Studies on the Coulomb Interaction of Double Acceptors in Magnetic Semiconductor Nanostructured Systems

Final Technical Report of the Major Research Project

University Grants Commission, New Delhi

(Reference No. F. No. 42 – 816/2013 (SR) dt. 22.03.2013)

SUBMITTED BY

Prof. K. JAYAKUMAR

and

Dr. P. NITHIANANTHI

Department of Physics

The Gandhigram Rural Institute - Deemed University

Gandhigram – 624302, Tamilnadu

November 2017

Acknowledgement

At the outset, let us express our thanks to the University Grants Commission, New Delhi for the finance assistance under Major Research Project

It is a pleasure to express our thanks to Ms. P. Kalpana, Project Fellow, UGC – MRP, Department of Physics, The Gandhigram Rural Institute – Deemed University, Gandhigram - 624302, Tamilnadu for assisting us to investigate the project.

We extend our heartfelt thanks to one and all in the Nanostructure Lab, Department of Physics, The Gandhigram Rural Institute – Deemed University, Gandhigram, Tamilnadu.

We are also immensely grateful to The Gandhigram Rural Institute – Deemed University for the successful completion of the Project

K. JAYAKUMAR

P. NITHIANANTHI

Contents

UNIVERSITY GRANTS COMMISSION

BAHADUR SHAH ZAFAR MARG

NEW DELHI – 110 002

PROFORMA FOR SUBMISSION OF INFORMATION AT THE TIMES OF SENDING THE FINAL REPORT OF THE WORK DONE ON THE PROJECT

1. **TITLE OF THE PROJECT** : **Study on the Coulomb Interaction of Double Acceptors in Magnetic Semiconductor Nanostructured Systems**

2. NAME AND ADDRESS OF THE PRINCIPAL INVESTIGATOR

PROF. K. JAYAKUMAR

Nanostructure Lab,Department of Physics,

Gandhigram Rural Institute – Deemed University, Gandhigram – 624302,

Tamilnadu

Mobile: +91 9443461177

E-mail: kjkumar_gri@rediffmail.com

3. NAME AND ADDRESS OF THE INSTITUTION

Gandhigram Rural Institute – Deemed University, Gandhigram – 624302,

Dindigul (Dt), Tamilnadu

4. UGC APPROVAL LETTER NO. AND DATE :

F. No. 42 – 816/2013 (SR) dt.22.03.2013

F. No. 42 – 816/2013 (SR) dt.26.08.2016

5. DATE OF IMPLEMENTATION : 13.05.2013

6. TENURE OF THE PROJECT : 3 + 1 = 4 years

7. TOTAL GRANT ALLOCATED : Rs. 10, 96, 800/=

8. TOTAL GRANT RECEIVED : Rs. 10, 21, 345/=

Grant Receivable as on 31.03.2017: Rs. 55, 605

9. FINAL EXPENDITURE : Rs. 10, 76, 950

10. TITLE OF THE PROJECT : Study on the Coulomb Interaction of Double Acceptors in Magnetic Semiconductor Nanostructured Systems

11. OBJECTIVES OF THE PROJECT :

- Effect of shape of Quantum Well, Quantum Wire and Quantum Dot on the Coulomb interaction of Magnetic Nanostructured systems.
- Effect of confining potential on the Coulomb interaction in the above said Magnetic Semiconductor Nanostructured Systems.
- Influence of external perturbation like magnetic field on the Coulomb interaction in these Semimagnetic / Magnetic Semimagnetic / Magnetic Nanostructured systems.

12. WHETHER OBJECTIVES WERE ACHIEVED: YES

(GIVE DETAILS)

- ✓ The influence of the shape of confining potential like square well and parabolic well on the acceptor binding and Coulomb interaction between the two holes has been studied for various impurity locations.

- When the correlation between holes are considered, the Coulomb interaction decreases.
- Coulomb interaction increases when an external magnetic field is applied in Quantum Well Wire (QWW) with parabolic confinement which is in contrary to the QWW with square well confinement.

✓ Donor/acceptor binding in CdTe/$Cd_{1-x}Mn_xTe$ Quantum Wire has been computed with square well along x – direction and parabolic confinement along y – direction has been investigated.

- Shape of confining potential along each direction plays an important role on the binding and the carriers can move with higher mobility when the directional dependent effective mass is employed in the calculation.

✓ Effect of geometry on the Coulomb interaction between the two holes in a Semimagnetic Quantum Dot (QD) has been studied by considering the spatially varying dielectric screening.

- The QD with spherical geometry gives more localization of the carriers as compared to the dot with cubical geometry.
- The spatially varying dielectric screening enhances the Coulomb interaction.

✓ Donor/Acceptor impurity states and the Bound Magnetic Polaron associated with them have been investigated in a Semimagnetic Double Quantum Well (DQW) and in a Triangular Quantum Well (TQW) have been studied.

- The donor/acceptor impurity is highly localised at the centre of the DQW and the applied magnetic field causes the counterintuitive behaviour for on centre well impurity and for other impurity locations.
- The Spin Polaronic Shift (SPS) depends only on the density of the magnetic ions separately concentrated in the well and in the barrier of DQW and TQW even though the effective concentration is same.
- The SPS is very much larger for the light hole than for heavy hole.

✓ Effect of magnetic field on the Coulomb interaction between the two electrons confined in a Low Dimensional Magnetic Nanostrucuted systems like QW, QWW and QD has been addressed.

- Coulomb interaction is tremendously affected by the applied magnetic field only when the impurity is confined inside the QD rather than in QW and QWW.

13. ACHIEVEMENTS FROM THE PROJECT :

- All the aspects of objectives were fulfilled
- Man Power trained : 1
- No. of Publications out of Project : International Journals : 9
  International/National Conferences: 4

14. SUMMARY OF THE FINDINGS: (IN 500 WORDS)

Irrespective of the nature of the confining potential the binding energy of the acceptor impurity with two holes and the Coulomb interaction between them is less both in Quantum Well Wire (QWW) and Quantum Dot (QD) when the correlation between them is considered in the wavefunction as compared to the case without considering the correlation. Moreover, the importance of accounting the correlation in the wavefunction has been emphasized by observing the increase of Coulomb repulsion with the increase of applied magnetic field in the case of parabolic confinement and the effect of impurity location on the Coulomb interaction between the two correlated holes is not significant as the strength of the interaction is consistently maintained for smaller wire size, when the impurity moves from the center to the edge of the wire. Moreover, a QD with spherical geometry which has bound states only for dot size greater than 30Å gives higher localization for the carriers since the Coulomb repulsion between them is less as compared to the Cubical Dot which could has bound states even for the dot size of 20Å. The spatially varying dielectric screening allows the carriers to have strong interaction (an enhancement of ≈ 20%) both in the absence and in the presence of applied magnetic field inside the QD. The influence of the shape of the confining potential along each direction of the confinement in QWW plays a crucial role to determine the strength of the binding of the carriers inside such QWW and the carriers can move with higher mobility when the directional dependent effective mass is employed in the calculation.

The effect of magnetic field on the acceptor ionization energy is very weak due to the high effective masses of the holes which leads to the smaller

Landau splitting as compared to the donor impurity. The carriers are highly localized only when it is situated at the centre of the Double Quantum Well (DQW) and also the applied magnetic field causes the counterintuitive behaviour for On Centre Well (OCW) impurity and for other impurity locations. the ground state donor binding energy and the SPS associated with it depends only on the density of the magnetic ions separately concentrated in the well $Cd_{1-x_{in}}Mn_{x_{in}}Te$ and in the barrier $Cd_{1-x_{out}}Mn_{x_{out}}Te$ of Semimagnetic Trianuglar Quantum Well (STQW) even though the effective concentration is same ($x_{out} - x_{in} = x = 0.1, 0.2$).

The results show that the effect of the increase of Mn^{2+} ion composition with different combinations on SPS is predominant for OCW impurity when compared to all other impurity locations for $\gamma = 0$ and the same is predominant for OCB impurity with $\gamma = 0.15$. The Spin Polaronic Shift (SPS) depends only on the density of the magnetic ions separately concentrated in the well and in the barrier of DQW and TQW even though the effective concentration is same and the SPS is very much larger for the light hole than for heavy hole.

The binding of the two electrons and their Coulomb interaction is tremendously affected by the applied magnetic field only when the impurity is confined inside the QD rather than in the QW and QWW.

15. CONTRIBUTION TO THE SOCIETY :

The field of Spintronics is how to manipulate the spin degree of freedom which is a purely quantum phenomenon in addition to the property called charge of the carrier to enhance the multifunctionality of the devices. Semimagnetic Semiconductors are ideal materials for spintronic applications

because of their tunable properties with the external perturbation like magnetic field. The Coulomb interaction between the carriers confined inside Semimagnetic Nanostructured systems with different band alignment is significant in the light of Coulomb blockade of transport. Hence, our investigation may give an understanding of the electronic and transport properties in such systems which can be exploited in various optoelectronic and spintronic devices such as spin based MOS structures and ultrahigh density non – volatile memory and reconfigurable logic devices based on novel spintronic concepts.

16. WHETHER ANY PH.D. ENROLLED / PRODUCED OUT OF THE PROJECT : YES, One Research Scholar

17. NO.OF PUBLICATIONS OUT OF THE PROJECT (PLEASE ATTACH) : International Journals - 9
International / National Conferences – 4

SEE ANNEXURE - I

PRINCIPAL INVESTIGATOR **REGISTRAR**

CO – INVESTIGATOR

23236351, 23232701, 23237721, 23234116
23235733, 23232317, 23236735, 23239437

विश्वविद्यालय अनुदान आयोग
बहादुरशाह जफर मार्ग
नई दिल्ली 110 002
UNIVERSITY GRANTS COMMISSION
BAHADURSHAH ZAFAR MARG
NEW DELHI-110 002

F. No. **42-816/2013 (SR)**

The Under Secretary (FD-III)
University Grants Commission
New Delhi-110002

22 MAR 2013

Sub:- UGC support for the Major Research Project in Physical Sciences, Bio-Sciences, Maths , Medical, Agricultural Sciences and Engineering & Chemistry to University/College Teachers – Project entitled,

"Study on the coulomb interaction of double acceptors in amgnetic semiconductor nanostructured systems"

Sir,

I am to refer to your letter forwarding the application of **Dr. K. Jayakumar** of your institution f financial assistance under the above scheme and to convey the Commission's approval & sanction an on account grant **Rs. 7,87,800/- (Rupees: seven lakh eighty seven thousand eight hundred only)** to the Registrar, **Gandhigram Ru Institute, Gandhigram-624302, TN** in r/o Major Research Project of **Dr. K. Jayakumar,** Department of **Physics** f the period of **3** years w.e.f. **1.4.2013** as detailed below:-

S.No	ITEMS	AMOUNT APPROVED	GRANT RELEASED AS Ist INSTALMENT	Cate ory
A.	**Non - Recurring**		**4,20,000/-**	GEN
1.	Books & Journals	nil		
2.	Equipment (work station & software)	4,20,000/-		
B.	**Recurring**			
1.	Honorarium to Retd. Teacher @ Rs. 12, 000/- p.m.	nil		
2.	Project Fellow @14,000/- p.m. for initial 2 years and Rs. 16,000/- p.m. from the third year onwards.	5,28,000/-		
3.	Chemical/ Glassware / Consumable	30,000/-	**3,67,800/-**	
4.	Hiring Services	nil		
5.	Contingency	30,000/-		
6.	Travel/Field Work	30,000/-		
7.	Special Need	nil		
8.	Overhead Charges @ Rs. 10% approved recurring Grant (Except Travel & Field Work)	58,800/-		
	Total (A + B)	**10,96,800/-**	**7,87,800/-**	

The acceptance Certificate in prescribed format (Annexure-I available on the UGC web-site) may be sent the undersigned within one month from the issue of the award letter failing which the project may be treated cancelled.

If the terms & conditions are acceptable, as per guideline which are available on UGC web-si www.ugc.ac.in the Demand Draft/ Cheque being sent may be retained. Otherwise the same may be returned in origi to the UGC by Registered Post in variably with in 15 days from the receipt of the Demand Draft Cheque in favour Secretary, UGC, New Delhi.

Principal Investigators should ensure that the statement of expenditure & utilization Certificate to the effect th the grant has been utilized for the purpose for which it has been sanctioned shall be furnished to the University Gra Commission in time.

The first instalment of the grant shall comprise of 100% of the Non –Recurrin including Over Head Charges, and 50% of the total Recurring grant.

1. The sanctioned amount is debitable to the Major Head **4. (i) .a (31) Rs. 3,67,800/- & 4. (i) .a (35) Rs. 4,20,000/-** and is valid for payment during financial year **2012-13**.
2. The amount of the Grant shall be drawn by the Under Secretary (drawing and Disbursing Office), University Grants Commission on the Grants-in-aid Bill and shall be disbursed to and credited to the Registrar, **Gandhigram Rural Institute, Gandhigram-624302, TN** through Cheque/Demand Draft/ Mail Transfer.
3. The Grants is subject to the adjustment of the basis of Utilization Certificate in the prescribed performa submitted by the University/Colleges/institution.
4. The University/College shall maintain proper accounts of the expenditure out of the grants which shall be utilized only on approved items of expenditure.
5. The Utilization Certificate of the effect that the grant has been utilized for the purpose for which it has been sanctioned shall be furnished to the University Grants Commission as early as possible after the close of the current financial year.
6. The assets acquired wholly or substantially out of University Grant Commission's grant shall not be disposed or encumbered of utilized for the purposes other that those for which the grant was given, without proper sanctioned of the University Grants Commission and should, at any time the College/University ceased in function such assets shall revert to the University Grant Commission.
7. A Register of assets acquired wholly or substantially out of the grant shall be maintained by the University/College in the prescribed form.
8. The grantee institution shall ensure the utilization of grant-in-aid for which it is being sanction/paid. In case non-utilization/part utilization, the simple interest @ 10% per annum as amended from time to time on unutilized amount from the date of drawl to the date of refund as per provisions contained in General Financial Rules of Govt. of India will be charged.
9. The interest earned by the University/College/Institute on this grants in aid shall be treated as additional grant and may be shown in the Utilization Certificate/Statement of expenditure to be furnished by grantee institution.
10. The University/College/Institute shall follow strictly all the instructions issued by the Government of India from time to time with regard to reservation of posts for Scheduled Castes/Scheduled Tribes/OBC/PH etc.
11. The University/College shall fully implement to Official Language Policy of Union Govt. and comply with the Official Language Act, 1963 and Official Languages (Use for Official purposes of the Union) Rules, 1978 etc.
12 The sanction issues in exercise of the delegation of powers vide Commission Office Order No. 25/92 dated May 01, 1992.
13. An amount of **Rs.** ---------- out the grant of **Rs.** ---------- sanctioned vide letter No. F. **42-816/2013 (SR)** dated has been utilized by University/College/Institution for he purpose for which it was sanctioned. Utilization Certificate for **Rs.** ---------- has already been entered at S. No. ------- now we may enter Utilization Certificate for **Rs.** ---------- S. No ------ and in the U. C. Registrar at page No. -----.
14. It is also certified from the B.C.R. that the funds are available under the scheme. Entered in BCR at S.No ------ 3141/53 The above grant is sanctioned against the budget provision of **Rs.** ..... during the current financial year leaving a balance of **Rs.** ---------- under the head of Account **4. (i) .a (31) Rs. 3,67,800/- & 4. (i) .a (35) Rs. 4,20,000/-**
15. The funds to the extent are available under the Scheme.
16. The University/Institution/College is strictly following the UGC regulations on curbing the menace of ragging in Higher Educational Institutions, 2009.

(Dr. (Mrs.) Urmila Devi)
Joint Secretary

Copy forwarded for information and necessary action for:-

1. The Registrar, **Gandhigram Rural Institute, Gandhigram-624302, TN,** Acknowledgement for the receipt of DD / Cheque / Mail Transfer for **Rs. 7,87,800/-** may be sent to the Under Secretary, Finance Division III, UGC,
2. **Dr. K. Jayakumar,** Principal Investigator, Department of **Physics** **Gandhigram Rural Institute, Gandhigram, 624302, TN**
3. office of the Director General of Audit, Central Revenues, A. G. C. R. Building, I. P. Estate, New Delhi.
4. The Registrar,

(Pramod Sharma)
Section Officer

सत्यमेव जयते

विश्वविद्यालय अनुदान आयोग
University Grants Commission
मानव संसाधन विकास मंत्रालय, भारत सरकार
(Ministry of Human Resource Development, Govt. of India)
बहादुरशाह जफर मार्ग नई दिल्ली –110002
Bahadurshah Zafar Marg, New Delhi-110002

ज्ञान-विज्ञान विमुक्तये

No. F. 42-816/2013 (SR)

March, 2016

26 MAR 2016

The Principal,
Gandhigram Rural Institute
Gandhigram, Dindigul District
Chinnalapatti, Tamil Nadu-624302.

Subject:- **Extension** of Major Research Project awarded **Dr. K. Jayakumar, Department of Physics** by UGC during 2013.

Sir,/ Madam,

I am directed to say that the tenure of the Major Research Project awarded to you has been extended by the UGC upto 31.03.2017 without any financial assistance for the extended period.

Yours faithfully,

(**G. S. Aulakh**)
Under Secretary

Copy to:-
Dr. K. Jayakumar,
Department of Physics,
Gandhigram Rural Institute
Gandhigram, Dindigul District
Chinnalapatti, Tamil Nadu-624302.

(**Arun Kumar Sinha**)
Section Officer

PFMS

UNIVERSITY GRANTS COMMISSION
BAHADUR SHAH ZAFAR MARG
NEW DELHI 110002
GEN

FD Diary No.4982
Dated : 21.06.2016

F .No.42-816/2013 (SR)

August 2016

26 AUG 2016

The Under Secretary (FD-III)
University Grants Commission
Bahadur Shah Zafar Marg
New Delhi – 110002

Sub: Release of Grant-in aid to **Gandhigram Rural Institute, Gandhigram - 624 302, Tamil Nadu** for the year 2016-17 under plan in respect of Major Research Project entitled **Study.....systems"** awarded to **Dr. K. Jayakumar Department of Physics,** tenure of project from **01.04.2013 to 31.03.2017.**

Sir,

I am directed to convey the sanction of the University Grants Commission for payment of grant of **Rs. 2,15,225/- (Rupees Two Lakh Fifteen Thousand Two Hundred Twenty Five Only)** as **2nd installment** for the year 2016-17 towards Major Research Project to **The Registrar, Gandhigram Rural Institute, Gandhigram - 624 302, Tamil Nadu** for the plan expenditure to be incurred during 2016-17.

I am also directed to say that the tenure of the above project has been extended by the UGC upto 31.03.2017 without any additional financial assistance for the extended period.

Name of the Item	Amount Allocated	Head of Account	Grant now Being Sanctioned	Grant already Released	Total Grant
Books & Journal	.....	3.A(56).35	.....		
Equipment	4,20,000/-		.....	4,20,000/-	4,20,000/-
Honorarium	.....	3.A(56).31	.....	.....	.....
Project fellow	5,05,806/-		1,91,225/-	2,64,000/-	4,55,225/-
HRA	.....		.....	.....	.....
Chemicals	30,000/-			15,000/-	15,000/-
Contingency	30,000/-		12,000/-	15,000/-	27,000/-
Hiring Services					
Travel/field work	30,000/-		12,000/-	15,000/-	27,000/-
Overhead Charges	58,800/-		.....	58,800/-	58,800/-
Additional Grant	.....		.....	.....	.....
Total	10,74,606/-		2,15,225/-	7,87,800/-	10,03,025/-

1. The sanctioned amount is debit able to **Major Research Project head Sector 3.A(56).31** and is valid for payment during the financial year **2016-17** only.
2. The amount of the Grant shall be drawn by the Under Secretary (Drawing and Disbursing Officer) UGC on the Grants-in-aid bill and shall be disbursed to and credited to **The Registrar, Gandhigram**

Rural Institute, Gandhigram - 624 302, Tamil Nadu through Electronic mode as per the following details:-

(a)	Bank Name & Address of Branch	**Canara Bank, Gandhirgram Branch, Code-8500, Gandhigram Rural Institute Campus, Gandhigram – 624 302.**
(b)	Account No	**85100101010000**
(c)	Type of Account : SB /Current /Cash Credit	**YES**
(d)	**IFSC Code**	**CNRB0008500**
(e)	MICR Code	**625015050**
(f)	Whether Bank Branch is RTGS or NEFT enabled : RTGS / NEFT /Both	**YES**
(g)	Name & Address of Account Holder	**The Registrar, Gandhigram Rural Institute, Gandhigram - 624 302, Tamil Nadu.**

3. The Grant is Subject to the adjustment on the basis of Utilization Certificate in the prescribed proforma submitted by the University / Institution.

4. The University / Institution shall maintain proper accounts of the expenditure out of the Grants, which shall be utilized, only on the approved items of expenditure.

5. The University / Institution may follow the General Financial Rules, 2005 and take urgent necessary action to amend their manuals of financial procedures to bring them in conformity with GFRs, 2005 and those don't have their own approved manuals on financial procedures may adopt the provisions of GFRs, 2005 and instructions / guidelines there under from time to time.

6. The Utilization Certificate to the effect that the grant has been utilized for the purpose for which it has been sanctioned shall be furnished to UGC as early as possible after the close of current financial year.

7. The assets acquired wholly for substantially out of University Grants Commission's Grant shall not be disposed or encumbered or utilized for the purposes other than those for which the grants waayanands given without proper sanction of the UGC and should at any time the University ceased to function, such assets shall revert to the University Grants Commission.

8. A Register of Assets acquired wholly or substantially out of the grant shall be maintained by the University in the prescribed proforma.

9. The grantee institution shall ensure the utilization of grants-in-aid for which it is being sanctioned / paid. In case of non-utilization / part utilization thereof, simple interest @ 10% per annum, as amended from time to time on the unutilized amount from the date of drawal to the date of refund as per provisions contained in General Financial Rules of Govt. of India, will be charged.

10. The University / Institutions shall follow strictly the Government of India / UGC guidelines regarding implementation of the reservation policy [both vertical (for SC, ST & OBC) and horizontal (for persons with disability etc.)] in teaching and non-teaching posts.

11. The University / Institution shall fully implement the Official Language Policy of Union Government and comply with the Official Language Act, 1963 and Official Languages (Use for Official Purposes of the Union) Rules, 1976 etc.

12. The sanction is issued in exercise of the delegation of powers vide UGC Order No. 69/2014 [F.No.10-11/12 (Admn. IA & B)] dated 26/3/2014.

13. The University / Institution shall strictly follow the UGC Regulations on curbing the menace of Ragging in Higher Education Institutions, 2009.

14. The University / Institution shall take immediate action for its accreditation by National Assessment & Accreditation Council (NAAC).

15. The accounts of the University / Institution will be open for audit by the Comptroller & Auditor General of India in accordance with the provisions of General Financial Rules, 2005.

16. The annual accounts i.e. balance sheet, income and expenditure statement and statement of receipts and payments are to be prepared strictly in accordance with the Uniform Format of Accounting prescribed by Government.

17. The grantee institution shall remit the amount the grants-in-aid and/or interest through e-mode (RTGS/NEFT) directly to UGC account as per following bank details:-

Account Holder	Secretary, UGC, New Delhi-110 002
Name of Bank & Address	Canara Bank, UGC Office, New Delhi-110 002
A/C No.	**8627101002122**
Type of A/C	Savings
IFSC Code	CNRB0008627
MICR Code	110015170

18. An amount of **Rs. 7,23,467/-** out the grant of **Rs. 7,87,800/-**..... Sanctioned vide letter No. **F. No. 42-816/2013 (SR)** dated **22-03-2013** has been utilized by University/College/Institution for the purpose for which it was sanctioned. Utilization Certificate for **Rs .....** ...NIL..... has been entered at S. No..... now we may enter Utilization Certificate for **Rs**...**7,23,467/-** .....S. No..197. and in the U.C. Register at page No..05...

19. Funds to the extent of Rs are available under the scheme or BE / RBE of the year 2016-17.

20. These issues with the concurrence of IFD vide **Diary No 8232 (IFD) dated 19/02/2016.**

21. This issues with the approval of Joint Secretary (MRP) vide **Diary No. 56418 dated 03/03/2016 and revalidated for the financial year 2016-17 with the approval of the Chairman, UGC vide Diary No. 58242 dated 28.04.2016.**

Your faithfully,

(G.S. AULAKH)
UNDER SECRETARY

Copy forwarded for information and necessary action for :-

1. **The Registrar, Gandhigram Rural Institute, Gandhigram - 624 302, Tamil Nadu.**
2. Office of The Finance Officer, General of Audit, Central Revenues, AGCR Building, I.P. Estate, New Delhi.
3. Accountant General, State Govt. of **Gandhigram Rural Institute, Gandhigram - 624 302, Tamil Nadu.**
4. **Dr. K. Jayakumar Department of Physics**
   Gandhigram Rural Institute, Gandhigram - 624 302, Tamil Nadu.
5. Guard file.

(ARUN KUMAR SINHA)
(SECTION OFFICER)

Annexure - VIII

UNIVERSITY GRANTS COMMISSION
UTILIZATION CERTIFICATE – From 19.09.2013 to 31.03.2017

It is certified that the amount of Rs.10,76,950/- (Rupees Ten lakhs seventy-six thousand nine hundred and fifty only) out of the grant of Rs.10,03,025/-(Rupees Ten lakhs three thousand and twenty-five only) Sanctioned to Dr. K. Jeyakumar Professor and PI, Department of Physics by the University Grants Commission vide its letter No.42-816/2013/(SR),dated.22.03.2013 towards UGC-MRP on "Study on the coulomb interaction of double acceptors in magnetic semiconductor nanostructured system" under UGC-MRP scheme has been utilized for the purpose for which it was sanctioned and in accordance with the terms and conditions as laid down by the commission.

If as a result of check or audit objection some irregularities are noticed at a later stage, action will be taken for refund, adjustment or regulation.

Signature
Registrar / Principal with seal

REGISTRAR
Gandhigram Rural Institute

Signature
Finance Officer with seal

Special Officer (Finance)
Gandhigram Rural Institute

Signature
Coordinator of the Programme /
Head of the Department
(as the case may be)

Principal Investigator / Co-Investigator
UGC-Major Research Project
'Coulomb Interaction in Nanostructures'
Department of Physics
Gandhigram Rural University
Gandhigram - 624 302, T.N.

For A.V. SUBRAMANIAN & CO
CHARTERED ACCOUNTANTS

Signature, Chartered Accountant
with seal and Registrar No.
(If the accounts were audited prior to the audit of Statutory Auditors)

C.A. J. Sumathi
M. 029617, Partne
ICAI: FRN: 010643S

Note: The University/ Institution will submit an audited statement of accounts, duly audited by the Statutory Auditors of the University / Institution as soon as the accounts of the University / Institution are audited.

Annexure - VII

The Gandhigram Rural Institute – Deemed University
Gandhigram - 624 302
UGC-MRP Project on "Study on the coulomb interaction of double acceptors in magnetic semiconductor nanostructured system"

Dr.K.Jeyakumar, Professor, Dept.of Physics.

University/Institution : **The Gandhigram Rural Institute-Deemed University, Gandhigram-624 302**
Sanction Letter No. and Date of UGC, New Delhi : **F.42-816/2013/(SR),dt: 22.03.2013**
Statement of Actual Expenditure during : **19.09.2013 to 31.03.2017**

Item of Expenditure	Total Grant approved	Actual Grant Received				Total (3 to 6)	Actual Expenditure incurred				Total (8 to 11)	Excess/Saving diff. of Co.7 & 12
1	2	3	4	5	6	7	8	9	10	11	12	13
		2013-14	2014-15	2015-16	2016-17		2013-14	2014-15	2015-16	2016-17		
(A) Non-Recurring												
1. Equipment	4,20,000	4,20,000	-	-	-	4,20,000	4,16,872	3,125	-	-	4,19,997	3
2. Books and Journals		0	-	-	-	0	0	0	-	-	0	0
Total (A)	**4,20,000**	**4,20,000**	-	-	-	**4,20,000**	**4,16,872**	**3,125**	**0**	**0**	**4,19,997**	**3**
(B) Recurring (Per Annum)												
1.Project Fellow - 2 Years	5,28,000	2,64,000	-	-	1,91,225	4,55,225	1,48,581	1,68,000	0	1,92,000	5,08,581	-53,356
2.Chemical/Glasswarc/Conumable	30,000	15,000	-	-	-	15,000	0	0	0	23,787	23,787	-8,787
2.Hiring Services	0	0	-	-	-	0	0	0	0	0	0	0
3.Contingencies	30,000	15,000	-	-	12,000	27,000	11,546	7,358	2,087	10,304	31,295	-4,295
4.Travel/Field Work	30,000	15,000	-	-	12,000	27,000	23,791	10,699	0	0	34,490	-7,490
5.Overhead Charges	58,800	58,800	-	-	-	58,800	58,800	0	0	0	58,800	0
Total (B)	**6,76,800**	**3,67,800**	-	-	**2,15,225**	**5,83,025**	**2,42,718**	**1,86,057**	**2,087**	**2,26,091**	**6,56,953**	**(73,928)**
Total (A) + (B)	**10,96,800**	**7,87,800**	-	-	**2,15,225**	**10,03,025**	**6,59,590**	**1,89,182**	**2,087**	**2,26,091**	**10,76,950**	**-73,925**
Interset on Grant received		8,262	4,864	2,877	2,317	18,320		**0**	**0**	**0**	0	18,320
Total	**10,96,800**	**7,96,062**	**4,864**	**2,877**	**2,17,542**	**10,21,345**	**6,59,590**	**1,89,182**	**2,087**	**2,26,091**	**10,76,950**	**-55,605**
Grant Receivable												(-)55605

Total Expenditure	**10,76,950**
Less: Grant received with interest	**10,21,345**
Grant Receivable as on 31.03.2017	**55,605**

Certified that the grant has been utilized for the purpose for which if was sanctioned and in accordence with terms and conditions attached

Special Officer (Finance)
Gandhigram Rural Institute

REGISTRAR

For A.V. SUBRAMANIAN & CO,
CHARTERED ACCOUNTANTS

CA. J. Sumathi
M. No. 029617, Partner
ICAI FRN: 010643S

Annexure – XI

Final Report Assessment / Evaluation Certificate

(Two Members Expert Committee Not Belonging to the Institute of Principal Investigator)

(to be submitted with the final report)

It is certified that the final report of Major Research Project entitled **"Studies on the Coulomb Interaction of Double Acceptors in Magnetic Semiconductor Nanostructured Systems"** by Prof. K. Jayakumar, Department of Physics, The Gandhigram Rural Institute – Deemed to be University has been assessed by the Committee consisting the following members for final submission of the report to the UGC, New Delhi under the scheme of Major Research Project.

Comments/Suggestions of the Expert Committee:-

Comments attached herewith

Name & Signatures of Experts with Date:-

Name of Expert	University/College Name	Signature with Date
1. Prof. T. R. Rajasekaran	Manonmaniam Sundaranar University, Tirunelveli, Tamilnadu	25.12.2018 Dr.T.R. RAJASEKARAN, M.Sc.,Ph.D., Professor of Physics Head,Dept. of Renewable Energy Sciences Manonmaniam Sundaranar University Tirunelveli-627.012.
2. Prof. S. Rajasekar	Bharathidasan University, Tiruchirapalli, Tamilnadu	25/6/2018 Prof. S. RAJASEKAR School of Physics Bharathidasan University Tiruchirapalli-620 024.

It is certified that the final Report has been uploaded on UGC – MRP portal on

It is also certified that the final report, Executive summary of the report, Research documents, monograph academic papers provided under Major Research Project have been posted on the website of the University / College.

(Registrar / Principal)

Seal

DEPARTMENT OF PHYSICS
MANONMANIAM SUNDARANAR UNIVERSITY
TIRUNELVELI – 627 012.

Dr.T.R. Rajsekaran
Professor

email: trrajasekaran@gmail.com
mobile: 9442327921

29.05.2018

Report of the UGC – Major Research Project submitted by Prof. K. Jayakumar and Dr. P. Nithiananthi, Department of Physics, The Gandhigram Rural Institute – Deemed to be University, Gandhigram – 624302, Tamilnadu

Title: Studies on the Coulomb Interaction of Double Acceptors in Magnetic Semiconductor Nanostructured Systems

To whomsoever it may concern

I am happy to go through the above said Report and fully satisfied by the objectives of the Project.

The report starts with nice Introduction on the exchange interaction on the wide gap Diluted Magnetic Semiconductors (DMS) and Chapter 2 discusses on the Coulomb interaction of double acceptors in Semimagnetic Quantum Well Wire (SMQWW). It gives the effective correlation of two holes in a SMQWW with the influence of shape of the confining potential on Coulomb interaction and also the effect of confining potential along in – plane directions also. The Spin Polaronic effect of donor and acceptor bound states have also been investigated.

Chapter 3 contains the Coulomb interaction of double acceptors in a Semimagnetic Quantum Dot (SQD) and in Chapter 4, the impurity states in a Semimagnetic Quantum Well (SMQW) have been thoroughly studied. Chapter 5 discusses the Coulomb Interaction of Electrons in Semimagnetic Nanostructured Systemsand ends up with the summary of the investigations in Chapter 6.

The highlight of the investigation is that the Principal Investigators and Project Fellow have published 9 papers in International refereed journals and 4 papers in International/National conferences. The Investigators have achieved the objectives. The outcome the Project is highly commended.

(T. R. RAJASEKARAN)

Dr. T.R. RAJASEKARAN
M.Sc., Ph.D.
Professor, Department of Physics
Manonmaniam Sundaranar University
TIRUNELVELI 627 012

School of Physics
Bharathidasan University
Tiruchirapalli - 620 024
Tamilnadu
INDIA

Prof. S. RAJASEKAR

Report on the UGC Major Project
Studies on the Coulomb Interaction of Double Acceptors in Magnetic Semiconductor Nanostructured Systems
Principal Investigators: Prof.K. Jayakumar & Dr.P.Nithiananthi

The prime objectives of the present project were investigation of the role of shape of the potentials of certain quantum nanostructures particularly on magnetic semiconductors. The goals of the project were achieved by employing theoretical analysis.

The Features of Objectives Performed and the Results Obtained

- Theoretical attack on the magnetic field produced interwell interaction in a DQW material. Binding energy was found enhanced. By solving the Schrodinger equation the binding energy of the donor impurity was computed.
- Solving the Schrodinger equation by employing the variational approach the effect of gamma-X-band cross-over in a TQW was explored. The results were explained and their usefulness were pointed out.
- The effect of applied magnetic field on the Coulomb interaction in a WQ was analysed. The predictions were illustrated through 3D plots.
- The computation of SPS as a result of the occurrence of BMP in DQW for impurity locations and for various concentrations of Mn^{2+} ions revealed several interesting results. The significance of the results have practical applications.
- The acceptor-acceptor Coulomb interaction in spherical and cubical QD has been investigated within the framework of effective mass theory. The results are very useful to understand the eigenspectra.

Highlights of the Outcomes of the Project

- 100% objectives were achieved.
- Appropriate theory were employed for the problems of interest.
- The statement of expenditures submitted clearly indicate the complete utilization of the grant received.

Phone : +91 (431) 2407057 Fax : +91 (431) 2407093 E-mail : rajasekar@physics.bdu.ac.in

- One man power has been trained.
- 9 publications in the internationally reputed high impact factor journals.
- 4 papers presented in conferences.
- Contributions to the society were mentioned.

In summary, the implementation and the outcomes of the project are high appreciable and commendable.

S. RAJASEKAR

PROF. S. RAJASEKAR
DEPARTMENT OF PHYSICS
BHARATHIDASAN UNIVERSITY
TIRUCHIRAPALLI - 620 024
TAMILNADU, INDIA

Chapter 1

INTRODUCTION

The relentless growth of microelectronics made Gordon E. Moore in 1965 to frame a law, called as Moore's law, which states that microprocessors will double in power every 18 months as electronic devices shrink and more logic is packed into every chip. But this law will run out of momentum one day as the size of the individual bits approaches the dimension of atoms – this has been called the end of the silicon road map. This induced the basic research community to focus their attention towards the subject called as "Spintronics", Spin + Electronics, which is a multidisciplinary field including magnetism, semiconductor, optics, mesoscopic physics, superconductivity and new connection to other fields. The central theme of this subject is how to manipulate the spin degree of freedom which is a purely quantum phenomenon in addition to the property called charge of the carrier to enhance the multifunctionality of the devices owing to its easy manipulation by externally applied magnetic field and long coherence or relaxation time. The key aspects of the spintronic devices rests on the three factors like efficient spin injection, slow spin relaxation and reliable spin detection and these requires materials with ferromagnetic ordering at operational temperatures compatible with existing semiconducting materials and the properties of the interface separating different materials used for forming the reliable spintronic devices.

Dilute Magnetic Semiconductors (DMS) also called as Semimagnetic Semicondcutors (SMSC), mainly $A^{II}_{1-x}Mn_xB^{VI}$ in which a fraction of the group II sublattice is replaced at random by Mn, suit this need. DMS are widely believed that they are ideal materials for spintronic applications because of their tunability of the band and lattice parameters by varying the composition of Mn^{2+} ion in $A^{II}_{1-x}Mn_xB^{VI}$ alloys, and the tuning of magnetic properties like paramagnetic, spin – glass and antiferromagnetic by varying externally applied magnetic field and subjected to thermal energy and thirdly the formation of Bound Magnetic Polaron (BMP) by the exchange interaction between the localized magnetic moments of Mn^{2+} ion and the conduction / valence band electrons. Moreover, these DMS structures have been proven to have high spin efficiency as measured by magnetic tunnelling and electroluminescence. The first narrow or zero gap materials that were studied experimentally was HgMnTe which revealed unusual transport and optical properties and the first of wide gap materials studied was CdMnTe and the studies of these wide gap crystals have been initiated by Komarov et.al and Gaj et.al. The reason for choosing Mn rather than other transition metal elements for the substitution of group II element is because of its high miscibility with the $A^{II}B^{VI}$ host without much affecting substantially the crystallographic quality of the resulting material. In the case of $Cd_{1-x}Mn_xTe$, the zinc – blende structure of the parent CdTe survives for 'x' as high as 0.77. This can be attributed to the fact that the 3d orbitals of Mn are exactly half filled which act as a completely filled shell as in the case of $4d^{10}$ shell in Cd atom and all five spins are parallel and it would require considerable energy to add an electron with opposite spin to the Mn atom. Moreover Mn^{2+} provides the spin polarized carriers only and does not give electrons or holes because it is electrically neutral and it possesses a relatively larger magnetic moment (s=5/2) due to the characteristic of a half filled d shell.

The lattice parameters of all DMS ternary alloys obey Vegard's law very closely and it is given for any composition of 'x' by $a = (1-x)\, a_{II-VI} + x\, a_{Mn-VI}$ where, a_{II-VI} and a_{Mn-VI} are lattice parameters of the binary constituents. The energy gap of all $A^{II}_{1-x}Mn_xB^{VI}$ alloys are temperature and composition dependent and they are all the direct gap semiconductors like their $A^{II}B^{VI}$ parent materials.

1.1. Exchange interaction in wide gap DMS

In view of spintronic applications, the crucial parameter that characterizes ferromagnetic materials is the degree of spin polarization of band carriers. The sp – d exchange interaction influences physical phenomena which involve electrons in the conduction and valence bands (e.g. magneto transport, interband magneto – optics), exciton levels (e.g., Faraday rotation) and impurity levels (e.g., Bound Magnetic Polaron, Giant magnetoresistance, metal – semiconductor transition). In nonmagnetic semiconductor, the Landau level structure of an electron which contains all the information required to describe the semiconductor can be denoted by the appropriate Hamiltonian H_0. When DMS alloy is formed, its band structure will be modified by this sp-d exchange interaction which can be described by adding the Kondo – like exchange term H_{exc} to the original Hamiltonian H_0. Therefore the total Hamiltonian H_T can be written as

$\mathbf{H}_T = \mathbf{H}_0 + \mathbf{H}_{exc} = H_T = H_0 + \sum_{R_i} J^{sp\text{-}d}(\mathbf{r}-\mathbf{R}_i)\mathbf{S}_i.\boldsymbol{\sigma}$, where, $\mathbf{S_i}$ and $\boldsymbol{\sigma}$ are the spin operators for the Mn^{2+} ion and for the band electrons or holes respectively. $J^{sp\text{-}d}$ is the electron – ion exchange coupling constant and $\mathbf{r}$ and $\mathbf{R_i}$ denote the coordinates of the band electron and of the Mn^{2+} ion respectively. The summation sign denotes over the lattice sites occupied by the Mn^{2+} ions. Since the electronic wavefunction is spatially extended, the probability for the electrons to include large number of Mn^{2+} ions within its Bohr orbit at any time is

more so that one can make use of molecular field approximation by replacing S_i by the thermal average $<S_z>$, which is qualitatively related to the magnetization of the system when the magnetic field is applied along z direction. Because of the electronic wavefunction spans a large number of lattice sites, the exchange interaction can be expressed in terms of virtual crystal approximation by replacing $J^{sp-d}(r-R_i)$ by $xJ^{sp-d}(r-R)$, where, R denotes the coordinate of every site of fcc cation sublattice, with the summation now carried out over all R. With these assumptions H_{exc} can be expressed as

$H_{exc}=\sigma_z \langle S_z \rangle x \sum_R J^{sp-d}(\mathbf{r-R})$. In the dilute limit, i.e. when the concentration of Mn^{2+} is small ($x < 0.01$), the Mn^{2+} spins can be regarded as isolated, i.e non interacting Mn^{2+} ions. The thermal average of $< S_z >$ is related to the magnetization of the material is therefore described by the Brillouin function and can be written as

$$M= - x N_0 g_{Mn} \mu_B \langle S_z \rangle = x N_0 g_{Mn} \mu_B S B_s [g_{Mn}\mu_B S B / k_B T]$$

where, $< S_z >$ is the average spin per Mn site, N_0 is the number of cations per unit volume, B is the applied magnetic field, S= 5/2 for Mn^{2+} ion, k_B is the Boltzmann constant and T is the temperature. B_s is the standard Brillouin function and is given by

$B_s(x)=\frac{2s+1}{2S}\coth\frac{2s+1}{2S}x-\frac{1}{2S}\coth\frac{x}{2S}$. For DMS of arbitrary 'x', the magnetization M cannot be expressed by the standard Brillouin function because of the antiferromagnetic interaction between the nearest neighbour Mn^{2+} ions rather it is expressed using modified Brillouin function incorporating semi phenomenological fitting parameters like S_0 and T_0 for which the numerical values can be taken from the work reported by Gaj et.al.

$M= x_{eff} N_0 g_{Mn} \mu_B S_0 B_s [g_{Mn}\mu_B S B / k_B T_{eff}]$, where, x_{eff} represents the existence of effective concentration of Mn^{2+} ions after considering antiferromagnetic interactions between them, S_0 therefore carries the information on the spatial distribution of the ions and T_0 expresses an influence of more distant neighbours. In wide band gap materials like

$Cd_{1-x}Mn_xTe$, because of its large effective mass m^*, the magnetic splitting due to H_{exc} is much greater than the Landau splitting predicted by ordinary sp band theory. H_{exc} can be diagonalized in the bases appropriate for the respective bands (i.e. Γ_6 conduction or Γ_8 valence). For these two cases, H_{exc} leads to the matices,

$$\left\langle \psi_{\Gamma_6} \left| H_{exc} \right| \psi_{\Gamma_6} \right\rangle = \begin{Vmatrix} 3A & 0 \\ 0 & -3A \end{Vmatrix}; \quad \left\langle \psi_{\Gamma_8} \left| H_{exc} \right| \psi_{\Gamma_8} \right\rangle = \begin{Vmatrix} 3B & 0 & 0 & 0 \\ 0 & B & 0 & 0 \\ 0 & 0 & -B & 0 \\ 0 & 0 & 0 & -3B \end{Vmatrix}$$

where, $A = \frac{1}{6} N_0 \alpha x \langle S_z \rangle$, $B = \frac{1}{6} N_0 \beta x \langle S_z \rangle$ and $\alpha N_0 = 220meV$, $\beta N_0 = -880meV$.

The positive and negative value of α and β respectively are based on the two processes which contribute to the exchange interaction between the band electrons or holes and the $3d^5$ electrons of the Mn^{2+} ions:

(i) The 1/r type potential exchange interaction between the band (s or p) and the d electrons align the spin of the electron parallel to the spin of the Mn^{2+} ion which is referred to as a ferromagnetic interaction and makes a positive contribution to the exchange constant.

(ii) The contribution due to the hybridization of the $3d^5$ levels with the p band electrons at the Γ point, where the s – d hybridization is forbidden by symmetry, leads to the antiferromagnetic interaction which makes a very strong negative contribution to the exchange constant which is much greater in magnitude than the potential contribution described above.

The low dimensionality is achieved by confinement, where the electrons are restricted from moving freely in all three directions. Squeezing one side of a 3-D plane until it is no thicker than one electron wavelength traps electron in a 2-D plane in which the density of states (DOS) gets quantized. Electrons are not really confined to any kind

of physical barriers rather it is confined artificially by sandwiching a smaller band gap semiconducing material between the two larger band gap materials and the electrons are trapped inside the smaller bandgap materials if the barrier layer is sufficiently thick. Many interesting and intriguing physical phenomena occurs when a narrow strip sliced from one of the plane to form 1-D Quantum Well Wire (QWW) and further dicing up a 1-D wire to form 0-D Quantum Dot (QD) . Reducing the number of dimensions in this manner one can make the electrons to behave in a more atom like manner. As the dimension of the system scales down from 3D $\rightarrow$ 2D $\rightarrow$ 1D $\rightarrow$ 0D, corresponding DOS also gets modified.

One of the most important development in DMS is the successful preparation of Low dimensional DMS superlattices and multiple quantum well structures by Molecualr Beam Epitaxy (MBE) because of the existence of strong exchange interaction in these quasi – low dimensional quantum structures as occurs in bulk DMS. The first high quality superlattices were prepared using $Cd_{1-x}Mn_xTe$/ $Cd_{1-y}Mn_yTe$.

Since the carriers are localized near magnetic impurities, it can strongly affect the magnetic properties of DMS with the possibility of spin – dependent tuning of the confining potential by magnetic field and the application of a perpendicular magnetic field also influences the strong correlations between the electrons / holes. The donor and acceptor type impurities play central role in determining the physical properties of these semiconductors. The acceptor impurities in barrier material which can be controlled by magnetic field, influence to a large extent the optical properties near the fundamental absorption edge in p –type structures in bulk and Quantum Well (QW) materials.

In the present report, an attempt has been made towards the theoretical investigation on how the reduction of dimensionality influences the electronic states of two holes / electrons **c**onfined in a CdTe / $Cd_{1-x}Mn_xTe$ and their Coulomb interaction and

also the spin polaronic shift due to the acceptor/donor BMP under the external perturbation like magnetic field.

1.2. Outline of the Report

The present report contains 6 chapters. The importance of accounting the correlation between the two holes in the spatially extended wavefunction when they are confined in a Semimagnetic Quantum Well Wire is discussed in detail in section I of **Chapter 2**. Section II presents the influence of the nature of the different confining potential along different directions of the confinement in QWW on the binding energy of the acceptor and donor impurities. The comparison has been made between the acceptor binding energy with accounting constant effective mass and directional dependent effective mass.

The study on the mutual Coulomb interactions of the electrons / holes in the dot is very much essential for the controlled electron/hole tunnelling to amplify the current. Such a study on the Coulomb interaction of the two correlated holes in a Semimagnetic Quantum Dot under the effect of the geometry of the dot and spatially varying dielectric screening is discussed in **Chapter 3**.

The modified density of states of DQW from 2D to 0D due to the formation of Landau levels under the influence of high magnetic field has induced the present author to consider the Coulomb interaction between the impurities and also to study its tunnelling properties in these systems. The triangular potential well could be the better approximation for modelling quantum mechanical effects in Metal Oxide Semiconductor (MOS) structures, for explaining the optical properties of the organic molecules and also in studying pyramid – shaped quantum confined systems easily obtained by etching of semiconductor surfaces. Therefore it shows some pronounced effects on the

acceptor/donor impurity energy levels and the BMP when they are confined in such shape of the QW. Hence, **Chapter 4** is dedicated to such investigation of acceptor and donor impurities confined in a Semimagnetic Double Quantum Well (SDQW) and TQW (STQW).

Chapter 5 discusses the Helium like impurity in some low dimensional systems like QW, QWW and QD under the effect of externally applied magnetic field.

Chapter 6 summarises the research findings that have been discussed in all the chapters from 2 to 5.

Chapter 2

COULOMB INTERACTION OF DOUBLE ACCEPTORS IN SEMIMAGNETIC QUANTUM WELL WIRE

Ever since the progress in semiconductor nanotechnology, such as Molecular Beam Epitaxy (MBE), Chemical lithography and etching were developed, it has been made possible to fabricate a wide variety of Low - Dimensional Semiconductor Nanostructures like Quantum Well Wires (QWW), Nanowires and Carbon Nanotubes with well controlled shape and composition to achieve the high carrier mobility [1]. Use of Diluted Magnetic Semiconductors (DMS) in such QWW has opened the doors for the researchers to break through entirely a new set of challenges which had been intimidating in the field of spintronics, since the physical nature of impurity energy levels associated with QWW made of DMS materials can be greatly controlled by the application of external magnetic field which manifest themselves into fascinating phenomena like Bound Magnetic Polaron [2], Giant Zeeman Splitting [3] at the band edges, Magneto optical [4-5] and Magneto transport [6-7].The shape of the confining potential and the impurity position along these structures mainly determine the spatial confinement of the wavefucntion in these QWW and thereby number of studies concerning QWW with rectangular [8], Parabolic [9], V-groove [10] and triangular [11] cross sections have been carried out. Moreover, these 1D systems provide the fantabulous space for the study of Coulomb interaction effects in many body problems because the reduced degree of

freedom for the carriers make qualitative changes in the role of interactions which leads to spin – charge separation [12], charge fractionalization [13] and Wigner crystallization [14]. Many researchers have put their considerable effort to investigate the electron – electron and hole – hole interaction under various confining potentials both in nonmagnetic [15-19]] and in Semimangetic [20] Semiconducting systems. However, in spite of theoretical activities on the hydrogenic acceptor impurity in DMS Nanostructures [21-24], the studies of impurity states concerning two holes are very few [25-28]. Therefore it necessitates to investigate the Coulomb interaction between the two holes confined in a Semimagnetic QWW (SQWW) made of $CdTe/Cd_{1-x}Mn_xTe$ which is discussed in section 2.1 of this Chapter. The effect of the nature of confining potential on the impurity states (acceptor and donor) in SQWW is treated separately in section 2.2.

2.1. Effective Correlation of Two Holes in a Semimagnetic Quantum Wire: Influence of Shape of the Confining Potential on Coulomb Interaction

In this section, the hole – hole interaction (E_{hh}) has been considered in a $CdTe/Cd_{1-x}Mn_xTe$ Semimagnetic Quantum Well Wire (SQWW). The influence of the shape of the confining potential like square well and parabolic well type on the binding energy of an acceptor impurity with two holes and their Coulomb interaction between them has been studied for various impurity locations. Magnetic field has been used as a probe to understand the carrier- carrier correlation in such Quasi 1- Dimensional QWW since it alters the strength of the confining potential tremendously. In order to show the significance of the correlation between the two holes, the calculations have been done with and without including the correlation effect in the ground state wavefunction of the

hyderogenic acceptor impurity and the results have been compared. The expectation value of the Hamiltonian, **H**, is minimized variationaly in the effective mass approximation through which E_{hh} has been obtained.

2.1.1. Theoretical Formalism

The Hamiltonian of the two holes bound to an acceptor impurity inside the SQWW made of CdTe/$Cd_{1-x}Mn_xTe$ in the effective mass approximation in the presence of applied magnetic field along the direction of growth axis (z-axis) is written as

$$\mathbf{H}_{hh} = -(\nabla_1^2 + \nabla_2^2) - 2z\left(\frac{1}{r_1}+\frac{1}{r_2}\right) + V_B(x_1,y_1) + V_B(x_2,y_2) + \gamma\,(L_{z_1}+L_{z_2}) + \frac{\gamma^2}{4}(\rho_1^2+\rho_2^2) + \frac{2}{|\vec{r_1}-\vec{r_2}|} \tag{2.1}$$

where, z = 2, since it is treated as a helium like impurity and $\gamma = \hbar\omega_c / 2R^*$ (ω_c – cyclotron frequency) is the parameter of the strength of the magnetic field and $\gamma = 1$ corresponds to ≈1131Tesla; $r_1 = \sqrt{\rho_1^2 + z_1^2}$, $r_2 = \sqrt{\rho_2^2 + z_2^2}$ is the mean distance of the parent acceptor atom and the carriers attached to it.

The profile of both the square and parabolic confining potential V_B for the carriers is given as,

$$\left.\begin{aligned} V_B &= \begin{cases} \frac{1}{2} m^*_w \omega^2 (\rho_1^2+\rho_2^2) & |x_1|,|y_1|,|x_2|,|y_2| \le L/2 \\ V_0 & |x_1|,|y_1|,|x_2|,|y_2| > L/2 \end{cases} \quad \rightarrow \textbf{Parabolic} \\ V_B &= \begin{cases} 0 & |x_1|,|y_1|,|x_2|,|y_2| \le L/2 \\ V_0 & |x_1|,|y_1|,|x_2|,|y_2| > L/2 \end{cases} \quad \rightarrow \textbf{Square} \end{aligned}\right\} \tag{2.2}$$

Here, L is the size of the QWW and V_0=30% ΔE_g^B, where, ΔE_g^B is the band gap difference with magnetic field and is given by [26]

$$\Delta E_g^B = \Delta E_g^0 \left[\frac{\eta\ \exp^{\zeta\gamma} - 1}{\eta - 1}\right] \tag{2.3}$$

and because of which, the strength of the confinement potential is rapidly reduced and results in the modifications of electrical and optical properties. $\eta = \exp[\alpha\gamma_0]$, where, α is a parameter (α=0.5) and γ_0 as the critical magnetic field. ΔE_g^B and ΔE_g^0 are the band gap difference with and without magnetic field respectively. The band gap of the material is given by E_g ($Cd_{1-x}Mn_xTe$) = 1606 + 1587x (meV). The critical magnetic field γ_0 depends upon the composition of magnetic impurity. This critical field (in Tesla) for various compositions can be obtained using the formula $B_0 = A_2 \exp[nx]$, where, A_2 = -0.57 and n=16.706.

The approximate ground state energy for confined acceptor impurity with two holes has been calculated using the variational method. The envelop function f (z) is considered for both square and parabolic confining potentials as,

$$\left.\begin{aligned} \phi_w(x_1,y_1,x_2,y_2) &= \mathrm{Cos}[\alpha_s x_1]\mathrm{Cos}[\alpha_s y_1]\,\mathrm{Cos}[\alpha_s x_2]\mathrm{Cos}[\alpha_s y_2] \\ \phi_b(x_1,y_1,x_2,y_2) &= B_s\, e^{-\beta_s(x_1+y_1)}\, e^{-\beta_s(x_2+y_2)} \end{aligned}\right\} \rightarrow \text{Square} \qquad (2.4)$$

$$\left.\begin{aligned} \phi_w(x_1,y_1,x_2,y_2) &= e^{-\frac{1}{2}\alpha_p(x_1^2+y_1^2)}\, e^{-\frac{1}{2}\alpha_p(x_2^2+y_2^2)} \\ \phi_b(x_1,y_1,x_2,y_2) &= B_p\, e^{-\beta_p(x_1+y_1)} e^{-\beta_p(x_2+y_2)} \end{aligned}\right\} \rightarrow \text{Parabolic} \qquad (2.5)$$

where, $\alpha_s = (m_w^* E_s/\hbar^2)^{1/2}$, $\beta_s = (m_b^*(V_0 - E_s)/\hbar^2)^{1/2}$; $\alpha_p = h\omega$, $\beta_p = (m_b^*(V_0 - E_p)/\hbar^2)^{1/2}$.

E_s and E_p are the lowest subband energy for square and parabolic potentials respectively. E_s, E_p and the constants B_s, B_p are obtained by choosing the proper boundary conditions. The trial wavefunction of the ground state of the two holes bound to an acceptor impurity is chosen as

$$\psi(x_1,y_1,x_2,y_2) = N_{hh} \begin{cases} \phi_w(x_1,y_1,x_2,y_2)\, e^{-\lambda\left|\vec{r_1}-\vec{r_2}\right|}, & |x_1|,|y_1|,|x_2|,|y_2| \le L/2 \\ & \rightarrow \text{With Correlation} \\ \phi_b(x_1,y_1,x_2,y_2)\, e^{-\lambda\left|\vec{r_1}-\vec{r_2}\right|}, & |x_1|,|y_1|,|x_2|,|y_2| > L/2 \\ \phi_w(x_1,y_1,x_2,y_2)\, e^{-\lambda(r_1+r_2)}, & |x_1|,|y_1|,|x_2|,|y_2| \le L/2 \\ & \rightarrow \text{Without Correlation} \\ \phi_b(x_1,y_1,x_2,y_2)\, e^{-\lambda(r_1+r_2)}, & |x_1|,|y_1|,|x_2|,|y_2| > L/2 \end{cases} \quad (2.6)$$

where, N_{hh} is the normalization constant and λ is the variational parameter.

The expectation value of **H** is minimized with respect to λ and the hole – hole interaction energy is obtained as follows:

$$H_{min} = \left\langle \psi(x_1,y_1,x_2,y_2) \left| H_{hh} \right| \psi(x_1,y_1,x_2,y_2) \right\rangle ; E_{hh} = \left\langle \psi(x_1,y_1,x_2,y_2) \left| \frac{2}{\left|\vec{r_1}-\vec{r_2}\right|} \right| \psi(x_1,y_1,x_2,y_2) \right\rangle \quad (2.7)$$

The binding energy of the acceptor impurity with two holes in the presence of magnetic field is found by solving the Schrödinger equation variationally and is given by

$$E_B = 2E_{sub} + \gamma - \langle H \rangle_{min} \quad (2.8)$$

2.1.2. Results and Discussion

2.1.2.1. Hole – Hole interaction in a Square Well Confinement

The results for the variation of two - hole binding energy of the acceptor impurity and the Coulomb interaction between them which are confined in a semimagnetic QWW with square band offset in various applied magnetic fields (γ = 0, γ = 0.04, γ = 0.06) by neglecting the correlation between the two holes (Case I) in the chosen wavefuntion as given in Eqn (2.6) are presented in fig.2.1a and 2.1b. The solid lines represent the results for the On Centre (OC; Z_i=0) acceptor impurity and the dotted lines show for On Edge

(OE; Z_i=L/2) acceptor impurity. One observes a fall in binding energy and interaction energy when a magnetic field is applied. The possible explanation for this fall of binding energy and the interaction with the applied magnetic field may be due to the reduction of the potential barrier (142meV, 66meV and 29meV for $\gamma = 0$, $\gamma = 0.04$, $\gamma = 0.06$ respectively which confines the interacting carriers (holes) and thereby the impurity energy levels become shallower which causes the tunnelling of the carriers through the barrier $Cd_{1-x}Mn_xTe$.

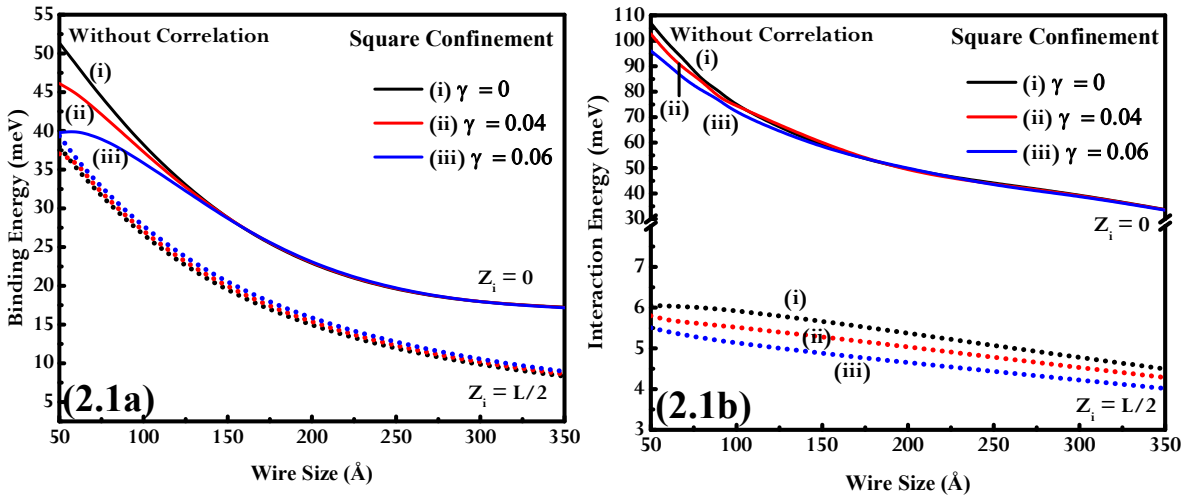

Figure 2.1: Variation of **(a)** binding energy and **(b)** interaction energy of the two holes bound to an acceptor impurity in a SQWW with square well type confining potential for different impurity locations and magnetic field by neglecting the correlation between the carriers.

This reduction in the binding and the interaction energy as a function of applied magnetic field is clearly seen only in the narrower wire size as one can see from the figure that both the energies converges irrespective of the applied magnetic field, when the wire size is increased from narrow to bulk limit. Moreover, the effect of magnetic field on the binding energy and the interaction energy is less pronounced when the impurity is placed at the interface between the non – magnetic and semimagnetic layers i.e. for OE impurity,

which has less binding inside the wire as compared to OC impurity. Though the impact of magnetic field on the strength of the interaction between the two holes is small for OE impurity case, it is not entirely negligible as one can see from the numerical value of interaction energy which scales down as the magnetic field increases. It is surprising to note that the strength of the Coulomb interaction between the two holes is comparatively negligible for OE impurity. This prodigious fall of interaction energy for OE impurity may be well understood from the fact that there is a fluctuation in the correlation of Mn^{2+} ions along the interface which produces the local changes in the total height of the potential barrier formed between the non – magnetic and magnetic layers of SQWW. Owing to this fluctuation, the carriers bound to the wire are driven closer to the interface region. In addition to this, the non-accounting of the correlation between the two holes which is chosen in wavefunction may also contribute to the substantial reduction in the strength of Coulomb interaction between the two holes.

Fig. 2.2a and 2.2b depict the variation of binding energy of the acceptor impurity with two holes and the interaction energy against the wire size in various magnetic field, when the correlation between the two holes is accounted (case II) in the wavefunction. The continuous lines represent the variation for OC impurity and the dotted lines for OE impurity. It is noted from fig. 2.2a that the trend of the binding energy against wire size for various magnetic field is as same as the trend of the binding energy in case I, but with lower in magnitude. The contribution of the correlation between the two holes to the binding energy is about 20 – 30% and to the Coulomb interaction is about 70 – 80%. The reason for this reduced binding and the Coulomb interaction can be explained through the kinetic energy and the potential energy variation of the carriers for both with and without including the correlation which has been compared in fig. 2.3. Despite an increase in the

kinetic energy of the carriers is observed for the case I, a large difference in the potential energy variation between the two cases is also noticed.

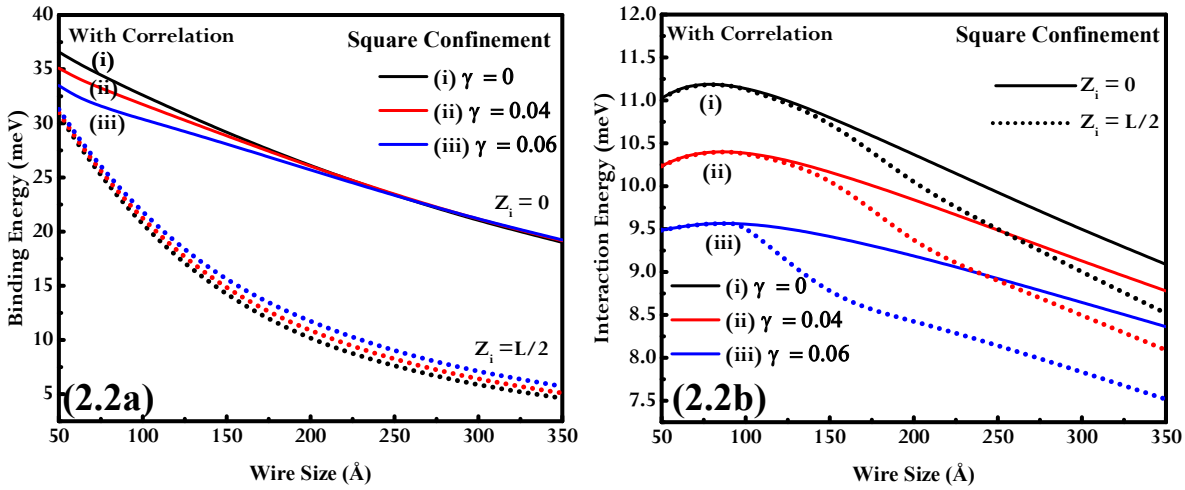

Figure 2.2: Variation of **(a)** binding energy and **(b)** interaction energy of the two holes bound to an acceptor impurity in a SQWW with square well type confining potential for different impurity locations and magnetic field by accounting the correlation between the carriers.

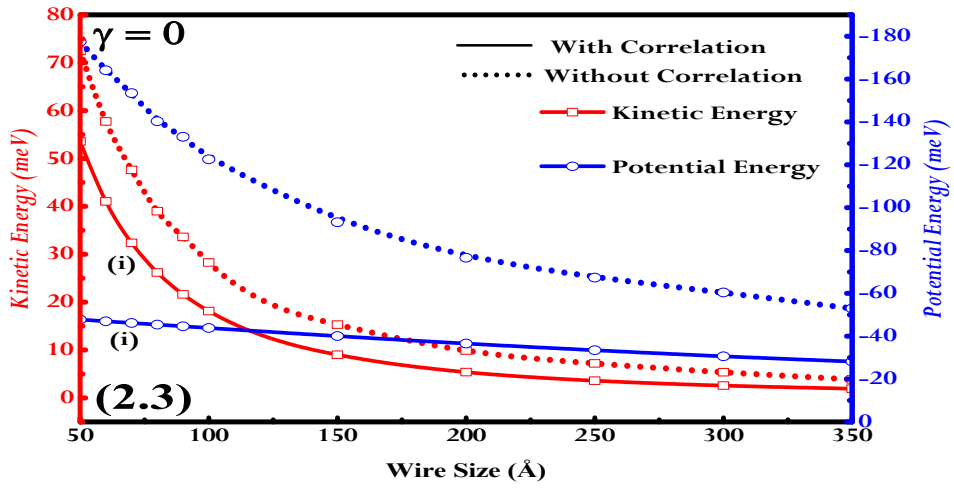

Figure 2.3: Comparison between the Case I and Case II by plotting kinetic energy and the potential energy variation against wire size for $\gamma = 0$.

The calculated potential energy is more negative for the case I compared to the case II which means that the carriers are strongly attached to the parent acceptor atom only when the correlation effect is ignored. Therefore the binding energy of the carriers will become very less when the correlation effect is taken into account between the two holes. It is also noted from fig. 2.2a that the fall of binding energy with respect to magnetic field is not as rapid as the fall of binding energy observed in the case I as one can compare the numerical values of the binding energy in both the cases from fig. 2.1a and 2.2a.

It is interesting to note the increase of Coulomb interaction between the two holes as the wire size is shrunk towards the narrower region and it attains the maximum around the wire size of 80Å and beyond which it starts to fall again which is contrary to the case I where no such turnover is noticed against the wire size. It clearly indicates that the wire of size 50Å makes the carriers to interact more with each other when the correlation is not considered between them. But, for Case II, a wire of size 80Å is needed for carriers to repel each other to a greater extent. Indeed, the applied magnetic field shows its prominent effect by suppressing the amplitude of the peak observed for the interaction energy at around 80Å. The effect of magnetic field on the binding of the carriers inside the QWW for OE impurity is not much appealing as expected. But, by comparing the results of Coulomb interaction for both the impurities from fig. 2.2b, it is noted that the effect of impurity location is not very significant on the Coulomb interaction between the two holes as the strength of the interaction is consistently maintained for smaller wire size, when the impurity moves from the center to the edge of the wire which reflects the importance of correlation dependence of the Coulomb interaction between the two holes.

2.1.2.2. Hole – Hole interaction in a Parabolic Well Confinement

The obtained results for both the binding energy and the interaction energy of the two holes as a function of wire size are plotted in fig. 2.4a and 2.4b for the QWW with

parabolic confinement. It is observed from the results that both the binding energy and the interaction energy are much larger in the parabolic confinement than in the square well confinement and it is again clear from the fig. 2.4a and 2.4b that both the energies decrease as the wire size increases as expected. When the applied magnetic field is increased ($\gamma = 0.06$) near to the critical magnetic field ($\gamma = 0.075$), a turnover is seen in the binding energy against the wire size.

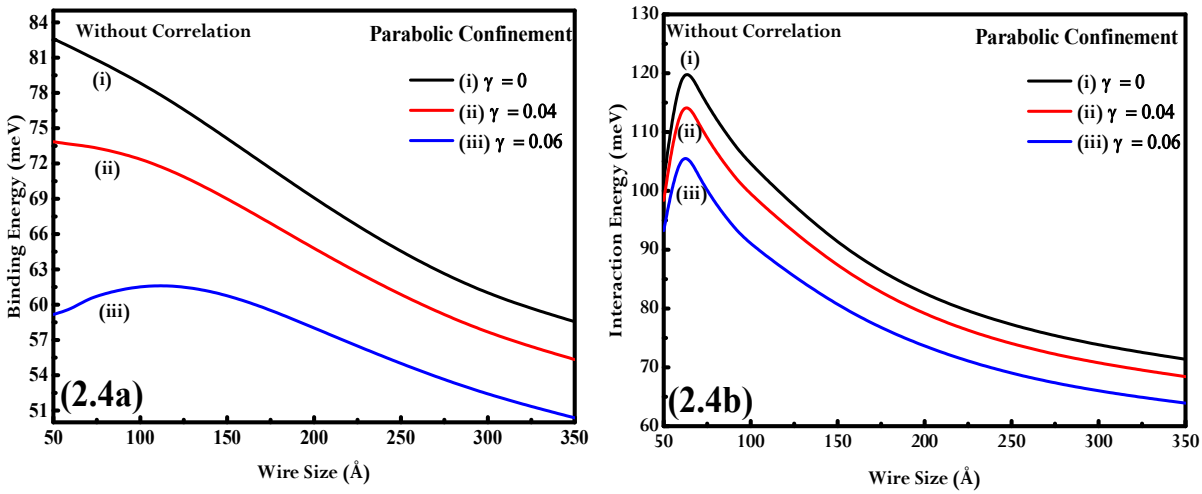

Figure 2.4: Carriers in Parabolic type confining potential. Variation of **(a)** binding energy and **(b)** interaction energy of the two holes bound to an acceptor impurity in a SQWW for various magnetic field by neglecting the correlation between the carriers.

The reason for this turnover may be attributed to the fact that the confining potential realized by the carriers is substantially reduced because of the applied magnetic field as discussed in section 3.1. Therefore, the wire of size 50Å does not favor for the larger confinement of the carriers inside the QWW for $\gamma = 0.06$ as in the case of zero ($\gamma = 0$) and lower magnetic field ($\gamma = 0.04$), since there is a finite probability for the carriers to tunnel through the barrier when they are bound to the wire with reported size. The mutual repulsion between the two holes is raised at the wire of size 60Å and it is noticed that this is the optimized wire size for the carriers to repel each other to greater extent irrespective

of the applied magnetic field. This may be due to the omission of correlation in the wavefunction. But the inclusion of correlation in the two hole wavefucntion shows a peculiar trend of the binding as well as the interaction energy as a function of both wire size and applied magnetic field as shown in fig. 2.5a and 2.5b.

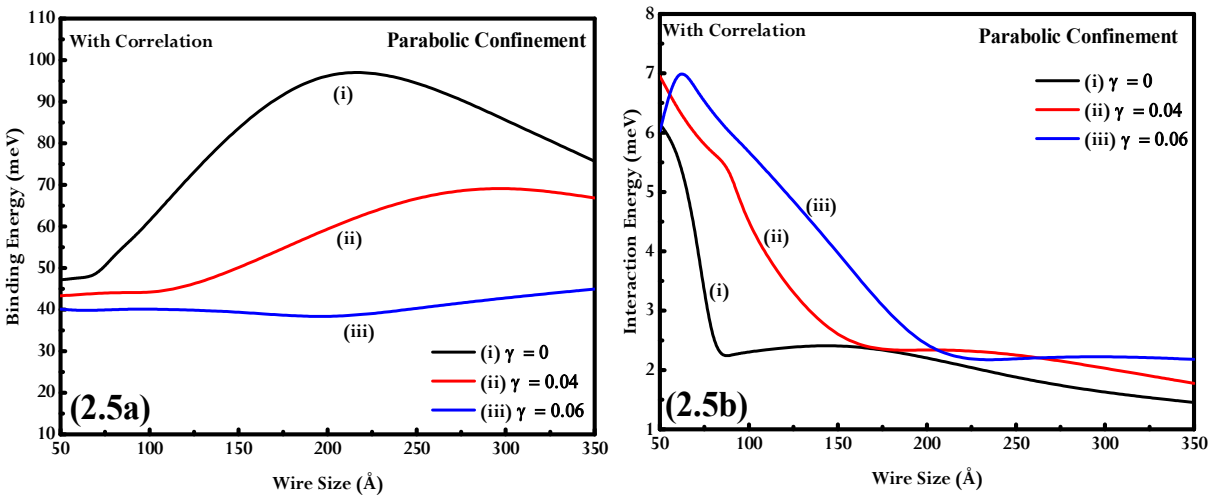

Figure 2.5: Carriers in Parabolic type confining potential. Variation of **(a)** binding energy and **(b)** interaction energy of the two holes bound to an acceptor impurity in a SQWW for various magnetic field by including the correlation between the carriers.

With increasing magnetic field the Coulomb repulsion increases, since the two holes are closer together. This behavior once again elucidates the importance of accounting the correlation in the wavefunction. But, by neglecting this correlation effect one would erroneously assume that with the applied magnetic field the Coulomb interaction between the holes is decreased instead of concluding that it is an increasing function of applied magnetic field. Moreover, one would clearly notice from fig. 2.5b that the interaction energy is a decreasing function of wire size and when the wire size is increased beyond 80Å, E_{hh} is nearly a constant.

However, interestingly the wire size at which the onset of saturation of E_{hh} occurs is shifted to higher values of wire size when the applied magnetic field is increased from

$\gamma = 0$ to $\gamma = 0.06$. The results presented in fig. 2.5a astonishes as the confinement of the carriers in the low dimensional region is very much less under such parabolic confinement when the correlation effect is included as compared to the bulk limit. The plots for the variation of kinetic energy, potential energy and the barrier potential against the wire size for both the cases are presented in fig. 2.6a and 2.6b.

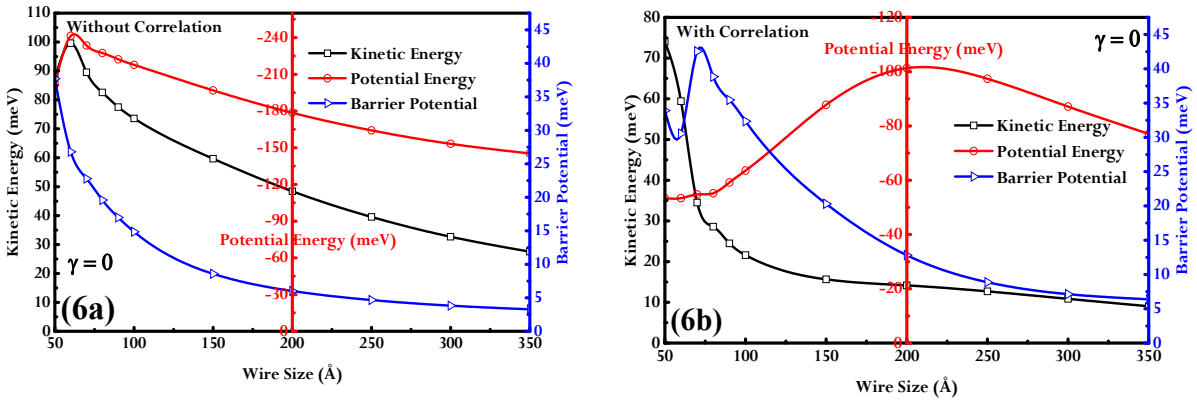

Figure 2.6: Comparison between the Case I and Case II by plotting kinetic energy and the potential energy variation against wire size for $\gamma = 0$ when carriers are confined in a parabolic potential. **(a)** Without including the Correlation and **(b)** With including the correlation.

Even though the interaction energy between the two holes reaches a constant value as seen from fig. 2.5b and the bulk limit may provide more space for the two holes to depart from each other, the Coulomb interaction of both the carriers with their parent acceptor atom is very strong as compared to the low dimensional region as shown in fig. 2.6b. This may be due to the Gaussian nature of the wavefunction in parabolic confinement. The reliability of these results could not be verified as there are no experimental results in such SQWW emphasized with hole – hole interaction. But, the results have been verified to some extent by reducing the two particle Hamiltonian to a single particle Hamiltonian by treating the carriers as non-interacting.

2.1.3. Concluding Remarks

An investigation of two – holes confined in a SQWW has been made under the effect of applied magnetic field and also the impurity location. Irrespective of the nature of the confining potential, the correlation effect contributes to a greater extent on the Coulomb interaction between the two holes confined in a SQWW. While, in the case of parabolic confinement, the percentage of contribution by correlation is about ≈40% to the binding energy and is about ≈90% to the Coulomb interaction energy for smaller wire size, in the case of square confinement, it is about 20 – 30% and 70-80% respectively. It is not possible to check the reliability of our results as the experimental results are not available.

2.2. *Impurity States in CdTe/ $Cd_{1-0.3}Mn_{0.3}Te$ Quantum Well Wire: Effect of Nature of the confining potential along in - plane directions*

This section aims to discuss the donor/acceptor impurity binding energy in CdTe / $Cd_{1-x}Mn_xTe$ QWW with square well confinement along x – direction and parabolic confinement along y – direction under the influence of externally applied magnetic field which has been computed using variational principle in the effective mass approximation. The Spin Polaronic Shift has been computed for the donor impurity. The impact of directional dependent effective mass calculated from the Luttinger parameters on the binding energy of the heavy hole bound to an acceptor impurity has also been investigated and compared with the results obtained for the constant effective mass used in the envelope function. From the observed results it is understood that the influence of the shape of the confining potential along each direction of the confinement in QWW plays a crucial role to determine the strength of the binding of the carriers inside such QWW and it is to be noted that the carriers can move with higher mobility when the directional dependent effective mass is employed in the calculation.

2.2.1. Theoretical Formalism

The Hamiltonian of a hydrogenic donor/acceptor impurity in the presence of magnetic field in CdTe/$Cd_{1-x}Mn_xTe$ Quantum Well Wire in the effective mass approximation is given as

$$\mathbf{H} = -\frac{\hbar^2}{2m^*}\frac{d^2}{dx^2} + V(x) - \frac{\hbar^2}{2m^*}\frac{d^2}{dy^2} + V(y) - \frac{\hbar^2}{2m^*}\frac{d^2}{dz^2} - \frac{e^2}{\varepsilon r} + \frac{eB}{2m^*c}\mathbf{L_z} + \frac{e^2B^2}{8m^*c^2}\mathbf{L^2} \qquad (2.9)$$

Defining effective Bohr radius $a_B^* = \hbar^2\varepsilon_0/m^*e^2$ as unit of length, effective Rydberg $R^* = e^2/2\varepsilon_0 a_B^*$ as unit of energy and the strength of the magnetic field parameter

$\gamma = \hbar\omega_c/2R^*$ (ω_c – cyclotron frequency and $\gamma = 1$ corresponds to 30.5604Tesla for donor impurity, 1131Tesla and 865Tesla for the acceptor impurity with constant and the directional effective mass approaches respectively**)**. m* is the effective mass of electron/heavy hole in CdTe/$Cd_{1-x}Mn_xTe$ and; ε is the static dielectric constant of CdTe. V(x) and V(y) are the finite confining potentials in the x- and y-direction, respectively. V(x) is a square well potential of height V_0 and V(y) is a parabolic well potential of $\frac{1}{2}m\omega^2y^2$, which are given by,

$$V(x)=\begin{cases}0 & ,|x|\le L/2\\ V_0 & ,|x|>L/2\end{cases}$$

$$V(y)=\begin{cases}\frac{1}{2}m\omega^2y^2 & ,|y|\le L/2\\ V_0 & ,|y|>L/2\end{cases} \qquad (2.10)$$

L is the width of the rectangular cross section of the wire and $V_0 = 70\%\Delta E_g^B$ for the conduction band and $V_0 = 30\%\Delta E_g^B$ for valence band; ΔE_g^B is the band gap difference with magnetic field and is given by Eqn (2.3) in which, the critical magnetic field B_0 in Tesla for different composition is given for the donor impurity as $B_0 = A\ e^{nx}$ with A = 0.734 and n = 19.082 [29] which gives the best fit to the extrapolated experimentally available critical fields.

The trial wavefunction for ground state donor/acceptor impurity in such QWW with different confinements along two directions is given by

$$\Psi = N_{1S}\ \psi(x)\ \psi(y)\ Exp[-\lambda r] \qquad (2.11)$$

where,

$$\psi(x)=\begin{cases}\mathrm{Cos}[\alpha_s x] & ,|x|\le L/2\\ B_s\ \mathrm{Exp}[-\beta_s x] & ,|x|>L/2\end{cases};\quad \psi(y)=\begin{cases}\mathrm{Exp}[-\frac{1}{2}\alpha_p y^2 & ,|x|\le L/2\\ B_p\ \mathrm{Exp}[-\beta_p y] & ,|y|>L/2\end{cases} \tag{2.12}$$

N_{1s} is the normalization constant. $\alpha_S=(2m_W^* E_S/\hbar^2)^{1/2}$, $\beta_S=(2m_b^*(V_0-E_S)/\hbar^2)^{1/2}$,

$\alpha_p=\frac{1}{2}h\omega$, $\beta_p=(2m_b^*(V_0-E_p)/\hbar^2)^{1/2}\lambda$ is the variational parameter, 'B_s' and 'B_p' are obtained from the continuity condition.

The binding energy of the donor / acceptor impurity in the presence of magnetic field is found by solving the Schrodinger equation variationally and is given by

$$E_B^{QWW}=E_x+E_y+\gamma-\langle H_{min}\rangle \tag{2.13}$$

2.2.1.1. Spin Polaronic effect

The modified Brillouin function [30] to invoke the exchange interaction between the carrier and magnetic impurity in the presence of an external magnetic field **B**, yielding the magnetic polaronic shift which is given by

$$E_{sp}=\tfrac{1}{2}\beta S N_0\left\{\langle\Psi_1|\,x_1 B_S(y_1)|\Psi_1\rangle+\langle\Psi_2|\,x_2 B_S(y_2)|\Psi_2\rangle\right\} \tag{2.14}$$

$$B_S(y_j)=\frac{2S+1}{2S}\coth\frac{2S+1}{2S}y_j-\frac{1}{2S}\coth\frac{y_j}{2S};\ y_j=\frac{S\beta|\Psi_j|^2}{2kT}+\frac{g\mu_B S\beta}{kT} \tag{2.15}$$

where, β - exchange coupling parameter, S is the spin of Mn^{2+} (=5/2), and xN_0 is the Mn ion concentration with $N_0 = 2.94 \times 10^{22}$ cm^{-3} and $\beta N_0 = 220$meV for CdMnTe. Also $g_{Mn} \approx 2$ and B is the strength of the external magnetic field, k is the Boltzmann constant and $B_s(y)$ is the modified Brillouin function.

2.2.2. Results and Discussion

2.2.2.1. Donor Bound States in QWW

Observations have been made on the binding energy and the Spin Polaronic Shift of the hydrogenic donor impurity confined in a QWW with square confinement along x-direction and parabolic confinement along y-direction for the various magnetic field ($\gamma = 0, \gamma = 3,$ and $\gamma = 6$) applied along the free direction 'z'. It can be seen from fig. 2.7 that the donor binding energy decreases with increase in magnetic field. This is due to the fact that the application of magnetic field reduces the confining potential barrier height according to Eqn (2.3) thus making the donor less confined in the wire.

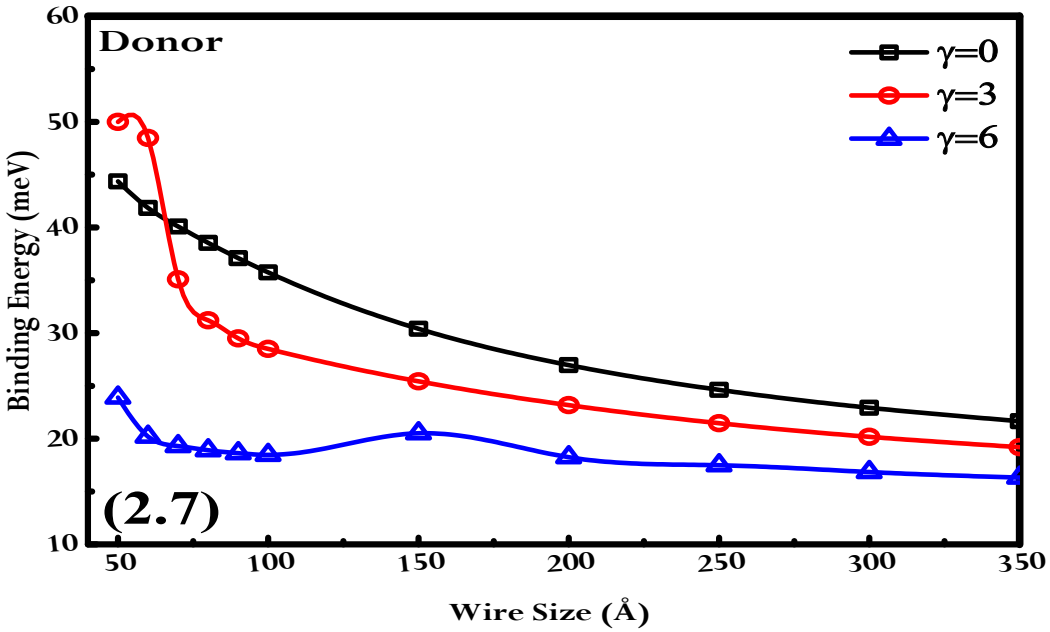

Figure 2.7: Donor Binding Energy *vs* Wire Size for x=0.3 for various magnetic field.

This can be justified from the probability distribution function plotted in fig. 2.8 for γ=0 and γ=6. It can be seen from the figure that the Probability density of the electron confined inside the wire is higher in magnitude in the absence of magnetic field than in the presence of magnetic field.

γ=0 and L=100Å **γ=6 and L=100Å**

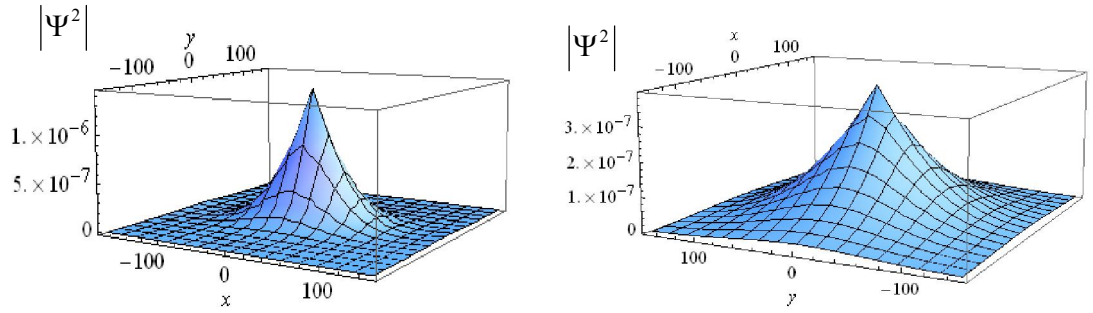

Figure 2.8: Probability distribution $|\Psi^2|$ of the electron in a QWW under γ=0 and γ=6 for wire size L=100Å.

It is also observed that the binding energy decreases as the wire size increases which is an expected one in any low dimensional system. The reliability of our results can be verified as:

$$E_B^{QWW} \text{approches to} \begin{cases} E_B^{\text{Square Well}} & , \quad \text{for } V(x,0) \\ E_B^{\text{Parabolic Well}} & , \quad \text{for } V(0,y) \end{cases}$$

where, $E_B^{\text{Square / Parabolic Well}}$ is the donor binding energy of a Quantum Well with Square / Parabolic potential confinement [8, 31].

The variation of magnetic polaronic shift of the donor impurity for γ = 0, γ = 3 and γ = 6 is given for x=0.3 in fig. 2.9. It is noticed that there is a drastic increase in the Spin Polaronic Shift with increase in magnetic field as there is an increase in the exchange interaction between the magnetic ions and donor impurity.

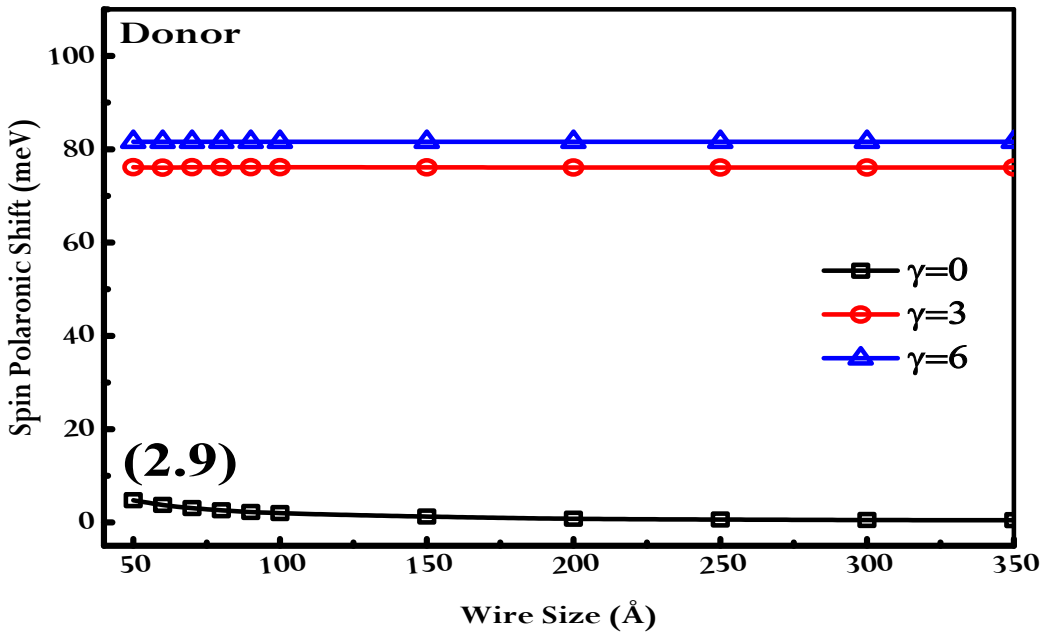

Figure 2.9: Spin Polaronic Shift due to the donor BMP *vs* Wire Size for x = 0.3 for various magnetic field.

2.2.2.2. Acceptor Bound States in QWW

This section discussed the investigation that has been made on the binding energy of the hydrogenic acceptor impurity confined in a QWW with square confinement along x direction and the parabolic confinement along y direction for various applied magnetic field ($\gamma = 0, \gamma = 0.03,$ and $\gamma = 0.06$) along the free direction 'z' for the Mn^{2+} ion composition of x = 0.3. Two different effective masses are employed. (i) The values of the effective masses of the heavy hole used in Eqn (2.9) are taken as a constant along all the directions within each material comprising the QWW which are appropriated to the bulk materials as defined through the bulk band structure (Called as approach I). (ii) Directional dependent effective masses (approach II) are used for the calculation derived from the Luttinger parameters using multiband **k**.**p** model for the heavy hole which are related to these band edge effective masses through the relations,

$m^*_{HH,(z)} = (\gamma_1 - 2\gamma_2)^{-1}$, along 'z' direction

$m^*_{HH,(x,y)} = (\gamma_1 + \gamma_2)^{-1}$, in plane effective mass

The numerical values of effective masses calculated through these two approaches for CdTe and $Cd_{1-0.3}Mn_{0.3}Te$ materials are listed as follows:

$$\left.\begin{aligned} m_w^* &= 0.60 \\ m_b^* &= 0.67 \end{aligned}\right\}$$ Constant effective mass approach; w, b represents the well and barrier region respectively.

$$\left.\begin{aligned} m_{w,z}^* &= 0.51 \\ m_{b,z}^* &= 0.586 \end{aligned}\right\}$$ along z direction ; $$\left.\begin{aligned} m_{w,xy}^* &= 0.1912 \\ m_{b,xy}^* &= 0.2677 \end{aligned}\right\}$$ in plane effective mass

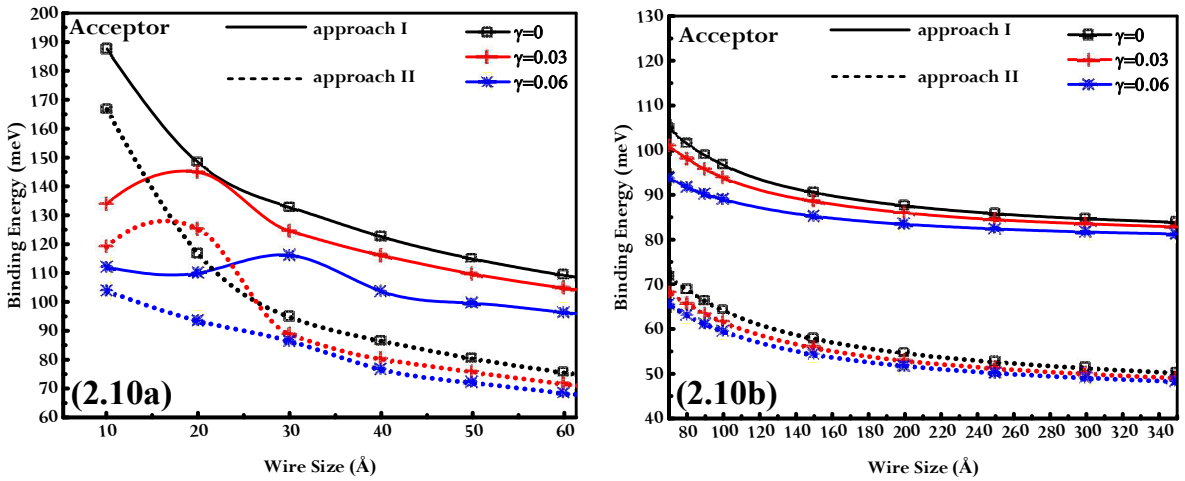

Figure 2.10: Variation of acceptor binding energy as a function of wire size for various magnetic field in approach I and II. Variation shows **(a)** for quite a large range of the narrow wires i.e. less than 60Å and **(b)** for the wire size limited towards the bulk limit.

The variation of binding energy as a function of the size of the CdTe QWW which is surrounded by $Cd_{1-0.3}Mn_{0.3}Te$ barrier material for (i) constant effective mass approach and (ii) directional dependent effective mass approach is presented in fig. 2.10. In order to show the significant effect of the two approaches on the carrier confinement observed for the wire size less than 30Å as shown in fig. 2.10a, 2.10b for the narrow size of the QWW less than 70Å and the wire size approaching towards the bulk limit. The concept of substantial reduction in the binding energy of the carriers and the occurrence of turnover and the notable shift in it as a function of wire size with the applied magnetic field do

agree well with the feature of any DMS Low dimensional system [20, 25, 26]. It is clear from the figure that the numerical values of the binding energy calculated in approach I is much larger than the results obtained in approach II. This is because of treating the effective masses as isotropic in the former which are three times larger than that of the masses taken along the confined directions $m^*_{w,xy}$ in the latter case. Since, the effective masses are very small along the confined directions in approach II, the carriers can move inside the QWW with higher mobility which leads to the lower binding of the carriers to the parent acceptor atom.

It is apparent from the fig. 2.11b that the discrepancy between the two approaches is larger for the wire size of 30Å and beyond which this difference becomes less and it reaches a saturation when the wire size approached to the bulk limit when the system is subjected to lower magnetic field strength ($\gamma = 0.04$) and for zero γ . This is attributed to a constant effective masses which are derived from the bulk band structure that has been used along all the directions even for narrow size of the wires.

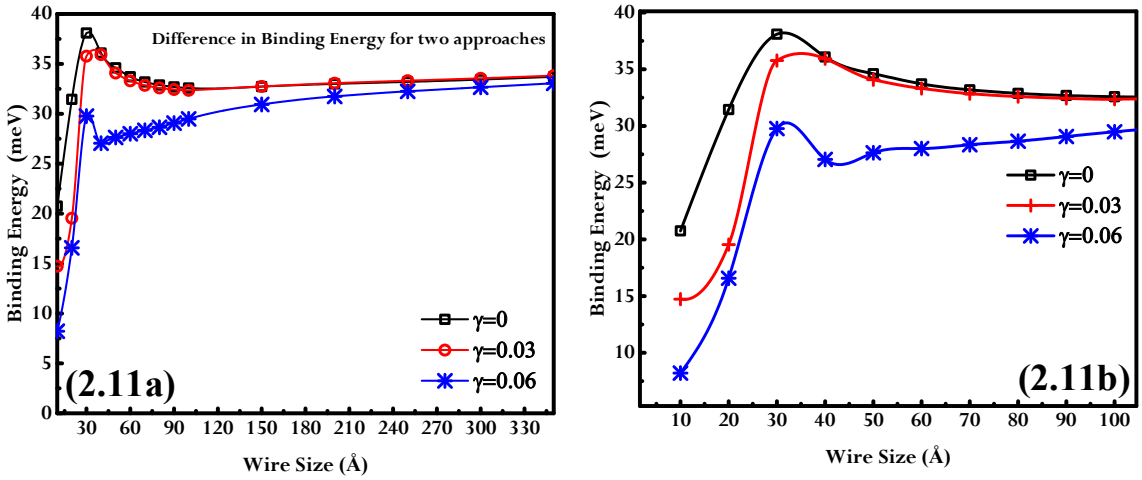

Figure 2.11: Difference in the acceptor binding energy between approach I and II as a function of wire size for various magnetic field. **(a)** Discrepancy shown for the whole range of the wire size and **(b)** shows for quite a large range of the narrow wires (< 100Å).

But for the applied magnetic field of higher strength, γ = 0.06, it is observed that the difference in the two approaches is larger only when the dimension of the QWW reaches the bulk limit than for the narrow dimension of the wire. Moreover, it is noted from the fig. 2.11a that the discrepancy between the two approaches decreases with the increase of applied magnetic field.

All the above results can be justified from the probability distribution function plotted in fig. 2.12 for γ=0 and γ=0.06. It can be seen from the figure that the Probability density of the confined heavy hole inside the wire is higher in magnitude in the absence of magnetic field and for the constant effective mass approach than in the presence of magnetic field and for the anisotropic effective mass approach.

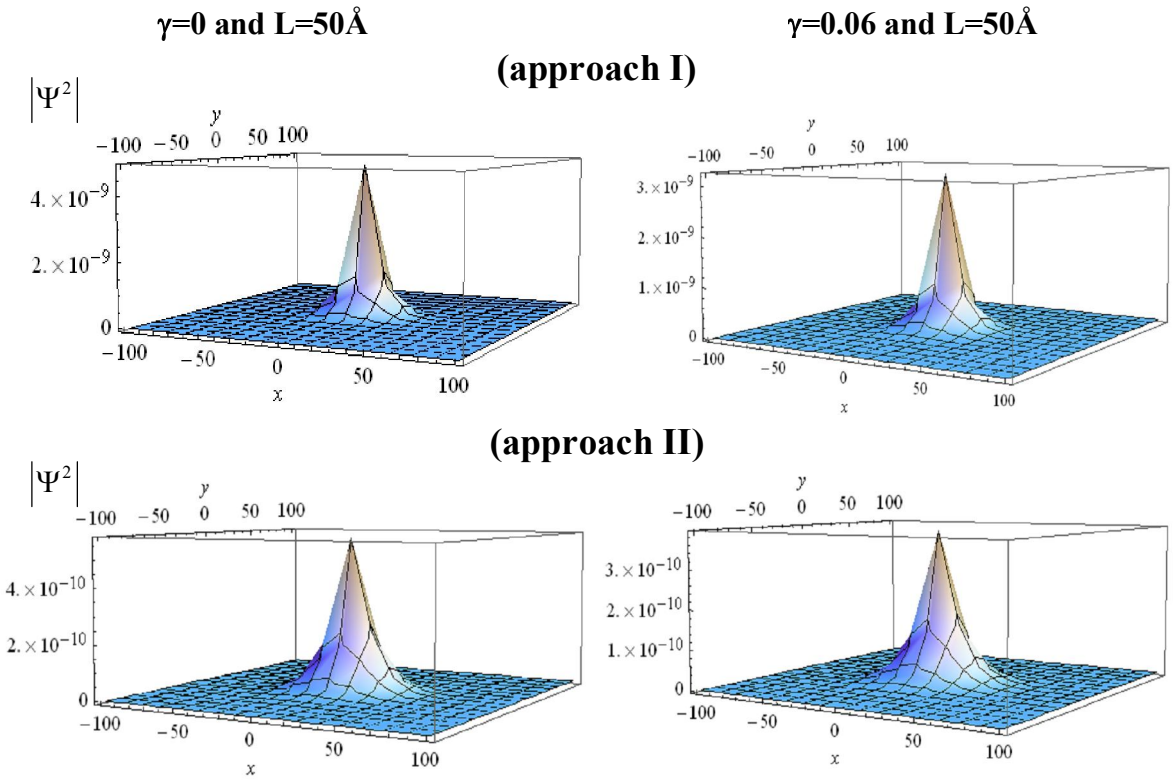

Figure 2.12: Probability distribution $|\Psi^2|$ for heavy hole bound to an acceptor impurity inside the QWW of size L=50Å under γ=0 and γ=0.06 for approach I and II.

2.2.3. Conclusion

The study of the magnetic effect on the donor / acceptor impurity confined in such a QWW with various confinements along two directions is important since it is possible to investigate the various properties like magnetic excitations and other magneto optical transitions and also to simulate and fabricate QWW of different cross sectional geometry and confining potential according to the requirement for various device applications.

References

1. H. Sakaki, *Jpn. J. Apply.Phys*. **1980**, *19*, 94.
2. P. Kalpana and K. Jayakumar, *Physica E*. (**Accepted**)

   DOI: 10.1016/j.physe.2017.06.025.
3. J.P. Lascaray, D. Coquillat, J. Deportes, A.K. Bhattacharjee, *Phys. Rev. B.* **1988**, *38*, 7602 – 7606.
4. Y. Harada, T. Kita, O.Wada and H. Ando, *Phys. Rev. B*. **2006**, *74*, 245323.
5. N. Takahashi, K. Takabayashi, E. Shirado, I. Soumal, J.X.Shen and Y. Oka, J. Crystal Growth. **2000**, *214/215*, 183 - 186.
6. K. Chang and F. M. Peters, *Phys. Rev. B*. **2003**, *68*, 205320.
7. D. D. Awschalom and N. Samarth, J. Magnetism and Magnetic Materials, **1999**, *200*, 130 - 147.
8. C. Raja Mohan and K. Jayakumar, *J. Nano. Electron.Phys*. **2011**, *3*, 1005 - 1009.
9. P. Kalpana, A. Merwyn Jasper D. Reuben, P. Nithiananthi and K. Jayakumar, *AIP Conf.Proc*.**2016**, *1731*,090027.
10. R. Khordad, A. Gharaati and M. Haghparast, Current Appl.Phys. **2010**, *10*, 199 - 202
11. S. Gangopadhyay and B. R. Nag, *J. Appl. Phys*.**1997**, *81*, 7885 - 7889.
12. O. M. Auslaender, H. Steinberg, A. Yacoby, Y. Tserkovnyak, B. Halperin, K. W. Baldwin, L. N. Pfeiffer and K. W. West, *Science* **2005**, *308*, 88 - 92.
13. H. Steinberg, G. Barak, A. Yacoby, L. N. Pfeiffer, K. W. West, B. I. Halperin and Karyn Le Hur, *Nature Phys*. **2008**, *4*, 116 – 119.
14. V. V. Deshpande and M. Bockrath, *Nature Phys*. **2008**, *4*, 314 - 318.
15. A. Sivakami and K. Navaneethakrishnan, *Physica E*. **2008**, *40*, 649 - 653.

16. S. Bednarek, B. Szafran, T. Chwiej and J. Adamowski, *Phys. Rev. B*.**2003**, *68*, 045328.
17. J. Adamowski, M.Sobkowicz, B. Szafran and S. Bednarek, *Phys. Rev. B.* **2000**, *62*, 4234 - 4237.
18. F. B. Pedersen, Yia – Chung Chang, Phys. Rev. B. **1997**, *55*, 4580 - 4588.
19. F. B. Pedersen, Yia – Chung Chang, Phys. Rev. B. **1996**, *53*, 1507 - 1516.
20. P. Kalpana and K.Jayakumar, *Superlatties. Microstruct*. **2017**, *111*, 115 – 122.
21. Sr. Gerardin Jayam and K. Navaneethakrishnan, *Int. J. Mod. Physics B*. **2002**, *16*, 3737 – 3757.
22. F. V. Kyrychenko and J. Kossut, *Phys. Rev. B*. **2000**, *61*, 4450 - 4452.
23. L. R. Ram – Mohan, Peter A. Wolff, *Phys. Rev. B*. **1988**, *38*, 1330 - 1339.
24. T. H. Nhung, R. Planel, C. Guillaume and A. K. Bhattacharjee, *Phys. Rev. B*. **1985**, *31*, 2388 - 2395.
25. P. Kalpana, A. Merwyn Jasper D. Reuben, P. Nithiananthi and K. Jayakumar, *AIP Conf.Proc*. **2014**, *1591*, 1176.
26. P. Kalpana, A. Merwyn Jasper D. Reuben, P. Nithiananthi and K. Jayakumar, *AIP Conf.Proc*.**2015**, *1665*, 090005.
27. A. Merwyn Jasper D Reuben and K. Jayakumar, *Superlattice. Microstruct*. **2012**, *52*, 732 – 737.
28. T. Jungwirth, Byounghak Lee, A. H. MacDonald, *Physica E*. **2001**, *10*, 153 – 156.
29. P. Nithiananthi and K. Jayakumar, *Int. J, Nanosci.* **2011***, 10*, 611-615.
30. P. Nithiananthi and K. Jayakumar, *J. Nano. Electron. Phys.* **2011***, 3*, 375-379.
31. P. Nithiananthi et.al. *Proc.ICONN-2010*, **2010**, 291-292.

Chapter 3

COULOMB INTERACTION OF DOUBLE ACCEPTORS IN SEMIMAGNETIC QUANTUM DOT

3.1. Introduction

Magnetic and Semi-magnetic nanostructure systems like $Cd_{1-x}Mn_xTe$ / CdTe Quantum Dot (QD) is drawing considerable attention due to Spintronic applications, possibility of realizing the optoelectronic devices and exhibiting the switch over of the system from type – I to type – II [1]. It is well known that Coulomb interaction between acceptor states leads to increase the significance of many body effects. The Mn concentration in nonmagnetic Semiconductor gives rise to ferromagnetism and metallic transport. Coulomb interaction within the QD gives rise to the phenomenon of Coulomb blockade of transport and its influence strongly depends on the size of the QD [2]. Moreover, the infrared spectra of acceptor-acceptor interaction in Si and Ge show a small splitting which cannot be explained unless one considers the acceptors interaction [3]. Recently, theoretical investigation has been carried out on the Coulomb interaction of the two holes in a Semimagnetic Quantum Dot (SMQD) [4, 5, 6, 7] and also on the energy levels of two holes in a non-magnetic QD with parabolic confining potential [8, 9]. But still there are uncertainties in the nature and type of potential that exists in QD. Brey et al. [10] and Yip [11] have demonstrated the evidences for the assumption of parabolic potential confinement in QD which is the motivation for the present work. In this work, we

investigate the effect of confining potential like harmonic oscillator type on the Coulomb interaction between the acceptors and their binding energy in the presence of magnetic field in $Cd_{1-x}Mn_xTe/CdTe$ Spherical/Cubical Quantum Dot (SQD/CQD) and the results have been compared with the results obtained for the case of abrupt band offset. The spatially varying dielectric screening also has been used to see the effect of screening on the Coulomb interaction of the two holes in such QD for Mn composition of x=0.3 using variational principle in the effective mass approximation. In order to show the significance of the correlation between the two holes, the calculations have been done with and wihout including the correlation effect in the ground state wavefunction of the acceptor impurity and the results have been compared.

3.2. Theoretical Formalism

Defining effective Bohr radius $a_B^* = \hbar^2\varepsilon_0/m^*e^2$ as unit of length, effective Rydberg $R^* = e^2/2\varepsilon_0 a_B^*$ as unit of energy and the strength of the magnetic field parameter $\gamma = \hbar\omega_c/2R^*$ (ω_c – cyclotron frequency), the Hamiltonian for the double acceptor impurity confined in a $CdTe/Cd_{1-x}Mn_xTe$ SQD /CQD is written as

$$\mathbf{H_{hh}} = -\nabla_1^2 - \nabla_2^2 - \frac{2}{r_1} - \frac{2}{r_2} + V_B(r_1) + V_B(r_2) + \gamma L_{z_1} + \gamma L_{z_2} + \frac{\gamma^2(r_1^2 \sin^2\theta_1)}{4} + \frac{\gamma^2(r_2^2 \sin^2\theta_2)}{4} + \frac{2}{|\vec{r_1} - \vec{r_2}|} \quad (3.1)$$

The parabolic and square confining potential for $Cd_{1-x}Mn_xTe$ SQD is given by,

$$V_B = \begin{cases} \frac{1}{2} m^*_w \omega^2 (r_1^2 + r_2^2) & |r_1|, |r_2| \le R \\ V_0 & |r_1|, |r_2| > R \end{cases} \rightarrow \text{Parabolic}$$

$$V_B = \begin{cases} 0 & |r_1|, |r_2| \le R \\ V_0 & |r_1|, |r_2| > R \end{cases} \rightarrow \text{Square} \quad (3.2)$$

where R is the radius of the Quantum Dot and V_0=30%ΔE_g^B, where, ΔE_g^B is the band gap difference with magnetic field and is given by Eqn (2.3).

The trial wavefunction for the ground state of double acceptor impurity in SQD / CQD with square and parabolic confinement is given by,

$$\left.\begin{aligned} f_w(r_1,r_2) &= e^{-\frac{1}{2}\alpha_p r_1^2} e^{-\frac{1}{2}\alpha_p r_2^2} \\ f_b(r_1,r_2) &= B_p \frac{e^{-\beta_p r_1}}{r_1} \frac{e^{-\beta_p r_2}}{r_2} \end{aligned}\right\} \rightarrow \text{SQD, Parabolic}; \quad \left.\begin{aligned} f_w(r_1,r_2) &= \frac{\sin \alpha_s r_1}{r_1} \frac{\sin \alpha s r_2}{r_2} \\ f_b(r_1,r_2) &= B_s \frac{e^{-\beta_s r_1}}{r_1} \frac{e^{-\beta_s r_2}}{r_2} \end{aligned}\right\} \rightarrow \text{SQD, Square} \quad (3.3)$$

$$\left.\begin{aligned} f_w(x_1,y_1,z_1,x_2,y_2,z_2) &= e^{-\frac{1}{2}\alpha_p (x_1^2+y_1^2+z_1^2)} e^{-\frac{1}{2}\alpha_p (x_2^2+y_2^2+z_2^2)} \\ f_b(x_1,y_1,z_1,x_2,y_2,z_2) &= B_p\, e^{-\beta_p (x_1+y_1+z_1)} e^{-\beta_p (x_2+y_2+z_2)} \end{aligned}\right\} \rightarrow \text{CQD, Parabolic}$$

$$\left.\begin{aligned} f_w(x_1,y_1,z_1,x_2,y_2,z_2) &= \text{Cos}\alpha_s x_1\ \text{Cos}\alpha_s y_1\ \text{Cos}\alpha_s z_1\ \text{Cos}\alpha_s x_2\ \text{Cos}\alpha_s y_2\ \text{Cos}\alpha_s z_2 \\ f_b(x_1,y_1,z_1,x_2,y_2,z_2) &= B_s\, e^{-\beta_s (x_1+y_1+z_1)} e^{-\beta_s (x_2+y_2+z_2)} \end{aligned}\right\} \rightarrow \text{CQD, Square} \quad (3.4)$$

where,

$$\alpha_s = (2m_w^* E_s/3\hbar^2)^{1/2}, \beta_s = (2m_b^*(V_0 - E_s)/3\hbar^2)^{1/2};\ \alpha_p = \frac{3}{2}\hbar\omega\ \beta_p = (2m_b^*(V_0 - E_p)/3\hbar^2)^{1/2}.$$

E_s and E_p are the lowest subband energy for square and parabolic potentials respectively. E_s, E_p and the constants B_s, B_p are obtained by choosing the proper boundary conditions. The trial wavefunction of the ground state of the two holes bound to an acceptor impurity is chosen as

$$\Psi(r_1,r_2) = N_{hh} \left\{ \begin{aligned} & f_w\ e^{-\lambda\left|\vec{r_1}-\vec{r_2}\right|} \\ & f_b\ e^{-\lambda\left|\vec{r_1}-\vec{r_2}\right|} \end{aligned} \right\} \rightarrow \textbf{With Correlation}; \quad \left\{ \begin{aligned} & f_w\ e^{-\lambda (r_1+r_2)} \\ & f_b\ e^{-\lambda (r_1+r_2)} \end{aligned} \right\} \rightarrow \textbf{Without Correlation} \quad (3.5)$$

where, N_{hh} is the normalization constant and λ is the variational parameter.

The expectation value of $\mathbf{H_{hh}}$ is minimized with respect to λ and the hole - hole interaction energy (E_{hh}) is obtained by

$$H_{min} = \langle \psi(r_1,r_2) \; |H_{hh}| \; \psi(r_1,r_2) \rangle \rightarrow \text{SQD} \; ; \; H_{min} = \langle \psi(x_1,y_1,z_1,x_2,y_2,z_2) \; |H_{hh}| \; \psi(x_1,y_1,z_1,x_2,y_2,z_2) \rangle \rightarrow \text{CQD}$$

$$E_{hh} = \left\langle \psi(r_1, r_2) \left| \frac{2}{|\vec{r_1} - \vec{r_2}|} \right| \psi(r_1, r_2) \right\rangle \rightarrow \text{SQD} \; ; \; E_{hh} = \left\langle \psi(x_1,y_1,z_1,x_2,y_2,z_2) \left| \frac{2}{|\vec{r_1} - \vec{r_2}|} \right| \psi(x_1,y_1,z_1,x_2,y_2,z_2) \right\rangle \rightarrow \text{CQD} \tag{3.6}$$

Among the several dielectric screening function worked out for semiconductors, the form given by Hermansen [12, 13, 14] has been considered for the calculation as follows:

$$\varepsilon^{-1}(r) = \varepsilon_0^{-1}{}_{(x)} + (1-\varepsilon_0^{-1}) \exp(-r/c) \tag{3.7}$$

where, ε_0 is the dielectric constant as a function of Mn composition and 'c' is a screening parameter chosen to provide a good fit of the Fourier transform of Eqn (3.7).

The binding energy of the two holes in the presence of magnetic field is found by solving the Schrödinger equation variationally and finally obtained using the Eqn (2.8.).

3.3. Results and Discussion

Fig. 3.1 presents the binding energy and the Coulomb Interaction energy of double acceptors as a function of dot size for three different barrier height (142meV, 66meV, 29meV) corresponding to the magnetic field strength of (γ = 0, 0.04, 0.06) respectively for both SQD and CQD by including the correlation (Case II) between the two holes in the wavefunction as given in Eqn (3.5). It can be seen from the figure that irrespective of the geometry of the QD there is a rapid reduction in the Coulomb interaction energy as well as the binding energy when the magnetic field (γ) is increased, since the applied magnetic field greatly alters the barrier height of the QD according to eqn.(2. 3). In both the cases (SQD & CQD), the binding and the interaction of the two holes increases to a maximum around 20Å without applying magnetic field (γ = 0) as shown in the figure.

This is due to the effective confinement frequency scales with the inverse square of the dot size ($\Omega \alpha 1/L^2$) and the typical interaction energy drops inversely with increasing dot size ($V_{Coulomb} \alpha 1/L$), which may be due to the fact that decreasing the dot size, the wavefunction is more squeezed in CdTe dot, leading to the stronger binding. However beyond a certain value of dot size, the wavefunction is spread into the barrier $Cd_{1-x}Mn_xTe$, leading to the reduced confinement of the holes in the well region. When the strength of the magnetic field is increased towards the critical value (vanishing of V_0), the energy maximum shifts towards the dot size of ≤ 60Å.

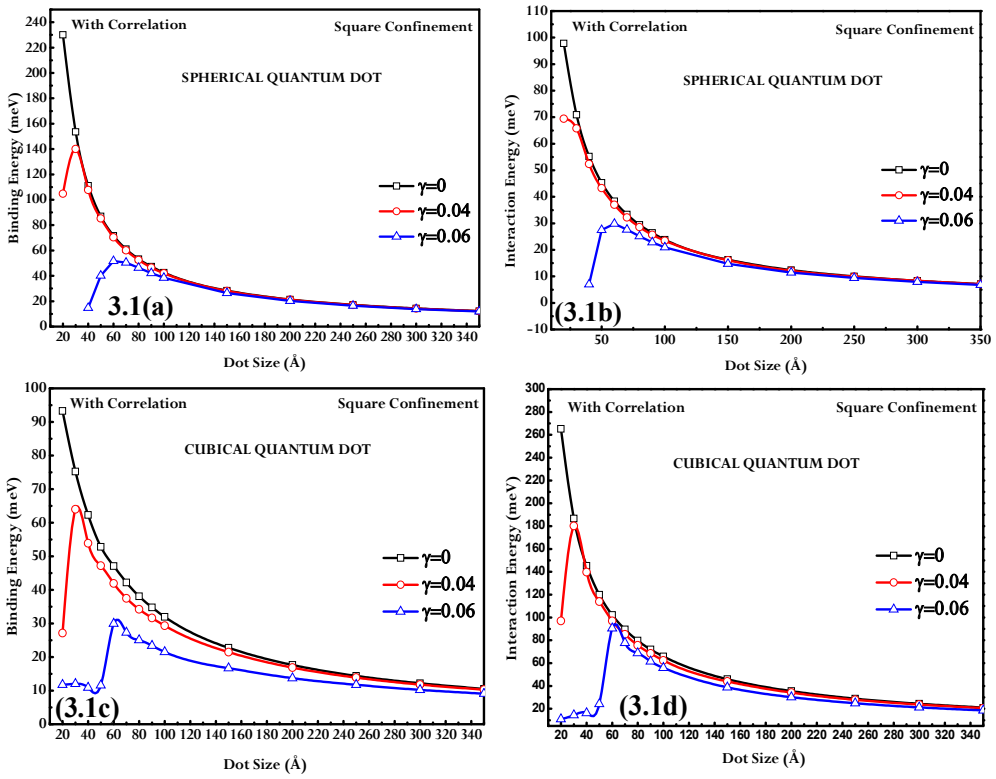

Figure 3.1: Variation of binding energy and the interaction energy as a function of dot size for SQD and CQD with square confining potential when the correlation between the holes are considered in various applied magnetic field.

This behavior of the energy as a function of dot size (for a given magnetic field) can be attributed by the following facts. (i) For extremely narrow dot size (~20Å) the repulsive

force between the two holes gain in strength and causes tunneling. (ii) When the dot size is larger (20Å< (R,L)< 60Å), an attractive force due to the confining potential and the magnetic field induced localization win over tunneling and tend to confine the holes together inside CdTe dot. From the above arguments, one expects the onset of quasi 0-dimensional effects to occur when the effective Bohr radius of the hole-hole pair is comparable to the size of the QD. The ionization energy of the double holes is larger in SQD than in CQD as shown in fig. 3.1a and fig. 3.1c which is justified by the distribution function of holes inside the dot as shown in fig.3.2.

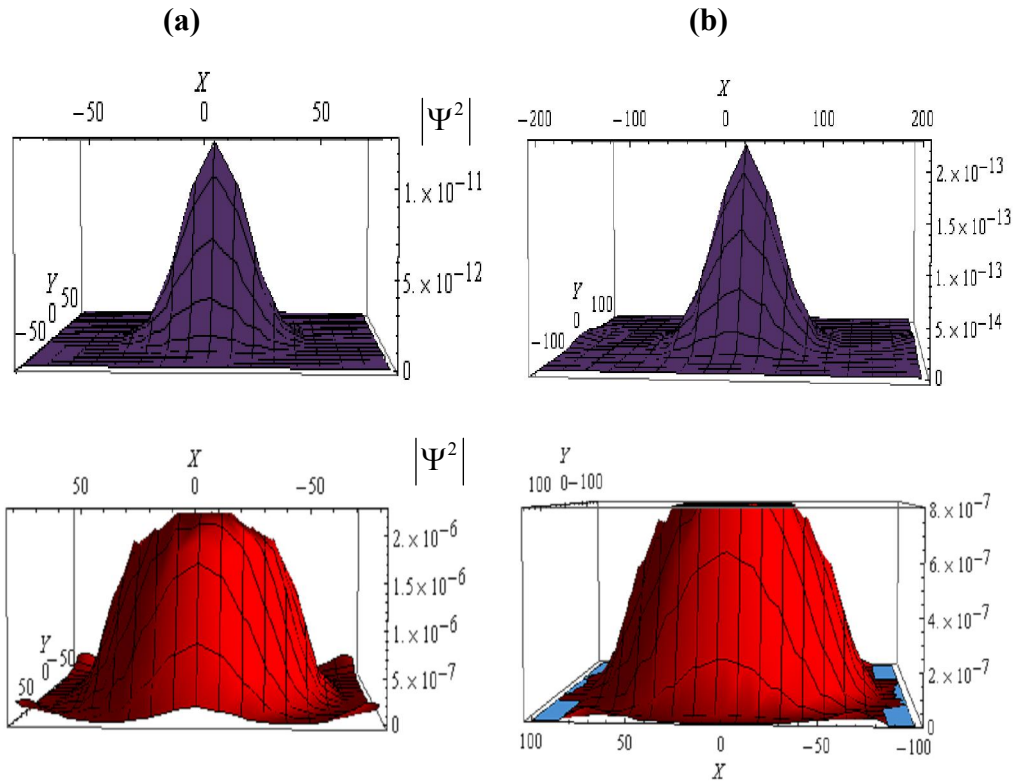

Figure 3.2: Probability distribution $|\Psi^2|$ of the holes inside the QD of size 50Å for **(a)** $\gamma = 0$, **(b)** $\gamma = 0.06$ for cubical (Blue) and Spherical (Red) Quantum Dot.

Hence, the Coulomb interaction between the holes is strongly enhanced only in dot with cubical geometry rather than in spherical geometry. This is due to the fact that the confinement in spherical geometry decreases the kinetic energy of the double holes thus

leading to the enhanced binding energy. Fig. 3.3 shows the results obtained using the spatially varying dielectric screening function ($\varepsilon^{-1}(r)$) as given in Eqn (3.7) and have been compared with the results obtained for static dielectric constant (ε_0) inside the spherical QD under both the square and parabolic confinement by neglecting the correlation (Case I) between the two holes in the chosen wavefunction as given in Eqn (3.5).

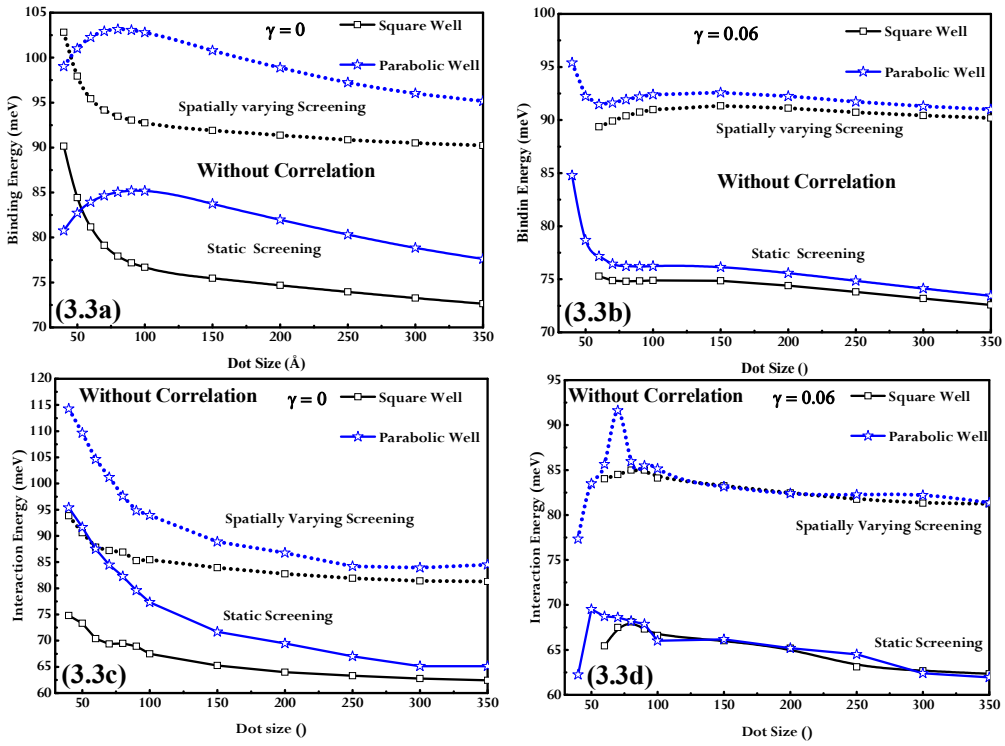

Figure 3.3: Variation of binding energy and E_{hh} as a function of dot size for SQD with both square and parabolic confining potential when the correlation between the holes are ignored for various γ. The results of static screening and the spatially dielectric screening have been reported and compared.

The results have been presented for $\gamma = 0$ and $\gamma = 0.06$. The Carriers show more interaction (an enhancement of ≅ 20%) between them as shown in fig. 3.3c and 3.3d with the spatially varying dielectric screening ε (r) rather than in static screening ε_0 in the absence ($\gamma = 0$) as well as in the presence of magnetic field ($\gamma = 0.06$) irrespective of the

nature of the confining potential inside the QD for both types of the confining potential. This interaction energy follows the same trend with the dot size in both the static screening and in the spatially varying dielectric screening for $\gamma = 0$ and $\gamma = 0.06$. In both the screening, the application of external magnetic field causes the Coulomb interaction to reduce especially in the narrower dot size because of the reduced barrier height. The effect of applied magnetic field on the E_{hh} is negligible when the dot radius is increased towards the bulk. Moreover, in the presence of the magnetic field a turnover occurs for the smaller radius of QD. This turnover feature is due to the interplay between three forces, the first being an attractive force due to the confining potential in a dot that tends to confine the holes together, the second being the repulsive force due to the Coulomb interaction between the hole themselves and the third being the magnetic field which reduces the confinement and aids the repulsive forces. At a smaller QD radius, the repulsive force gains in strength and causes tunnelling which in turn reduce the interaction energy when the magnetic field is applied. The binding energy follows the same trend with the dot radius in both types of screening as given in fig. 3.3a and fig. 3.3b. The spatially varying dielectric screening causes the acceptors to be more bound inside the QD. The externally applied magnetic field does not show any turnover effect on the binding energy except causing the acceptors to be less bound inside the dot with the applied magnetic field. Both the binding energy and the interaction energy is more for the double acceptors when it is confined with parabolic type potential rather than square type potential inside the QD. It is interesting to note from fig. 3.3a and 3.3b that there are no bound states for the double acceptors below 60Å for the applied magnetic field of $\gamma = 0.06$ in QD with Square well confinement but the bound states are available for the QD with parabolic confinement. But, when the correlation effect is considered in the

chosen wavefunction of the double acceptor, the bound states for the SQD with square confinement start to appear even from the dot size of 40Å as shown in fig. 3.1a and 3.1b. The results obtained for the CQD with Square confinement by neglecting the correlation between the two holes are presented in fig. 3.4a and 3.4b. It is noted from fig. 3.4a that the trend of the binding energy and the interaction energy against the dot size for various magnetic field is as same as the trend of the binding and the interaction energy in case I, but with higher in magnitude. This may be due to the less attachment of the carriers with their parent acceptor atom when the correlated holes are considered. Moreover, irrespective of the applied magnetic field, the fall of binding energy in the case II is not as rapid as the fall in the binding energy in the case I.

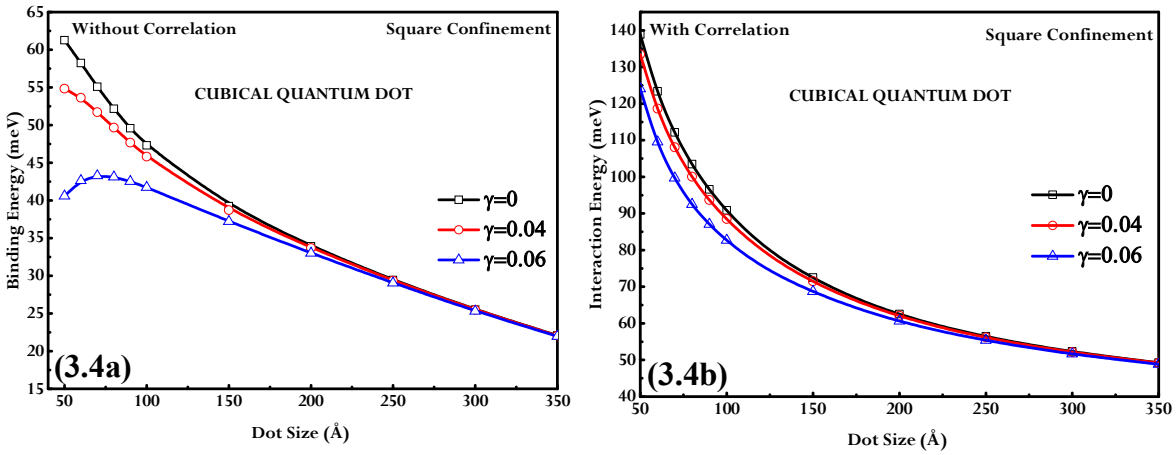

Figure 3.4: Variation of binding energy and E_{hh} as a function of dot size for CQD with square confining potential when the correlation between the holes are ignored under various applied magnetic field.

The obtained results for both the binding energy and the interaction energy of the two holes as a function of dot size are plotted in fig. 3.5a for the CQD with parabolic confinement. It is observed from the results that both the binding energy and the interaction energy are much larger in the parabolic confinement than in the square well

confinement and it is again clear from fig. 3.5 that both the energies decrease with the increase of dot size and the applied magnetic field as expected.

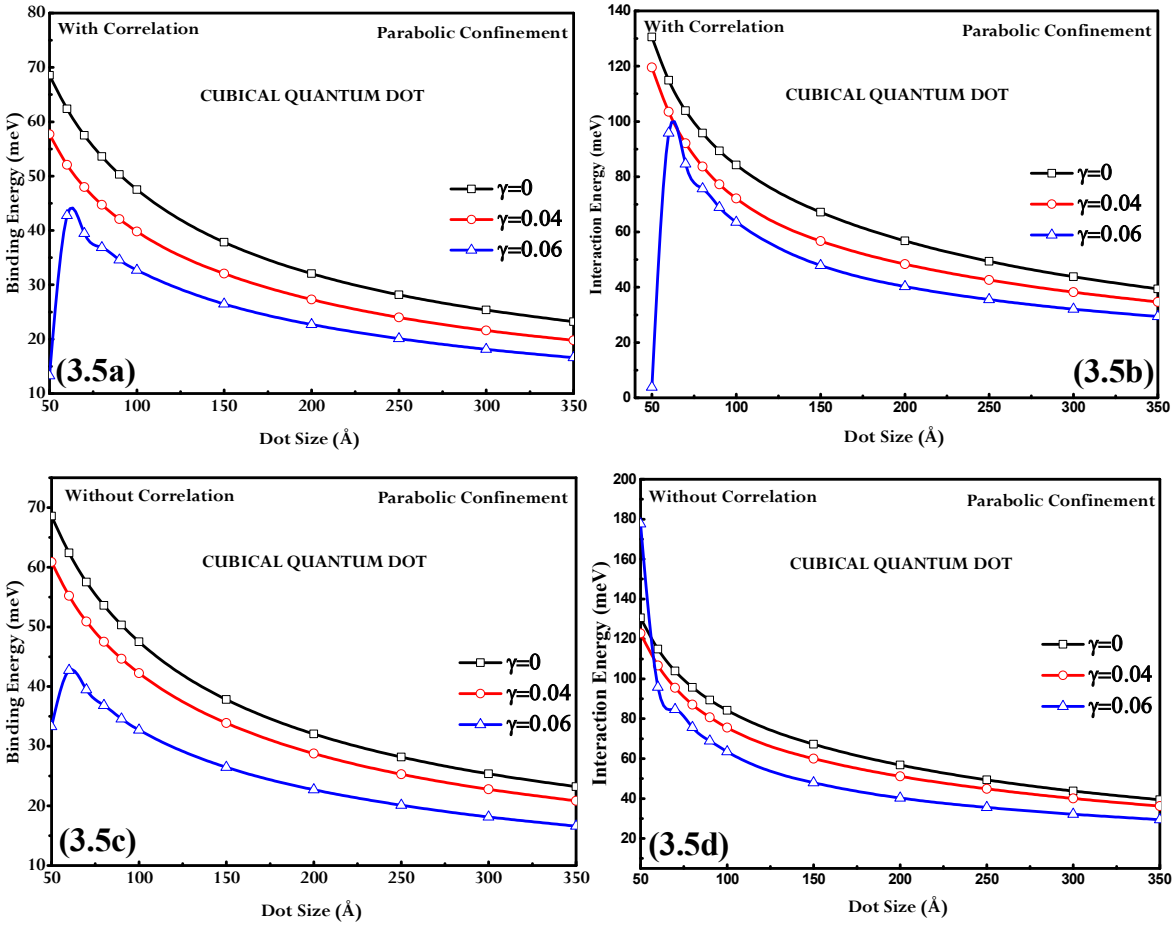

Figure 3.5: Variation of binding energy and E_{hh} as a function of dot size for CQD with paraolic confining potential under various applied magnetic field for both the inclusion and exclusion of the correlation between the two holes.

To conclude, the Coulomb interaction of the two holes bound to an acceptor impurity in SQD and CQD is very effective and can be controlled by the external magnetic field. This Coulomb interaction in Semimagnetic QD is significant in the light of Coulomb blockade of transport. Moreover, this two particle interaction can be very helpful to understand the two particle energy spectra and the formation of Wigner crystal in low dimensional systems llike Quantum Dot, Quantum Wire and Quantum Well.

References

1. G.Bastard, J.A.Brum and R.Rerreire, *Solid St.Phys,* **1991**, *44*, 229.
2. U. Merkt, J. Huser and M. Wagner, *Phys. Rev. B*, **1991**, *43*, 7320.
3. A.Giesekus, *Phys. Rev. B*, **1991**, *42*, 11725.
4. A. Merwyn Jasper D Reuben, K. Jayakumar, *Superlat. and Microstruct*, **2012**, *52*, 732–737.
5. A. Merwyn Jasper D Reuben, K. Jayakumar, J. Nano. Electron. Phys. **2011**, *3*, 236-239.
6. A. Merwyn Jasper D Reuben, K. Jayakumar, *Book of Abstracts: 2nd Int. Symposium. Semiconductor Materials and Devices (ISSMD – 2),* **2013**, *52*, 324 – 325.
7. T. Jungwirth, Byounghak Lee, A. H. MacDonald, *Physica E*. **2001**, *10*, 153 – 156.
8. F. B. Pedersen, Yia – Chung Chang, Phys. Rev. B. **1997**, 55, 4580 - 4588.
9. F. B. Pedersen, Yia – Chung Chang, Phys. Rev. B. **1996**, *53*, 1507 - 1516.
10. L. Brey, N. F. Johnson and B. I. Halperin, *Phys. Rev. B*, **1989**, *40*, 10647-10649
11. S. K. Yip, *Phys. Rev. B*, **1991**, *43*.
12. J. Hermanson, *Phys. Rev. B*. **1966**, *150*, 660.
13. M. Latha, S. Rajashabala and K. Navaneethakrishnan, *phys. stat.s ol. (b).* **2006**, *243*, 1219 – 1228.
14. H. ParedesGutierrez, J. C. CueroYepez and N. PorrasMontenegro, *J. Appl. Phys.* **1994**, *75*, 5150.

Chapter 4

IMPURITY STATES IN A SEMIMAGNETIC QUANTUM WELL

A. Impurity states in a Semimagnetic Double Quantum Well

With the advantage of having Molecular Beam Epitaxy (MBE), one can easily fabricate the Double Quantum Well (DQW) Nanostructured systems with various barrier widths or heights. The modification of the barrier height in these DQWs made up of DMS materials can be achieved either by adjusting the composition of the alloy used in the barrier material or by the application of the external magnetic field [1]. The presence of a quantised motion in the growth direction of the DQW structures has a huge impact on their physical properties, which strongly differ from properties of narrow single quantum wells representing a physical realisation of a quasi-2-Dimensional system. The distinctive behaviour of DQWs becomes apparent especially when the density of states are modified from 3D to 2D due to the formation of Landau levels in these structures under the influence of high magnetic field which has a very profound effects on physical phenomenon in 2D systems. Therefore the DQWs made out of DMS materials provides a new path to explore the rich variety of phenomena through which one can investigate the role of impurities confined in such systems to understand its electrical transport and magneto optical properties.

4.1. *Donor States in a Semimagnetic* $Cd_{1-x_{in}}Mn_{x_{in}}Te / Cd_{1-x_{out}}Mn_{x_{out}}Te$ *Double Quantum Well*

Our knowledge about the influence of magnetic impurity on semiconductors has been extended to study the extensive transport properties in DMS heterostructures over the past few decades [1-8]. Considerable attention has been focused by many researchers on the theoretical investigation of the ground state energy of hydrogenic donor impurity in GaAs /$Al_xGa_{1-x}As$ Single and DQW systems by accounting various effects [9-15]. Copious literatures are available on the study of electronic and excitonic states in a DQW with non-magnetic materials under the application of strong magnetic field [16-20]. The magneto-optical study has been carried out by Lee *et. al* [21] both theoretically and experimentally to demonstrate the interwell coupling in DQWs using DMS materials. Detailed spectroscopic measurements and their successful theoretical interpretation [6] is favourable for DMS to offer an appealing opportunity to elucidate how the BMP affect transport phenomena. Therefore it becomes necessary to account this polaronic corrections to the impurity binding energy and this has been investigated in various DMS heterostructures by many researchers [22-26]. But this kind of study has not been touched yet in DQW made from DMS barrier layers especially with $Cd_{1-x}Mn_xTe$. Hence the present work is mainly intended for the study of electronic states of the donor impurity as well as the influence of BMP on the impurity states in $Cd_{1-x_{in}}Mn_{x_{in}}Te / Cd_{1-x_{out}}Mn_{x_{out}}Te$ QW under the external applied magnetic field for the composition of magnetic impurity like Mn ion of $x_{in} = 0.005$ and $x_{out} = 0.3$, where x_{in} and x_{out} are the composition of Mn^{2+} ion in the well and the barrier regions respectively, and also for various impurity locations. The results are computed in the effective mass approximation using variational technique.

4.1.1. Theoretical Formalism

4.1.1.1. *Donor Binding Energy for Various Impurity Locations*

The Hamiltonian of a hydrogenic donor impurity inside the DQW made up of $Cd_{1-x_{in}}Mn_{x_{in}}Te / Cd_{1-x_{out}}Mn_{x_{out}}Te$ DMS materials in the effective mass approximation in the presence of magnetic field applied along the growth direction (z-axis) is written as

$$\mathbf{H} = \mathbf{H}_0 + \mathbf{H}_{exc} \tag{4.1}$$

$$\mathbf{H_0} = -\nabla^2 - \frac{2}{r} + V_B(z) + \gamma L_z + \frac{\gamma^2 \rho^2}{4} \tag{4.2}$$

The contribution from the exchange interaction between the electron and the Mn^{2+} ion to the Hamiltonian can be written as given in section 1.1.

Using the mean field theory with modified Brillouin function [24], the exchange interaction between the carrier and the magnetic impurity in the presence of an external magnetic field **B** can be written as

$$E_{exc} = \frac{\beta N_0}{2}\left\{ \langle \Psi \mid x_{in} S_0(x_{in}) B_s(y_1) \mid \Psi \rangle + \langle \Psi \mid x_{out} S_0(x_{out}) B_s(y_2) \mid \Psi \rangle \right\} \tag{4.3}$$

where, $B_s(y)$ is the modified Brillouin function and is given by Eqn (2.15). For the DMS of arbitrary x, it is inevitable to choose the phenomenological fitting parameters [27] of saturation value $S_0(x_{in} = 0.005) = 2.11$, $S_0(x_{out} = 0.3) = 0.52$ and the effective temperature $T_{eff} = T + T_0$ with $T_0(x_{in} = 0.005) = 0.29$ and $T_0(x_{out} = 0.3) = 14.9$.

The various impurity positions (z_i) accounted for the study is as follows.

(i) On Centre Barrier impurity (OCB) ($z_i = 0$)

(ii) On Edge Barrier impurity (OEB) ($z_i = L_b / 2$)

(iii) On Centre Well impurity (OCW) ($z_i = L_b / 2 + L_w / 2$)

(iv) On Edge Well impurity (OEW) ($z_i = L_b / 2 + L_w = L_e$)

According to the scheme of fig. 4.1, the profile of the confining potential V_B (z) for the carriers in symmetric DQW structures is given as

$$V_B(z) = \begin{cases} 0 & \frac{L_b}{2} \le |z| \le (\frac{L_b}{2} + L_W) \\ V_0 & |z| \le \frac{L_b}{2} \text{ and } (\frac{L_b}{2} + L_W) < |z| < \infty \end{cases} \tag{4.4}$$

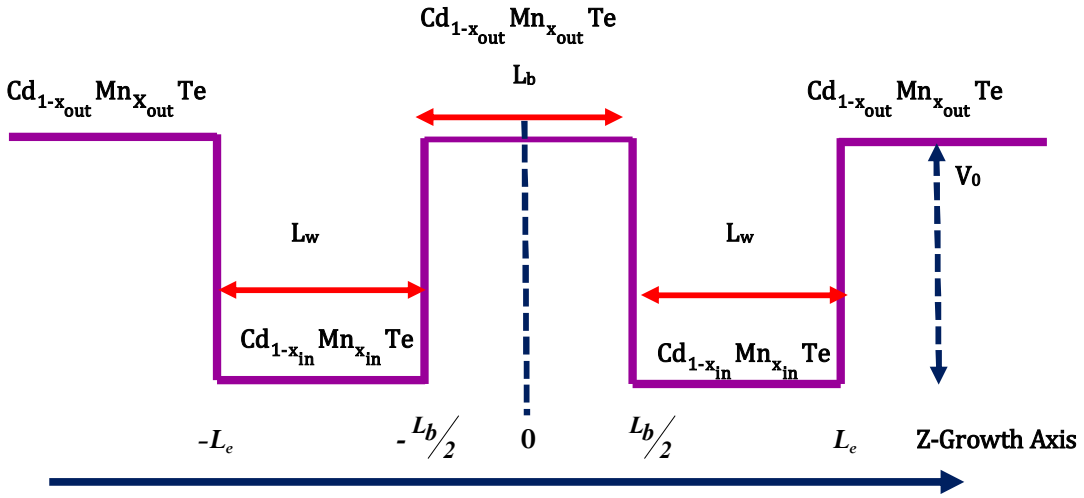

Figure 4.1: Schematic view of the potential profile for a DQW

L_w is the width of the each well and L_b is the central barrier width and V_0=70% ΔE_g^B.

The approximate ground state for confined donor impurity has been calculated using the variational method. The envelop function f (z) is considered as

$$f(z) = \begin{cases} A \exp[\beta (z + L_e)] & z \le -L_e \\ -B \sin[\alpha (z + \frac{L_b}{2})] + C \cos[\alpha (z + \frac{L_b}{2})] & -Le < z < -\frac{L_b}{2} \\ \cosh[\beta z] & -\frac{L_b}{2} < z < \frac{L_b}{2} \\ B \sin[\alpha (z - \frac{L_b}{2})] + C \cos[\alpha (z - \frac{L_b}{2})] & \frac{L_b}{2} < z < Le \\ A \exp[-\beta (z - L_e)] & z \ge L_e \end{cases} \tag{4.5}$$

Here, $\alpha=(2m_w^* E/\hbar^2)^{1/2}$ and $\beta=(2m_b^*(V_0 - E)/\hbar^2)^{1/2}$. The unknown constants A, B and C are found out using the proper boundary conditions at the interfaces $z_i = L_b / 2$ and $z_i = L_e$.

The trial wavefunction of the ground state is chosen as,

$$\psi(r) = N f(z) e^{-\lambda r} \tag{4.6}$$

where, N is the normalization constant and λ is the variational parameter.

The lowest energy level E_0 without donor impurity can be computed by solving the transcendental equation [13]

$$2\cos(\alpha L_W)+(\mu-\frac{1}{\mu})\sin(\alpha L_W)-(\mu+\frac{1}{\mu})\sin(\alpha L_W)\exp(-\beta L_b)=0 \quad \text{with} \quad \mu=m_W^*\beta \,/\, m_b^*\alpha \qquad (4.7)$$

m_w^* and m_b^* are the electron effective masses in the well and barrier region respectively.

The expectation value of **H** is minimized with respect to λ and the binding energy of the donor impurity in the presence of magnetic field is found by solving the Schrödinger equation variationally, and is given by,

$$E_B = E + \gamma - \langle H \rangle_{min} \qquad (4.8)$$

The CdTe parameters used in our calculation are ε = 10.2; m_w^*= 0.090. Energies for electron are scaled by effective Rydberg $R_e^* = m_w^* e^2 / 2\hbar^2\varepsilon^2$ and the effective Bohr radius $a_B^* = \hbar^2\varepsilon / m_w^* e^2$.

4.1.2. Results and Discussion

The estimation of $< r^2 >$ i.e. the effective distance of the carrier from the parent donor atom plays a vital role in determining the carrier localization in the nanostructured systems. Therefore, one can examine the impact of the central barrier width and the external magnetic field on the behaviour of hydrogenic donor impurity confined inside the DQW through the observation of $< r^2 >$. To start with, the variation of the binding energy of a donor impurity confined in a $Cd_{1-x_{in}}Mn_{x_{in}}Te$ / $Cd_{1-x_{out}}Mn_{x_{out}}Te$ DQW and the $< r^2 >$ as a function of central barrier width for the Mn composition of x_{in} = 0.005 and x_{out} = 0.3 without the application of magnetic field has been calculated and is presented in section 4.1.2.1. The effect has been analysed for the two well widths (i) L_w = 50Å (quasi

2D region) and (ii) L_w = 300Å (almost bulk region) for various impurity positions. The first observation we have made is, irrespective of the well widths, applied magnetic field and the impurity positions, when the barrier width is limited to zero (i.e.) $L_b \rightarrow 0$Å, we reproduce the E_B of the single quantum well which is available in the literature [28] as a limiting case. On the other hand, when the width of the central barrier between the two wells is as large as the bulk value, the symmetric wells are completely decoupled and it makes the donor impurity to behave in a single isolated quantum well. Therefore, it is apparent from this observation that the interwell coupling is possible only for the narrow barrier width which should be in the limit 0Å < L_b < 100Å which can be seen from fig. 4.2a showing a saturation value of E_B for L_b > 100Å. The behaviour of the donor impurity with the central barrier width can be understood for various impurity locations in the presence and in the absence of the magnetic field as follows:

4.1.2.1. DQW under zero applied magnetic field ($\gamma = 0$)

This section discusses the variation of binding energy of the donor impurity when the system is not subjected to the perturbation due to the external magnetic field.

On Centre Barrier Impurity (OCB)

A clear inspection of fig. 4.2a indicates that the binding energy decreases as L_b increases, when the impurity resides at the centre of the central barrier. This is because of the increased $< r^2 >$ for larger L_b which makes the donor atom and the carrier to be weekly coupled due to the reduction in Coulomb interaction (fig. 4.2b). The inset in the fig. 4.2b gives variation of $< r^2 >$ for OEB, OCW and OEW impurities in different scale.

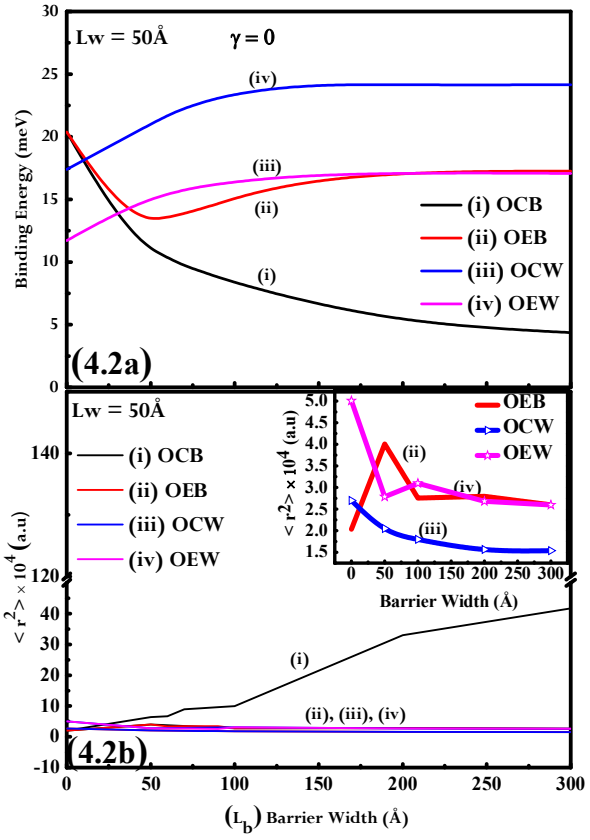

Figure 4.2: Variation of **(a)** binding energy and **(b)** $<r^2>$ against barrier width for lower well dimension L_w = 50Å without the application of magnetic field (γ =0) for the Mn concentration of x = 0.3. Graphs have been plotted against various impurity locations (z_i).

On Edge Barrier Impurity (OEB)

In the case of OEB impurity, the effect of the central barrier width is almost negligible upto particular barrier width which can be clearly seen from the figure that the binding energy of OEB impurity coincides with the binding energy of OCB impurity. But when the barrier width crosses the particular value of L_b~ 100Å, the onset of bulk limit, E_B behaves differently which is discussed subsequently. Initially binding energy decreases as L_b increases and thereafter it starts increasing again and reaches a saturation. This can be understood that when the barrier width increases in between the two wells, the $< r^2 >$ increases and results in the reduction of Coulomb interaction between the carrier impurity

and the parent donor atom. But after reaching the critical barrier width of L_b ~ 100Å, the carrier confinement is limited in the DQW and makes the donor atom and carrier to be closed to each other and thereby increasing their Coulomb interaction which results in larger binding energy in that region.

On Centre Well (OCW) and On Edge Well (OEW) Impurity

Unlike the other two impurity locations discussed earlier, the binding energy for OCW and OEW impurities follow the same trend and these two impurity locations are found to favour for the tunnelling of the carriers through the central barrier layer, which can also be interpreted that the interwell coupling becomes stronger for these two impurity locations as in the case of non-magnetic DQW [13]. It is worth noticing that the gradual and smooth increase of binding energy occurs upto L_b = 100Å but beyond that it becomes saturated. This can be understood in terms of interwell coupling i.e. when the barrier width is reduced below the critical value, there is a finite probability for the carriers to tunnel through the central barrier layer. But, when the barrier width is increased beyond the critical value, it starts to squeeze the impurity wavefuntion more and the carrier is localized only within the isolated well space of 50Å and eventually reduces the degree of freedom of the carrier to move through the entire DQW. Because of this, the distance between the donor atom and the carrier is rapidly decreased which leads to the strong Coulomb interaction between them and it is almost constant for all the barrier widths beyond L_b > 100Å.

The computed results of the binding energy and $< r^2 >$ against barrier width for L_w = 300Å are displayed in fig. 4.3a and 4.3b**.** It is very clear from the figure that the binding energy for all the impurity positions exhibit a similar behaviour with smaller well width like L_w = 50Å with the following exception.

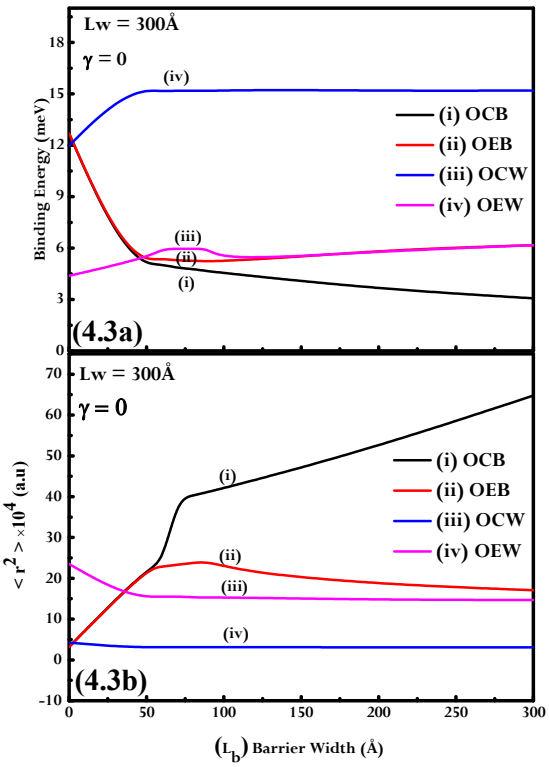

Figure 4.3: Variation of **(a)** binding energy and **(b)** $<r^2>$ against barrier width for larger well dimension L_w = 300Å without the application of magnetic field (γ =0) for the Mn ion concentration of x = 0.3. Graphs have been plotted against various impurity locations (z_i).

The shift in the binding occurs towards smaller barrier width of $L_b \sim 50$Å when compared with $L_b \sim 100$Å as discussed in the earlier case at which the saturation in the binding energy is observed. This can be substantiated with the fact that once the well width is increased towards the bulk value, the DQW starts to behave like two isolated quantum wells irrespective of the barrier width which is increased beyond 50Å.

4.1.2.2. DQW under applied Magnetic field (γ = 3, 5 and 6)

As reported in Ref. [21], one can investigate the interwell coupling in a DQW and its relation to barrier parameters through the magneto absorption study under the effect of magnetic field. Therefore, in order to understand the transitions of carriers involving both symmetric and antisymmetric states in diluted magnetic DQW systems, it is inevitable to

make a comparative study on the carrier behaviour at various impurity locations under the applied magnetic field. Hence this section is mainly addressed for such discussion. It is well known that the applied magnetic field tremendously reduces (Eqn (2.3)) the potential barrier height (333meV, 67.7meV, 19.4meV and 8.4meV corresponding to $\gamma = 0$, 3, 5 and 6 respectively) in which the carrier has been confined. When analysing the effect of applied magnetic field, one observes that an increase of the strength of magnetic field beyond $\gamma = 5$ (~150Tesla) results in the complete delocalization of the carriers confined inside the DQW structures which has been studied for all the impurity locations. For the strength of magnetic field $\gamma > 5$, the unbound states are formed above the potential barrier height instead of bound states inside the well. Therefore, this fact eliminates the need to discuss the results for $\gamma \geq 6$.

On Centre Barrier Impurity (OCB)

Fig. 4.4 presents the variation of binding energy and $< r^2 >$ for the OCB impurity as a function of central barrier width for $L_w = 50$Å It is seen from fig. 4.4a that, when the barrier width is limited to zero, $L_b \rightarrow 0$Å, the binding energy decreases as the strength of the magnetic field increases. This can be understood from the fact that when the central barrier vanishes, the two QWs effectively becomes the SQW of width $L_{SQW} = 2L_{DQW}$ and exhibits the same characteristic behavior ascribed to the SQW under the external magnetic field. An interesting influence of magnetic field upon the confinement of the carrier relies on the rapid increase of binding energy when γ increases for $L_b > 0$Å, even though the barrier height is reduced due to the applied magnetic field as one can justify from the probability distribution for the impurity located at the centre of the barrier as shown in fig. 4.5 (Ia, Ib and IIa, IIb).

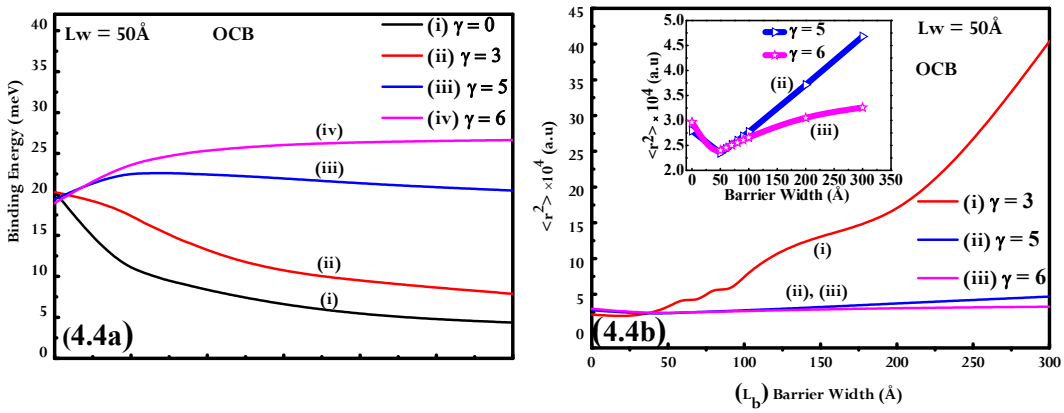

Figure 4.4: Variation of **(a)** binding energy and **(b)** $\langle r^2 \rangle$ against barrier width for lower well dimension L_w = 50Å with the application of magnetic field (γ =3, 5 and 6) for the Mn ion concentration of x = 0.3. Graphs have been plotted for OCB impurity.

I. L_b = 100Å and Lw = 50Å

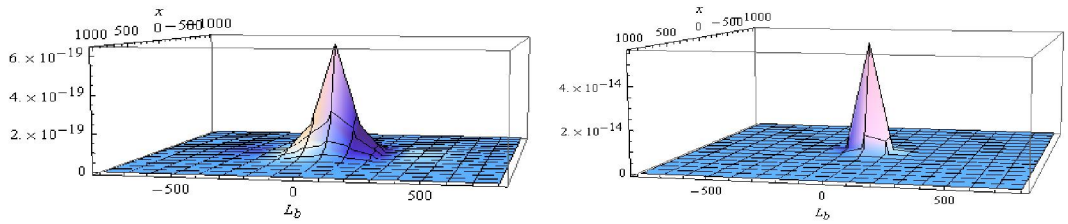

II. L_b = 100Å and Lw = 300Å

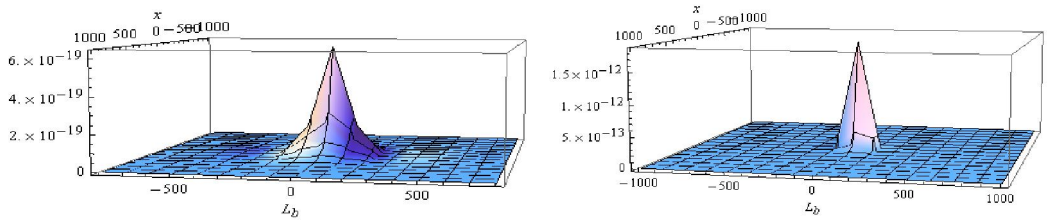

(a) γ =0 *(b) γ = 5*

Figure 4.5: Probability density $|\psi^2|$ of the donor placed at OCB for various dimensions of the barrier and well under γ = 0 and γ = 5 for Mn ion concentration of x=0.3.

The mechanism by which the magnetic field gives rise to the strong localization of the carrier when it resides at OCB is the strong exchange interaction between the spin of

confined carriers and the spins of localized Mn^{2+} ions. As a result, there is an existence of ferromagnetic clouds around the singly occupied electronic states which enhances the binding energy and shrinks the localization radius of localized electrons. When the well width is increased beyond the effective Bohr radius towards the bulk, the binding energy associated with all γ converges to the same value when the barrier width approaches the bulk limit as one can see from fig. 4.6a.

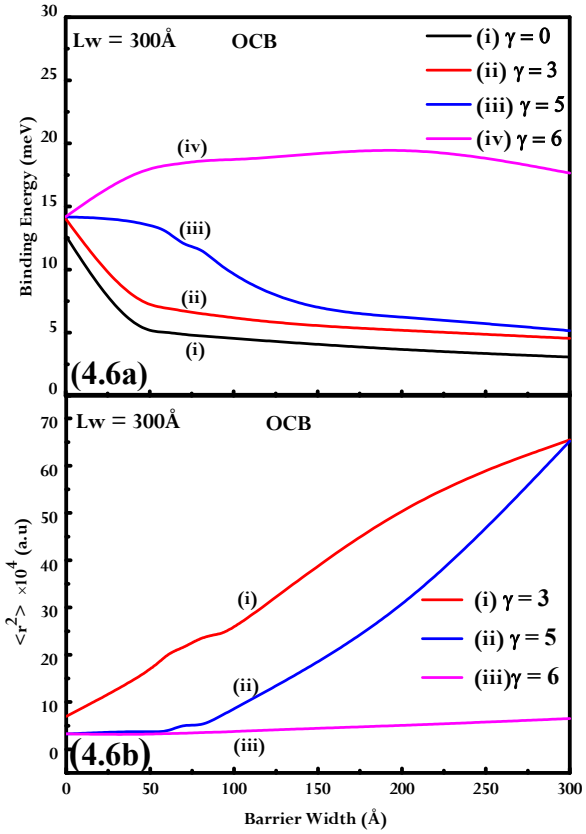

Figure 4.6: Variation of **(a)** binding energy and **(b)** $<r^2>$ against barrier width for larger well dimension L_w = 300Å with the application of magnetic field (γ =3, 5 and 6) for the Mn ion concentration of x = 0.3. Graphs have been plotted for OCB impurity.

On Centre Well Impurity (OCW)

When the Impurity is at OCW, the reduction in the barrier height causes the $< r^2 >$ larger and results in very weak Coulomb interaction between the carrier and the parent donor

atom thereby reducing the binding energy with respect to the applied magnetic field as shown in fig. 4.7a & 4.7b.

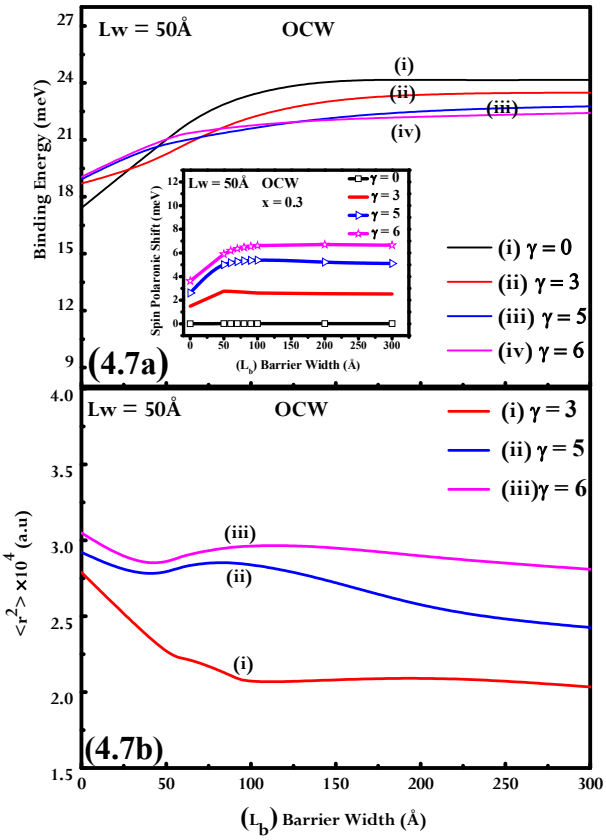

Figure 4.7: Variation of **(a)** binding energy and **(b)** $\langle r^2 \rangle$ against barrier width for lower well dimension L_w = 50Å with the application of magnetic field (γ =3, 5 and 6) for the Mn ion concentration of x = 0.3. Graphs have been plotted for OCW impurity.

Moreover the binding energy increases as the barrier width increases. This is due to the fact that for the thinner barrier, a greater fraction of the wavefunction starts to penetrate into the central barrier which can be seen from fig.4.8 (Ia, Ib and IIa, IIb) giving $|\psi^2|$ against L_b. When the barrier becomes thick, then the DQW structure effectively becomes two decoupled SQWs and the properties associated with the applied magnetic field becomes the same as that of the SQW thereby one can see the increased binding energy in that region.

I. L_b = 100Å and Lw = 50Å

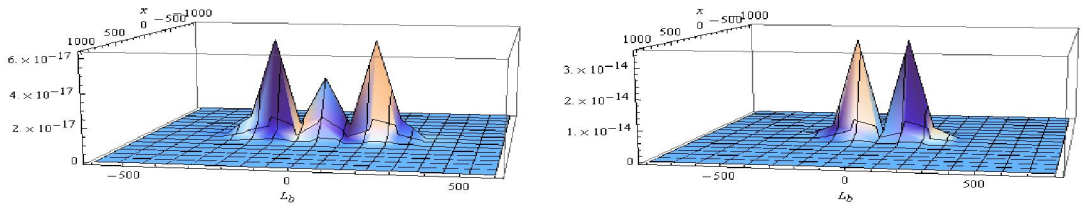

II. L_b = 100Å and Lw = 300Å

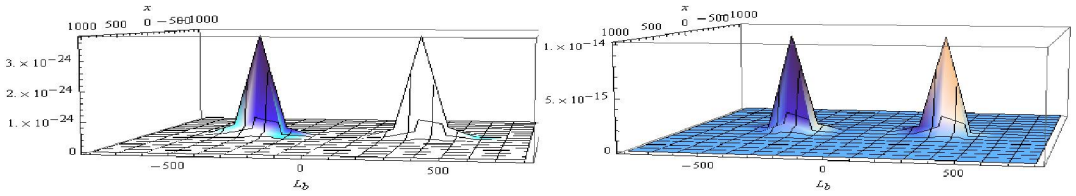

(a) γ =0 ***(b) γ = 5***

Figure 4.8: Probability density $|\psi^2|$ of the donor placed at OCW for various dimensions of the barrier and well under γ = 0 and γ = 5 for Mn ion concentration of x=0.3.

When the well width is increased towards the bulk value, there is no much appreciable effect of magnetic field on the binding energy has been noticed (fig. 4.9a) which can be understood from the variation of $< r^2 >$ as shown in fig. 4.9b. Though the effect due to spin polaronic shift is perceptible for smaller well width of L_w = 50Å as given in the inset of fig.4.7a, the overall effect on the binding does not alter the trend without considering the spin polaronic shift. But the effect due to spin polaronic shift as given in the inset of fig. 4.9a shows the reverse effect on the trend of the donor binding without considering the polaronic correction as there is no much effect on the exchange energy when the magnetic field is applied as can be seen from the inset of fig. 4.9a.

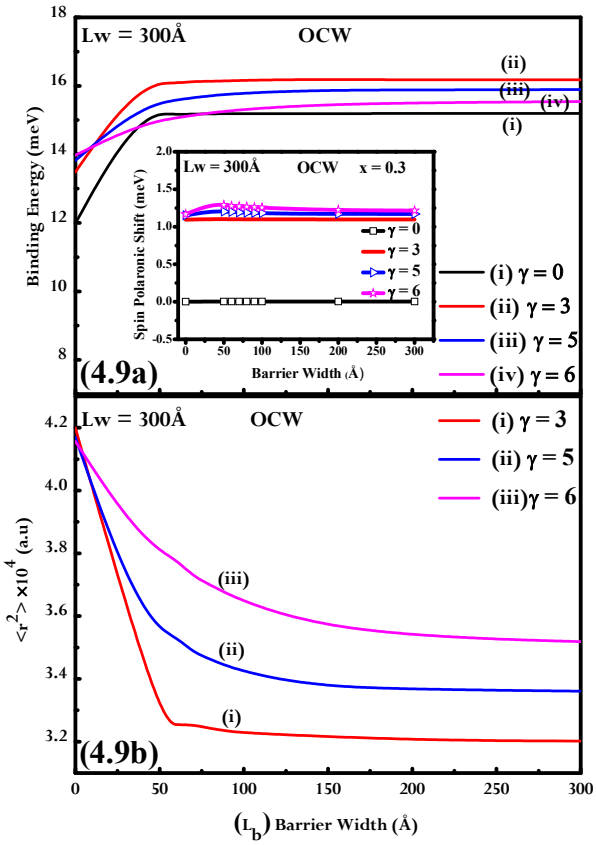

Figure 4.9: Variation of **(a)** binding energy and **(b)** $\langle r^2 \rangle$ against barrier width for larger well dimension L_w = 300Å with the application of magnetic field (γ =3, 5 and 6) for the Mn ion concentration of x = 0.3. Graphs have been plotted for OCW impurity.

On Edge Barrier (OEB) and On Edge Well (OEW) Impurity

When the donor impurity is placed at the interface between the two magnetic semiconducting layers for a given smaller width like L_w =50Å, it experiences a striking effect with respect to magnetic field which contradicts to other two impurity locations like OCB, OCW. There is a drastic increase of the binding energy with respect to magnetic field for OEW impurity as shown in fig. 4.10a when the barrier width is limited to zero in contrast to the situation for non – magnetic wells [29]. This result can be justified from the interpretation given by S.Lee et.al [21] and Mukesh Jain [30] as follows:

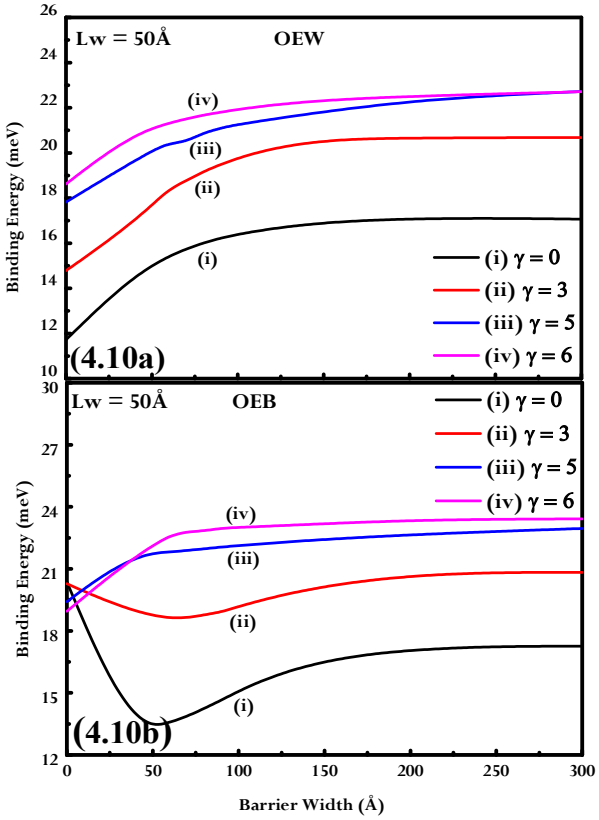

Figure 4.10: Variation of binding energy against barrier width for lower well dimension L_w = 50Å with and without the application of magnetic field (γ = 0, 3, 5 and 6) for the Mn ion concentration of x = 0.3. Graphs have been plotted for **(a)** OEW and **(b)** OEB impurity.

There is a possibility of finding less number of antiferromagnetically paired Mn^{2+} ions along the interface of the heterostructure, which can effectively contribute to a larger $\langle S_z \rangle$ (i.e.) the thermal average of the spin of the contributing ions. Therefore, the magnetization of the material becomes larger since these ions can easily be aligned in the external magnetic field. Hence it can show its influence to the full extent with the carrier through a strong exchange interaction when it resides at the well interface. The results of fig. 4.10a can be justified from the probability distribution for the carrier plotted in fig. 4.11(Ia, Ib and IIa, IIb).

I. L_b = 100Å and Lw = 50Å

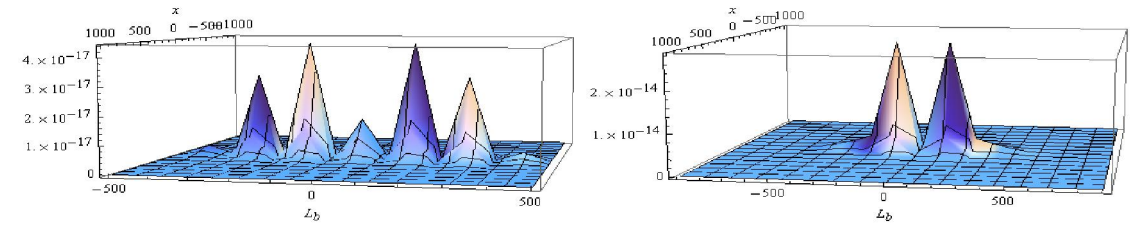

II. L_b = 100Å and Lw = 300Å

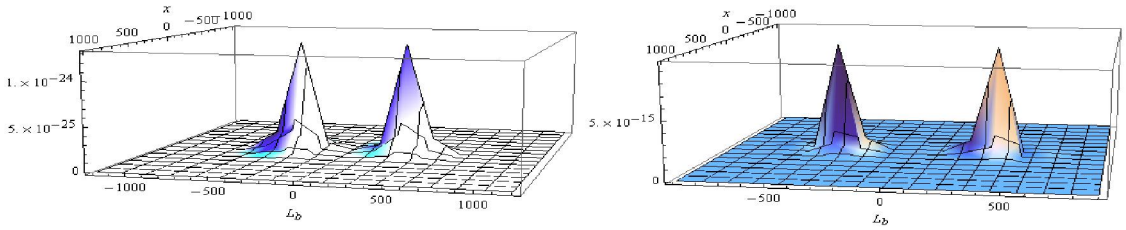

(a) γ =0 ***(b) γ = 5***

Figure 4.11: Probability density $|\psi^2|$ of the donor placed at OEW for various dimensions of the barrier and well under γ = 0 and γ = 5 for Mn ion concentration of x=0.3.

But the applied magnetic field shows the reverse effect on the carrier confinement when the impurity is placed at OEB even though this is the interface between the two magnetic semiconducting layers as this exhibits the behaviour of the donor binding in a SQW including BMP effect (fig. 4.10b). The influence of magnetic field is predominant for the larger well width since it drastically alters the binding energy as shown in fig. 4.12a and 4.12b**.** The substantiated argument is given to this point through the understanding of the behaviour of the carriers in two isolated quantum wells in this bulk limit which does not favour the tunnelling phenomena to occur.

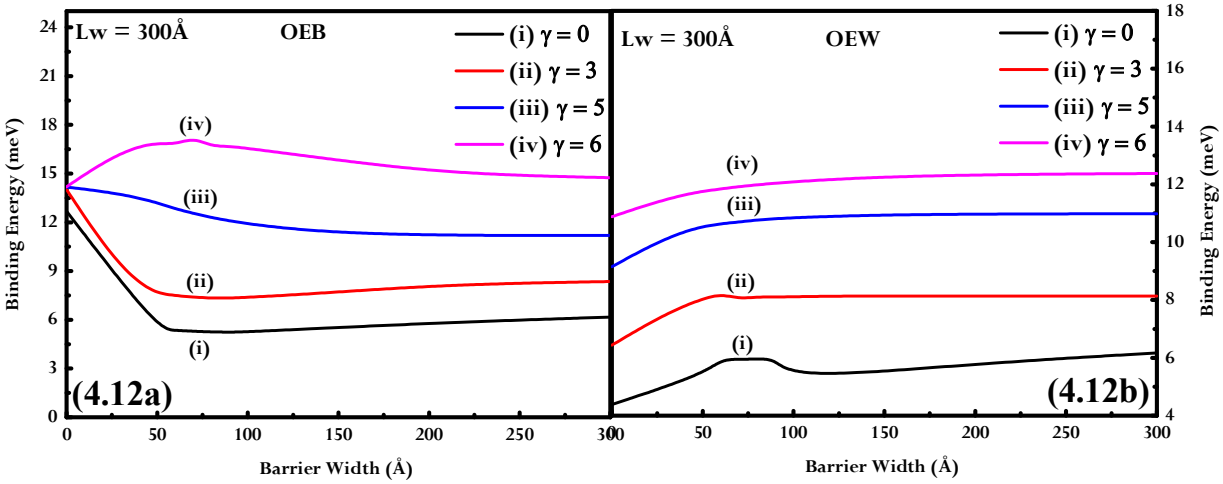

Figure 4.12: Variation of binding energy against barrier width for larger well dimension L_w = 300Å with and without the application of magnetic field (γ =0, 3, 5 and 6) for the Mn ion concentration of x = 0.3. Graphs have been plotted for **(a)** OEB and **(b)** OEW impurity.

4.1.3. Conclusion

This work presents a comprehensive description of the theoretical investigation on the magnetic field induced interwell coupling in a in a $Cd_{1-x_{in}}Mn_{x_{in}}Te / Cd_{1-x_{out}}Mn_{x_{out}}Te$ DQW materials in which the carrier has been confined. To sum up, the above results presented clearly demonstrate that without the application of magnetic field, the binding energy increases as the impurity position goes from OCB and reaches a maximum value when it is at OCW and starts to decrease when it resides at well interface. But once the magnetic field is applied, it favours the interwell coupling by allowing the penetration of the impurity wavefunction via central barrier thereby it reduces the binding energy for OCW impurity and shift the binding energy to higher value for all other impurity locations. These conclusions are further confirmed from the fig. 4.13 which represents

how the binding energy varies with the various impurity locations for various barrier dimensions.

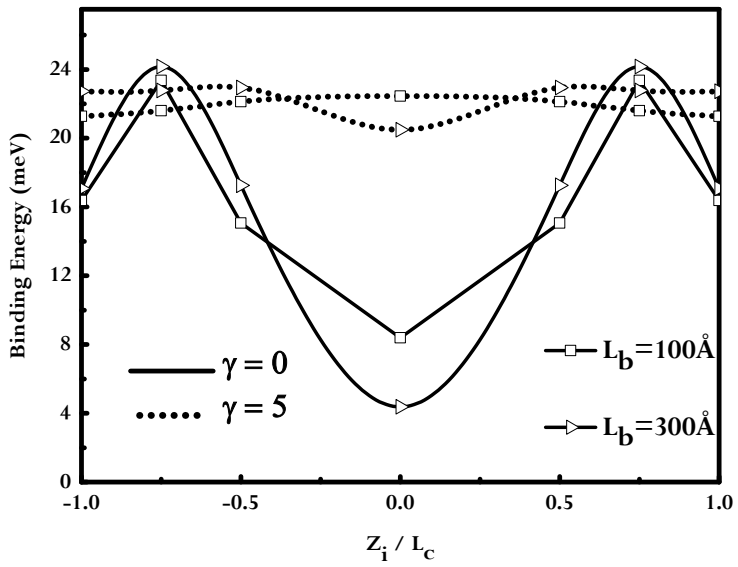

Figure 4.13: Variation of Binding energy as a function of impurity position is plotted for DQW with a well width of 50Å. The solid and dashed lines are corresponding to $\gamma = 0$ and $\gamma = 5$ respectively. The square and triangle symbols represents L_b = 100Å and L_b = 300Å respectively.

The calculations devoted to the polaronic effects may be helpful to understand how the transport properties of the confined carriers are indirectly altered by the applied external magnetic field. It is very clear from the available literatures that no much effort has been dedicated for such a study exhibited by the DQWs with DMS. Hence this work may give an understanding of the transport properties accounting the BMP effect associated with the electrons confined in a diluted magnetic DQW systems which can be exploited in various optoelectronic and spintronic devices.

4.2. *Bound Magnetic Polaron in a Semimagnetic Double Quantum Well*

Many theoretical investigations [23, 24, 31, 32] on the energy levels of Bound Magnetic Polaron do already exist. However, no such investigations have been made to study the effect of BMP on the energy levels especially in a DQW with respect to the impurity position as a function of various combinations of the composition of Mn^{2+}ion in the well (x_{in}) and the barrier (x_{out}) of DMS materials in such a way that the difference between the two composition ($x_{out} - x_{in} = x$) is same. The present study attempts for such an investigation in $Cd_{1-x_{in}}Mn_{x_{in}}Te/Cd_{1-x_{out}}Mn_{x_{out}}Te$ DQW with and without the application of magnetic field for the resultant composition of x = 0.1 as a function of central barrier width and the impurity positions.

The various combinations (C_i) of x_{in} and x_{out} in such a way that the difference between x_{out} and x_{in} is 0.1 ($x_{out} - x_{in} = x = 0.1$) accounted for the study are as follows:

$$\begin{aligned} C_1 &: x_{in} = 0.005, x_{out} = 0.1 \\ C_2 &: x_{in} = 0.01, x_{out} = 0.1 \\ C_3 &: x_{in} = 0.1, x_{out} = 0.2 \\ C_4 &: x_{in} = 0.2, x_{out} = 0.3 \end{aligned} \tag{4.9}$$

4.2.1. Results and Discussion

The Fig. 4.14a, 4.14b, 4.14c and 4.14d corresponding to OCB, OEB, OCW and OEW impurity locations shows the variation of Spin Polaronic Shift (SPS) against the central barrier width in a $Cd_{1-x_{in}}Mn_{x_{in}}Te/Cd_{1-x_{out}}Mn_{x_{out}}Te$ DQW for various combinations of x_{in} and x_{out} in such a way that the difference between x_{out} and x_{in} is 0.1 ($x_{out} - x_{in} = x = 0.1$). It is noted from the figure that the trend of the variation of SPS with the barrier width is as same as the trend of the variation of binding energy of the donor impurity with the

barrier width of the DQW under zero magnetic field (γ = 0) as discussed in section 4.1.2.1.

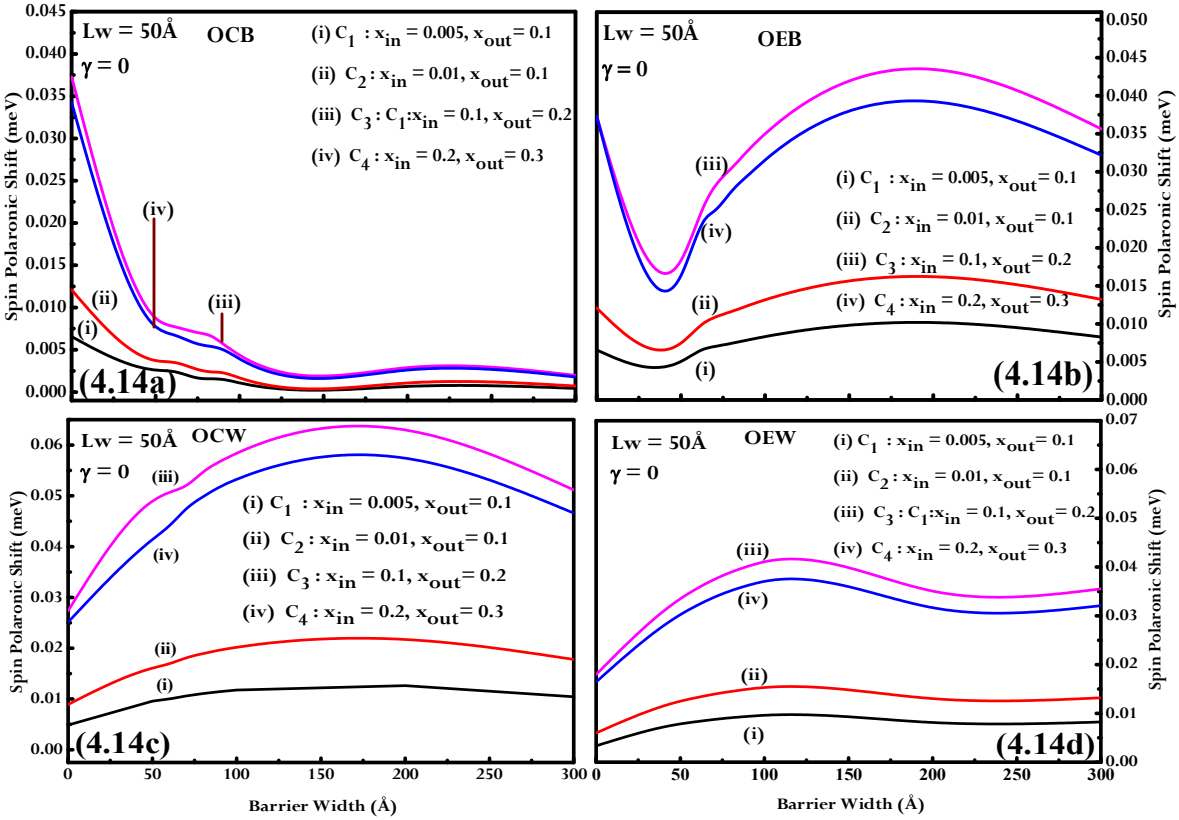

Figure 4.14: Variation of SPS against the barrier width for different combinations C_i of concentration of Mn^{2+} for composition of x = 0.1 (x_{out} -x_{in}=C_i) in a DQW with well width of L_w = 50Å for **(a)** OCB, **(b)** OEB, **(c)** OCW and **(d)** OEW impurities without the application of magnetic field (γ = 0).

An attempt has been made on how the exchange interaction between the Mn^{2+} ions and the confined carrier in a DQW is affected by the composition of the magnetic impurity ion (x_{in} and x_{out}) which are varied simultaneously as given in Eqn (4.9) both in the well and in the barrier material. For all the impurity locations, the SPS increases with the increase of the composition of Mn^{2+} ion except for the combination (C_4) of x_{in} = 0.2 and x_{out} = 0.3. This is because, when the concentration of Mn^{2+} ion in both well and barrier increases, the exchange interaction between the magnetic moment of the Mn^{2+} ions and

the spin of the localized carrier also increases which results in larger shift in the polaronic energy. This may be justified as follows: When the concentration of Mn^{2+} ions is low , $x < 0.005$, the interaction between the magnetic moments of the Mn^{2+} ions is very low [21]. Hence, all the Mn^{2+} ions can contribute to the total magnetic moment with the average spin per magnetic ions $<S_z>$.But when x increases beyond 0.005, spins of nearest neighbour cancels out due to the antiferromagnetic interaction between the Mn^{2+} ions which reduces the number of ions contributing to the total magnetic moment. Eventually only an effective concentration $\bar{x}$ of Mn^{2+} ions which is always less than x contributes to the total magnetic moment. From the results reported in [21], one can understand that the $\bar{x}$ increases upto x = 0.2 and then starts to decrease when x increases beyond 0.3. It is because of this fact one gets lower SPS for the combination of Mn^{2+} ions which involves $x_{out} = 0.3$. When the barrier width is limited to zero ($L_b \rightarrow 0$), the rate of increase of the shift with respect to the increase of the concentration of Mn^{2+} ions as in Eqn (4.9) is high, only when the impurity is at OCB and OEB when compared to the other two impurity locations. This is due to the fact that the DQW effectively becomes the Single Quantum Well (SQW) as $L_b \rightarrow 0$ and it exhibits the characteristic behaviour ascribed to the SQW. However, when the barrier width starts to increase in between the two wells, the rate of increase of SPS is high, only for the OCW impurity compared to all the other impurity locations as shown in Fig 4.14c.

The results of SPS against barrier width is presented in Fig. 4.15 for $L_w = 300$Å. It is seen from the figure that the effect on SPS due to the variation of the concentration of Mn^{2+} ion for any combinations ($C_i : x_{out} - x_{in}$) is predominant only for the lower well width of L_w=50Å rather than for the well width approaching the bulk value like L_w=300Å.

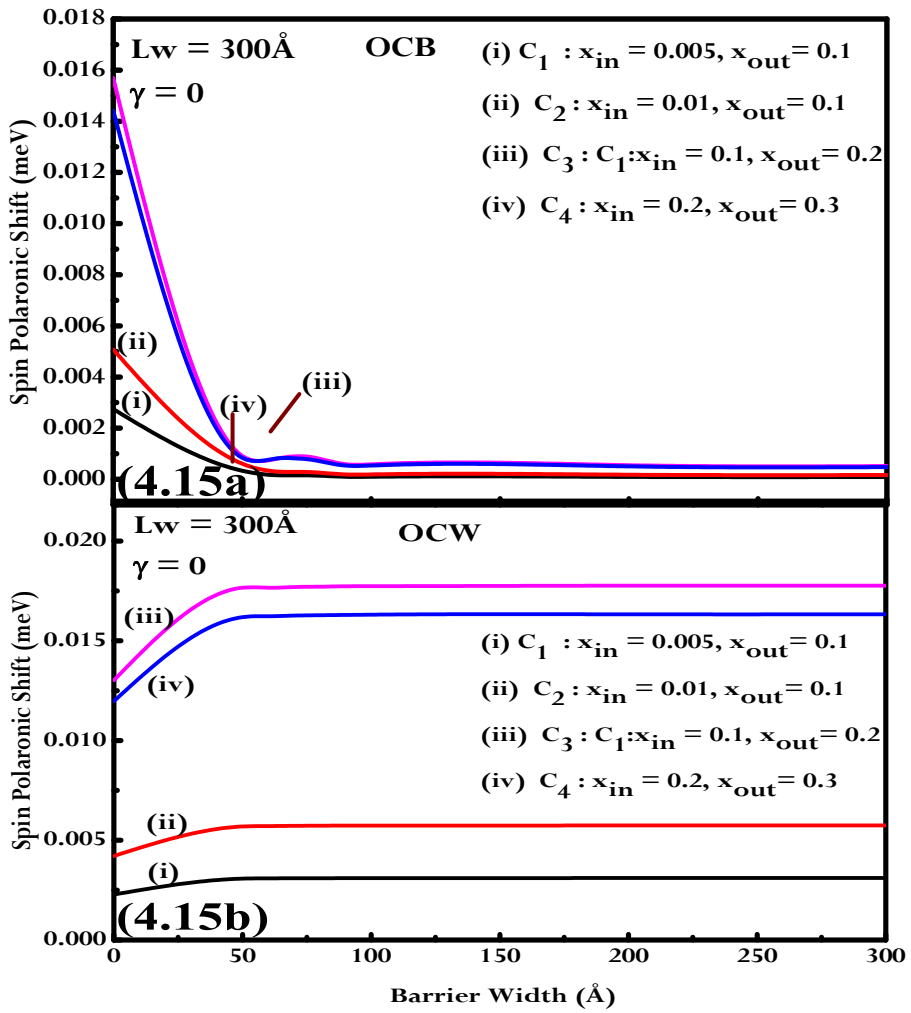

Figure 4.15: Variation of SPS against the barrier width for different combinations C_i of concentration of Mn^{2+} for composition of x = 0.1 (x_{out} -x_{in}=C_i) in a DQW with a well width of L_w = 300Å for **(a)** OCB, **(b)** OCW impurities without the application of magnetic field.

The variation of the SPS against the barrier width for all the combinations of composition of Mn^{2+} ions and for all the impurity locations under the external applied magnetic field is given in Fig. 4.16. It is well known that the applied magnetic field tremendously reduces the confining potential (111. 09meV, 7.865meV for γ = 0 and γ = 0.15 respectively) in which the carrier has been confined. When the external magnetic field is applied, the exchange interaction between the Mn^{2+} ions and the carrier is enhanced thereby

increasing the shift largely as one can see from the numerical values of SPS for both $\gamma = 0$ and $\gamma = 0.15$ from the respective figures.

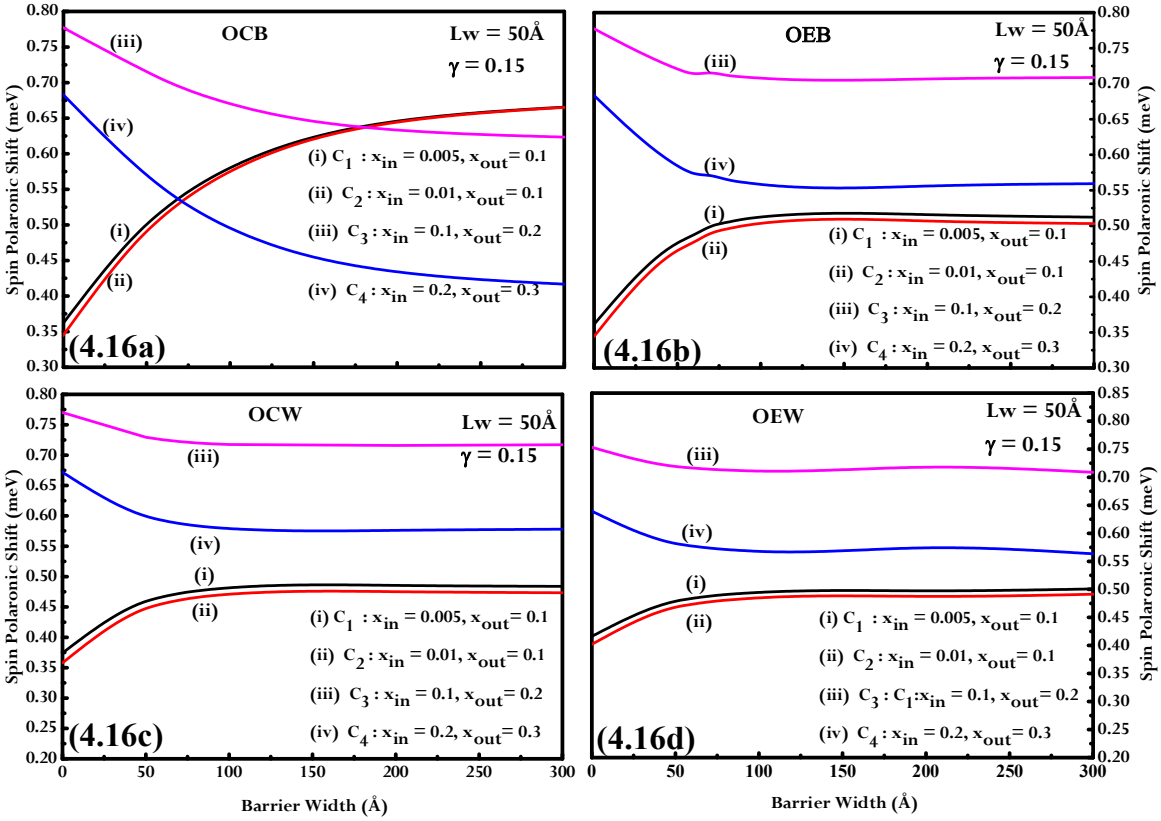

Figure 4.16: Variation of SPS against the barrier width for different combinations C_i of Mn^{2+} composition of x = 0.1 in a DQW with L_w = 50Å for **(a)** OCB, **(b)** OEB, **(c)** OCW and **(d)** OEW impurities with the application of magnetic field ($\gamma = 0.15$).

The trend of the variation of SPS with the barrier width under the applied magnetic field is same for all the impurity locations except for OCB impurity with respect to different combinations of Mn^{2+} ions as shown in Fig. 4.16. In the case of OCB impurity as given in Fig. 4.16a, when the combinations of C_1 and C_2 are considered, the SPS increases as the barrier width increases and one observes the reverse trend for the combinations of C_3 and C_4. This is because when the barrier width increases, the coupling between the two QWs is reduced which causes the carrier to interact with the Mn^{2+} ions presented in the well

material alone. Therefore, only for the combination for which $x_{in} \leq 0.01$ alone shows its influence to the maximum extent with the carrier, thereby increasing the shift. But when the width of the central barrier becomes thin, the maximum of SPS is observed only for the combinations of C_3 and C_4 which is due to the strong alignment of the spins of Mn^{2+} ions with the applied magnetic field. It is also worth to note from the Fig.4.16d that the SPS is maximum for OEW impurity as compared to all other impurity locations for the combination of C_1 and C_2. This is because there is a possibility of finding lesser number of antiferromagnetically paired Mn^{2+} ions along the interface of DQW, which can effectively contribute to a larger <Sz>. Therefore, the magnetization of the material becomes larger since these ions can easily be aligned in the external magnetic field.

4.2.2. Conclusion

The calculation of the SPS due to the formation of BMP with and without the application of external magnetic field in DQW for various impurity locations and for the different combinations of the concentration of Mn^{2+} ions in the well and the barrier DMS materials giving rise to x = 0.1 has been made. From our investigation it has been observed that even though the Mn^{2+} concentration x = 0.1 ($x_{out} - x_{in} = 0.1$) determines the effective confining potential well of the DQW, the SPS is different and depends on the concentration of Mn^{2+} ion in the well (x_{in}) and in the barrier (x_{out}). The large spin – splitting of energy levels due to the sp-d exchange interaction in such DMS materials corresponds to the far – infrared (FIR) region of the spectrum which causes the possibility of a tunable coherent circularly polarized FIR emitter and for the resonant tunnelling devices using superlattices involving wide – gap DMS for which our study may throw some light.

4.3. *Acceptor Bound States in a Semimagnetic CdTe /$Cd_{1-x}Mn_xTe$ Double Quantum Well under Magnetic Field*

The case of p-type materials requires a special attention because of the complex influence of the exchange interaction on the fourfold degenerate acceptor states. The quantum confinement of the valence band holes in a square quantum well was first considered by Nedorezov [33] and a proper theoretical interpretation for the acceptor centre in DMS was given in [34-36].The effect of the magnetic field and the exchange interaction on the acceptor states is weaker in wide gap semiconductors like $Cd_{1-x}Mn_xTe$ because of the high effective masses of the holes which leads to the smaller Landau splitting and the higher shallow acceptor binding energy. The influence of the external magnetic field on the energy levels of acceptor states was treated by Mycielski and Rigaux [37] using perturbation approach at small magnetic fields and by Mycielski and Mycielski [38], Gawron and Mycielski [39] when the Landau splitting of the valence band is much greater than the acceptor binding energy at the quantum limit. Gawron [40] investigated the energy levels of acceptors by incorporating the exchange interaction into the Γ_8 valence band effective – mass Hamiltonian and used the spherical tensor operators and the reduced matrix element technique [41] in order to solve the eigenvalue problem variationally. Very few literatures are available on the acceptor impurities in DMS [40-42]. The purpose of the present work is to deal with the acceptor impurity at various impurity locations in a DQW made up of Semimagnetic materials like CdTe/ $Cd_{1-x}Mn_xTe$ under the influence of magnetic field by solving the Schrodinger equation variationally in the effective mass approximation.

According to the scheme of fig. 4.17, the profile of the confined potential V_B (z) for the carriers in symmetric DQW structures is given as

$$V_B(z)=\begin{cases} 0 & \frac{L_b}{2} \le |z| \le (\frac{L_b}{2}+L_W) \\ V_0 & |z| \le \frac{L_b}{2} \text{ and } (\frac{L_b}{2}+L_W) < |z| < \infty \end{cases} \quad (4.10)$$

L_w is the width of the each well and L_b is the central barrier width and V_0=30% ΔE_g^B, where, ΔE_g^B is given by Eqn (2.3).

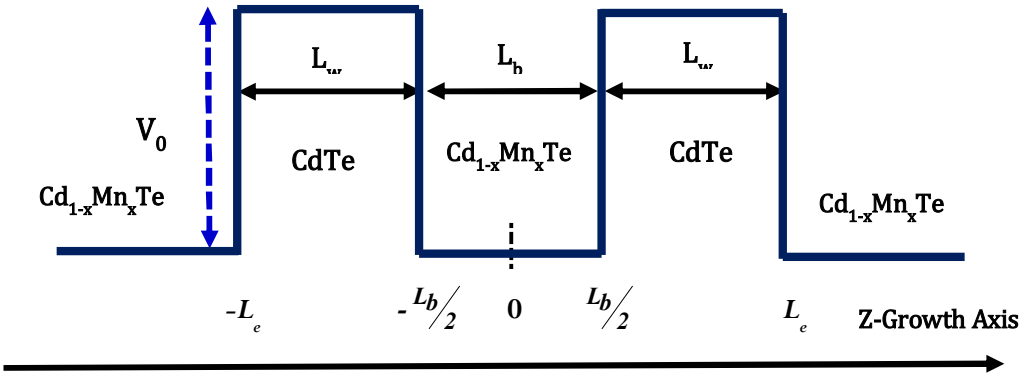

Figure 4.17: Schematic view of the potential profile of the valence band in DQW.

4.3.1. Results and Discussion

The theoretical calculations of the acceptor binding energy against the central barrier width for various impurity locations in the absence of applied magnetic field is presented in fig. 4.18. The results are analysed for the two well widths (i) L_w = 50Å (quasi 2D region) and (ii) L_w = 300Å (almost bulk region). In the absence of magnetic field, there is no net exchange interaction of the magnetic ions with a hole due to the randomness in the spin alignment of these ions. Therefore, the results shown in fig. 4.18a and 4.18b are then similar to those obtained with the non-magnetic semiconductors like GaAs/$Ga_{1-x}Al_xAs$.

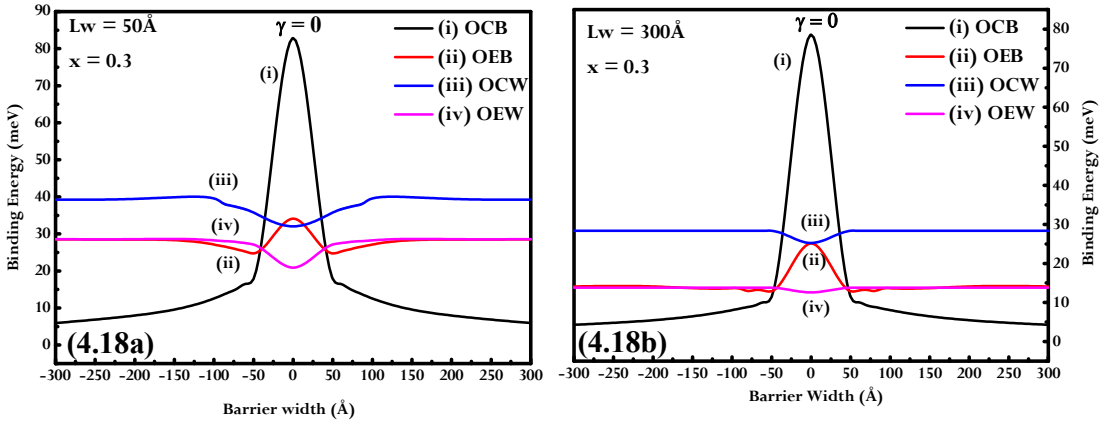

Figure 4.18: Variation of binding energy against barrier width for **(a)** lower well dimension of L_w = 50Å and **(b)** larger well dimension of L_w = 300Å without the application of magnetic field (γ =0) for the Mn^{2+} ion concentration of x = 0.3. Graphs have been plotted against various impurity locations (Z_i)

The justification for the behaviour followed by the binding energy of the impurity situated at various impurity locations like OCB, OEB, OCW and OEW can be referred from the results demonstrated by N. Raigoza, A. L. Morales et al. [13] except for the order of magnitude due to the changes in the material parameters. The reliability of our results lies in the reproduction of the results of single quantum well when the central barrier width is limited to zero [42]. Because of the influence of the exchange interaction on the four – fold degenerate acceptor states in the presence of applied magnetic field, there is a decrease in the acceptor binding energy and also the concentration of holes thermally activated to the valence band increases with the magnetic field [37]. It is well known that the applied magnetic field tremendously reduces the potential barrier height (142.83meV, 85.53meV and 29.1meV corresponding to γ = 0, 0.03 and 0.06 respectively) according to the equation given by Eqn (2.3) in which the carrier has been confined. This leads to a change over from type – I to the type-II band alignment at the critical magnetic

field and beyond which the hole and the negative ion exist in the $Cd_{1-x}Mn_xTe$ and in CdTe region respectively which in turn will strongly affect the optical properties of the system. With respect to all the impurity positions, it is also found that the dependence of binding energy on the central barrier width follows the same trend for all the values of magnetic field as in the case of $\gamma = 0$.

Fig. 4.19 shows the variation of binding energy for the OCB impurity as a function of the central barrier width for the well width of L_w =50Å and L_w =300Å under the influence of applied magnetic field and the inset in the fig. 4.19a gives variation of binding energy of the acceptor impurity in different scale. Moreover, the inset in the fig.4.19a shows that the influence of magnetic field on the binding energy is strong only when the barrier is thinner but when the barrier width approaches the bulk limit, the binding energy associated with all γ converges to the same value. For the higher well width like L_w = 300Å, the binding energy follows the same trend to that of L_w = 50Å but less in magnitude Fig. 4.19b. It is seen from the same figure that the binding energy increases as the barrier width increases.

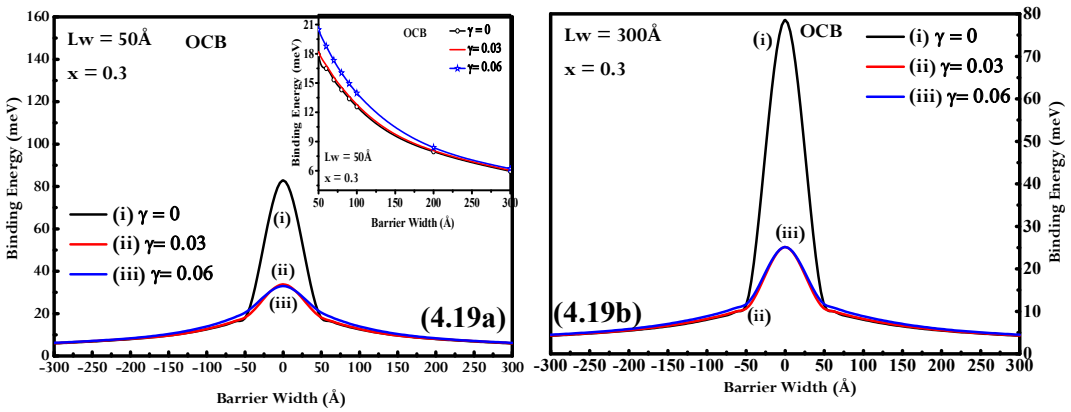

Figure 4.19: Variation of binding energy against width of the central barrier with the application of magnetic field. Results have been plotted in for **(a)** lower well width of L_w = 50Å and **(b)** higher well width of L_w = 300Å with Mn^{2+} ion concentration of x = 0.3 for OCB impurity.

This is due to the fact that when the barrier width is very narrow, there is a possibility of the hole to penetrate the barrier layer thereby reducing the binding energy. When the barrier becomes thick, the DQW effectively becomes the two decoupled SQWs and it exhibit the magnetic properties associated with the SQW which result in increased binding energy in that region. The binding energy decreases as a function of magnetic field when the impurity is situated at the centre of the well region for the smaller well width L_w = 50Å (fig. 4.20a) and there is no appreciable effect of magnetic field on the binding energy when the well width is increased towards the bulk value i.e L_w = 300Å (fig. 4.20b). It is seen from the same figures that the binding energy increases as the barrier width increases. This is due to the fact that when the barrier width is very narrow, there is a possibility of the hole to penetrate the barrier layer thereby reducing the binding energy. When the barrier becomes thick, the DQW effectively becomes the two decoupled SQWs and it exhibit the magnetic properties associated with the SQW which result in increased binding energy in that region.

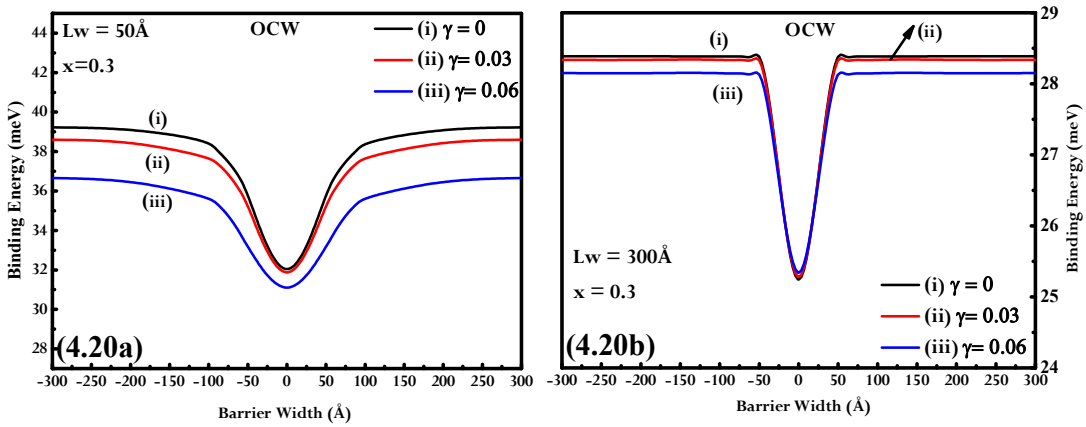

Figure 4.20: Variation of binding energy against width of the central barrier with the application of magnetic field. Results have been plotted in for **(a)** lower well width of L_w = 50Å and (**b)** higher well width of L_w = 300Å with Mn ion concentration of x = 0.3 for OCW impurity.

It is worth noticing from the fig. 4.21 that when the impurity resides at the interface between non-magnetic and magnetic semiconducting layer, the binding energy increases with the applied magnetic field which is in contrast to OCW impurity. The effective concentration of the Mn^{2+} ions along the interface is very large and it can easily be aligned in the external magnetic field which results in larger magnetization of the material. Therefore, the exchange interaction of the Mn^{2+} ion with the carrier becomes very strong and it increases the binding energy of the impurity when it resides at the well interface. The same trend is obeyed by the binding energy at OEW compared to other impurity locations when the central barrier width is limited zero as shown in fig.4.21b and 4.21d.

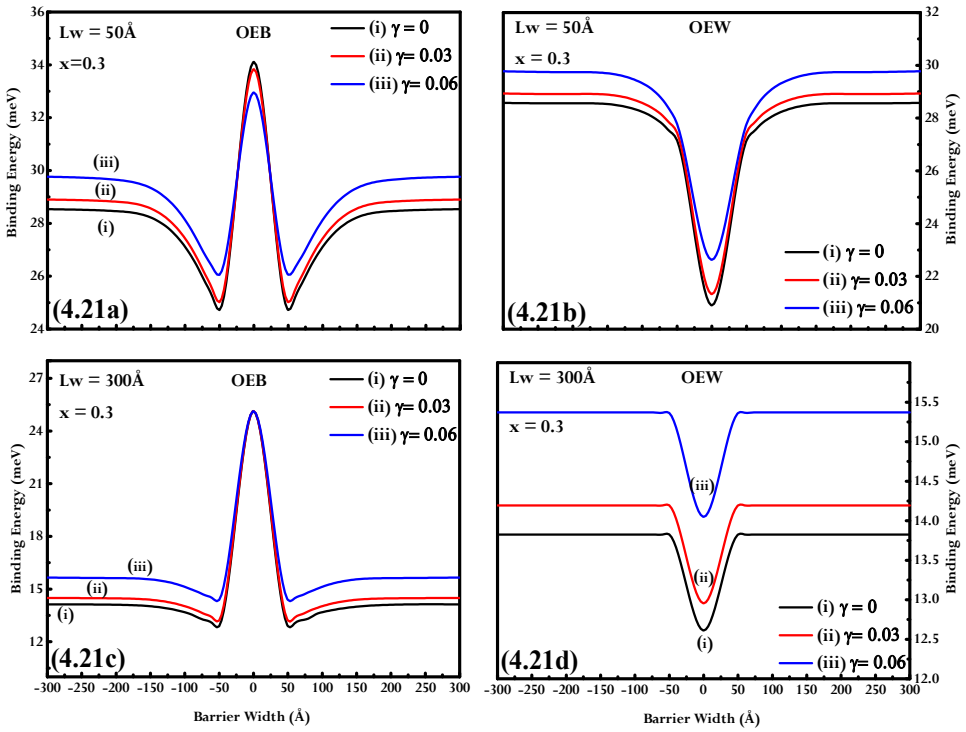

Figure 4.21: Variation of binding energy against width of the central barrier with the application of magnetic field. Results have been plotted for lower well width of L_w = 50Å for **(a)** OEB and **(b)** OEW as well as for higher well width of L_w = 300Å for **(c)** OEB and **(d)** OEW with Mn^{2+} ion concentration of x = 0.3.

These results can be justified from the probability distribution $|\psi^2|$ of holes as shown in fig. 4.22 for the above mentioned impurity locations with and without magnetic field.

OCB Impurity

γ = 0 **γ = 0.06**

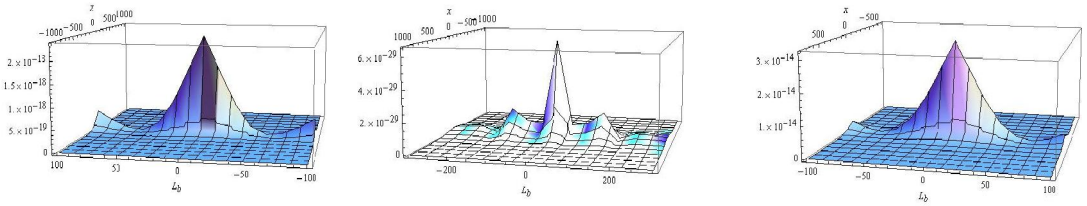

Lb = 100Å, Lw=50Å **Lb = 300Å, Lw=50Å** **Lb = 100Å, Lw=50Å**

OCW Impurity

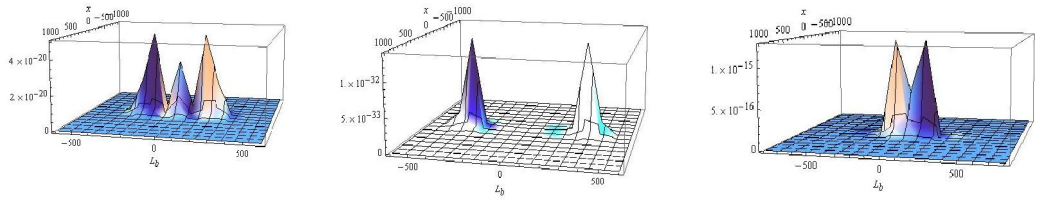

OEW Impurity

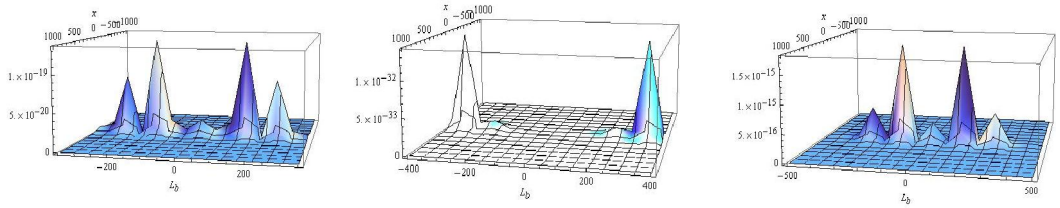

Figure 4.22: Probability density $|\psi^2|$ of the acceptor impurity placed at various impurity locations for various dimensions of the barrier and well under γ = 0 and γ =0.06 for Mn^{2+} ion concentration of x=0.3.

4.3.2. Conclusion

The acceptor impurity is highly localized only when it is situated at the centre of the DQW both in the absence and presence of magnetic field. The magnetic field reduces the confinement for the OCW impurity by reducing the potential barrier height and allowing the interwell coupling between the two Quantum Wells. But, it shows the reverse effect for all other impurity locations due to the strong exchange interaction of Mn^{2+} ions with hole. This gives the insight for extending the investigation on the acceptor impurity considering its complex nature of the valence band splitting in the presence of magnetic field.

B. Impurity states in a Semimagnetic Triangular Quantum Well

With the advantage of Molecular Beam Epitaxy (MBE), one can easily fabricate the QW systems with graded confining potential of different shapes like parabolic [43] and triangular [44] instead of abrupt band offset like rectangular QW [24]. Among them, Triangular Quantum Well (TQW) structures have attracted much attention in recent years because of their unique properties of quantum energy levels which is used for modelling Metal- Oxide Semiconductor structures which has been widely studied by many researchers [45-51]. An abundance of experimental [36] and theoretical [32, 52] investigations exists on both the acceptor and donor BMP in bulk DMS and the Quantum wells made of DMS materials with square confinement [23, 31]. Though lot of research works have been devoted to the study of impurity states in a Semimagnetic Quantum Well with square band – offset, studies of impurity states and the BMP associated with it in a Semimagnetic Triangular Quantum Well (STQW) are conspicuously missing. Hence, considerable attention has to be given on this field for theoretical research and practical applications since combining the DMS materials with the triangular shaped confining potential may be viable for spintronic applications.

4.4. *Magnetic field Driven Bound Magnetic Polaron with Compostional Effect in Semimagnetic Triangular Quantum Well*

The strength of the coupling between the sp- band electrons and the d-electrons of Mn^{2+} ions are precisely determined by the effective concentration of the Mn^{2+} ions present in these DMS materials. However studies on the effect of BMP on the energy levels with respect to the various combinations of the composition of Mn^{2+} ions in the well (x_{in}) and in the barrier (x_{out}) of DMS materials are conspicuously missing at lower dimensionalities. In the present communication, an attempt has been made to investigate the binding energy of the donor impurity and the Spin Polaronic Shift (SPS) due to the formation of BMP with and without the application of magnetic field as a function of different combinations of the composition of Mn^{2+} ions in the well $Cd_{1-x_{in}}Mn_{x_{in}}Te$ and in the barrier $Cd_{1-x_{out}}Mn_{x_{out}}Te$ of Semimagnetic Triangular Quantum Well (STQW) in such a way that the difference between the two composition ($x_{out} - x_{in} = x = 0.1, 0.2$) is same.

4.4.1. Theoretical Formalism

The Hamiltonian of a hydrogenic donor impurity inside the STQW made of $Cd_{1-x_{in}}Mn_{x_{in}}Te/Cd_{1-x_{out}}Mn_{x_{out}}Te$ DMS materials in the effective mass approximation in the presence of applied magnetic field along the direction of growth axis (z-axis) is written as in Eqn (4.2). The scheme of the BMP in STQW is shown in fig. 4.23 for which the profile of the confining potential V_B (z) for the carriers in symmetric TQW structures is given as

$$V_B(z)=\begin{cases}\dfrac{V_0|z|}{b} & ,-b<z<b\\ V_0 & ,|z|>b\end{cases} \tag{4.11}$$

Here, L = 2b is the width of the well and V_0=70% ΔE_g^B, where, ΔE_g^B is the band gap difference with magnetic field and is given by Eqn (2.3) for which the parameters has been defined in section 2.2.1.

The various combinations (C_i) of x_{in} and x_{out} in such a way that the difference between x_{out} and x_{in} is 0.1 and 0.2 (x_{out} - x_{in} = x =0.1, 0.2) accounted for the study is as follows:

x = 0.1	**x = 0.2**
$C_1 : x_{in} = 0, x_{out} = 0.1$	$C_1 : x_{in} = 0, x_{out} = 0.2$
$C_2 : x_{in} = 0.01, x_{out} = 0.1$	$C_2 : x_{in} = 0.005, x_{out} = 0.2$
$C_3 : x_{in} = 0.1, x_{out} = 0.2$	$C_3 : x_{in} = 0.02, x_{out} = 0.2$
$C_4 : x_{in} = 0.2, x_{out} = 0.3$	$C_4 : x_{in} = 0.1, x_{out} = 0.3$

(4.12)

The approximate ground state energy for confined donor impurity has been calculated using the variational method. The envelop function f (z) is considered as [45],

$$f(z)=\begin{cases}c_1 e^{\beta(z+b)} & , \quad z<-b\\ c_2 Ai\left[\left(\dfrac{2m_w^* V_0}{b\,h^2}\right)^{1/3}\left(-z-\dfrac{b\,E_0}{V_0}\right)\right]+c_3 Bi\left[\left(\dfrac{2m_w^* V_0}{b\,h^2}\right)^{1/3}\left(-z-\dfrac{b\,E_0}{V_0}\right)\right] & , \quad -b<z<0\\ c_4 Ai\left[\left(\dfrac{2m_w^* V_0}{b\,h^2}\right)^{1/3}\left(z-\dfrac{bE_0}{V_0}\right)\right]+c_5 Bi\left[\left(\dfrac{2m_w^* V_0}{b\,h^2}\right)^{1/3}\left(z-\dfrac{bE_0}{V_0}\right)\right] & , \quad 0<z<b\\ c_5 e^{-\beta(z-b)} & , \quad z>b\end{cases} \tag{4.13}$$

where, $\beta = 2m_b^*[(V_0 - E_0])^{1/2}$ and Ai[z], Bi[z] are Airy functions, E_0 is the energy of the lowest conduction band. The constants c_1, c_2, c_3, c_4 and c_5 and E_0 are obtained by choosing the proper boundary conditions.

The trial wavefunction of the ground state is chosen as given in Eqn (4.6) and the expectation value of **H** is minimized with respect to λ and the binding energy of the donor

impurity in the presence of magnetic field is found by solving the Schrödinger equation variationally using Eqn (4.8). The Spin Polaronic shift is calculated using Eqn (4.3) for various combinations of the composition of Mn^{2+} ion as given in Eqn (4.12).

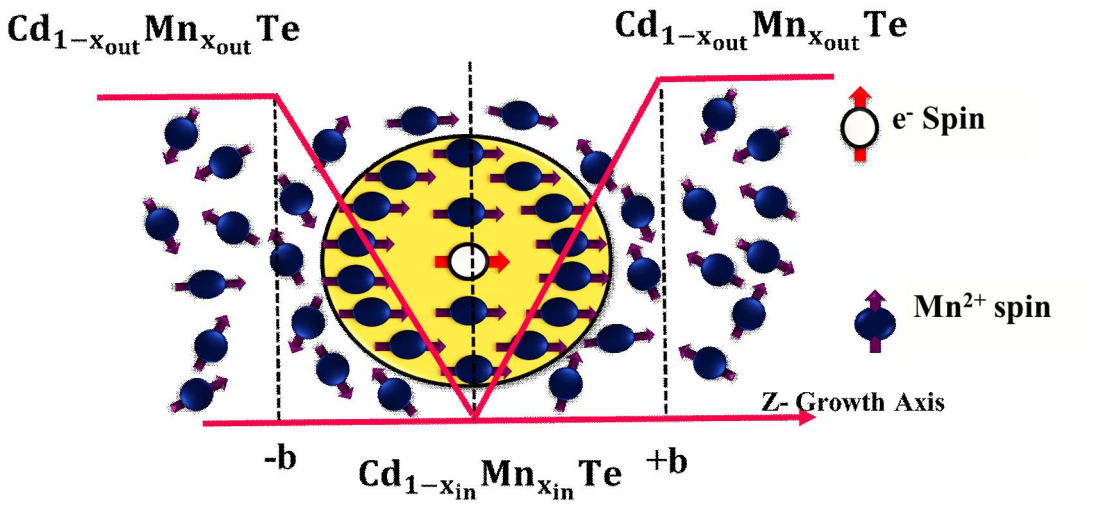

Figure 4.23: Formation of Bound Magnetic Polaron (BMP) in a Semimagnetic Triangular Quantum Well (STQW).

4.4.2. Results and Discussion

4.4.2.1. *Binding Energy of the donor impurity in a STQW*

The results for the variation of binding energy of the donor impurity confined in a $Cd_{1-x_{in}}Mn_{x_{in}}Te/Cd_{1-x_{out}}Mn_{x_{out}}Te$ TQW as a function of well width is reported in fig. 4.24 for various combinations of Mn^{2+} ion in the well and in the barrier materials for the resultant composition $x_{out} - x_{in} = x = 0.1$ without the application of magnetic field. The figure clearly shows that the donor binding energy increases as the well width decreases from the bulk towards the low dimensional region and it attains the maximum when the size of the well is shrunk to the effective Bohr Radius (≈14 meV) and below which it starts to fall again which is the well-known characteristic behavior of any low dimensional structures approaching towards strictly 2 Dimensional [24, 26, 31]. The carrier confinement in a STQW is being much affected by the composition of the magnetic

impurity ion (x_{in} and x_{out}) which are varied simultaneously as given in Eqn (4.12) both in the well and in the barrier material.

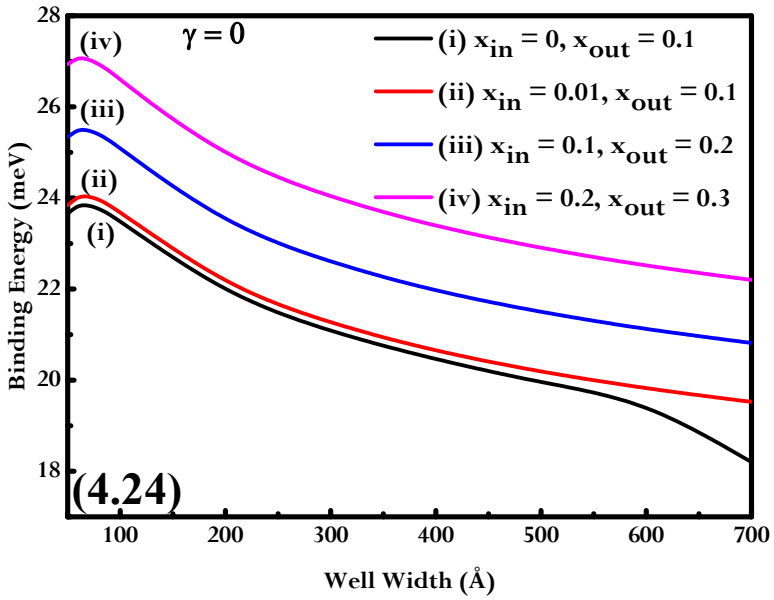

Figure 4.24: Variation of Binding Energy against the well width for different combinations of concentration of Mn^{2+} for composition of x = 0.1 (x_{out} -x_{in} = x = 0.1) in a STQW without the application of magnetic field ($\gamma = 0$).

This can be clearly seen from the figure that the binding energy increases as x_{in} and x_{out} increases simultaneously. This can be understood on the basis of the following qualitative argument: when the composition of magnetic impurity ion (Mn^{2+}) increases simultaneously there is a possibility for the electrons to have exchange interaction with the large number of magnetic moments of the Mn^{2+} ions within its orbit since the electron wavefunction is a spatially extended one. Therefore the probability for the spin of the electron being strongly polarized and trapped in the field created by the average magnetic moments of Mn^{2+} ions is very high which leads to the larger confinement of the carrier in such STQW. When the external magnetic field of strength $\gamma = 0.05$ and $\gamma = 0.1$ is applied, the binding energy gets decreased as shown in fig. 4.25. This is because, the applied magnetic field tremendously reduces the confining potential (100.8meV, 68.27meV,

36.56meV for $\gamma = 0, \gamma = 0.05$ and $\gamma = 0.1$ respectively) in which the carrier has been confined and thereby the impurity energy levels become shallower which causes the tunneling of the carrier through the barrier material $Cd_{1-x_{out}}Mn_{x_{out}}Te$.

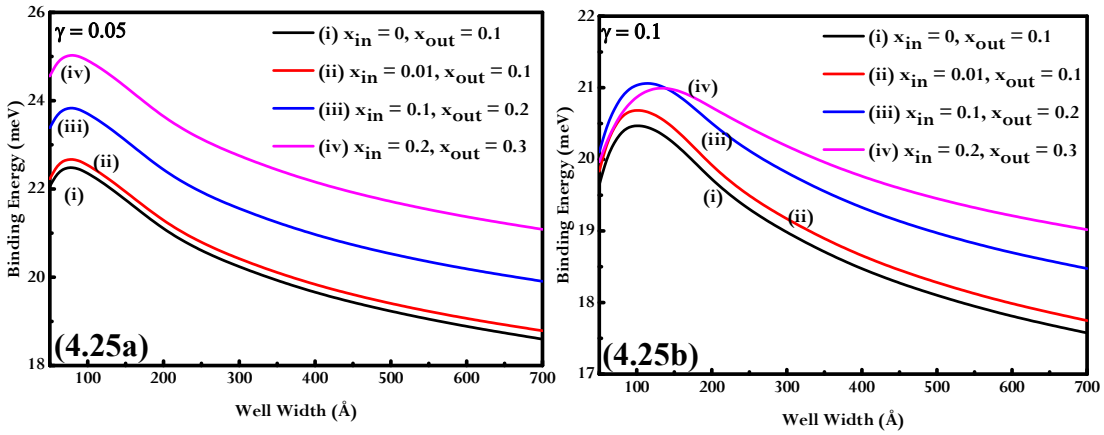

Figure 4.25: Variation of Binding Energy against the well width for different combinations of concentration of Mn^{2+} for composition of x = 0.1 (x_{out} -x_{in} = x = 0.1) in a STQW with the application of magnetic field (a) $\gamma = 0.05$ and (b) $\gamma = 0.1$.

A shift in the maximum of binding energy is seen conspicuously in the low dimensional region when the magnetic field of strength $\gamma = 0.1$ is applied which is again the well-known feature of any Semimagnetic Nanostructured Systems under the application of magnetic field. It is noted from the figure that the variation of binding energy with the well width for $\gamma = 0.1$ is not as rapid as the variation observed for $\gamma = 0$ and $\gamma = 0.05$ and the same is the case with the various combinations of Mn^{2+} ion as well. The fact lies behind this trend of the binding energy is very clear as the strength of the applied magnetic field $\gamma = 0.1$ is very nearer to the critical magnetic field ($\approx\gamma = 0.16$) at which the barrier vanishes completely ($V_0 = 0.08$meV) and the QW almost vanishes which leads the carriers to become free as in the bulk system. Moreover the binding energy for all the values of γ converges when the well width is increased towards the bulk limit as one can see from the numerical values of the binding energy for various γ.

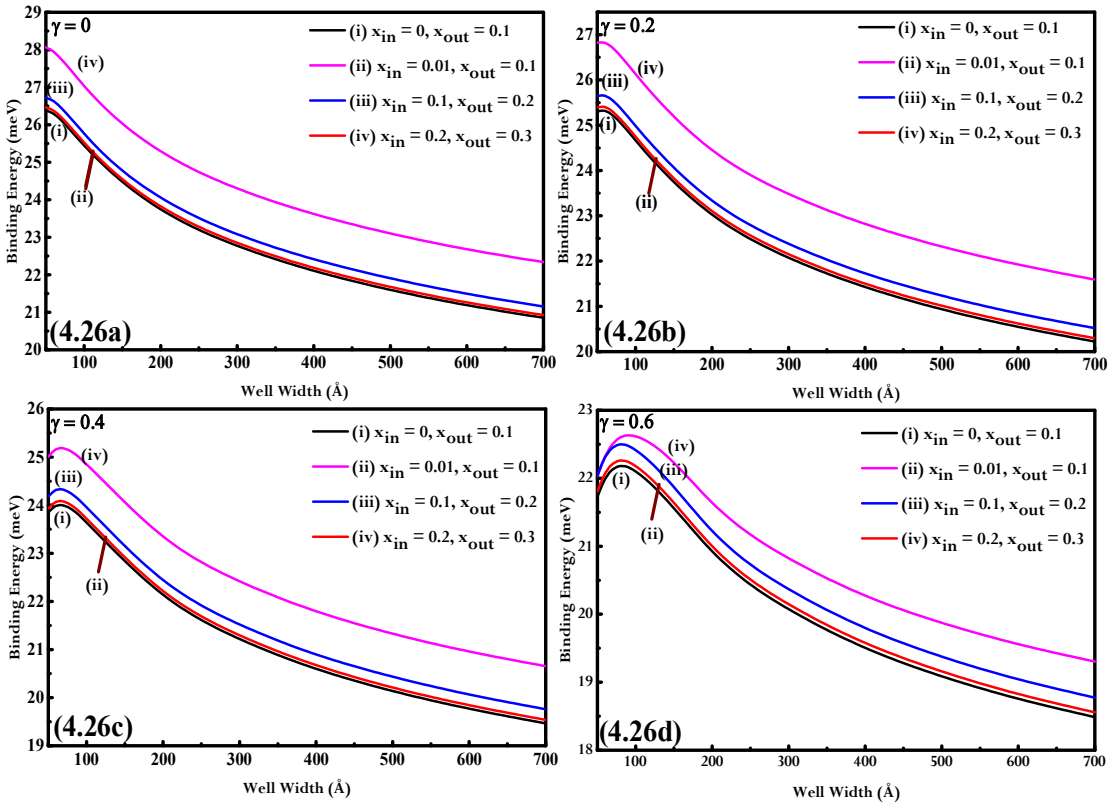

Figure 4.26: Variation of Binding Energy against the well width for different combinations of concentration of Mn^{2+} for composition of x = 0.2 (x_{out} -x_{in} = x = 0.2) in a STQW with and without the application of magnetic field **(a)** γ = 0, **(b)** γ = 0.2, **(c)** γ = 0.4 and **(d)** γ = 0.6.

The graphs for binding energy of the donor impurity for the resultant composition of Mn^{2+} ion x = 0.2 are plotted in fig. 4.26 with and without the application of magnetic field for various combinations of x_{in} and x_{out} ($x_{out} - x_{in}$ = x = 0.2) as given in Eqn (4.12). It is apparent from the said figure that the trend of the binding energy with the Mn^{2+} ion composition of x = 0.2 is as same as the trend seen for x = 0.1 but with the larger magnitude in binding energy. The reason for this behavior may be given as the potential barrier height is directly proportional to the composition of Mn^{2+} ion substituted into the host lattice which makes the impurity energy levels to become deeper thereby leads to the larger confinement of the carrier inside the well.

4.4.2.2. *Spin Polaronic Shift (SPS) due to BMP in STQW*

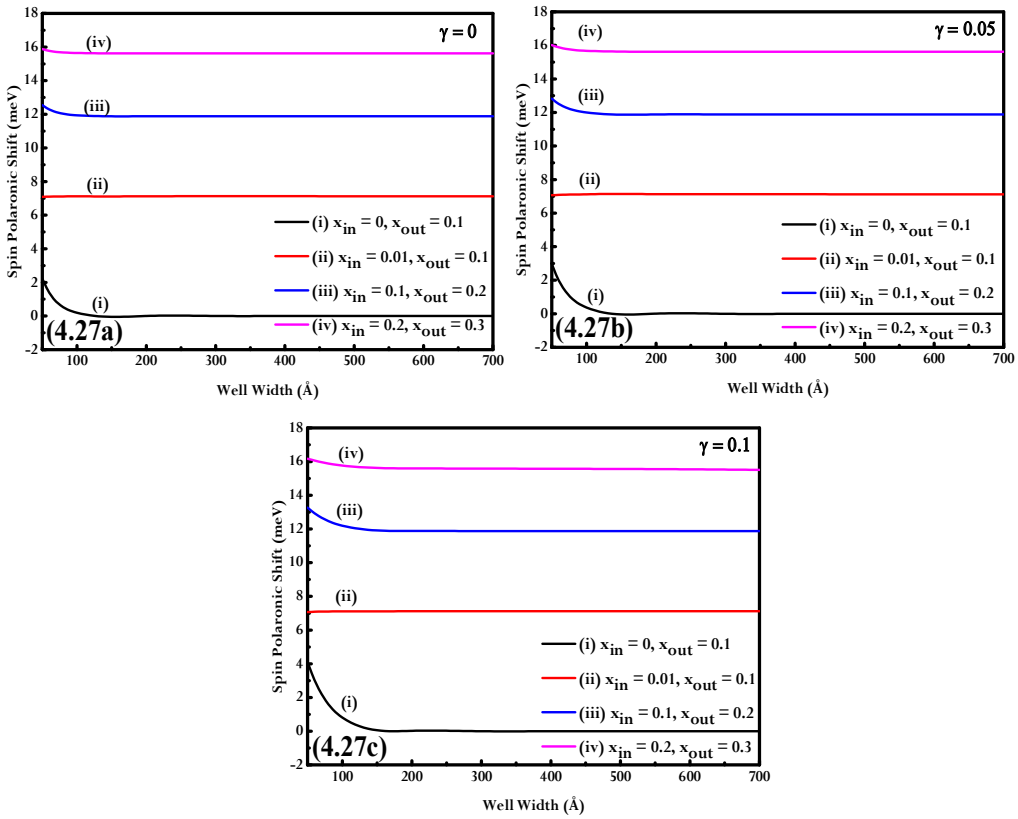

Figure 4.27: Variation of Spin Polaronic Shift against the well width for different combinations of concentration of Mn^{2+} for composition of x = 0.1 (x_{out} -x_{in} = x = 0.1) in a STQW with and without the application of magnetic field **(a)** γ = 0, **(b)** γ = 0.05 and **(c)** γ = 0.1.

The SPS as a function of well width and various combinations of x_{in} and x_{out} ($x_{out} - x_{in}$ = x = 0.1) is presented in fig. 4.27 for the cases with and without the application of magnetic field. The figure shows the increase of SPS, once the composition of Mn^{2+} ion x_{in} and x_{out} increases simultaneously and when the carrier is subjected to the external applied magnetic field also. The behavior attributed to this increase of SPS for various combinations of Mn^{2+} ion is as same as the reason stated earlier for the binding energy variation. All the spins of the Mn^{2+} ions and the carrier are in random directions in the absence of magnetic field. Hence, they cannot contribute to the net magnetic moment

with the average spin per magnetic ion i.e.$< S_z > = 0$. Once the magnetic field is applied all the spins align parallel to the applied magnetic field which results in magnetic ordering in the semiconducting lattice.

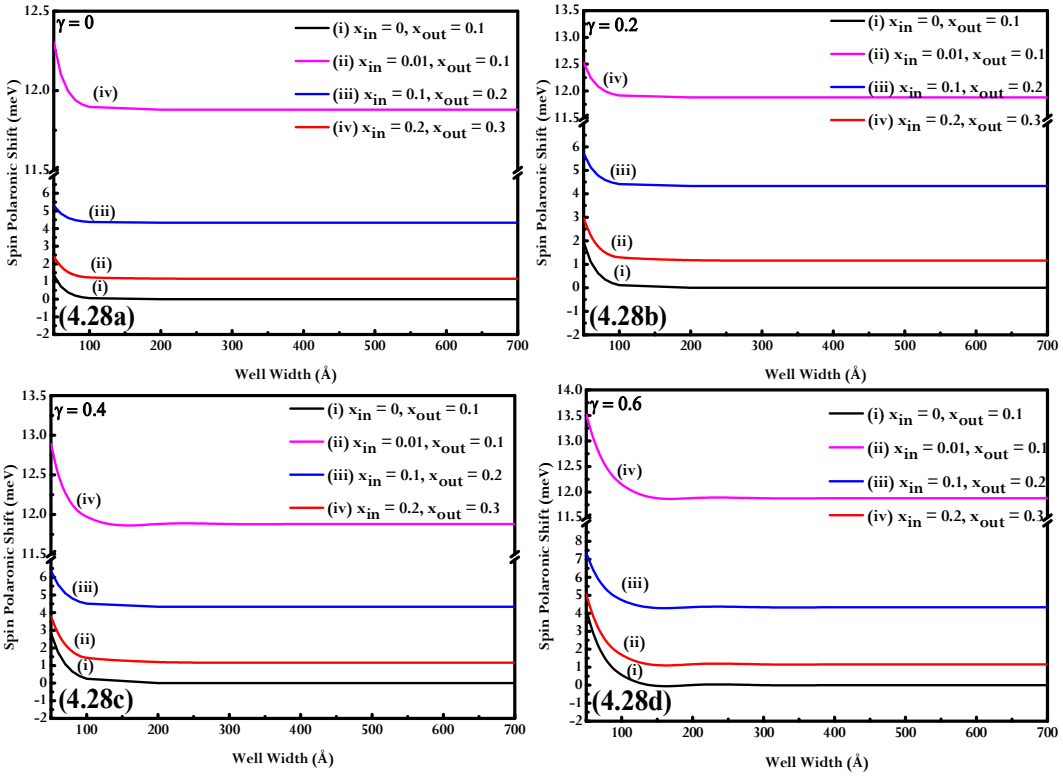

Figure 4.28: Variation of Spin Polaronic Shift against the well width for different combinations of concentration of Mn^{2+} for composition of x = 0.1 (x_{out} -x_{in} = x = 0.2) in a STQW with and without the application of magnetic field **(a)** γ = 0, **(b)** γ = 0.2, **(c)** γ = 0.4 and **(d)** γ = 0.6.

Hence the exchange interaction between the Mn^{2+} ions and the carrier is greatly enhanced thereby increasing the shift largely as one can see from the numerical results of SPS reported in fig. 4.27b and 5c for γ = 0.05 and γ = 0.1. When Mn^{2+} ions substituted with higher concentration like x = 0.2, the trend of the variation of SPS is as same as in the case with x = 0.1 except for the lower in numerical value as displayed in fig. 4.28. This can be justified from the fact that when the concentration of Mn^{2+} ions is low, x < 0.005, the interaction between the magnetic moments of the Mn^{2+} ions is very low [21]. Hence,

all the Mn^{2+} ions can contribute to the total magnetic moment with the average spin per magnetic ions $<S_z>$. But when x increases beyond 0.005, spins of nearest neighbour cancels out due to the antiferromagnetic interaction between the Mn^{2+} ions which reduces the number of ions contributing to the total magnetic moment. Eventually, only an effective concentration $\bar{x}$ of Mn^{2+} ions which is always less than x contributes to the total magnetic moment. It is evident from the results reported by Gaj et.al. [27] that the numerical value of the spin of Mn^{2+} ion is not at all consistently maintained as 5/2 rather it decreases because of the interaction between the nearest neighbour Mn^{2+} ions is antiferromagnetic in nature which has been included in the SPS calculation through the semi phenomenological fitting parameters S_0 and T_0 as given in Eqn (4.3).

4.4.3. Conclusion

The effect of various combinations of the composition of Mn^{2+} ions on the bound states of STQW and also on the properties of BMP have been investigated. It is found that the ground state binding energy and the SPS depends only on the density of the magnetic ions separately concentrated in the well $Cd_{1-x_{in}}Mn_{x_{in}}Te$ and in the barrier $Cd_{1-x_{out}}Mn_{x_{out}}Te$ of STQW even though the effective concentration is same ($x_{out} - x_{in} = x = 0.1, 0.2$). A counterintuitive behaviour is observed for the ground state binding energy and the SPS when the effective concentration of Mn^{2+} ion is increased from x = 0.1 to x = 0.2 under different magnetic field strength. Since the TQW is mainly used to model the Metal – Oxide Semiconductor (MOS) Devices, the present study may be useful in spin based MOS structures where the properties of the spin can be exploited to device an ultrahigh density non-volatile memory and reconfigurable logic devices based on novel spintronic concepts.

4.5. *Acceptor Bound Magnetic Polaron in a Semimagnetic Triangular Quantum Well*

In this work, we investigate to what extent the confinement of the heavy and light holes (hh and lh) bound to an acceptor impurity gets affected when it is confined in a STQW made of $Cd_{1-x_{in}}Mn_{x_{in}}Te/Cd_{1-x_{out}}Mn_{x_{out}}Te$ with composition of Mn^{2+} ion x = 0.2 with x_{in} = 0.1 and x_{out} = 0.3 and its impact on the shift in the polaronic energy under the external applied magnetic field. Using the mean field theory with modified Brillouin function function, the exchange interaction between the carrier and magnetic impurity which causes the Spin Polaronic Shift (SPS) in the presence of an external magnetic field **B** can be written as

$$E_{exc} = \frac{q}{6}\beta N_0 \left\{ \langle \Psi | x_{in} S_0(x_{in}) B_s(y_1) | \Psi \rangle + \langle \Psi | x_{out} S_0(x) B_s(y_2) | \Psi \rangle \right\} \tag{4.14}$$

Here, q=3, 1 for heavy hole of spin 3/2 and light hole of spin ½ respectively.

4.5.1. Results and Discussion

The results for the variation of binding energy of the heavy hole (hh) and light hole (lh) bound to an acceptor impurity confined in a $Cd_{1-x_{in}}Mn_{x_{in}}Te/Cd_{1-x_{out}}Mn_{x_{out}}Te$ TQW as a function of well width are reported in fig. 4.29a for the resultant composition of Mn^{2+} ion x = 0.2 ($x_{out} - x_{in} = x$) with and without the application of magnetic field. The results apparently shows that the hh is tightly bound inside the well rather than the lh. This may be due to the fact that the effective mass of the hh is about six times larger than the lh effective mass. Moreover, the smaller band – offset created in the valence band during the formation of heterostructure between CdTe/CdMnTe may lead to the less number of lh states as compared to the hh states. For each kind of the carrier i.e hh and lh, the semimagnetic barrier height vanishes completely and the quantum size effects are

suppressed for different values of critical magnetic field ($\gamma = 0.014$, $\gamma = 0.15$ for hh and lh respectively). With reference to the aforesaid values of the critical magnetic field, all the calculations for hh have been carried out under the applied magnetic field of strength $\gamma = 0.004$, 0.008, 0.01 and for the lh subjected to the magnetic field of strength $\gamma = 0.05$, 0.1.

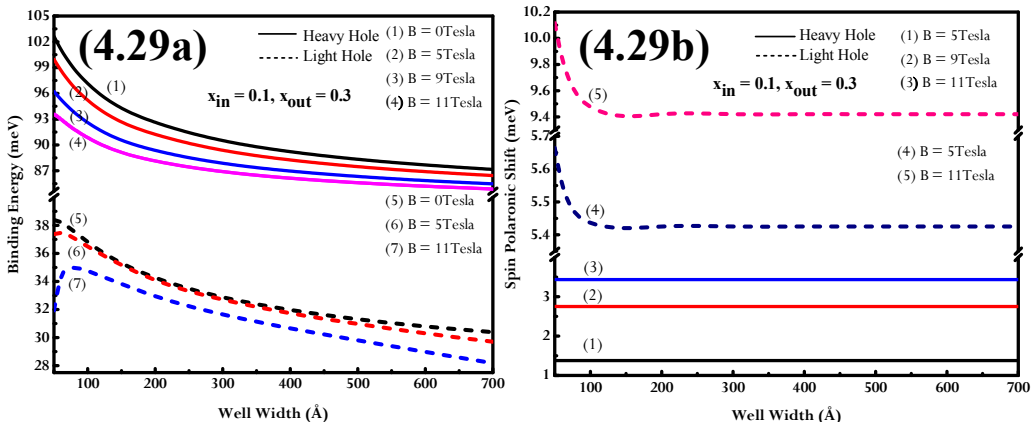

Figure 4.29: Variation of **(a)** Binding Energy, **(b)** Spin Polaronic Shift of the acceptor impurity as a function of well width for various magnetic fields with Mn^{2+} ion concentration of x = 0.2. Solid line shows the variation for heavy hole and dashed line shows for light hole.

The binding energy decreases as a function of applied magnetic field for both type of holes which is a well-known and unique feature of the CdMnTe QW. The reason for this behavior may be attributed as: the applied magnetic field tremendously reduces the Semimagnetic potential barrier created by the band – offset ($30\%\Delta E_g^B$) as given in Eqn (2.3). It is conspicuous from the figure that the turnover in the binding energy with respect to the well width is seen only for the lh states rather than for hh states. This remarkable feature of the lh may be understood as follows: because of the larger difference in the effective masses between these two carriers, there is a possibility for the envelop function ascribed to the lh to penetrate into the semimagnetic barrier even at a well width of L = 50Å which is the promising well width for hh where it finds the

maximum localization inside the well. But one can find from the figure that there is a noticeable shift in the turnover of the binding energy towards higher well width when the applied magnetic field approaches the critical value. This can be understood that the QW will have bound states associated with the lh, only from the well width of L = 80Å because the applied magnetic field drastically reduces the potential barrier. When the well width is reduced below this value, the changes in the total height of the barrier with magnetic impurity leads the envelope function of the lh to penetrate into the barrier material. The veracity of our results can be checked by the limiting case of $L \rightarrow \infty$, when the well width approaches the bulk value, the binding energy E_B approaches towards $1R^*$ for 1s state (81.34meV, 24.54meV for hh and lh respectively). The peculiar feature of the magnetic semiconductor is the motion of Bloch hole bound to an acceptor impurity across the magnetic ions present in the semiconducting lattice and thus polarizing the spin of the magnetic ions present within its hydrogenic orbit which leads to the formation of BMP. This creates the magnetic potential and has a pronounced effects on the hole states due to the larger value of $N_0\beta \approx$-880meV and the smaller value of the band – offset.

Fig. 4.29b depicts the variation of SPS as a function of well width for both heavy and lhs bound to an acceptor impurity inside a STQW with the application of external magnetic field for the Mn^{2+} composition of x = 0.2 (x_{out} - x_{in} = x). Two interesting aspects that should be pointed out from these figures are: (i) The SPS is very much larger for the lh as compared with the hh which is juxtaposition to the binding energy case. This can be understood that the Bohr radius of hydrogenic orbit associated with the lh in CdMnTe QW is very larger (28.7Å) than the radius of the hh orbit (8.6Å), and there is a possibility for the lh encompassing a large number of magnetic ions within its orbit. Therefore the energy required for the lh to polarize all the spins of large number of magnetic ions is very large. (ii) The applied magnetic field drastically affects the BMP as one can see that

the increase of SPS as a function of magnetic field as shown in fig. 4.29b. For increasing magnetic field, the magnetic potential created by the strong exchange interaction between the spins of Mn^{2+} ions and the spin of the band holes also increases which causes an increase in shift. But the increase of SPS for the hh with the applied magnetic field is not as rapid as seen in the case of lh. This is due to the larger effective mass and the smaller effective Bohr radius of the hh which causes the magnetic potential (resulting from the spin – spin exchange interaction) amounts to just few meV, even for higher magnetic fields. Due to the Quantum size effects the SPS for lh has a maximum only for the lower well width and decreases as a function of increasing the size of the well and attains a saturation once it approaches the bulk limit. On the other hand, there is no much attention is paid to the variation of SPS associated with the hh since no new quantum size effects can be observed.

It is very clear from the available literatures that not much effort has been made to investigate on the BMP in STQW. Hence, the present work may be helpful in understanding the impurity states accounting the BMP associated with the hh and lh confined in such TQW which can be exploited in various optoelectronic and spintronic devices.

References

1. P. Nithiananthi, K. Jayakumar, *Int. J. Nanosci.* **2011**, *10*, 611–615.
2. J.A. Gaj, J. Ginter, *Phys. Status Solidi Basic Res.* **1978**, 655–662.
3. G. Rebmann, C. Rigaux, G. Bastard, M. Menant, R. Triboulet, W. Giriat, *Phys. B+C.* **1983**, *117–118*, 452–454.
4. J.P. Lascaray, D. Coquillat, J. Deportes, A.K. Bhattacharjee,, *Phys. Rev. B.* **1988**, *38*, 7602–7606.
5. T. Kasuya, *Rev. Mod. Phys.* **1968**, *40*, 684–696.
6. U. Thibblin, *Int. J. Mod. Phys. B*.**1989**, *3*, 337–366.
7. T. Dietl, J. Cibert, P. Kossacki, D. Ferrand, S. Tatarenko, A. Wasiela, Y. Merle D'Aubigné, F. Matsukura, N. Akiba, H. Ohno, *Phys. E Low-Dimensional Syst. Nanostructures.* **2000**, *7*, 967–975.
8. C. Camilleri, F. Teppe, D. Scalbert, Y. Semenov, M. Nawrocki, M. Dyakonov, J. Cibert, S. Tatarenko, T. Wojtowicz, *Phys. Rev. B.* **2001**, *64*, 1–7.
9. P. Nithiananthi, K. Jayakumar, *Phys. Status Solidi Basic Res.* **2009**, *246*, 1238.
10. P. Nithiananthi, K. Jayakumar, *Int. J. Mod. Phys. B.* **2005**, *19*, 3861–3868.
11. H. Chen, S. Zhou, *Phys. Rev. B.* **1987**, *36*, 9581.
12. D.B.T. Thoai, *Phys. B.* **1991**, *175*, 373–380.
13. N. Raigoza, A. L. Morales, A. Montes, N. Porras – Montenegro,C. A. Duque, *Phys. Rev. B.* **2004**, *69*, 045323.
14. P. Kalpana, K. Jayakumar, P. Nithiananthi, *Int. J. Comput. Mater. Sci. Eng.* **2015**, *4*, 1550018.
15. G. Vignesh, P. Nithiananthi, *Superlattices Microstruct*. **2016**, *92*, 232–241.
16. D. Yoshioka and Allan H. Macdonald, *J. Phys. Soc. Jap*. **1990**, *59*, 4211–4214.

17. G.S. Boebinger, H.W. Jiang, L.N. Pfeiffer, K.W. West, *Phys. Rev. Lett.* **1990**, *64*, 1793–1796.

18. L. Brey, *Phys. Rev. Lett.* **1990**, *7*, 903–906.

19. G.S. Boebinger, A. Passner, L.N. Pfeiffer, K.W., *Phys. Rev. B.* **1991***, 43*, 12673.

20. M. Orlita, R. Grill, S. Malzer, M. Byszewski, *Phys. Rev. B.* **2005**, *72*, 165314.

21. S. Lee, M. Dobrowolska, J.K. Furdyna, H. Luo, L.R. RamMohan, *Phys. Rev. B.***1996***, 54*, 16939–16951.

22. B.E. Larson, K.C. Hass, H. Ehrenreich, A.E. Carlsson, **Solid State Commun**. **1985**, *56*, 347–350.

23. A. Elangovan, D. Shyamala, K. Navaneethakrishnan, *Solid State Commun*. **1994**, *89,* 869 – 873.

24. K. Gnanasekar, K. Navaneethakrishnan, *Mod. Phys. Lett. B.* **2004**, *18*, 419–426.

25. C. Rajamohan, K. Jayakumar, *J. Nano. Electron. Phys*. **2011**, *3*, 1005-1009.

26. A. Merwyn Jasper De Reuben, K. Jayakumar, *Int. J. Nanosci.* **2011***, 10*, 665–668.

27. J.A. Gaj, R. Planel, G. Fishman, *Solid State Commun.* **1979**, *29*, 435–438.

28. P. Nithiananthi, D. Varshney, K. Jayakumar, *Conference*, *Int. Conf. Nanosci. Nanotech.* **1985**, 6962–6964.

29. C. E. T. Gonvalves da Silva, *Phys. Rev. B.* **1985**, *32*, 6962–6964.

30. M. Jain, Diluted Magnetic Semiconductors, in: G.E.Marques (Eds.), *World Scientific*; Singapore, USA, UK, **1991**, pp. 492, 518.

31. K. Jayakumar, P. Nithiananthi, *J. Nano. Electron. Phys.* **2011**, *3*, 375-379.

32. W. E. Hagston, T. Stirner, P. Harrison, O. F. Holbrook and J. P. Goodwin, *Phys. Rev. B*. **1994**, *50*, 5264-5271.

33. S. S. Nedorezov, *Fiz. Tverdogo Tela*.**1970**, *12*, 2269.

34. J. Warnock and P. A. Wolf, *Phys. Rev. B.* **1985**, *31*, 6579.

35. A. K. Bhattarjee, *Solid State Commun*.**1986**, *57*, 31.

36. T. H. Nhung, R. Planel, C.Benot a la Guillaume and A.K.Bhattacharjee, *Phys.Rev. B*. **1985**, *31*, 2388.

37. J. Mycielski and C. Rigaux, *J. de Phys*. **1984**, *44*, 1041.

38. A. Mycielski and J. Mycielski, *J. Phys. Soc.Japan Suppl. A*. **1980**, *49*, 807**.**

39. T. R. Gawron and J. Mycielski, *Phys. Status Solidi b.* **1984**, *125*, 341.

40. T. R. Gawron, *J. Phys. C: Solid State Phys.***1986***, 19*, 21.

41. A. Baldereschi and N. Lipari, *Phys. Rev. B.* **1973***, 8*, 2697.

42. Sr. Gerardin Jayam, K. Navaneethakrishnan, *Int.J.Mod.Phys. B.* **2002**, *16*, 3737.

43. T. Wojtowicz, M. Kutrowski, M.Surma, K. Kopalko, G. Karczewski, J. Kossut, M. Godlewski, P. Kossacki and Nguyen The Khoi, *J. Appl. Phys. Lett.* **1996***, 68*, 3326.

44. T. Wojtow, G. Karczewski, J. Kossut, *Thin solid Films*, **1997**, *306*, 271.

45. P. Kalpana and K. Jayakumar, *J.Phys.Chem.Solids*. **2017**, *110,* 364.

46. Guang –Zuo Jiang and Cheng – Zhong Wen, *Phys. Rev. B*. **1994**, *50*, 2689.

47. R. F. Kopf, M. H. Herman, M. Lamont Schnoes, A. P. Perley, G. Livescu and M. Ohring, *J.Appl.Phys.* **1992**, *71,* 5004.

48. Jun Wang, Shu Shen Li, Yan – Wu Lü, Xiang – Lin Liu, Shao –Yan Yang, Qin – Sheng Zhu, Zhan-Guo Wang, *Nanoscal Res Lett.* **2009**, *4*, 1315.

49. Zhang Hairui and Sun Yong, *J. Semicond.* **2014**, *35*, 102001- 1.

50. P. Kalpana, A. Merwyn Jasper D Reuben, P. Nithiananthi and K. Jayakumar, *AIP. Conf. Proc.***2017**, *1832*, 090032

51. R. Khordad, *Solid State Sci.* **2013**, *19*, 63.

52. M. I. Auslender, I. I. Zyapilin, A. B. Zolotovitskii and V. V. Karyagin, *Solid State Commun.* **1988**, *67*, 535-539.

Chapter 5

COULOMB INTERACTION OF ELECTRONS IN SEMIMAGNETIC NANOSTRUCTURED SYSTEMS

5.1. Introduction

The influence of high magnetic field has very profound effects on physical phenomenon in Low Dimensional Semiconducting Systems (LDSS) like Quantum Well (QW), Quantum Well Wire (QWW) and Quantum Dot (QD) which modifies the density of states due to the formation of Landau levels in these structures. Therefore, the nature of the impurity states associated with such LDSS is a subject of considerable technical and scientific relevance because of its potential applications in Optoelectronic and Spintronic devices. Moreover, the prospect of understanding electron correlations in a simple system like QW, QWW and QD Helium which are occupied by two electrons in each has been a driving force for much of the theoretical work since the Coulomb interaction between them leads to unusual magnetic – field dependence of the ground state and its excitations. Many researchers have put their considerable effort to investigate the single and double donor / acceptor impurities widely on GaAs systems [1-14]. The effective mass theory for helium – like donors in bulk semiconductors was first carried out by Glodeanu [15] and various experimental studies for the same were carried out by Grimmeiss et al [16,17]. The energy spectra of two electrons in a parabolic QWW and QD have been thoroughly studied by G.Y. Hu et.al [18] and D. Pfannkuche et. al [19], Metkit et.al [20] respectively.

Correa et.al [21] have analysed the spectrum of two electrons confined inside a non-isotropic parabolic QD using the fractional dimensional formulation. Though the role of hydrogen – like donors in DMS systems have received some attention, studies of the helium –like donors have not been paid much attention. Therefore, studies in this field are still important for both theoretical research and practical applications. The present investigation discusses how the electron – electron interaction gets affected by the applied magnetic field and alters the binding of the carriers confined in a CdTe/ $Cd_{1-x}Mn_xTe$ QW, QWW and QD DMS systems for the composition of Mn^{2+} ion, x = 0.3.

5.2. Theoretical Formalism

The Hamiltonian for the He – like impurity confined in a $CdTe/Cd_{1-x}Mn_xTe$ Square Quantum Well / Wire / Dot is written as,

$$\mathbf{H}_{ee} = -(\nabla_1^2 + \nabla_2^2) - 2z\left(\frac{1}{r_1}+\frac{1}{r_2}\right) + V_B(q_1) + V_B(q_2) + \gamma\,(L_{z_1}+L_{z_2}) + \frac{\gamma^2}{4}(\rho_1^2+\rho_2^2) + \frac{2}{|\vec{r_1}-\vec{r_2}|} \tag{5.1}$$

The effective confinement potential for the two electrons in a QW is given as,

$$V_B = \begin{cases} 0 & |q_1|, |q_2| \le L/2 \\ V_0 & |q_1|, |q_2| > L/2 \end{cases} \tag{5.2}$$

$$q_1 = \begin{cases} z_1 \\ x_1, y_1 \\ x_1, y_1, z_1 \end{cases} \quad ; \quad q_2 = \begin{cases} z_2 & \rightarrow \text{QW} \\ x_2, y_2 & \rightarrow \text{QWW} \\ x_2, y_2, z_2 & \rightarrow \text{QD} \end{cases}$$

The envelop function is chosen to be a product of the lowest subband energy states of the two electrons confined inside the QW is given by,

$$f(z_1, z_2) = N_{1s} \begin{cases} B\, e^{\beta z_1} e^{\beta z_2} & z_1, z_2 \le -L/2 \\ \mathrm{Cos}\,\alpha z_1\, \mathrm{Cos}\,\alpha z_2 & -L/2 < z_1, z_2 < L/2 \\ B\, e^{-\beta z_1} e^{-\beta z_2} & z_1, z_2 \ge L/2 \end{cases} \rightarrow \textbf{QW} \tag{5.3}$$

$\alpha = \sqrt{\frac{2m_w^* E}{\hbar^2}}$, $\beta = \sqrt{\frac{2m_b^* (V_0 - E)}{\hbar^2}}$; for QWW and QD, it is given by Eqn (2.4) and Eqn (3.4) respectively.

The approximate ground states for the confined two electrons have been calculated using the variational approach. The variational ansatz is written as

$\Psi_{QW} = f(z_1, z_2)\, e^{-\lambda (r1+r2)}$ in QW and for QWW, QD, it is given by Eqn (2.6) and Eqn (3.5) respectively which are correspond to without considering correlation.

The expectation value of $\mathbf{H_{ee}}$ is minimized with respect to λ and the electron-electron interaction energy is obtained by,

$$E_{e\text{-}e} = \left\langle \Psi_{QW,QWW,QD}(r_1, r_2) \left| \frac{2}{|\vec{r_1} - \vec{r_2}|} \right| \Psi_{QW,QWW,QD}(r_1, r_2) \right\rangle \tag{5.4}$$

The binding energy of the two electrons in the presence of magnetic field is found by solving the Schrödinger equation variationally using the Eqn (2.8).

5.3. Results and Discussion

The variation of binding energy for the He-like impurity confined inside a CdTe / $Cd_{1-x}Mn_xTe$ Square Quantum Well with and without the application of magnetic field ($\gamma = 0$, $\gamma = 3$, $\gamma = 6$) as a function of well width is depicted in fig. 5.1 for the composition of Mn^{2+} ion x = 0.3. It is noted from the figure that for the case with $\gamma = 0$, the binding energy increases gradually as the well width is reduced from the bulk regime towards the Quasi two dimensional regime and it attains maximum when the well width reaches approximately the effective Bohr radius of the confining system (60Å).

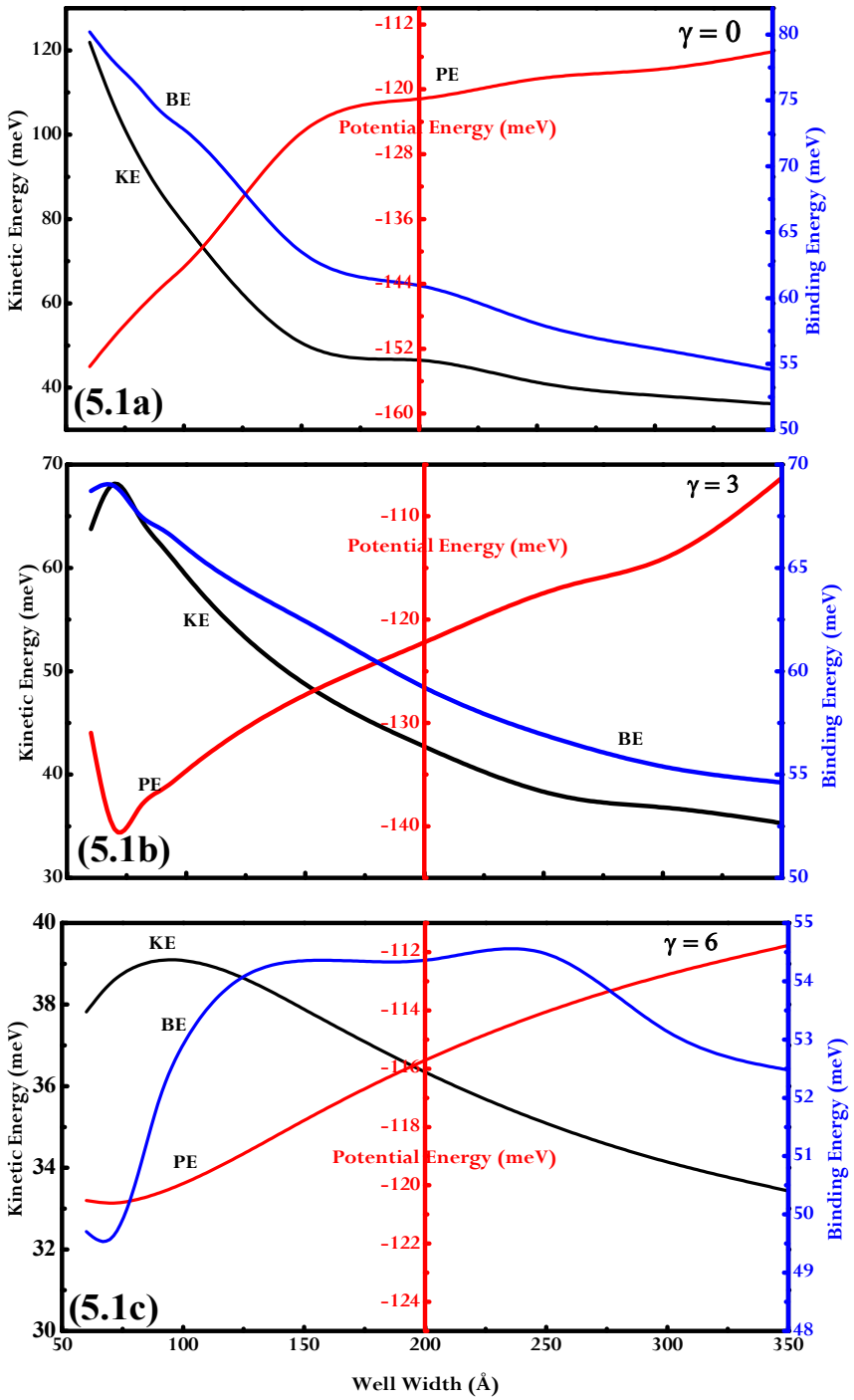

Figure 5.1: Variation of **(a)** Kinetic Energy, **(b)** Potential energy and **(c)** Binding energy of the two electrons confined inside the QW as a function of well width for $\gamma = 0$, $\gamma = 3$ and $\gamma = 6$.

This is due to the fact that the impurity potential energy becomes more negative with decreasing well width which leads to larger binding of the carriers in that regime even

though there is an increase in the kinetic energy of the particles. The variation of Coulomb interaction between the two electrons as a function of well width is plotted in fig. 5.2.

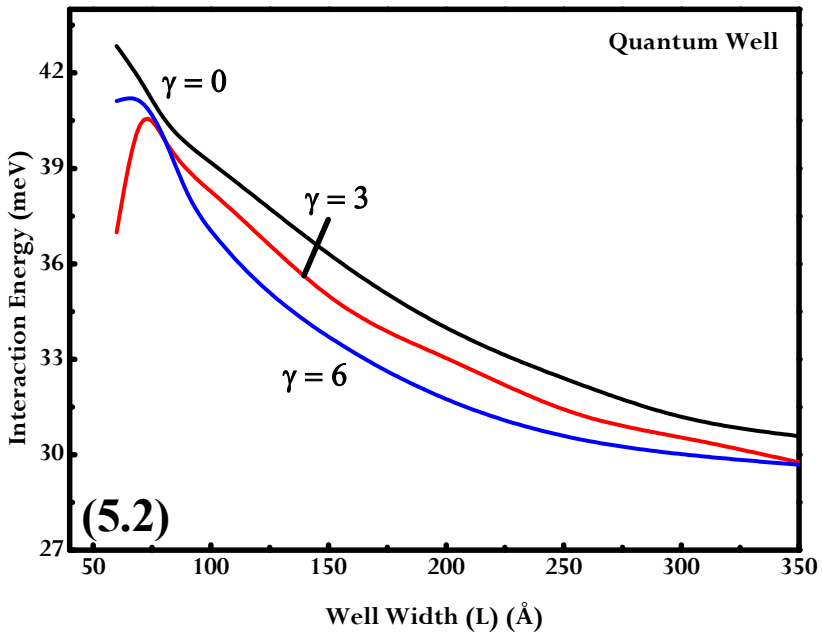

Figure 5.2: Variation of interaction energy of the two electrons confined inside the QW as a function of well width for $\gamma = 0$, $\gamma = 3$ and $\gamma = 6$.

The interaction energy is maximum for the narrower well width where the confinement is more and thereafter a gradual decrease is observed as the well width increases since the Coulomb interaction scales inversely proportional to the dimension of the well as $V_{Coulomb} \sim 1 / L$ [29]. But, when the external magnetic field of strength $\gamma = 3$ and $\gamma = 6$ are applied, the Coulomb interaction gets decreased as shown in fig. 5.2. This is because, the applied magnetic field tremendously suppresses the confining potential barrier (333.27meV, 67.65meV, 8.39meV for $\gamma = 0$, $\gamma = 3$ and $\gamma = 6$ respectively) and thereby shrinking the spatial extend of the two particle wavefunction which causes tunnelling of electrons through the barrier $Cd_{1-x}Mn_xTe$. In addition to this, when the strength of magnetic field is more the angular momentum gets increased and the electrons in states

with higher angular momentum are further apart from each other and thereby decreasing the Coulomb interaction between them. The expectation value of binding energy of the two electrons confined in a QW also follows the same trend (given in fig.5.1) with the magnetic field as that of the interaction energy. The decrease of the binding energy (fig.5.1) with the magnetic field can be attributed to the decrease in the kinetic energy, impurity potential energy as well as the subband energy due to the reduction in the potential barrier height. The variation of subband energy with the magnetic field for the two electrons confined inside the QW for various well widths is reported in Table 1.

Table 1: Subband Energy *vs* well width for different magnetic fields in QW

Well Width (Å)	**Subband Energy (meV)**		
	$\gamma = 0$	**$\gamma = 3$**	**$\gamma = 6$**
60	63.27	33.42	7.34
100	28.70	18.97	6.08
150	14.39	10.79	4.63
200	8.614	6.90	3.54
300	4.08	3.5026	2.19

When the magnetic field of strength $\gamma = 3$ is applied, the turnover in the binding energy is seen in the Quasi 2D region. This is because, the reduction in the potential barrier height due to the application of magnetic field keeps the expectation value of impurity potential to be more negative until the well width reaches around the effective Bohr radius when it is decreased from the bulk value. But, thereafter, it allows the carrier to be far apart from each other and leads to less negative value in the impurity potential with decreasing well width and therefore the carriers get loosely bound to the donor atom which results in

lower binding energy. But when the magnetic field of strength $\gamma = 6$ is applied, the binding energy increases as the well width increases and attains a maximum value around L = 100Å and thereafter it gets saturated until L reaches 250Å and beyond that the binding energy starts to fall again. The reason for this behaviour is the competition between the kinetic energy and the potential energy as shown in fig. 5.1c. The contribution of the kinetic energy to the total energy is much greater than the potential energy in the range L < 100Å and vice versa in the ranges L > 100Å. But this variation of the binding energy with the well width for $\gamma = 6$ is not as rapid as the variation observed for $\gamma = 0$ and $\gamma = 3$.

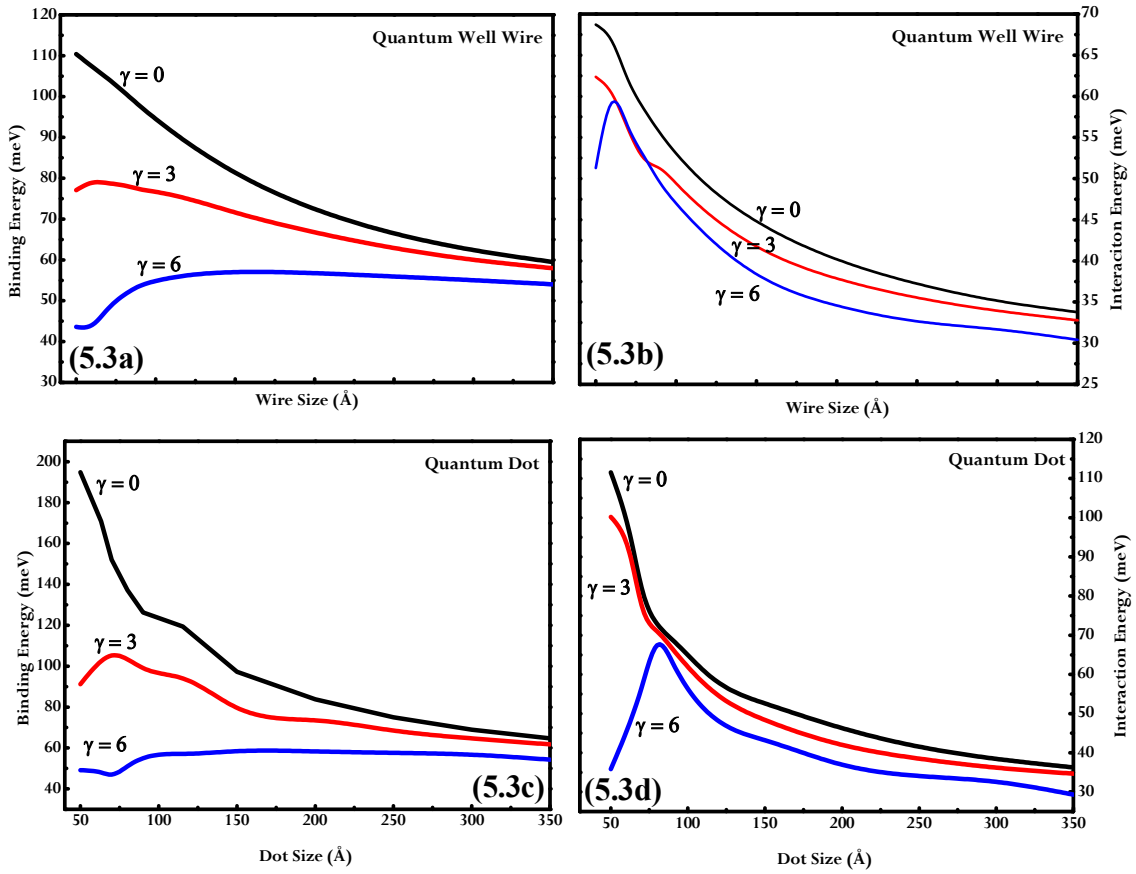

Figure 5.3: Variation of binding energy for the two electrons confined inside **(a)** QWW, **(c)** QD and the interaction energy in **(b)** QWW, **(d)** QD as a function of well width for different magnetic fields.

This can be understood on the basis of the following qualitative argument. The strength of the applied magnetic field $\gamma = 6$ is very nearer to the critical magnetic field ($\gamma = 7.35$) at which the barrier vanishes completely and the QW gets disappeared and the carriers become unconfined as in the bulk system. Moreover, the binding energy for all the values of magnetic field converges when the well width is increased towards the bulk value.

The graphs for binding energy and interaction energy for QWW and QD are plotted in fig. 5.3 for the cases with and without the application of magnetic field and the variation of subband energy for these QWW and QD have also been presented in Table 2.

Table 2: Subband Energy *vs* Well Width for various γ in QWW and QD

Well Width (Å)	Subband Energy (meV)					
	QWW			QD		
	$\gamma = 0$	$\gamma = 3$	$\gamma = 6$	$\gamma = 0$	$\gamma = 3$	$\gamma = 6$
60	100.807	43.93	7.82	127.945	49.44	8.0013
100	49.648	28.422	7.02	66.844	34.60	7.411
150	26.035	17.5738	5.886	36.224	22.655	6.507
200	15.952	11.77	4.854	22.583	15.684	5.59645
300	7.74	6.27316	3.323	11.57684	8.666	4.080

It is clearly seen from these figures that the trend of the binding energy with the dimension of the system is as same as the trend seen in the QW but with the larger magnitude in binding as well as interaction energy as the confinement of the system is increased from 2D $\rightarrow$ 1D (QW $\rightarrow$ QWW) and then 1D $\rightarrow$ 0D (QWW $\rightarrow$ QD). This is because, when the confinement is increased, there is a less possibility for the electrons to

undergo tunnelling because of its highly localized wavefunction. Since the degree of freedom for the two electrons is restricted as the dimensionality of the system is reduced which increases the effective strength of the Coulomb interaction between them and hence affects the binding energy. The Binding energy and the interaction energy for QW, QWW and QD for a typical value of $\gamma = 3$, has been given in fig. 5.4a and 5.4b respectively.

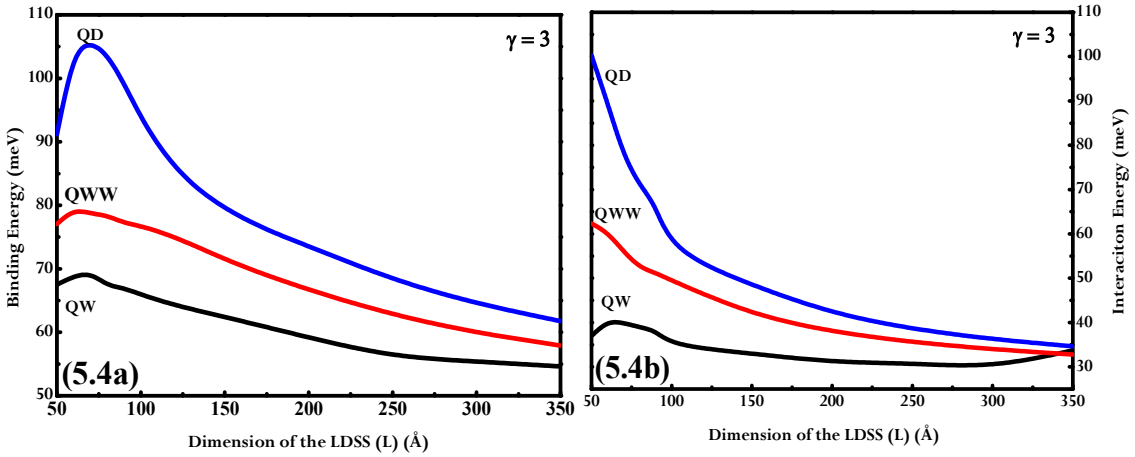

Figure 5.4: Variation of **(a)** binding energy and **(b)** interaction energy for the two electrons confined inside QW, QWW and QD as a function of dimension of the LDSS for the magnetic field $\gamma = 3$.

It is worth noticing from all the graphs portrayed above that the binding of the two electrons and their Coulomb interaction is tremendously affected by the applied magnetic field only when the impurity is confined inside the QD rather than in the QW and QWW. This can be justified as one can note that the magnitude of decrease in the binding energy and the interaction energy with respect to the applied magnetic field increases as the confinement of the carrier increases from 2D $\rightarrow$ 1D $\rightarrow$ 0D.

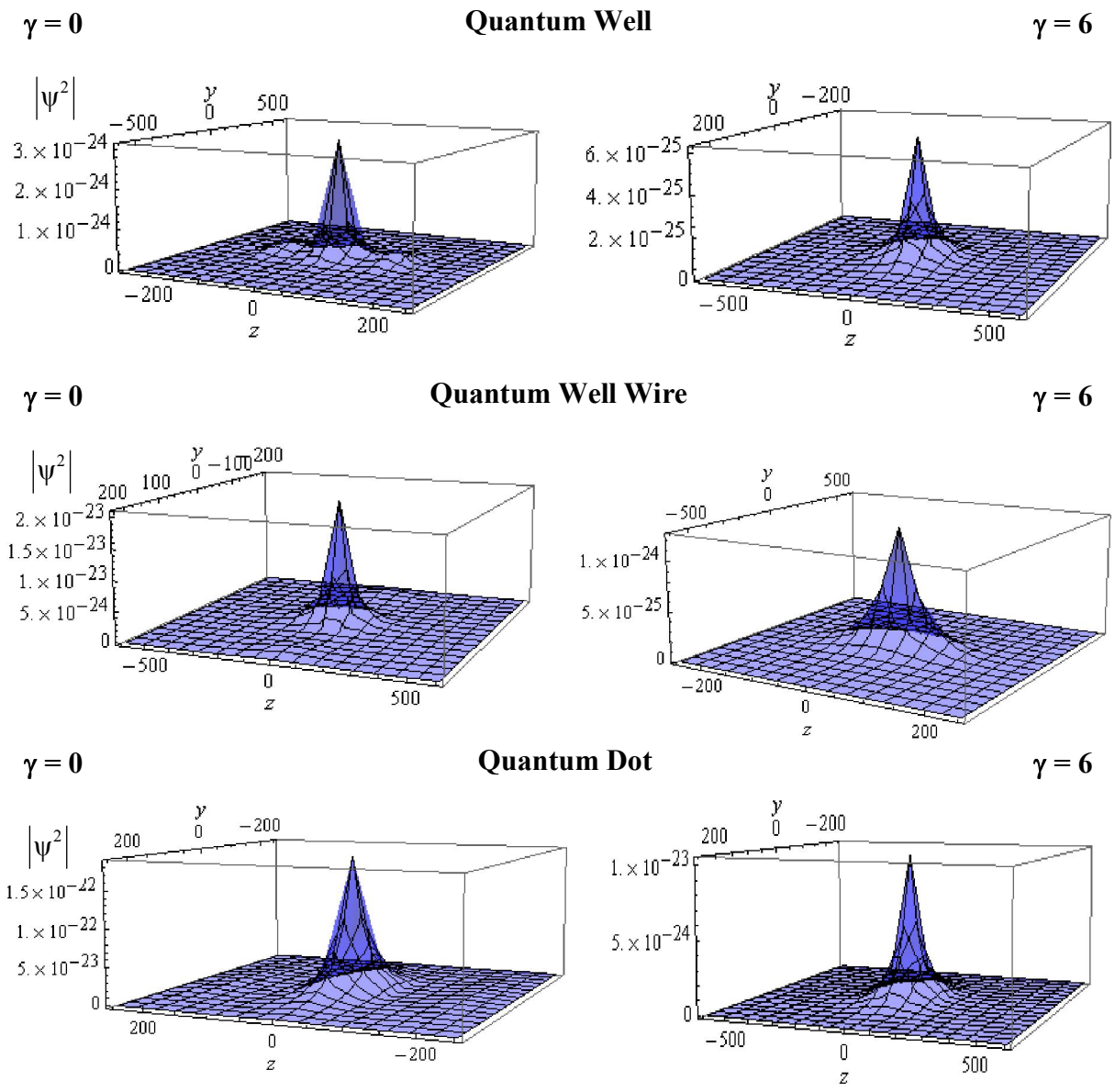

Figure 5.5: Probability density $|\Psi^2|$ of the He – like impurity confined inside the QW, QWW and QD under $\gamma = 0$ and $\gamma = 6$ for Mn ion concentration of x=0.3.

The above said qualitative arguments can be justified from the three dimensional probability function shown in fig.5.5 for the two electrons confined inside the CdTe /$Cd_{1-x}Mn_xTe$ QW, QWW and QD with $\gamma = 0$ and $\gamma = 6$ by noticing, the $|\Psi^2|$ decreases when the magnetic field is applied and it increases as the dimensionality of the system is reduced.

5.4. Conclusion

We have calculated the Coulomb interaction between the two electrons confined in the LDSS and their binding to the donor impurity as a function of magnetic field. The most appealing feature of the Coulomb interaction in DMS systems in response to the applied magnetic field as compared to other non-magnetic systems may be instrumental in understanding the strong influence of the spectral properties of the LDSS which can be interpreted as transition to Quantum Chaos and may also shed some light on the fabrication of spintronic devices.

References

1. T. Kasuya, Anamalous, *Rev. Mod. Phys.***1968**, *40*, 684–696.
2. U. Thibblin, *Int. J. Mod. Phys. B*. **1989**, *3*, 337–366.
3. J.A. Gaj, J. Ginter, *Phys. Status Solidi Basic Res.***1978**, *655*, 655–662.
4. J.P. Lascaray, D. Coquillat, J. Deportes, A.K. Bhattacharjee, *Phys. Rev. B*. **1988**, *38,* 7602–7606.
5. P. Nithiananthi, K. Jayakumar, *Int. J. Nanosci.* **2011**, *10*, 611–615.
6. P. Kalpana, P. Nithianathi and K. Jayakumar, *Superlatt.Microstruct*. **2017**, *102*, 246-258.
7. R. Khordad, H. R. Rastegar Sedhi, *Superlatt. Microstruct*. **2017**, *101*, 559.
8. R. Khordad, *Int. J. Theor. Phys*. **2013,** *52*, 837 – 848.
9. P. Nithiananthi, K. Jayakumar, *Phys. Status. Solidi (b)*, **2009**, *246*, 1238 – 1242.
10. P. Nithiananthi, K. Jayakumar, *Superlatt. Microstruct.***2006**, *40*, 174- 179.
11. A. Merwyn Jasper D Reuben, K. Jayakumar, *Phys. Status. Solidi (b)*. **2006**, *243* 4020-4024.
12. Zhen – Yan Deng, Tatsuki Ohji and Xiaoshuang Chen, *J. Phys. Condens. Mattter*. **2000**, *12*, 3019 - 3027
13. Y. Yakar, B. Cakir and A. Ozman, *Int. J. Quantum Chem*. **2011**, *111*, 4139-4149.
14. Frederico V. Prudente, Luis S. Costa and Jose David M. Vianna, *J. Chem. Phys*. **2005**, *123*, 224701.
15. R K Pandey, Manoj H Harbola and Vijay A Singh, *J. Phys.:Condens. Matter*. **2004**, *16*, 1769-1776.
16. S. E. Okan, H. Akbas and S. Aktas, *Superlatt.Microstruct*. **2000**, *28*, 171-176.
17. M. Brasken, M. Lindberg, D. Sundholm and J. Olsen, *Phys. stat. sol. (b)*. **2000**, *221,* 37- 41.

18. Ya. M. Blanter, N.E. Kaputkina and Yu. E. Lozovik, *Phys. Scripta*. **1996**, *54*, 539- 541.
19. E C. Niculescu, *Phys. Lett. A*. **1995**, *197*, 330-334.
20. P. A. Maksym, T. Chakraborty, *Phys. Rev. Lett*. **1990**, *2*, 108-111.
21. A. Glodeanu, *Phys. stat. sol. (b)*. **1967**, *19*, K43.
22. H G. Grimmeiss, E. Janzen and B. Skarstam, *J. Appl. Phys*. **1980**, *51*, 4212.
23. H G. Grimmeiss, E. Janzen and K. Larsson, *Phys. Rev. B*. **1982**, *25*, 2627.
24. G. Y. Hu, R. F. O'Connell, *Phys. Rev. B*. **1990**, *42*, 1290.
25. D. Pfannkuche, R. Gerhardts, A. Maksym, V. Gudmundsson, *Physica B*. **1993**, *189*, 6-15.
26. U. Merkt, J. Huser and M. Wagner, *Phys. Rev. B*. **1991**, *43*, 7320-7323.
27. R. Correa, W. Gutierrez, I. Mikhailov, M. R. Fulla and J. H. Marin, *Physics Letters,* **2015**, *379*, 1457-1463.
28. A. Merwyn Jasper D Reuben, K. Jayakumar, *Superlatt. Microstruct*. **2012**, *52*, 732-737.
29. Pancakes, Daniela, Aspects of Coulomb Interaction in Semiconductor Nanostrucutres, Physics, Habil – Schr. 28, **1999**.

Chapter 6

SUMMARY OF THE RESEARCH FINDINGS

The hole – hole interaction (E_{hh}) in a $CdTe/Cd_{1-x}Mn_xTe$ Semimagnetic Quantum Well Wire (SQWW) has been studied in **section 2.1 of Chapter 2**. The influence of the shape of the confining potential like square well and parabolic well type on the binding energy of an acceptor impurity with two holes and their Coulomb interaction between them has been studied for various impurity locations. Magnetic field has been used as a probe to understand the carrier- carrier correlation in such Quasi 1- Dimensional QWW since it alters the strength of the confining potential tremendously. In order to show the significance of the correlation between the two holes, the calculations have been done with and without including the correlation effect in the ground state wavefunction of the hydrogenic acceptor impurity and the results have been compared. From the observed results, it is understood that irrespective of the nature of the confining potential the binding energy of the acceptor impurity and the Coulomb interaction between them is less when the correlation between them is considered in the wavefunction as compared to the case without considering the correlation. Moreover, the importance of accounting the correlation in the wavefunction has been emphasized by observing the increase of Coulomb repulsion with the increase of applied magnetic field in the case of parabolic confinement and the effect of impurity location on the Coulomb interaction between the two correlated holes is not significant as the strength of the interaction is consistently

maintained for smaller wire size, when the impurity moves from the center to the edge of the wire.

The donor/acceptor impurity binding energy in CdTe / $Cd_{1-x}Mn_xTe$ QWW with square well confinement along x – direction and parabolic confinement along y – direction under the influence of externally applied magnetic field has been computed in **section 2.2 of Chapter 2**. The impact of directional dependent effective mass calculated from the Luttinger parameters on the binding energy of the heavy hole bound to an acceptor impurity has also been investigated and compared with the results obtained for the constant effective mass used in the envelope function. From the observed results it is understood that the influence of the shape of the confining potential along each direction of the confinement in QWW plays a crucial role to determine the strength of the binding of the carriers inside such QWW and it is to be noted that the carriers can move with higher mobility when the directional dependent effective mass is employed in the calculation.

The same work of Section 2.1 of Chapter 2 has been extended in Semimagnetic QD with various geometry like Spherical and Cubical and with the effect of spatially varying dielectric screening which has been presented in **Chapter 3**. The observed results show that the QD with spherical geometry which has bound states only for dot size greater than 30Å gives higher localization for the carriers since the Coulomb repulsion between them is less as compared to the CQD which could has bound states even for the dot size of 20Å. It has also been found that the spatially varying dielectric screening allows the carriers to have strong interaction (an enhancement of ≈ 20%) both in the absence and in the presence of applied magnetic field.

Donor and Acceptor impurity sates and the BMP associated with them have been investigated in a Semimagnetic DQW as a function of central barrier width for various well dimensions and in a STQW. The magnetic field can act as a tool to continuously change the interwell coupling inside this DQW systems and its effect on donor and acceptor binding has also been studied. Moreover, the polaronic corrections, which is due to the strong exchange interaction between the magnetic moment of Mn^{2+} ion and the spin of the confined electron to the binding energy of the hydrogenic donor impurity has also been estimated with and without the application of magnetic field in **section 4.1 of chapter 4**.

The effect of different combinations of the concentration of Mn^{2+} ion in the Quantum well $Cd_{1-x_{in}}Mn_{x_{in}}Te$ and the barrier $Cd_{1-x_{out}}Mn_{x_{out}}Te$ on the BMP in a DQW has been investigated in **section 4.2**. The results show that the effect of the increase of Mn^{2+} ion composition with different combinations on SPS is predominant for OCW impurity when compared to all other impurity locations when there is no application of magnetic field ($\gamma = 0$) and the same is predominant for OCB impurity with the application of external magnetic field ($\gamma = 0.15$).

The effect of magnetic field on the acceptor ionization energy is very weak due to the high effective masses of the holes which leads to the smaller Landau splitting. It is found from the calculations that the acceptor impurity is highly localized only when it is situated at the centre of the DQW and also the applied magnetic field causes the counterintuitive behaviour for OCW impurity and for other impurity locations which has been discussed in details in **section 4.3**.

The concept of section 4.2 has been extended for the donor impurity in STQW for which has been presented in detail in **section 4.4**. It is found that the ground state donor binding energy and the SPS associated with it depends only on the density of the

magnetic ions separately concentrated in the well $Cd_{1-x_{in}}Mn_{x_{in}}Te$ and in the barrier $Cd_{1-x_{out}}Mn_{x_{out}}Te$ of STQW even though the effective concentration is same ($x_{out} - x_{in} = x = 0.1, 0.2$). A counterintuitive behaviour is observed for the ground state binding energy and the SPS when the effective concentration of Mn^{2+} ion is increased from x = 0.1 to x = 0.2 under different magnetic field strength.

The effect of heavy and light holes on the Bound Magnetic Polaron (BMP) confined in a Semimagnetic $Cd_{1-x_{in}}Mn_{x_{in}}Te/Cd_{1-x_{out}}Mn_{x_{out}}Te$ STQW has been investigated and discussed in **section 4.5**. The SPS is very much larger for the light hole as compared with the heavy hole which is in contrary to the binding energy case.

The effect of magnetic field on the Coulomb interaction between the two electrons confined inside a CdTe/ $Cd_{1-x}Mn_xTe$ QW, QWW and QD for the composition of Mn^{2+} ion, x = 0.3 has been addressed in **Chapter 5**. It is found from the reported results that the binding of the two electrons and their Coulomb interaction is tremendously affected by the applied magnetic field only when the impurity is confined inside the QD rather than in the QW and QWW and the results has been justified from the three dimensional probability distribution function for the two electrons confined inside such LDSS.

ANNEXURE – I

LIST OF PUBLICATIONS

International Journals

1. Coulomb Interaction of Acceptors in Cd1-xMnxTe/CdTe Quantum Dot,

   P.Kalpana**,** A.Merwyn Jasper D Reuben, P.Nithiananthi and **K. Jayakumar**,

   AIP Conf.Proc. **2014**, *1591*, 1176 **doi: 10.1063/1.4917985**

2. Effect of Geometry on the pressure induced donor binding energy in semiconductor nanostructures

   P. Kalpana, **K. Jayakumar** and P. Nithiananthi, *Int.J.Comp.Mat.Sci.Eng.* **2015***, 4*, 1550018 **doi: 10.1142/S2047684115500189**

3. Magnetic field Effect on the Coulomb Interaction of Acceptors in Semimagnetic Quantum Dot

   P.Kalpana**,** A.Merwyn Jasper D Reuben, P.Nithiananthi and **K. Jayakumar**,

   AIP Conf.Proc. **2015**, *1665*, 090005 **doi: 10.1063/1.4872894**

4. Effect of magnetic field on the Donor impurity in CdTe/$Cd_{1-x}Mn_xTe$ Quantum Well Wire

   P.Kalpana**,** A.Merwyn Jasper D Reuben, P.Nithiananthi and **K. Jayakumar**,

   AIP Conf. Proc. **2016**, *1731*, 090027 **doi: 10.1063/1.4947991**

5. Impurity States and Diamagnetic Susceptibility of a donor in a Triangular Quantum Well

   P.Kalpana, A.Merwyn Jasper D Reuben, P.Nithiananthi and **K. Jayakumar**, *AIP Conf. Proc*. **2017**, *1832*, 090032 **doi: 10.1063/1.4980585**

6. Donor States in a Semimagnetic $Cd_{1-xin}Mn_{xin}Te$ / $Cd_{1-xout}Mn_{xout}Te$ Double Quantum Well,

   P. Kalpana, P. Nithiananthi and **K.Jayakumar**, *Suplatt.Microstruct*. **2017**, *102*, 246 – 258 **doi: 10.1016/j.spmi.2016.12.042**

7. Impurity states and the Diamagnetic Susceptibility of a donor in a GaAs/ $Al_xGa_{1-x}As$ Triangular Quatnum Well under Hydrostatic Pressure

   P. Kalpana and **K. Jayakumar**, *J. Phys. Chem. Solids*., **2017**, *110*, 364-369

   doi: 10.1016/j.jpcs.2017.06.031

8. Bound Magnetic Polaron in a Semimagnetic Double Quantum Well

   P.Kalpana, **K.Jayakumar,** Physica E, **2017** (**Accepted Manuscript)**

   doi: 10.1016/j.physe.2017.06.025

9. Helium like impurity in CdTe / $Cd_{1-x}Mn_xTe$ Semimagnetic Semiconductors under Magnetic Field: Dimensionality Effect on Electron – Electron Interaction

   P. Kalpana and **K. Jayakumar,** *Superlatt.Microstruct*., **2017,** *111*, 115-122.

   doi: 10.1016/j.spmi.2017.06.017

Papers presented in International / National Conferences

1. Enhanced Coulomb Interaction due to Spatial dielectric Screening in Semimagnetic Quantum Dot

   P.Kalpana, A.Merwyn Jasper D Reuben, P.Nithiananthi and **K. Jayakumar**

   Proc. International Conference on Nano science and Technology (ICONSAT - 2014), Chandigarh, India, March 3-5, **2014**

2. Coulomb Interaction of He – like Impurity in a Quantum Dot

   P. Kalpana, P. Nithiananthi and **K.Jayakumar**

   Proc. National Conf. on Frontiers of Chemistry and Materials (NCFCM-2015) Tuljaram Chaturchand College, Baramati, Pune, 12-14th Feb, 2015.

3. Acceptor States in a Semimagnetic $Cd_{1-xin}Mn_{xin}Te$ / $Cd_{1-xout}Mn_{xout}Te$ Double Quantum Well

   P. Kalpana, P. Nithiananthi and **K.Jayakumar**

   Proc. International Conference on Materials Science and Tehcnology (ICMST – 2016), St.Thomas College, Palai, Kottayam, 5-8 June 2016.

4. Donor States in a Semimagnetic Triangular Quantum Well

   P. Kalpana and **K. Jayakumar**

   4th International Conf. on Nanoscience and Nanotechnology (ICONN 2017), SRM University, Chennai, India **(2017)**

REPRINTS

Superlattices and Microstructures 102 (2017) 246–258

Contents lists available at ScienceDirect

Superlattices and Microstructures

journal homepage: www.elsevier.com/locate/superlattices

Donor states in a semimagnetic $Cd_{1-x_{in}}Mn_{x_{in}}Te/Cd_{1-x_{out}}Mn_{x_{out}}Te$ Double Quantum Well

Panneer Selvam Kalpana, Perumal Nithiananthi, Kalyanasundaram Jayakumar*

Nanostructure Lab, Department of Physics, Gandhigram Rural University, Gandhigram, 624 302, Tamilnadu, India

ARTICLE INFO

Article history:
Received 12 November 2016
Received in revised form 18 December 2016
Accepted 20 December 2016
Available online 23 December 2016

Keywords:
Semimagnetic semiconductor
Double Quantum Well
Donor impurity location
Binding energy
Bound Magnetic Polaron
Magnetic field

ABSTRACT

The theoretical investigation has been carried out on the binding energy of donor associated with the electrons confined in a $Cd_{1-x_{in}}Mn_{x_{in}}Te/Cd_{1-x_{out}}Mn_{x_{out}}Te$ Double Quantum Well (DQW) as a function of central barrier width for various well dimensions and impurity locations in the barrier and the well. The magnetic field can act as a tool to continuously change the interwell coupling inside this DQW systems and its effect on donor binding has also been studied. Moreover, the polaronic corrections, which is due to the strong exchange interaction between the magnetic moment of Mn^{2+} ion and the spin of the confined carrier, to the binding energy of the hydrogenic donor impurity has also been estimated with and without the application of magnetic field. The binding energy of the donor impurity is determined by solving the Schrodinger equation variationally in the effective mass approximation and the effect due to Bound Magnetic Polaron (BMP) is included using mean field theory with the modified Brillouin function. The results are reported and discussed.

1. Introduction

The unique features, such as Giant Zeeman Splitting [1–3] and Bound Magnetic Polaron (BMP) [4,5] due to the strong exchange interaction between the magnetic moments of the magnetic ions and the spins of band electrons, of Diluted Magnetic Semiconductors (DMS) has opened the doors for Spintronic device applications. This has made DMS an interesting test ground for various theoretical ideas since its bandstructure can be tailored so that both the electronic and magnetic properties can also be investigated. With the advantage of having Molecular Beam Epitaxy (MBE), one can easily fabricate the Double Quantum Well (DQW) Nanostructured systems with various barrier widths or heights. The modification of the barrier height in these DQWs made up of DMS materials can be achieved either by adjusting the composition of the alloy used in the barrier material or by the application of the external magnetic field [6]. The presence of a quantised motion in the growth direction of the DQW structures has a huge impact on their physical properties, which strongly differ from properties of narrow single quantum wells representing a physical realisation of a quasi-2-Dimensional system. The distinctive behaviour of DQWs becomes apparent especially when the density of states are modified from 3D to 2D due to the formation of Landau levels in these structures under the influence of high magnetic field which has a very profound effects on physical phenomenon in 2D systems. Therefore the DQWs made out of DMS materials provides a new path to explore the rich variety of phenomena through which one can investigate the role of impurities confined in such systems to understand its electrical

* Corresponding author.
E-mail address: kjkumar_gri@rediffmail.com (K. Jayakumar).

http://dx.doi.org/10.1016/j.spmi.2016.12.042
0749-6036/

transport and magneto optical properties. Our knowledge about the influence of magnetic impurity on semiconductors has been extended to study the extensive transport properties in DMS heterostructures over the past few decades [1–8]. Considerable attention has been focused by many researchers on the theoretical investigation of the ground state energy of hydrogenic donor impurity in GaAs/$Al_xGa_{1-x}As$ Single and DQW systems by accounting various effects [9–15]. Copious literatures are available on the study of electronic and excitonic states in a DQW with non magnetic materials under the application of strong magnetic field [16–20]. The magneto-optical study has been carried out by Lee et al. [21] both theoretically and experimentally to demonstrate the interwell coupling in DQWs using DMS materials. Haacke [22] et al. have studied carrier tunnelling in CdTe/(Cd, Zn)Te asymmetric DQW through photoluminescence experiments and demonstrated the strong dependence of the tunnelling on barrier thickness. Lawrence et al. [23] have demonstrated the tunnelling dynamics of exciton in CdTe/CdMnTe asymmetric DQW by time resolved and steady state photoluminescence experiments. Detailed spectroscopic measurements and their successful theoretical interpretation [5] is favourable for DMS to offer an appealing opportunity to elucidate how the BMP affect transport phenomena. Therefore it becomes necessary to account this polaronic corrections to the impurity binding energy and this has been investigated in various DMS heterostructures by many researchers [24–28]. But this kind of study has not been touched yet in DQW made from DMS barrier layers especially with $Cd_{1-x}Mn_xTe$. Hence the present work is mainly intended for the study of electronic states of the donor impurity as well as the influence of BMP on the impurity states in $Cd_{1-x_{in}}Mn_{x_{in}}Te/Cd_{1-x_{out}}Mn_{x_{out}}Te$ DQW under the external applied magnetic field for the composition of magnetic impurity like Mn ion of xin = 0.005 and $x_{out} = 0.3$, where x_{in} and x_{out} are the composition of Mn^{2+} ion in the well and the barrier regions respectively, and also for various impurity locations. The results are computed in the effective mass approximation using variational technique.

2. Theoretical formalism

2.1. Donor binding energy for various impurity locations

The Hamiltonian of a hydrogenic donor impurity inside the DQW made up of $Cd_{1-x_{in}}Mn_{x_{in}}Te/Cd_{1-x_{out}}Mn_{x_{out}}Te$ DMS materials in the effective mass approximation in the presence of magnetic field applied along the growth direction (z-axis) is written as

$$\mathbf{H} = \mathbf{H}_0 + \mathbf{H}_{exc} \tag{1}$$

$$\mathbf{H}_0 = -\nabla^2 - \frac{2}{r} + V_B(z) + \gamma L_z + \frac{\gamma^2\rho^2}{4} \tag{2}$$

where $\gamma = \hbar\omega_c/2R^*$ (ω_c – cyclotron frequency) is the parameter of the strength of the magnetic field and $\gamma = 1$ corresponds to ≈ 30 T; $r = \sqrt{x^2 + y^2 + z^2}$ is the mean distance of the parent donor atom and the carrier attached to it.

The contribution from the exchange interaction between the electron and the Mn^{2+} ion to the Hamiltonian can be written as [29],

$$\mathbf{H_{exc}} = -\sum_i \mathbf{J_e}(\boldsymbol{r_e} - \boldsymbol{R_i})\mathbf{s_e}\cdot\mathbf{S_i} \tag{3}$$

where, J_e is the coupling constant for the exchange interaction between the electron of spin $\mathbf{s_e}$ located at $\mathbf{r_e}$ and Mn^{2+} ions of spin $\mathbf{S_i}$ located at $\mathbf{R_i}$. Using the mean field theory with modified Brillouin function [26], the exchange interaction between the carrier and magnetic impurity in the presence of an external magnetic field **B** can be written as

$$E_{exc} = \frac{\beta N_0}{2}\{\langle\Psi|x_{in}S_0(x_{in})B_s(y_1)|\Psi\rangle + \langle\Psi|x_{out}S_0(x_{out})B_s(y_2)|\Psi\rangle\} \tag{4}$$

$$B_s\left(y_j\right) = \frac{2S+1}{2S}\coth\frac{2S+1}{2S}y_j - \frac{1}{2S}\coth\frac{y_j}{2S};\quad y_j = \frac{S\beta|\Psi_j|^2}{2k_BT_{eff}} + \frac{g\mu_B SB}{k_BT_{eff}} \tag{5}$$

where, S is the spin of Mn^{2+} (=5/2), $N_0 = 2.94 \times 10^{22}$ cm^{-3} and β - exchange coupling parameter and its value is obtained from the experimental value of the s − d coupling constant, $\beta N_0 = 220$ meV. Also $g_{Mn} \approx 2$, k_B is the Boltzmann constant and $B_s(y)$ is the modified Brillouin function. For the DMS of arbitrary x, it is inevitable to choose the phenomenological fitting parameters [29] of saturation value S_0 ($x_{in} = 0.005$) = 2.11, S_0 ($x_{out} = 0.3$) = 0.52 and the effective temperature $T_{eff} = T + T_0$ with T_0 ($x_{in} = 0.005$) = 0.29 and T_0 ($x_{out} = 0.3$) = 14.9.

The various impurity positions (z_i) accounted for the study is as follows.

(i) On Centre Barrier impurity (OCB) ($z_i = 0$)
(ii) On Edge Barrier impurity (OEB) ($z_i = L_b/2$)

(iii) On Centre Well impurity (OCW) ($z_i = L_b/2 + L_w/2$)
(iv) On Edge Well impurity (OEW) ($z_i = L_b/2 + L_w = L_e$)

According to the scheme of Fig. 1, the profile of the confining potential $V_B(z)$ for the carriers in symmetric DQW structures is given as

$$V_B(z) = \begin{cases} 0 & \frac{L_b}{2} \le |z| \le \left(\frac{L_b}{2} + L_w\right) \\ V_0 & |z| \le \frac{L_b}{2} and \left(\frac{L_b}{2} + L_w\right) < |z| < \infty \end{cases} \tag{6}$$

L_w is the width of the each well and L_b is the central barrier width and $V_0 = 70\%\ \Delta E_g^B$, where, ΔE_g^B is the band gap difference with magnetic field and is given by Ref. [6].

$$\Delta E_g^B = \Delta E_g^0 \left[\frac{\eta\ \exp^{\varsigma\gamma} - 1}{\eta - 1}\right] \tag{7}$$

ΔE_g^0 is the band gap difference without magnetic field. $\eta = e^{\varsigma\gamma_0}$ is chosen with ς as a parameter (=0.5) and γ_0 as the critical magnetic field which depends upon the value of the composition 'x' of Mn^{2+} ion. The critical magnetic field B_0 in Tesla for different composition is given as $B_0 = A\ e^{nx}$ with A = 0.734 and n = 19.082 which gives the best fit to the extrapolated experimentally available critical fields and the band gap of $Cd_{1-x}Mn_xTe$ is 1.606 + 1.587× eV [6].

The approximate ground state for confined donor impurity has been calculated using the variational method. The envelop function f (z) is considered as

$$f(z) = \begin{cases} A\exp[\beta(z + L_e)] & z \le -L_e \\ -B\ Sin\left[\alpha\left(z + \frac{L_b}{2}\right)\right] + C\ Cos\left[\alpha\left(z + \frac{L_b}{2}\right)\right] & -Le < z < -\frac{L_b}{2} \\ Cosh[\beta z] & -\frac{L_b}{2} < z < \frac{L_b}{2} \\ B\ Sin\left[\alpha\left(z - \frac{L_b}{2}\right)\right] + C\ Cos\left[\alpha\left(z - \frac{L_b}{2}\right)\right] & \frac{L_b}{2} < z < L_e \\ A\exp[-\beta\ (z - L_e)] & z \ge L_e \end{cases} \tag{8}$$

Here, $\alpha = (2m^*E)^{1/2}$ and $\beta = (2m^*(V_0\text{-}E))^{1/2}$. The unknown constants A, B and C are found out using the proper boundary conditions at the interfaces $z_i = L_b/2$ and $z_i = L_e$.

The trial wavefunction of the ground state is chosen as,

$$\psi(r) = Nf(z)e^{-\lambda r} \tag{9}$$

where, N is the normalization constant and λ is the variational parameter.

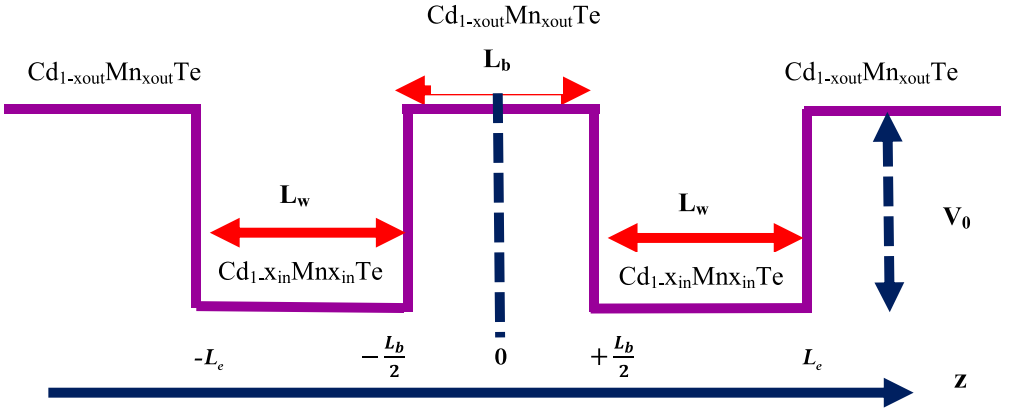

Fig. 1. Schematic view of the potential profile for a DQW.

The lowest energy level E_0 without donor impurity can be computed by solving the transcendental equation [13].

$$2\cos(\alpha L_w) + \left(\mu - \frac{1}{\mu}\right)\sin(\alpha L_w) - \left(\mu + \frac{1}{\mu}\right)\sin(\alpha L_w)\exp(-\beta L_b) = 0 \quad with \quad \mu = m_w^*\beta/m_b^*\alpha \tag{10}$$

m_w^* and m_b^* are the electron effective masses in the well and barrier region respectively.

The expectation value of **H** is minimized with respect to λ and the binding energy of the donor impurity in the presence of magnetic field is found by solving the Schrödinger equation variationally, and is given by

$$E_B = E + \gamma - \langle \mathbf{H} \rangle_{min} \tag{11}$$

The CdTe parameters used in our calculation are $\varepsilon = 10.2$; $m_w^* = 0.090$. Energies for electron are scaled by effective Rydberg $R_e = m_w^* e^2/2\hbar^2\varepsilon^2$ and the effective Bohr radius $a_B = \hbar^2\varepsilon/m_w^* e^2$.

3. Results and discussion

The estimation of $<r^2>$ i.e. the effective distance of the carrier from the parent donor atom plays a vital role in determining the carrier localization in the nanostructured systems. Therefore, one can examine the impact of the central barrier width and the external magnetic field on the behaviour of hydrogenic donor impurity confined inside the DQW through the observation of $<r^2>$. To start with, the variation of the binding energy of a donor impurity confined in a $Cd_{1-xin}Mn_{xin}Te/Cd_{1-xout}Mn_{xout}Te$ DQW and the $<r^2>$ as a function of central barrier width for the Mn composition of $x_{in} = 0.005$ and $x_{out} = 0.3$ without the application of magnetic field has been calculated and is presented in section 3.1. The effect has been analysed for the two well widths (i) $L_w = 50$ Å (quasi 2D region) and (ii) $L_w = 300$ Å (almost bulk region) for various impurity positions. The first observation we have made is, irrespective of the well widths, applied magnetic field and the impurity positions, when the barrier width is limited to zero (i.e.) $L_b \rightarrow 0$ Å, we reproduce the E_B of the single quantum well which is available in the literature [30] as a limiting case. On the other hand, when the width of the central barrier between the two wells is as large as the bulk value, the symmetric wells are completely decoupled and it makes the donor impurity to behave in a single isolated quantum well. Therefore, it is apparent from this observation that the interwell coupling is possible only for the narrow barrier width which should be in the limit 0 Å < L_b < 100 Å which can be seen from Fig. 2a showing a saturation value of E_B for L_b > 100 Å. The behaviour of the donor impurity with the central barrier width can be understood for various impurity locations in the presence and in the absence of the magnetic field as follows:

3.1. DQW under zero applied magnetic field ($\gamma = 0$)

This section discusses the variation of binding energy of the donor impurity when the system is not subjected to the perturbation due to the external magnetic field.

3.1.1. On centre barrier impurity (OCB)

A clear inspection of Fig. 2a indicates that the binding energy decreases as L_b increases, when the impurity resides at the centre of the central barrier.

This is because of the increased $<r^2>$ for larger L_b which makes the donor atom and the carrier to be weekly coupled due to the reduction in Coulomb interaction (Fig. 2b). The inset in Fig. 2b gives variation of $<r^2>$ for OEB, OCW and OEW impurities in different scale.

3.1.2. On edge barrier impurity (OEB)

In the case of OEB impurity, the effect of the central barrier width is almost negligible upto particular barrier width which can be clearly seen from the figure that the binding energy of OEB impurity coincides with the binding energy of OCB impurity. But when the barrier width crosses the particular value of L_b~100 Å, the onset of bulk limit, E_B behaves differently which is discussed subsequently. Initially binding energy decreases as L_b increases and thereafter it starts increasing again and reaches a saturation. This can be understood that when the barrier width increases in between the two wells, the $<r^2>$ increases and results in the reduction of Coulomb interaction between the carrier impurity and the parent donor atom. But after reaching the critical barrier width of L_b ~100 Å, the carrier confinement is limited in the DQW and makes the donor atom and carrier to be closed to each other and thereby increasing their Coulomb interaction which results in larger binding energy in that region.

3.1.3. On centre well (OCW) and On edge well (OEW) impurity

Unlike the other two impurity locations discussed earlier, the binding energy for OCW and OEW impurities follow the same trend and these two impurity locations are found to favour for the tunnelling of the carriers through the central barrier layer, which can also be interpreted that the interwell coupling becomes stronger for these two impurity locations as in the case of non-magnetic DQW [13]. It is worth noticing that the gradual and smooth increase of binding energy occurs upto $L_b = 100$ Å but beyond that it becomes saturated. This can be understood in terms of interwell coupling i.e. when the barrier

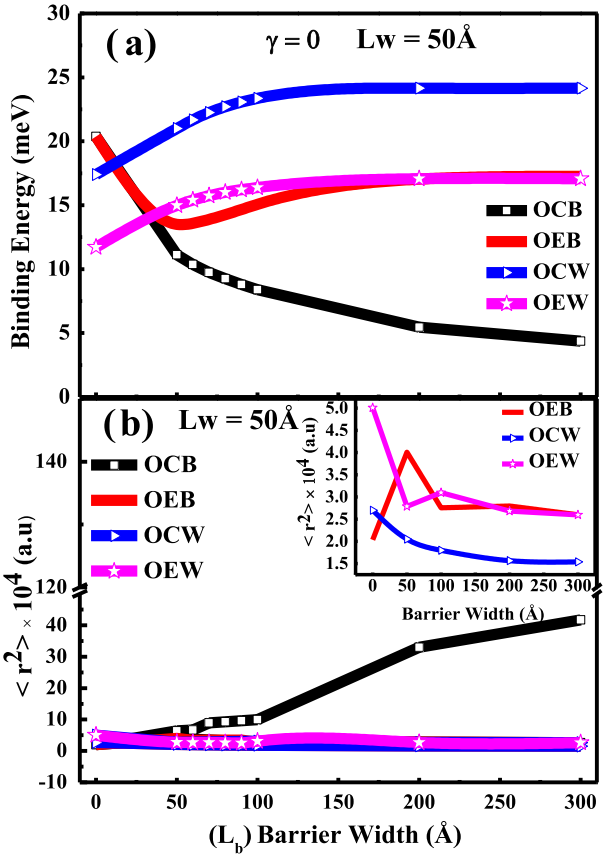

Fig. 2. Variation of **(a)** binding energy and **(b)** $<r^2>$ against barrier width for lower well dimension $L_w = 50$ Å without the application of magnetic field ($\gamma = 0$) for the Mn ion concentration of $x = 0.3$. Graphs have been plotted against various impurity locations (z_i).

width is reduced below the critical value, there is a finite probability for the carriers to tunnel through the central barrier layer. But, when the barrier width is increased beyond the critical value, it starts to squeeze the impurity wavefunction more and the carrier is localized only within the isolated well space of 50 Å and eventually reduces the degree of freedom of the carrier to move through the entire DQW. Because of this, the distance between the donor atom and the carrier is rapidly decreased which leads to the strong Coulomb interaction between them and it is almost constant for all the barrier widths beyond $L_b > 100$ Å.

The computed results of the binding energy and $<r^2>$ against barrier width for $L_w = 300$ Å are displayed in Fig. 3a and b.

It is very clear from the figure that the binding energy for all the impurity positions exhibit a similar behaviour with smaller well width like $L_w = 50$ Å with the following exception. The shift in the binding occurs towards smaller barrier width of L_b ~50 Å when compared with L_b ~100 Å as discussed in the earlier case at which the saturation in the binding energy is observed. This can be substantiated with the fact that once the well width is increased towards the bulk value, the DQW starts to behave like two isolated quantum wells irrespective of the barrier width which is increased beyond 50 Å.

3.2. DQW under applied magnetic field ($\gamma = 3$, 5 and 6)

As reported in Refs. [21–23], one can investigate the interwell coupling in a DQW and its relation to barrier parameters through the magneto absorption study under the effect of magnetic field. Therefore, in order to understand the transitions of carriers involving both symmetric and antisymmetric states in diluted magnetic DQW systems, it is inevitable to make a comparative study on the carrier behaviour at various impurity locations under the applied magnetic field. Hence this section is mainly addressed for such discussion. It is well known that the applied magnetic field tremendously reduces (Eqn. (7)) the potential barrier height (333 meV, 67.7 meV, 19.4 meV and 8.4 meV corresponding to $\gamma = 0$, 3, 5 and 6 respectively) in which the carrier has been confined. When analysing the effect of applied magnetic field, one observes that an increase of the strength of magnetic field beyond $\gamma = 5$ (~150 T) results in the complete delocalization of the carriers confined inside the DQW structures which has been studied for all the impurity locations. For the strength of magnetic field $\gamma > 5$, the unbound states are formed above the potential barrier height instead of bound states inside the well. Therefore, this fact eliminates the need to discuss the results for $\gamma \geq 6$.

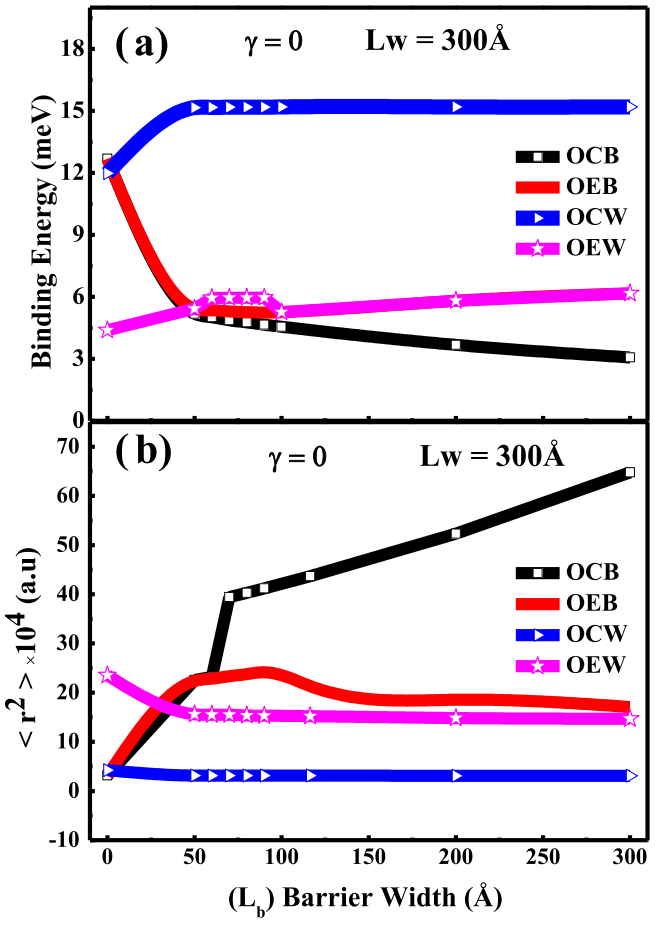

Fig. 3. Variation of **(a)** binding energy and **(b)** $<r^2>$ against barrier width for larger well dimension $L_w = 300$ Å without the application of magnetic field ($\gamma = 0$) for the Mn ion concentration of $x = 0.3$. Graphs have been plotted against various impurity locations (z_i).

3.2.1. On centre barrier impurity (OCB)

Fig. 4 presents the variation of binding energy and $<r^2>$ for the OCB impurity as a function of central barrier width for $L_w = 50$ Å It is seen from Fig. 4a that, when the barrier width is limited to zero, $L_b \rightarrow 0$ Å, the binding energy decreases as the strength of the magnetic field increases.

This can be understood from the fact that when the central barrier vanishes, the two QWs effectively becomes the SQW of width $L_{SQW} = 2L_{DQW}$ and exhibits the same characteristic behaviour ascribed to the SQW under the external magnetic field. An interesting influence of magnetic field upon the confinement of the carrier relies on the rapid increase of binding energy when γ increases for $L_b > 0$ Å, even though the barrier height is reduced due to the applied magnetic field as one can justify from the probability distribution for the impurity located at the centre of the barrier as shown in Fig. 5 (Ia, Ib and IIa, IIb).

The main mechanism by which the magnetic field gives rise to the strong localization of the carrier when it resides at OCB is the strong exchange interaction between the spin of confined carriers and the spins of localized Mn^{2+} ions. As a result, there is an existence of ferromagnetic clouds around the singly occupied electronic states which enhances the binding energy and shrinks the localization radius of localized electrons. When the well width is increased beyond the effective Bohr radius towards the bulk, the binding energy associated with all γ converges to the same value when the barrier width approaches the bulk limit as one can see from Fig. 6a.

3.2.2. On Centre Well impurity (OCW)

When the Impurity is at OCW, the reduction in the barrier height causes the $< r^2 >$ larger and results in very weak Coulomb interaction between the carrier and the parent donor atom thereby reducing the binding energy with respect to the applied magnetic field as shown in Fig. 7a and b.

Moreover the binding energy increases as the barrier width increases. This is due to the fact that for the thinner barrier, a greater fraction of the wavefunction starts to penetrate into the central barrier which can be seen from Fig. 8 (Ia, Ib and IIa, IIb) giving $\left|\psi^2\right|$ against L_b, as demonstrated by Refs. [22,23] justifying the veracity of our model. When the barrier becomes thick,

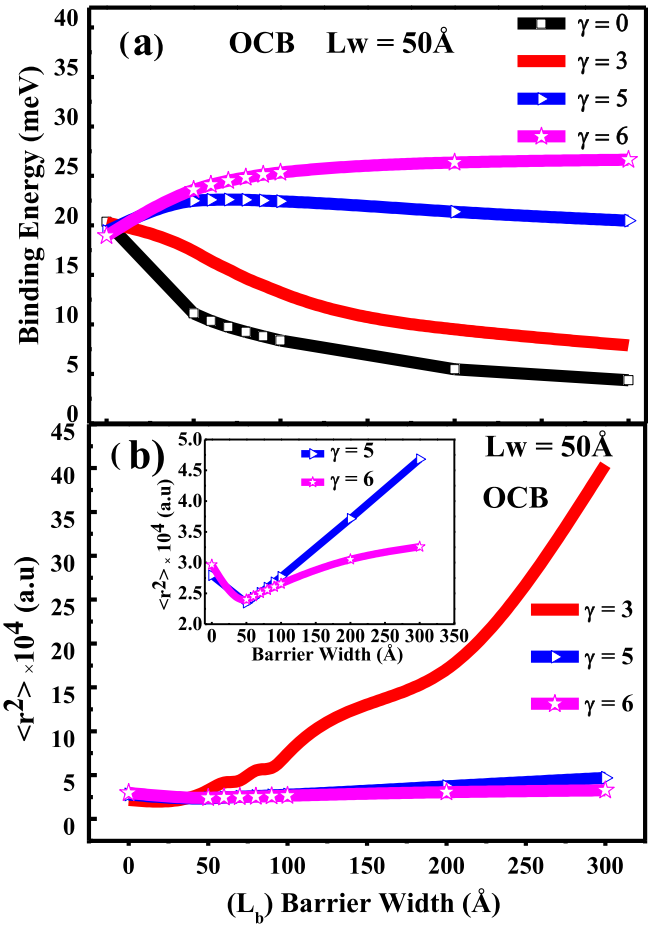

Fig. 4. Variation of **(a)** binding energy and **(b)** $\langle r^2 \rangle$ against barrier width for lower well dimension $L_w = 50$ Å with the application of magnetic field ($\gamma = 3$, 5 and 6) for the Mn ion concentration of $x = 0.3$. Graphs have been plotted for OCB impurity.

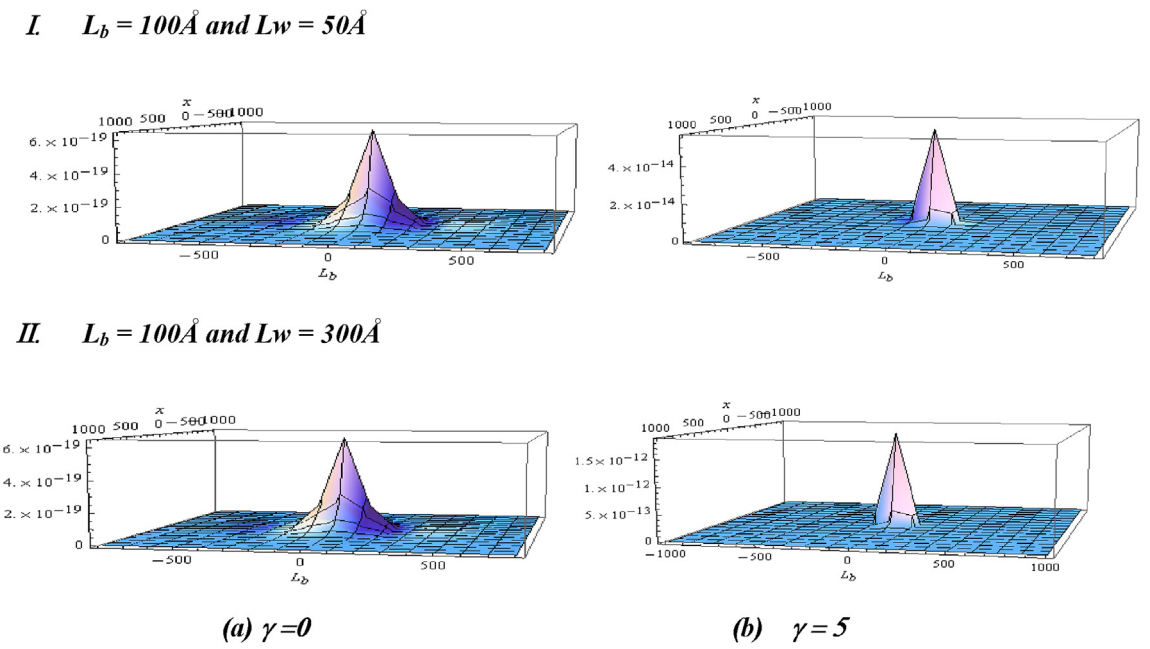

Fig. 5. Probability density $|\psi^2|$ of the donor placed at OCB for various dimensions of the barrier and well under $\gamma = 0$ and $\gamma = 5$ for Mn ion concentration of $x = 0.3$.

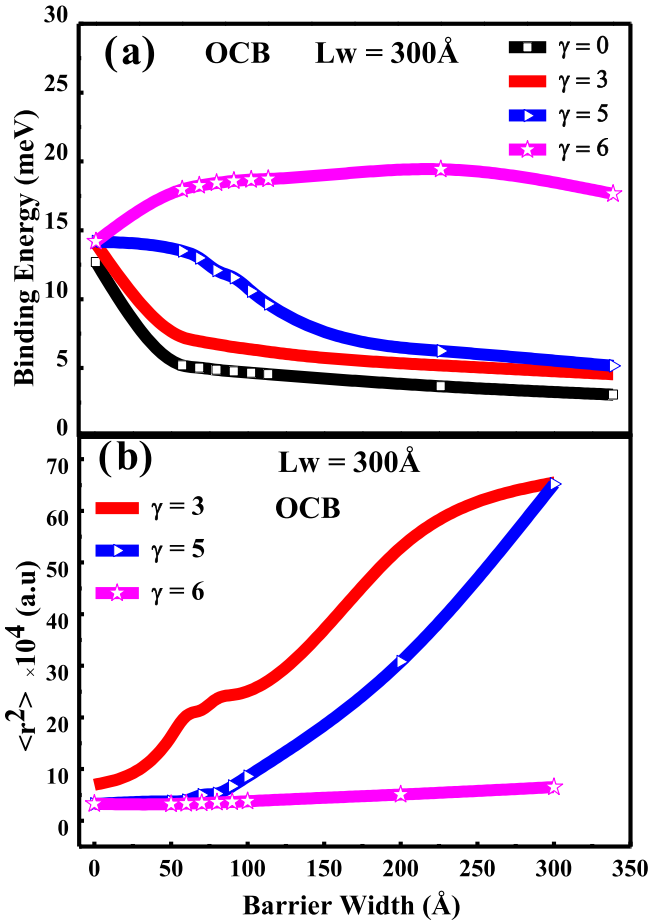

Fig. 6. Variation of **(a)** binding energy and **(b)** $\langle r^2 \rangle$ against barrier width for larger well dimension $L_w = 300$ Å with the application of magnetic field ($\gamma = 3$, 5 and 6) for the Mn ion concentration of $x = 0.3$. Graphs have been plotted for OCB impurity.

then the DQW structure effectively becomes two decoupled SQWs and the properties associated with the applied magnetic field becomes the same as that of the SQW thereby one can see the increased binding energy in that region.

When the well width is increased towards the bulk value, there is no much appreciable impact of magnetic field on the binding energy has been noticed (Fig. 9a) which can be understood from the variation of $\langle r^2 \rangle$ as shown in Fig. 9b.

Though the effect due to spin polaronic shift is perceptible for smaller well width of $L_w = 50$ Å as given in the inset of Fig. 7a, the overall effect on the binding does not alter the trend without considering the spin polaronic shift.

But the effect due to spin polaronic shift as given in the inset of Fig. 9a shows the reverse effect on the trend of the donor binding without considering the polaronic correction as there is no much effect on the exchange energy when the magnetic field is applied as can be seen from the inset of Fig. 9a.

3.2.3. On edge barrier (OEB) and On edge well (OEW) impurity

When the donor impurity is placed at the interface between the two magnetic semiconducting layers for a given smaller width like $L_w = 50$ Å, it experiences a striking effect with respect to magnetic field which contradicts to other two impurity locations like OCB, OCW.

There is a drastic increase of the binding energy with respect to magnetic field for OEW impurity as shown in Fig. 10a when the barrier width is limited to zero in contrast to the situation for non − magnetic wells [31]. This result can be justified from the interpretation given by S. Lee et al. [21] and Mukesh Jain [32] as follows: There is a possibility of finding less number of antiferromagnetically paired Mn^{2+} ions along the interface of the heterostructure, which can effectively contribute to a larger $< S_z >$ (i.e.) the thermal average of the spin of the contributing ions. Therefore, the magnetization of the material becomes larger since these ions can easily be aligned in the external magnetic field. Hence it can show its influence to the full extent with the carrier through a strong exchange interaction when it resides at the well interface. The results of Fig. 10a can be justified from the probability distribution for the carrier plotted in Fig. 11(Ia, Ib and IIa, IIb).

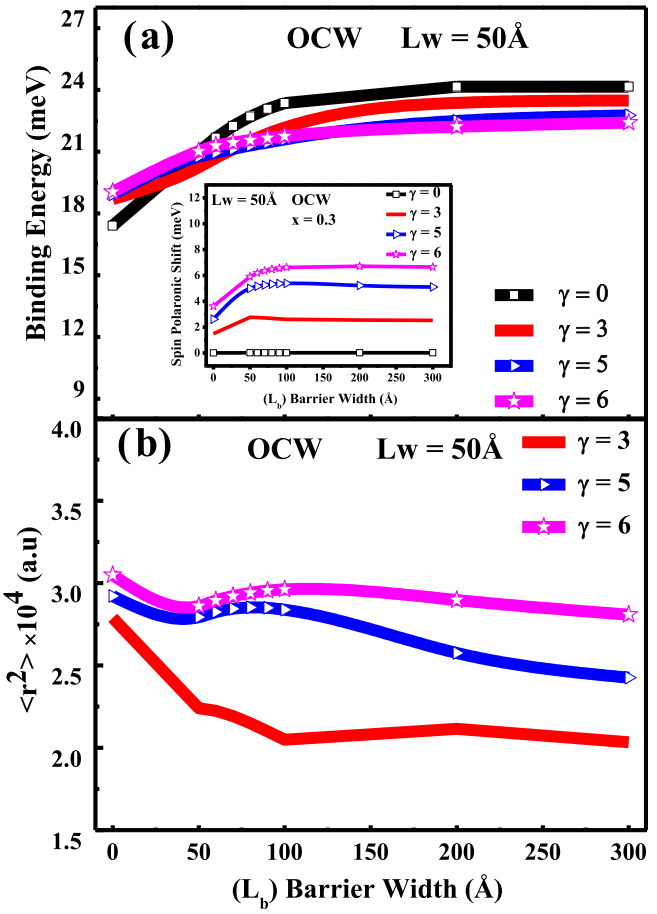

Fig. 7. Variation of **(a)** binding energy and **(b)** $\langle r^2 \rangle$ against barrier width for lower well dimension $L_w = 50$ Å with the application of magnetic field ($\gamma = 3$, 5 and 6) for the Mn ion concentration of $x = 0.3$. Graphs have been plotted for OCW impurity.

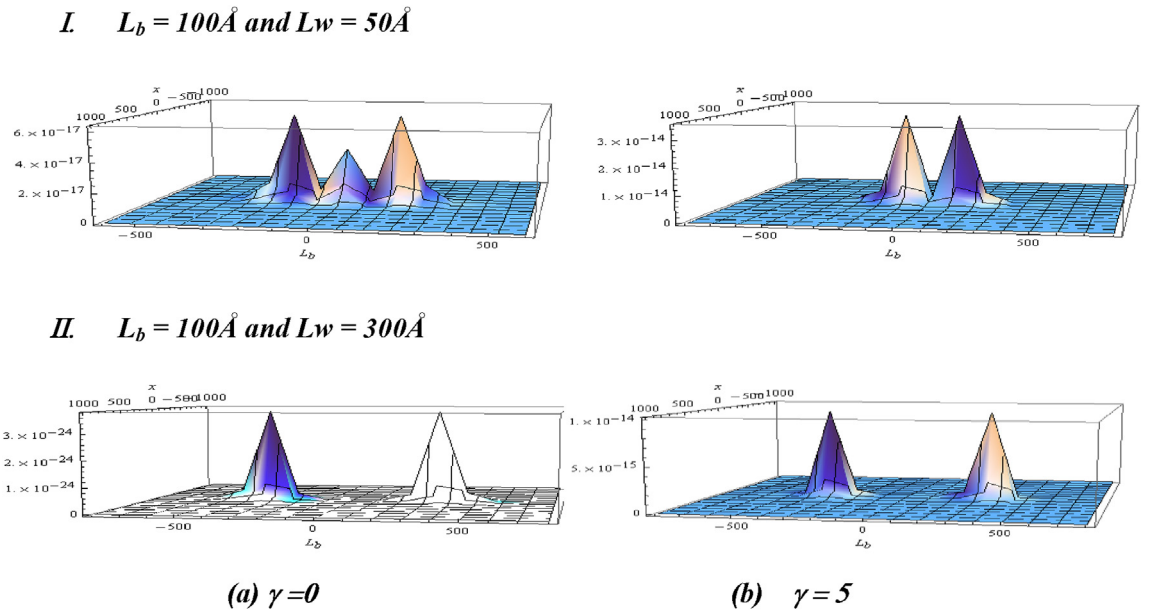

Fig. 8. Probability density $|\psi^2|$ of the donor placed at OCW for various dimensions of the barrier and well under $\gamma = 0$ and $\gamma = 5$ for Mn ion concentration of $x = 0.3$.

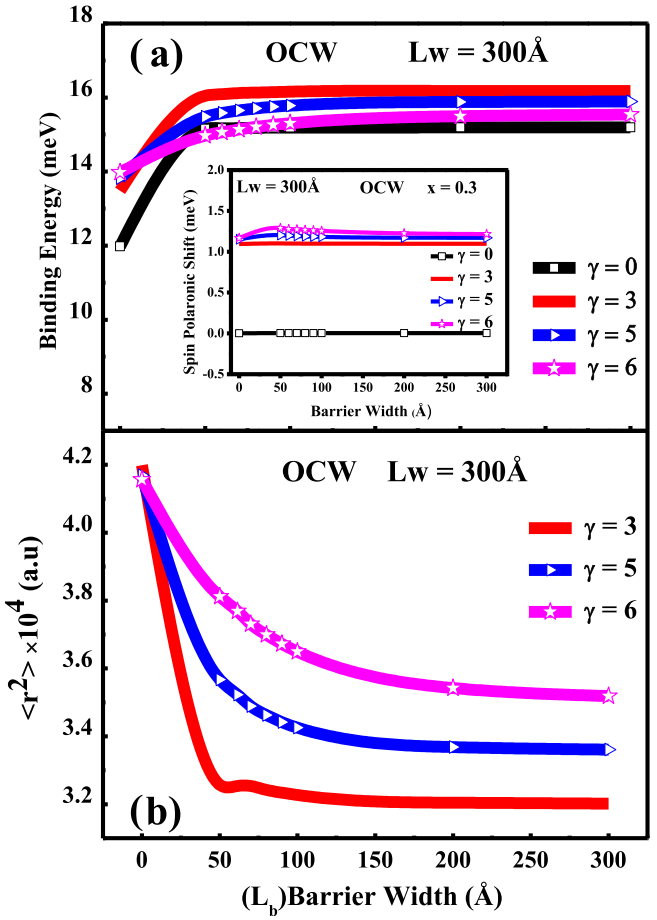

Fig. 9. Variation of **(a)** binding energy and **(b)** $<r^2>$ against barrier width for larger well dimension $L_w = 300$ Å with the application of magnetic field ($\gamma = 3$, 5 and 6) for the Mn ion concentration of $x = 0.3$. Graphs have been plotted for OCW impurity.

But the applied magnetic field shows the reverse effect on the carrier confinement when the impurity is placed at OEB even though this is the interface between the two magnetic semiconducting layers as this exhibits the behaviour of the donor binding in a SQW including BMP effect (Fig. 10b). The influence of magnetic field is predominant for the larger well width since it drastically alters the binding energy as shown in Fig. 12a and b. The substantiated argument is given to this point through the understanding of the behaviour of the carriers in two isolated quantum wells in this bulk limit which does not favour the tunnelling phenomena to occur.

4. Conclusion

This work presents a comprehensive description of the theoretical investigation on the magnetic field induced interwell coupling in a in a Cd1-xinMnxinTe/Cd1-xoutMnxoutTe DQW materials in which the carrier has been confined. To sum up, the above results presented clearly demonstrate that without the application of magnetic field, the binding energy increases as the impurity position goes from OCB and reaches a maximum value when it is at OCW and starts to decrease when it resides at well interface. But once the magnetic field is applied, it favours the interwell coupling by allowing the penetration of the impurity wavefunction via central barrier thereby it reduces the binding energy for OCW impurity and shift the binding energy to higher value for all other impurity locations. These conclusions are further confirmed from the Fig. 13 which represents how the binding energy varies with the various impurity locations for various barrier dimensions.

The calculations devoted to the polaronic effects may be helpful to understand how the transport properties of the confined carriers are indirectly altered by the applied external magnetic field. It is very clear from the available literatures that no much effort has been dedicated for such a study exhibited by the DQWs with DMS. Hence this work may give an understanding of the transport properties accounting the BMP effect associated with the electrons confined in a diluted magnetic DQW systems which can be exploited in various optoelectronic and spintronic devices.

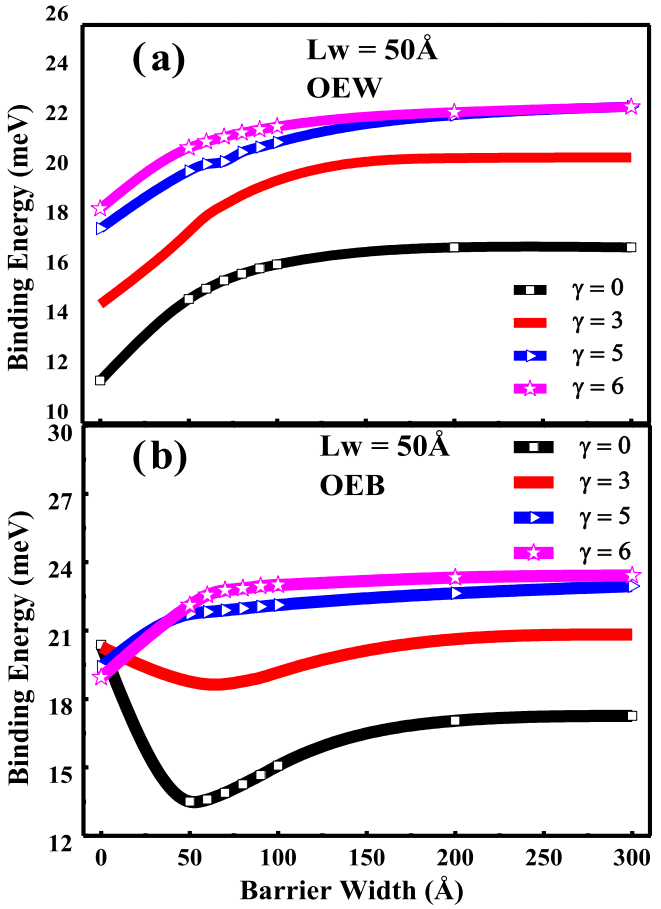

Fig. 10. Variation of **(a)** binding energy and **(b)** $\langle r^2 \rangle$ against barrier width for lower well dimension $L_w = 50$ Å with the application of magnetic field ($\gamma = 3$, 5 and 6) for the Mn ion concentration of $x = 0.3$. Graphs have been plotted for OEB and OEW impurity.

I. $L_b = 100\text{Å}$ *and* $Lw = 50\text{Å}$

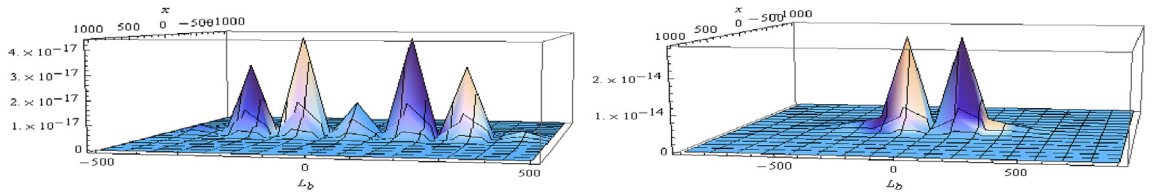

II. $L_b = 100\text{Å}$ *and* $Lw = 300\text{Å}$

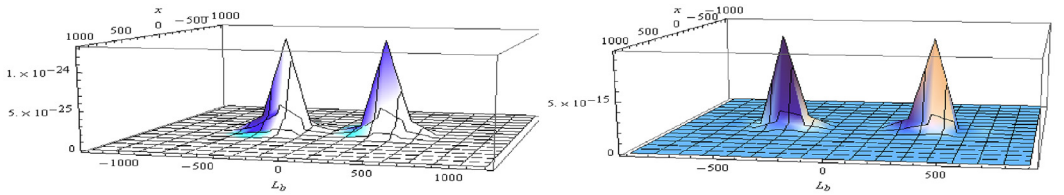

(a) $\gamma = 0$ *(b)* $\gamma = 5$

Fig. 11. Probability density $|\psi^2|$ of the donor placed at OEW for various dimensions of the barrier and well under $\gamma = 0$ and $\gamma = 5$ for Mn ion concentration of $x = 0.3$.

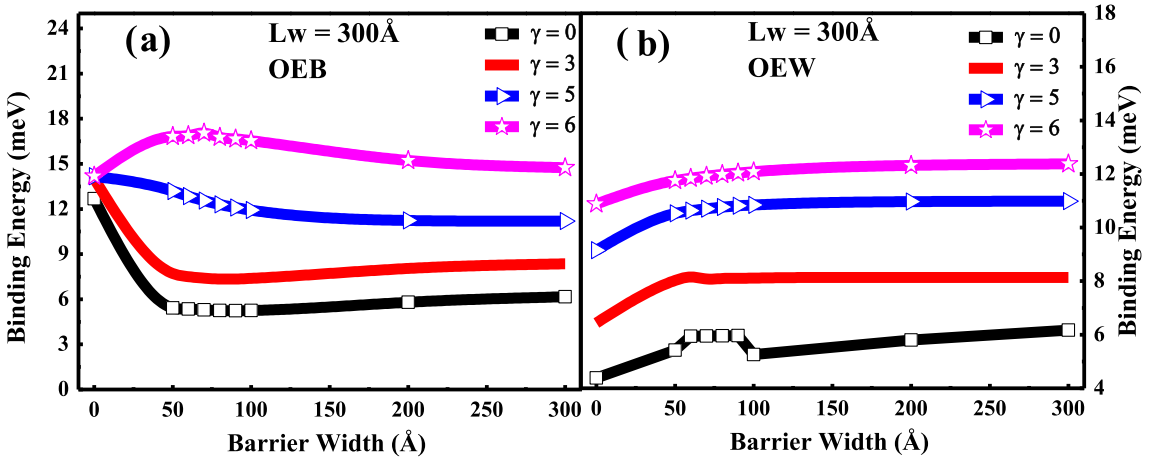

Fig. 12. Variation of **(a)** binding energy and **(b)** $<r^2>$ against barrier width for larger well dimension $L_w = 300$ Å with the application of magnetic field ($\gamma = 3$, 5 and 6) for the Mn ion concentration of $x = 0.3$. Graphs have been plotted for OEB and OEW impurity.

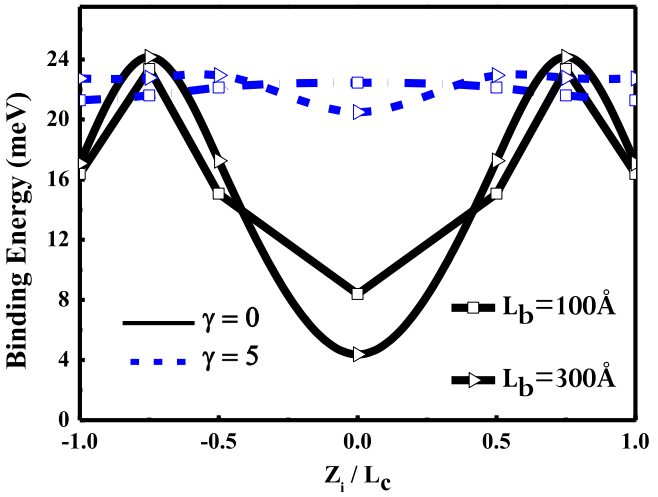

Fig. 13. Variation of **(a)** Binding energy as a function of impurity position is plotted for DQW with a well width of 50 Å. The solid and dashed lines are corresponding to $\gamma = 0$ and $\gamma = 5$ respectively. The square and triangle symbols represents $L_b = 100$ Å and $L_b = 300$ Å respectively.

Acknowledgement

The authors thank University Grants Commission, New Delhi, India for the financial support under Major Research Project. (F.No.42-816/2013 (SR)).

References

[1] J.A. Gaj, J. Ginter, Exchange interaction of manganese, Phys. Status Solidi Basic Res. 655 (1978) 655–662, http://dx.doi.org/10.1002/pssb.2220890241.
[2] G. Rebmann, C. Rigaux, G. Bastard, M. Menant, R. Triboulet, W. Giriat, Magnetooptical study of semimagnetic alloys $Cd_{1-x}Mn_xTe$, Phys. B+C 117–118 (1983) 452–454, http://dx.doi.org/10.1016/0378-4363(83)90556-9.
[3] J.P. Lascaray, D. Coquillat, J. Deportes, A.K. Bhattacharjee, Zeeman splitting of exciton and magnetization in $Cd_{1-x}Mn_xTe$:anomalous behavior at high x, Phys. Rev. B 38 (1988) 7602–7606, http://dx.doi.org/10.1103/PhysRevB.38.7602.
[4] T. Kasuya, Anomalous transport phenomena in Eu-chalcogenide alloys, Rev. Mod. Phys. 40 (1968) 684–696, http://dx.doi.org/10.1103/RevModPhys.40.684.
[5] U. Thibblin, Theory of bound magnetic polarons in diluted magnetic semiconductors, Int. J. Mod. Phys. B 3 (1989) 337–366, http://dx.doi.org/10.1142/S0217979289000269.
[6] P. Nithiananthi, K. Jayakumar, Laser induced semiconductor- metal transition in A semimagnetic quantum well, Int. J. Nanosci. 10 (2011) 611–615, http://dx.doi.org/10.1142/S0219581X11009180.
[7] T. Dietl, J. Cibert, P. Kossacki, D. Ferrand, S. Tatarenko, A. Wasiela, Y. Merle D'Aubigné, F. Matsukura, N. Akiba, H. Ohno, Ferromagnetism induced by free carriers in p-type structures of diluted magnetic semiconductors, Phys. E Low-Dimens. Syst. Nanostructures 7 (2000) 967–975, http://dx.doi.org/10.1016/S1386-9477(00)00098-9.

[8] C. Camilleri, F. Teppe, D. Scalbert, Y. Semenov, M. Nawrocki, M. Dyakonov, J. Cibert, S. Tatarenko, T. Wojtowicz, Electron and hole spin relaxation in modulation-doped CdMnTe quantum wells, Phys. Rev. B 64 (2001) 1–7, http://dx.doi.org/10.1103/PhysRevB.64.085331.
[9] P. Nithiananthi, K. Jayakumar, Pressure study on the semiconductor-metal transition in a quantum well, Phys. Status Solidi Basic Res. 246 (2009) 1238–1242, http://dx.doi.org/10.1002/pssb.200945023.
[10] P. Nithiananthi, K. Jayakumar, Effect of Γ-X crossover on the donor binding energy in a quantum well, Int. J. Mod. Phys. B 19 (2005) 3861–3868, http://dx.doi.org/10.1142/S0217979205032486.
[11] H. Chen, S. Zhou, Effect of a finite width barrier on binding energy in modulation doped quantum well structures, Phys. Rev. B 36 (1987) 9581, http://dx.doi.org/10.1103/PhysRevB.
[12] D.B.T. Thoai, Hydrogenic impurity in double quantum wells: effects of the image charges, Phys. B 175 (1991) 373–380, http://dx.doi.org/10.1016/0921-4526(91)90073-N.
[13] N. Raigoza, A.L. Morales, C.A. Duque, Effects of hydrostatic pressure on donor states in symmetrical GaAs-$Ga_{0.7}Al_{0.3}As$ double quantum wells, Phys. B Condens. Matter 363 (2005) 262–270, http://dx.doi.org/10.1016/j.physb.2005.03.031.
[14] P. Kalpana, K. Jayakumar, P. Nithiananthi, Effect of geometry on the pressure induced donor binding energy in semiconductor nanostructures, Int. J. Comput. Mater. Sci. Eng. 4 (2015) 1550018, http://dx.doi.org/10.1142/S2047684115500189.
[15] G. Vignesh, P. Nithiananthi, Diamagnetic susceptibility: an indicator of pressure induced donor localization in a double quantum well, Superlattices Microstruct. 92 (2016) 232–241, http://dx.doi.org/10.1016/j.spmi.2016.02.017.
[16] D. Yoshioka, Allan H. Macdonald, Double Quantum Well Electron - Hole Systems in Strong Magnetic Fields, 1990, pp. 4211–4214, http://dx.doi.org/10.1143/JPSJ.59.4211.
[17] G.S. Boebinger, H.W. Jiang, L.N. Pfeiffer, K.W. West, Magnetic-field-driven destruction of quantum hall states in a double quantum well, Phys. Rev. Lett. 64 (1990) 1793–1796, http://dx.doi.org/10.1103/PhysRevLett.64.1793.
[18] L. Brey, Energy spectrum and CDW instability of a DQW in a magnetic field, Phys. Rev. Lett. 7 (1990) 903–906, http://dx.doi.org/10.1103/PhysRevLett.65.903.
[19] G.S. Boebinger, A. Passner, L.N. Pfeiffer, K.W. West, Measurement of Fermi-surface distortion in double quantum wells from in-plane magnetic fields, Phys. Rev. B 43 (1991) 12673–12676, http://dx.doi.org/10.1103/PhysRevB.43.12673.
[20] M. Orlita, R. Grill, S. Malzer, M. Byszewski, Luminescence of double quantum wells subject to in-plane magnetic fields, Phys. Rev. B 72 (2005) 165314, http://dx.doi.org/10.1103/PhysRevB.72.165314.
[21] S. Lee, M. Dobrowolska, J.K. Furdyna, H. Luo, L.R. RamMohan, Magneto-optical study of interwell coupling in double quantum wells using diluted magnetic semiconductors, Phys. Rev. B 54 (1996) 16939–16951, http://dx.doi.org/10.1103/PhysRevB.54.16939.
[22] S. Haacke, N.T. Pelekanos, H. Mariette, M. Zigone, A.P. Heberle, W.W. Rühle, Tunneling dynamics in CdTe/(Cd, Zn) Te asymmetric double-quantum well structures, Phys. Rev. B 47 (1993) 16643–16646, http://dx.doi.org/10.1103/PhysRevB.47.16643.
[23] I. Lawrence, S. Haacke, H. Mariette, W.W. Rühle, H. Ulmer – Tuffigo, J. Cibert, G. Feuillet, Exciton tunneling revealed by magnetically tuned interwell coupling in semiconductor double quantum wells, Phys. Rev. Lett. 73 (1994) 2131–2134, http://dx.doi.org/10.1103/PhysRevLett.73.2131.
[24] B.E. Larson, K.C. Hass, H. Ehrenreich, A.E. Carlsson, Exchange mechanisms in diluted magnetic semiconductors, Solid State Commun. 56 (1985) 347–350, http://dx.doi.org/10.1016/0038-1098(85)90399-0.
[25] A. Elangovan, D. Shyamala, K. Navaneethakrishnan, Solid State Commun. 89 (1994) 869–873, http://dx.doi.org/10.1016/0038-1098(94)90073-6.
[26] K. Gnanasekar, K. Navaneethakrishnan, Spin polaron in a quantum dot of the diluted magnetic semiconductors, Mod. Phys. Lett. B 18 (2004) 419–426, http://dx.doi.org/10.1142/S0217984904006962.
[27] C. Rajamohan, K. Jayakumar, Effect of laser on the bound magnetic polaron in a semimagnetic quantum wire, J. Nano. Electron. Phys. 3 (2011) 1005–1009.
[28] A. Merwyn Jasper De Reuben, K. Jayakumar, Shape effect of semimagnetic quantum dot on the bound magnetic polaron, Int. J. Nanosci. 10 (2011) 665–668, http://dx.doi.org/10.1142/S0219581X11009131.
[29] J.A. Gaj, R. Planel, G. Fishman, Relation of magneto-optical properties of free excitons to spin alignment of Mn^{2+} ions in CdMnTe, Solid State Commun. 29 (1979) 435–438, http://dx.doi.org/10.1016/0038-1098(79)91211-0.
[30] P. Nithiananthi, D. Varshney, K. Jayakumar, Conf. Int. Conf. Nanosci. Nanotech. (2010) 291–292.
[31] C.E.T. Gonvalves da Silva, Bound magnetic polarons in semimagnetic quantum wells, Phys. Rev. B 32 (1985) 6962–6964, http://dx.doi.org/10.1103/PhysRevB.32.6962.
[32] M. Jain, in: G.E. Marques (Ed.), Diluted Magnetic Semiconductors, World Scientific, Singapore, USA, UK, 1991, pp. 492–518.

Journal of Physics and Chemistry of Solids 110 (2017) 364–369

Contents lists available at ScienceDirect

Journal of Physics and Chemistry of Solids

journal homepage: www.elsevier.com/locate/jpcs

Impurity states and the diamagnetic susceptibility of a donor in a GaAs/$Al_xGa_{1-x}As$ Triangular Quantum Well under hydrostatic pressure

Panneer Selvam Kalpana, Kalyanasundaram Jayakumar *

Nanostructure Lab, Department of Physics, Gandhigram Rural University, Gandhigram, 624 302, Tamilnadu, India

ARTICLE INFO

Keywords:
Triangular Quantum Well
Diamagnetic susceptibility
Donor impurity
Binding energy
Hydrostatic pressure
Impurity states

ABSTRACT

We study the effect of Γ-X band crossover due to the application of hydrostatic pressure of a hydrogenic donor confined in a Triangular GaAs/$Al_{1-x}Ga_xAs$ Quantum Well (TQW) for x = 0.3 and the diamagnetic susceptibility (χ_{dia}) for such an impurity in 1s and some few low lying excited states have been investigated. The Schrodinger equation has been solved using variational technique in the effective mass approximation. The results show that the diamagnetic susceptibility (χ_{dia}) of a hydrogenic donor abruptly increases at a particular pressure for 1s and $2p_{\pm}$ states but a steady increase for 2s state as a function of applied pressure.

1. Introduction

Triangular Quantum Well (TQW) structures have attracted much attention in recent years because of their unique properties of quantum levels which is used for modelling Metal Oxide Semiconductor Structures. Recently, many theoretical investigations [1–8] have been devoted to the study of donor impurity confined in a Triangular Nanostructure systems. The combined effects of hydrostatic pressure and the applied electric field on the binding energy of a hydrogenic impurity states in GaAs/$Ga_{1-x}Al_xAs$ Triangular Quantum Well Wires (TQWW) has been investigated by Restrepo et al. [9]. Khordad [10] has investigated in his work that the wire size and pressure have small influences on the spin - orbit interaction of a V-shaped Quantum Well Wire (QWW).

The importance of crossed electric and magnetic field applied to the V – shaped QW on the binding energy of a donor impurity has been theoretically studied by Kasapoglu et al. [11]. The fabrication and the mechanism of any Semiconductor Devices is not possible without considering impurity states since its energy levels are considerably different from the bulk which mainly affects the electronic, optical and transport properties of these devices. Many researchers have focussed their attention on the experimental [12] and theoretical[13–24] investigations of the diamagnetic susceptibility (χ_{dia}) of a donor impurity in Low Dimensional Semiconductor Systems (LDSS) because it acts as a probe to understand the carrier localization as well as the Semiconductor to Metal Transition (SMT) in such LDSS. The study on the influence of pressure on the Diamagnetic Susceptibility of hydrogenic donor in some low – lying excited states in a QW with square confinement has been carried out by Nithiananthi et al. [25]. The diamagnetic susceptibility of a hydrogenic donor in a QW has been investigated by Kasapoglu et al. [26] including different mass anisotropy parameters and found that the χ_{dia} in such anisotropic materials converges rapidly to the bulk limit as the well size increases. Considerable effort has been made by Avazzadeh et al. [27] to analyse the impact of the cross-sectional are of various QWW on the χ_{dia} of the hydrogenic donor impurity and reported that the absolute value of the diamagnetic susceptibility increases with increasing cross-sectional area (TQWW) and also observed that the highest energy gap renormalization corresponds to Triangular cross section only. In the light of all these works, in the present communication, we report the binding energy and the χ_{dia} of a donor impurity confined in a GaAs/$Al_{1-x}Ga_xAs$ TQW under the effect of Γ-X band crossover due to the application of hydrostatic pressure.

2. Theoretical formalism

The pressure dependent Hamiltonian of the donor electron in a GaAs Quantum Well in atomic unit is given by

$$\mathbf{H} = \frac{-\nabla^2}{2m^*_{w,b}(P,T)} - \frac{1}{\varepsilon_{w,b}(z,P,T)r} + v_B(z,P,T) \quad (1)$$

with the first, second and third terms are the Kinetic Energy, Potential Energy due to the ionized donors and the confining barrier potential, which arises due to the band discontinuities when two different materials are placed adjacent to each other to form the heterojunction

* Corresponding author.
E-mail address: kjkumar_gri@rediffmail.com (K. Jayakumar).

http://dx.doi.org/10.1016/j.jpcs.2017.06.031
Received 9 May 2017; Received in revised form 11 June 2017; Accepted 29 June 2017
Available online 1 July 2017

respectively.where $m^*_{w,b}$ is pressure dependent effective mass of electron in GaAs and is given by Ref. [20]

$$m^*_w(P,T) = 1/\left[1 + 7.51\left\{2/\Gamma_w(P,T) + [\Gamma_w(P,T) + 0.341]^{-1}\right\}\right] \quad (2)$$

Γ_w(P,T) is the pressure dependent energy gap of GaAs at the Γ point and is given by Ref. [20]

$$\Gamma_w(P,T) = 1.519 + \alpha^{\Gamma}_w P - 5.405x10^{-14}T^2/(T+204) \quad (3)$$

where α^{Γ}_w is the pressure coefficient of GaAs at the Γ point.

The effective mass of the Al_xGa_{1-x} As barrier is [20]

$$m*_b(P,T) = m*_w(P,T) + 0.083x, \; x \text{ being the Al composition} \quad (4)$$

The pressure dependent dielectric constant for GaAs and Al_xGa_{1-x} As are given by

$$\varepsilon_w(P) = \varepsilon_w(0)\exp(\varsigma P) \quad (5)$$

where, $\varepsilon_w(0) = \varepsilon_0(T_0)\exp[\gamma_0(T - T_0)]$ and $\varepsilon_b(P) = \varepsilon_w(P) - 3.12\,x$

Pressure dependent potential energy of Al_xGa_{1-x}As barrier is

$$v_B(z,P,T) = \begin{cases} \dfrac{v_0(z,P,T)|z|}{L(P)} & , -L(P) < z < L(P) \\ v_0(z,P,T) & , |z| > L(P) \end{cases} \quad (6)$$

$$v_0(z,P,T) = \begin{cases} \Gamma_b(P,T) - \Gamma_w(P,T) & P \le P_1 \\ x_b(P,T) - \Gamma_w(P,T) + S_{\Gamma X}(P) & P_1 < P < P_2 \end{cases} \quad (7)$$

The pressure dependent Γ - X band mixing strength coefficient [20]

$$S_{\Gamma X}(P) = S_0 x(P - P_1)/P \quad (8)$$

P_1 and P_2 are the critical crossover pressures between X_b - band and Γ_b – band, X_b - band and Γ_w - band respectively.

The variation of X_b band with pressure is [20]

$$X_b(P,T) = X_b(0,T) + \alpha^X_b P \quad (9)$$

where,α^X_b being the pressure coefficient for the barrier.

The envelop function without the donor impurity inside the TQW is defined as

$$f_i(z) = \begin{cases} c_1 e^{\beta(z+L(P))} & , z < -L(P) \\ c_2 Ai\left[\left(\dfrac{2m^*_w(P,T)v_0(z,P,T)}{L(P)\hbar^2}\right)^{1/3}\left(-z - \dfrac{L(P)E_0(P,T)}{v_0(z,P,T)}\right)\right] + c_3 Bi\left[\left(\dfrac{2m^*_w(P,T)v_0(z,P,T)}{L(P)\hbar^2}\right)^{1/3}\left(-z - \dfrac{L(P)E_0(P,T)}{v_0(z,P,T)}\right)\right] & , -L(P) < z < 0 \\ c_4 Ai\left[\left(\dfrac{2m^*_w(P,T)v_0(z,P,T)}{L(P)\hbar^2}\right)^{1/3}\left(z - \dfrac{L(P)E_0(P,T)}{v_0(z,P,T)}\right)\right] + c_5 Bi\left[\left(\dfrac{2m^*_w(P,T)v_0(z,P,T)}{L(P)\hbar^2}\right)^{1/3}\left(z - \dfrac{L(P)E_0(P,T)}{v_0(z,P,T)}\right)\right] & , 0 < z < L(P) \\ c_5 e^{-\beta(z-L(P))} & , z > L(P) \end{cases} \quad (10)$$

where, $\beta = 2m^*_b(P,T)[(v_0(P,T) - E_0(P,T)])^{1/2}$ and Ai[z], Bi[z] are Airy functions, E_0 (P,T) is the Pressure dependent energy of the lowest conduction band. Here the subscript 'i' in $f_i(z)$ corresponds to i = 1, 2, 3, 4 in the respective regions of the TQW. The constants c_1, c_2, c_3, c_4 and c_5 and E_0 (P, T) are obtained by choosing the proper boundary conditions as given below:

(i) $\left.\frac{\partial f_1(z)}{\partial z}\right|_{z=-L} = \left.\frac{\partial f_2(z)}{\partial z}\right|_{z=-L}$ (ii) $\left.\frac{\partial f_2(z)}{\partial z}\right|_{z=0} = \left.\frac{\partial f_3(z)}{\partial z}\right|_{z=0}$

Table 1
Experimental parameters used.

Γ_b(0,T) (eV)	X_b(0,T) (eV)	$\alpha^{\Gamma}_{w,b}$ (meV/Kbar)	α^{x}_{b} (meV/Kbar)	Critical pressure		S_0 (meV)
				P_1 (Kbar)	P_2 (Kbar)	
1.755	1.918	10.7	−1.3	13.5	33.2	250

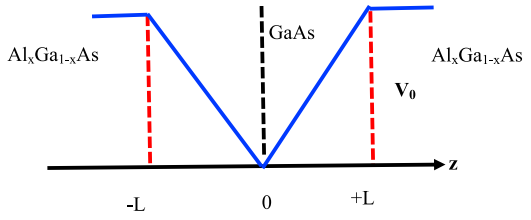

Fig. 1. The Potential profile of the Triangular Quantum Well along the z-axis.

(iii) $\left.\frac{\partial f_2(z)}{\partial z}\right|_{z=L} = \left.\frac{\partial f_3(z)}{\partial z}\right|_{z=L}$

The trial wavefunction of the donor impurity for 1s state, 2s and $2p_{\pm}$ states are given by,

$$\begin{aligned} \Psi_{1s} &= N_{1s} f(z) e^{(-\lambda_{1s} r)} \\ \Psi_{2s} &= N_{2s} f(z)(1 - \delta r) e^{(-\lambda_{2s} r)} \\ \Psi_{2p_{\pm}} &= N_{2p_{\pm}} f(z) \rho e^{(\pm i m\varphi)} e^{\left(-\lambda_{2p_{\pm}} r\right)} \end{aligned} \quad (11)$$

N_{1s}, N_{2s}, $N_{2p\pm}$ and λ_{1s}, λ_{2s}, $\lambda_{2p\pm}$ are the Normalization constants and variational parameters for 1s, 2s and $2p_{\pm}$ states respectively. δ is the orthogonality parameter which is calculated through $\iiint \Psi^*_{2s}\Psi_{1s}\rho d\rho\phi dz = 0$.

The variation of the width of the well as a function of the pressure is given by Ref. [20]

$$L(P) = L(0)[1 - (S_{11} + 2S_{12})P] \quad (12)$$

where S_{11} and S_{12} are the elastic constants of GaAs.

The Schrodinger equation is solved variationally and the donor binding is found from

$$E_B(P,T) = E_0(P,T) - <H(P,T)>_{min} \quad (13)$$

The Diamagnetic susceptibility (χ_{dia}) of the hydrogenic donor confined in a GaAs/Al_xGa_{1-x}As TQW in atomic units, is given by Ref. [25]

$$\chi_{dia} = \frac{-e^2}{6m^*_w(P)\varepsilon_0(P)c^2}\langle r(P)^2\rangle \quad (14)$$

Though we have investigated the effect of pressure alone on the donor binding energy as well as the χ_{dia}, we have given the parameters as a function of both P and T and in all our calculation, T is considered as T = 4 K.

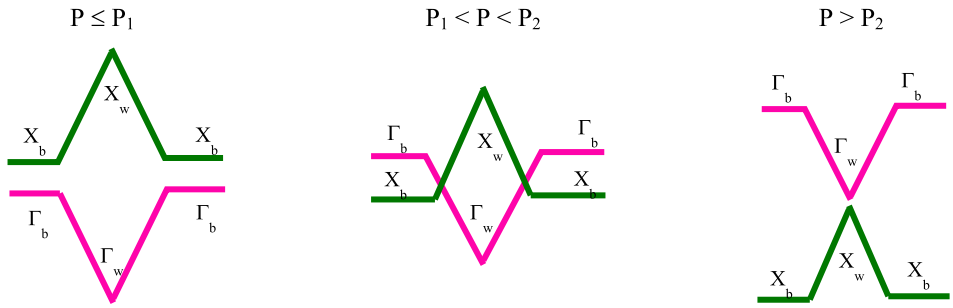

Fig. 2. Schematic band diagram for the Γ – X crossover due to the applied hydrostatic pressure in TQW.

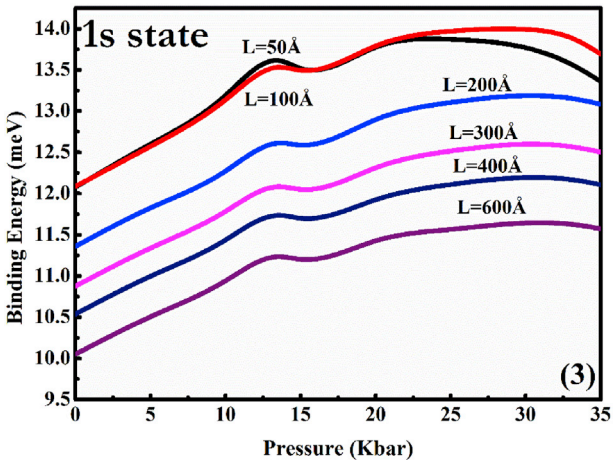

Fig. 3. Variation of binding energy of donor impurity against pressure for 1s state for various well widths.

The parameters used in the calculation are taken from the experimental results [28] and is given in Table 1.

The potential profile of the GaAs/$Al_xGa_{1-x}As$ TQW is given in Fig. 1.

The band diagram for the Γ – X crossover due to the applied hydrostatic pressure in TQW is sketched in Fig. 2.

3. Results and discussion

It is seen from the Fig. 3 that the binding energy varies linearly with the applied pressure upto the first critical value (P_1 = 13.5 Kbar) for 1s state with a fall in the binding upto a pressure of 15 Kbar consistently for all the well widths.

Thereafter it starts to increase with an increase in pressure upto 30 Kbar and again starts to decrease near the second critical pressure (P_2 = 33.2 Kbar).

This may be due to the fact that there is no reduction in the barrier height as presented in Fig. 4 upto P_1 and thereafter that the barrier height starts decreasing and the well becomes shallower as a result of the Γ - X band crossover due to external pressure.

This is an unexpected trend of the binding energy with the applied pressure in a TQW as compared to the reported results of Square Quantum Well (SQW) by Nithiananthi et al. [29]. Perhaps, this may be due to the trend in the variation of subband energy with pressure in TQW as against the SQW given in Fig. 4b.

Moreover, this trend is predominantly seen in the ground state binding energy rather than for the low lying excited states as shown in Fig. 5a and b. For 2s and $2p_{\pm}$ states, the binding energy keeps on increasing as a function of pressure upto an applied pressure of 35 Kbar. The clear splitting up in the binding energy is seen near the first critical pressure for $2p_{\pm}$ state when the well width is increased towards the bulk.

Fig. 6 shows the variation of binding energy as a function of well dimension for the cases with (P_1 = 13.5 Kbar and P_2 = 33.2 Kbar) and without (P = 0 Kbar) the application of external pressure in GaAs/$Al_xGa_{1-x}As$ TQW for 1s, 2s and $2p_{\pm}$ states. It is seen from the figure that the turnover in the binding energy occurs for 1s state with respect to well width as in the case of SQW which is an expected one in any low dimensional systems. One can see from the figure that there is a shift in the turnover towards the higher well width beyond the first critical pressure P_1. These results can be justified from the fact that the applied pressure shrinks the well dimension as given in (12) thereby squeezing the wavefunction causing the binding more.

A similar trend in the binding energy is observed with respect to well width for $2p_{\pm}$ state also but it is found that the shift in the turnover occurs around L ~50 Å at narrow well width itself when the pressure is increased beyond P_1 which can be seen from the results presented in Fig. 6c. But for the 2s state, no turnover is seen upto the pressure of

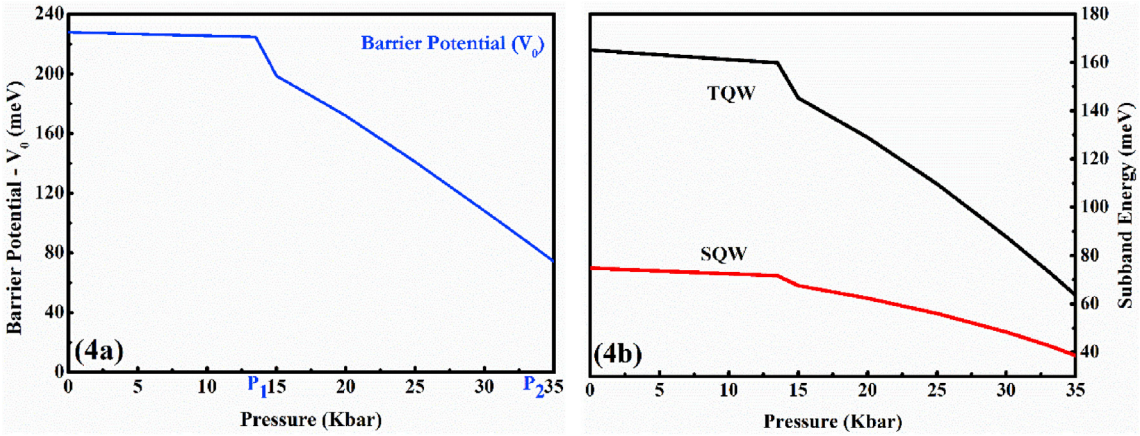

Fig. 4. (a) Variation of Confining Potential of TQW and (b) comparison of Subband Energy of TQW and SQW against Pressure.

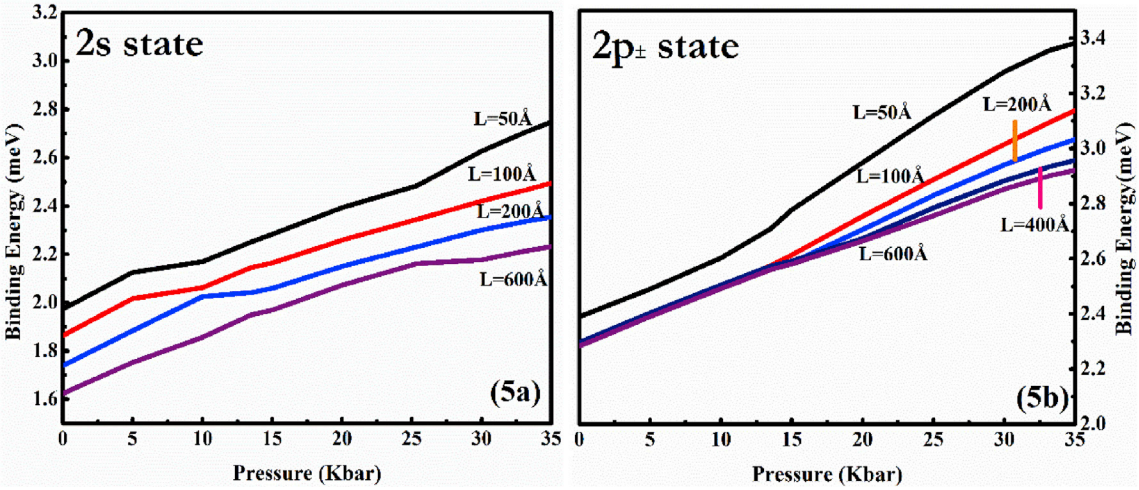

Fig. 5. Variation of binding energy of donor impurity against pressure for (a) 2s state and for (b) $2p_{\pm}$ state for various well widths.

13.5 Kbar and the same occurs when L < 50 Å at pressure P_2 as shown in Fig. 6b. The binding energy of 2s state is considerably less than that of $2p_{\pm}$ state. This is due to the fact that the shape of the lobes of the $2p_{\pm}$ orbital is aligned along the perpendicular direction to that of growth axis (**z**) so that the repulsive potential of barrier has less influence on it when compared to the 2s state which decreases the impurity energy ($<H_{min}>$) thereby increasing the binding E_B of the carrier. The veracity of our results have been found by the limiting cases L→ 0 and L→ ∞. In both the limiting cases, the binding energy E_B should approach towards 1R* (5.3 meV) for 1s state and 0.25R* (1.3 meV) for 2s and $2p_{\pm}$ state [30]. The evidence for our calculation can be found by calculating the ratio between the binding energy of 1s and 2s states for the larger well widths approaching to 4 which exactly reproduces the results of bulk hydrogen atom.

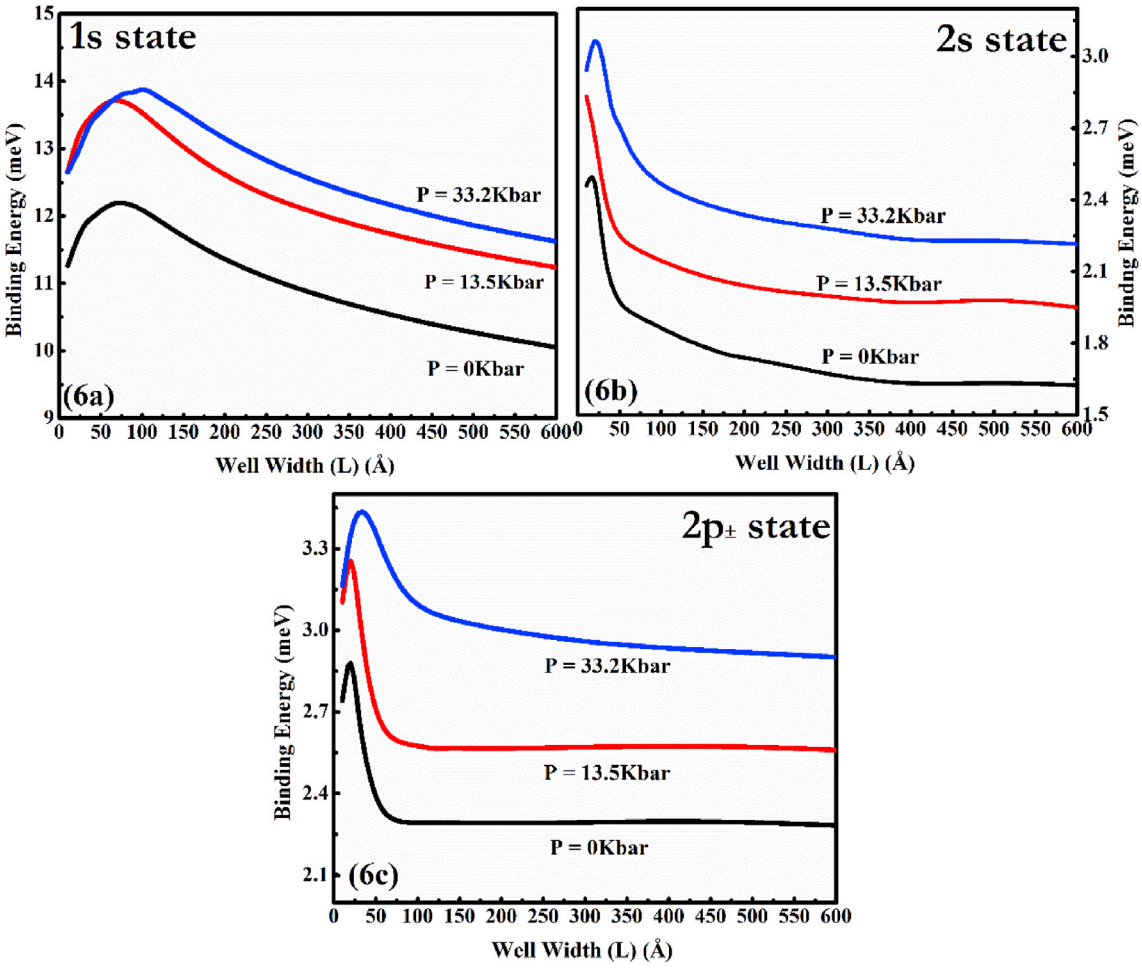

Fig. 6. Variation of binding energy of donor impurity against well width for (a) 1s state, (b) for 2s state and (c) for $2p_{\pm}$ state for various pressures.

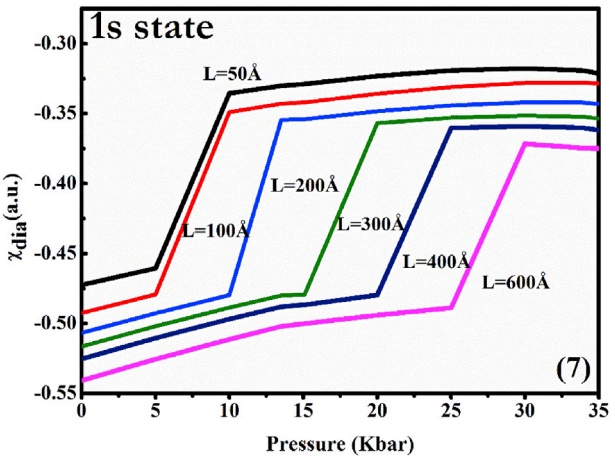

Fig. 7. Variation of χ_{dia} of donor impurity against pressure for 1s state for various well widths.

The behaviour of the variation of χ_{dia} of the donor impurity with the pressure for 1s state is presented in Fig. 7. When the pressure increases, the χ_{dia} increases linearly to a smaller value until the applied pressure reaches 5 Kbar when the well width is of $L_w = 50$ Å. When the pressure goes from 5 Kbar to 10 Kbar, interestingly the χ_{dia} increases very rapidly as shown in figure. Thereafter, when the pressure is larger than 10 Kbar (P > 10 Kbar), the χ_{dia} is nearly a constant. However, the threshold pressure at which the diamagnetic susceptibility shoots up rapidly is shifted to higher pressure values with an increment of 5 Kbar when the confining well width increases from quasi 2D region of $L_w = 50$ Å to bulk region of $L_w = 300$ Å in steps of 50 Å. It is observed that the difference between the pressure at which the onset of drastic increase in χ_{dia} and the onset of saturation of χ_{dia} is always 5 Kbar for all L_w.

The χ_{dia} for $2p_{\pm}$ state follows the same trend with the applied pressure as in the case of 1s state which is presented in Fig. 8. Interestingly one finds from the figure that the χ_{dia} increases rapidly with the applied pressure for all the well widths and attains the same saturation value of $\chi_{dia} \sim -3.25$a.u. with the shift of the onset of saturation of χ_{dia} towards higher pressure with the increase of well width.

Unlike1s and $2p_{\pm}$ state, the behaviour of χ_{dia} with the external applied pressure for 2s state is almost linear which can be seen form the Fig. 9.

Higher the external applied pressure, higher is the χ_{dia} and attains the maximum for pressure of 35 Kbar which leads to the indirect band gap regime in the bandstructure. The results again have been checked for its

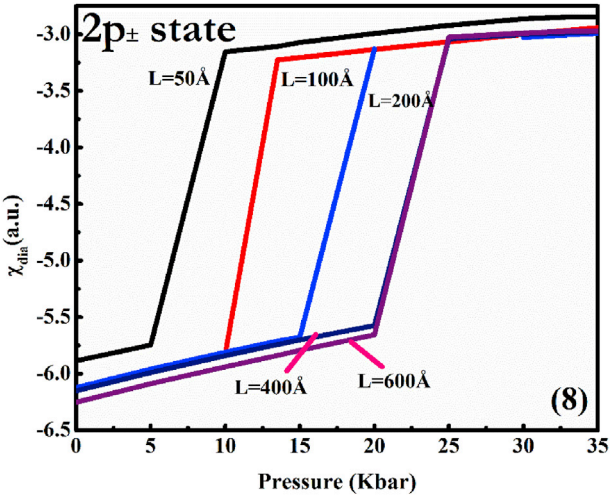

Fig. 8. Variation of χ_{dia} of donor impurity against pressure for $2p_{\pm}$ state for various well widths.

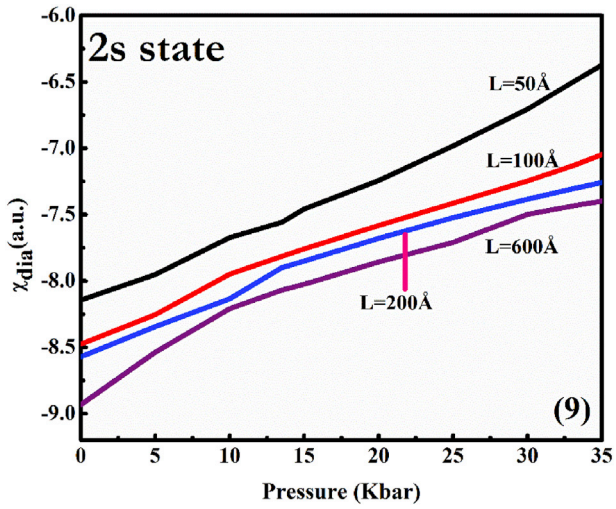

Fig. 9. Variation of χ_{dia} of donor impurity against pressure for 2s state for various well widths.

veracity by setting the limiting cases. In the bulk limit, $L \to \infty$, $\chi_{dia} \to -15.82$ a.u. for 2s state and $\chi_{dia} \to -11.3$ a.u $2p_{\pm}$ state. In the limit $L \to 0$, $\chi_{dia} \to -10.53$ a.u. for 2s state and $\chi_{dia} \to -7.52$ a.u. for $2p_{\pm}$ state [17]. We could not compare our results with any experimental data as it is not available explicitly for variation of binding energy with pressure for TQW.

4. Conclusion

In this paper, the steady and abrupt response of the χ_{dia} of a hydrogenic donor impurity to the applied pressure for various impurity states have been found. The binding energy of the donor impurity has also been estimated for various well widths and pressures. The drastic increase of χ_{dia} under pressure and an unexpected trend of the binding energy with the applied pressure shows the possibility of SMT in such triangular nanostructure systems for which the present study can be useful. Moreover, the present work may be useful to understand the performance of Quantum – Well Lasers since it becomes difficult to operate in stimulated emission at pressures corresponding to Γ – X band crossover of the barrier and waveguide region [31].

Acknowledgement

The authors thank University Grants Commission, New Delhi, India for the financial support under Major Research Project (F. No. 42-816/2013(SR)).

References

[1] Guang –Zuo Jiang, Cheng – Zhong Wen, Donors and excitons in triangular GaAs – $Ga_{1-x}Al_xAs$ quantum wells, Phys. Rev. B 50 (1994) 2689–2692.
[2] R.F. Kopf, M.H. Herman, M. Lamont Schnoes, A.P. Perley, G. Livescu, M. Ohring, Band offset determination in analog graded parabolic and Triangular Quantum Wells of GaAs/AlGaAs and GaInAs/AlInA, J. Appl. Phys. 71 (1992) 5004–5011.
[3] Ji – ye Zhang, Xi –xia Liang, Binding energy of donors in symmetric Triangular Quantum Wells, Optoelectron Lett. 1 (2005) 0088–0091.
[4] Jun Wang, Shu Shen Li, Yan – Wu Lü, Xiang – Lin Liu, Shao –Yan Yang, Qin – Sheng Zhu, Zhan-Guo Wang, Binding energy and spin – orbit splitting of a hydrogenic donor impurity in AlGaN/GaN triangle shaped potential quantum well, Nanoscal Res. Lett. 4 (2009) 1315–1318.
[5] S. Rabbaa, J. Stiens, Validation of a Triangular Quantum Well model for GaN-based HEMTs used in pH and dipole moment sensing, J. Phys. D Appl. Phys. 45 (2012), 475101 (1-9).
[6] Zhang Hairui, Sun Yong, Properties of polaron in a Triangular Quantum Well induced by the Rashba effect, J. Semicond. 35 (2014), 102001–1 – 102001 -4.
[7] E. Kasapoglu, H. Sari, I. Sökmen, Geometrical effects on shallow donor impurities in quantum wires, Phys. E 19 (2003) 332–335.

[8] P. Kalpana, A. Merwyn Jasper D Reuben, P. Nithiananthi, K. Jayakumar, Impurity states and the diamagnetic susceptibility of a donor in a Triangular Quantum Well, AIP. Conf. Proc. 1832 (2017) 090032.
[9] R.L. Restrepo, E. Giraldo, G.L. Miranda, W. Ospina, C.A. Duque, Hydrogenic donor impurity in parallel – triangular quantum wires: hydrostatic pressure and applied electric field effects, Phys. B 404 (2009) 5163–5166.
[10] R. Khordad, Effect of pressure on spin – orbit interaction in a quantum wire with V-shaped cross – section, Solid State Sci. 19 (2013) 63–68.
[11] E. Kasapoglu, I. Sökmen, Shallow donor impurity binding energy in the V- shaped quantum well under the crossed electric and magnetic fields, Phys. E 27 (2005) 198–203.
[12] J. Kundrotas, et al., Radiative recombination spectr of p-type δ-doped GaAs/AlAs multiple quantum wells near the Mott transition, J. Appl. Phys. 103 (2008), 123108–1-123108-6.
[13] P. Nithiananthi, K. Jayakumar, Diamagnetic susceptibility of hydrogenic donor impurity in low – dimensional semiconducting systems, Solid State Commun. 137 (2006) 427–430.
[14] R. Khordad, Diamagnetic Susceptibility of hydrogenic donor impurity in a V – groove GaAs/$Ga_{1-x}Al_xAs$ quantum wire, Eur. Phys. J. B 78 (2010) 399–403.
[15] P. Nithiananthi, K. Jayakumar, Diamagnetic susceptibility of a hydrogenic donor in low lying excited states in a quantum well, Superlattice Microstruct. 40 (2006) 174–179.
[16] N. Muthu Irulayee, K. Navaneetha Krishann, Diamagnetic Susceptibility of a shallow donor in a quantum well, Phys. E 41 (2008) 193–195.
[17] G. Vignesh, P. Nithiananthi, Diamagnetic Susceptibility: an indicator of pressure induced donor localization in a double quantum well, Superlattice Microstruct. 92 (2016) 232–241.
[18] P. Nithiananthi, K. Jayakumar, Pressure study on the semiconductor – metal transition in a quantum well, Phys. Status. Solidi (b) 246 (2009) 1238–1242.
[19] A. Merwyn Jasper, D. Reuben, K. Jayakumar, Diamagnetic susceptibility of a hydrogenic donor in a quantum dot, Phys. Status. Solidi (b) 243 (2006) 4020–4024.
[20] P. Kalpana, K. Jayakumar, P. Nithiananthi, Effect of geometry on the pressure induced donor binding energy in semiconductor nanostructures, Int. J. Comput. Mater. Sci. Eng. 4 (2015) 1550018.
[21] Z. Avazzadeh, H. Bahramiyan, R. Khordad, S.A. Mohammadi, Diamagnetic susceptibility of an off – center hydrogenic donor in pyramid – like and cone – like quantum dots, Eur. Phys. J. Plus 131 (2016), 121:1–8.
[22] R. Khordad, Hydrogenic impurity states in a quantum pseudodot: spin – orbit interaction, relativistic correction and diamagnetic susceptibility, Int. J. Theor. Phys. 52 (2013) 837–848.
[23] U. Yesilgul, F. Ungan, E. Kasapoglu, H. Sari, I. Sökmen, The effects of temperature on the diamagnetic susceptibility of a donor in a quantum well, Surf. Rev. Lett. 18 (2011) 147–152.
[24] A. Mmadi, I. Zorkani, K. Rahmani, A. Jorio, Magnetic field effect on the diamagnetic susceptibility of hydrogenic donor in cylinderical quantum dot, Afr. Rev. Phys. 8 (2013) 219–226.
[25] P. Nithiananthi, K. Jayakumar, Influence of pressure on the diamagnetic susceptibility of hydrogenic donor in some low-lying excited states in a quatnum well, Int. J. Nano Sci. 6 (2007) 37–40.
[26] E. Kasapglu, F. Ungan, H. Sari, I. Sökmen, The Diamagnetic Susceptibilities of donors in Quantum wells with anisotropic effective mass, Superlattice Microstruct. 46 (2009) 817–822.
[27] Z. Avazzadh, R. Khordad, H. Bahramiyan, S.A. Mohammadi, Energy gap renormalization and diamagnetic susceptibility in quantum wires with different cross – sectional shape, J. Comput. Electron 15 (2016) 931.
[28] H. Burnett, H.M. Cheong, W. Paul, E.S. Koteles, B. Elman, Γ –X mixing in GaAs/$Al_xGa_{1-x}As$ coupled double quantum wells under hydrostatic pressure, Phys. Rev. B 47 (1993) 1991–1997.
[29] P. Nithiananthi, K. Jayakumar, Effect of Γ – X crossover on the donor binding energy in a quantum well, Int. J. Mod. Phys. B 19 (2005) 3861–3868.
[30] K. Jayakumar, S. Balasubramanian, M. Tomak, Low lying excited states of a hydrogenic donor and resonant states in a quantum well, Phys. Rev. B 34 (1986) 8794–8799.
[31] M.D. Camras, N. Holonyak Jr., J.J. Coleman, H.G. Drickamer, R.D. Bumham, W. Streifer, D.R. Scifres, C. Lindström, T.P. Paoli, High pressure measurements on photopumped low threshold $Al_xGa_{1-x}As$ quantum well lasers, J. Appl. Phys. 54 (1983) 4386.

Superlattices and Microstructures 111 (2017) 115–122

Contents lists available at ScienceDirect

Superlattices and Microstructures

journal homepage: www.elsevier.com/locate/superlattices

Helium like impurity in CdTe/ $Cd_{1-x}Mn_xTe$ semimagnetic semiconductors under magnetic field: Dimensionality effect on electron – Electron interaction

Panneer Selvam Kalpana, Kalyanasundaram Jayakumar*

Nanostructure Lab, Department of Physics, Gandhigram Rural University, Gandhigram 624 302, Tamilnadu, India

ARTICLE INFO

Article history:
Received 7 May 2017
Received in revised form 4 June 2017
Accepted 6 June 2017
Available online 9 June 2017

Keywords:
Semimagnetic quantum well
Quantum well wire
Quantum dot
Magnetic field
Helium like impurity
Coulomb interaction
Binding energy

ABSTRACT

We study the effect of magnetic field on the Coulomb interaction between the two electrons confined inside a CdTe/$Cd_{1-x}Mn_xTe$ Quantum Well (QW), Quantum Well Wire (QWW) and Quantum Dot (QD) for the composition of Mn^{2+} ion, x = 0.3. The two particle Schrodinger equation has been solved using variational technique in the effective mass approximation. The results show that the applied magnetic field tremendously alters the Coulomb interaction of the electrons and their binding to the donor impurity by shrinking the spatial extension of the two particle wavefunction and leads to tunnelling through the barrier. The qualitative phenomenon involved in such variation of electron – electron interaction with the magnetic field has also been explained through the 3D – plot of the probability density function.

1. Introduction

The random distribution of magnetic ions over the cation sublattice in Diluted Magnetic Semiconductors (DMS) leads to important magnetic effects like the formation of Bound Magnetic Polaron (BMP) [1,2], Giant Zeeman Splitting [3,4] etc … The effective confinement of the carrier confined in such DMS systems can be manipulated by the modification of the barrier height either by adjusting the composition of the alloy used in the barrier material or by the application of the external magnetic field [5,6].

The influence of high magnetic field has very profound effects on physical phenomenon in Low Dimensional Semiconducting Systems (LDSS) like Quantum Well (QW), Quantum Well Wire (QWW) and Quantum Dot (QD) which modifies the density of states due to the formation of Landau levels in these structures. Therefore, the nature of the impurity states associated with such LDSS is a subject of considerable technical and scientific relevance because of its potential applications in Optoelectronic and Spintronic devices. Moreover, the prospect of understanding electron correlations in a simple system like QW, QWW and QD Helium which are occupied by two electrons in each has been a driving force for much of the theoretical work since the Coulomb interaction between them leads to unusual magnetic – field dependence of the ground state and its excitations. Many researchers have put their considerable effort to investigate the single and double donor/acceptor impurities widely on GaAs systems [7–20]. The effective mass theory for helium – like donors in bulk semiconductors was first

* Corresponding author.
E-mail address: kjkumar_gri@rediffmail.com (K. Jayakumar).

http://dx.doi.org/10.1016/j.spmi.2017.06.017
0749-6036/

carried out by Glodeanu [21] and various experimental studies for the same were carried out by Grimmeiss et al. [22,23]. The energy spectra of two electrons in a parabolic QWW and QD have been thoroughly studied by G.Y. Hu et al. [24] and D. Pfannkuche et al. [25], Metkit et al. [26] respectively. Correa et al. [27] have analysed the spectrum of two electrons confined inside a non-isotropic parabolic QD using the fractional dimensional formulation. Though the role of hydrogen − like donors in DMS systems have received some attention, studies of the helium −like donors and acceptors [28] have not been paid much attention. Therefore, studies in this field are still important for both theoretical research and practical applications. In the present communication, an effort has been taken to study how the electron − electron interaction gets affected by the applied magnetic field and alters the binding of the carriers confined in a CdTe/$Cd_{1-x}Mn_xTe$ QW, QWW and QD DMS systems for the composition of Mn^{2+} ion, x = 0.3.

2. Theoretical formalism

Defining effective Bohr radius $a_B^* = \hbar^2\varepsilon_0/m^*e^2$ as unit of length, effective Rydberg $R^* = e^2/2\varepsilon_0 a_B^*$as unit of energy and the strength of the magnetic field parameter $\gamma = \hbar\omega_c/2R^*$ (ω_c − cyclotron frequency), the Hamiltonian for the He − like impurity confined in a CdTe/$Cd_{1-x}Mn_xTe$ Square Quantum Well/Wire/Dot is written as

$$H_{ee} = -\nabla_1^2 - \nabla_2^2 - \frac{2}{r_1} - \frac{2}{r_2} + V_B(r_1) + V_B(r_2) + \gamma L_{z_1} + \gamma L_{z_2} + \frac{\gamma^2(x_1^2+y_1^2)}{4} + \frac{\gamma^2(x_2^2+y_2^2)}{4} + \frac{2}{|\vec{r}_1 - \vec{r}_2|} \tag{1}$$

where, m^* is the effective mass of electron in CdTe and $r = \sqrt{x^2+y^2+z^2}$; ε_0 is the static dielectric constant of CdTe.

The effective confinement potential for QW, QWW and QD is given as,

$$\begin{aligned} V_B &= \begin{cases} 0 & |z| \le L/2 \\ V_0 & |z| > L/2 \end{cases} \rightarrow \text{Q W} \\ V_B &= \begin{cases} 0 & |x|,|y| \le L/2 \\ V_0 & |x|,|y| > L/2 \end{cases} \rightarrow \text{Q W W} \\ V_B &= \begin{cases} 0 & |x|,|y|,|z| \le L/2 \\ V_0 & |x|,|y|,|z| > L/2 \end{cases} \rightarrow \text{Q D} \end{aligned} \tag{2}$$

The external applied magnetic field strongly alters the difference in the band gap between $Cd_{1-x}Mn_xTe$ and CdTe is given by Ref. [6].

$$\Delta E_g^B = \Delta E_g^0 \left[\frac{\eta e^{\zeta\gamma} - 1}{\eta - 1}\right] \tag{3}$$

Hence, the strength of the confinement potential is rapidly reduced and results in the modifications of electrical and optical properties. ΔE_g^B and ΔE_g^0 are the band gap difference with and without magnetic field respectively. $\eta = e^{\zeta\gamma_0}$ is chosen with ζ as a parameter (=0.5) and γ_0 as the critical magnetic field which depends upon the value of the composition of Mn^{2+} ion 'x'. This critical field (in Tesla) for other values of composition of Mn^{2+} ion can be obtained using formulae [6] $B_0 = Ae^{nx}$ with A = 0.734 and n = 19.082 which gives the best fit to the extrapolated experimentally available critical fields. The band gap of $Cd_{1-x}Mn_xTe$ is given by 1.606 + 1.587× eV. The envelop function is chosen to be a product of the lowest subband energy states of the two electrons confined inside the QW, QWW and QD and is given by,

$$f(z) = N_{1s}\begin{cases} Be^{\beta z_1}e^{\beta z_2} & z_1, z_2 \le -L/2 \\ Cos\alpha z_1 Cos\alpha z_2 & -L/2 < z_1, z_2 < L/2 \\ Be^{-\beta z_1}e^{-\beta z_2} & z_1, z_2 \ge L/2 \end{cases} \rightarrow \text{QW} \tag{4}$$

$$f(x,y) = N_{1s}\begin{cases} Be^{\beta_1(x_1+y_1)}e^{\beta_1(x_2+y_2)} & x_1, y_1, x_2, y_2 \le -L/2 \\ Cos\alpha_1 x_1 Cos\alpha_1 y_1 Cos\alpha_1 x_2 Cos\alpha_1 y_2 & -L/2 < x_1, y_1, x_2, y_2 < L/2 \\ Be^{\beta_1(x_2+y_2)}e^{\beta_1(x_2+y_2)} & x_1, y_1, x_2, y_2 \ge L/2 \end{cases} \rightarrow \text{QWW}$$

$$f(x,y,z) = N_{1s}\begin{cases} Be^{\beta_2(x_1+y_1+z_1)}e^{\beta_2(x_2+y_2+z_2)} & x_1, y_1, z_1, x_2, y_2, z_2 \le -L/2 \\ Cos\alpha_2 x_1 Cos\alpha_2 y_1 Cos\alpha_2 z_1 Cos\alpha_2 x_2 Cos\alpha_2 y_2 Cos\alpha_2 z_2 & -L/2 < x_1, y_1, z_1, x_2, y_2, z_2 < L/2 \\ Be^{\beta_2(x_2+y_2+z_2)}e^{\beta_2(x_2+y_2+z_2)} & x_1, y_1, z_1, x_2, y_2, z_2 \ge L/2 \end{cases} \rightarrow \text{QD}$$

Here,

$$\left.\begin{aligned}\alpha &= \sqrt{\frac{2m_w^* E}{\hbar^2}}\\ \beta &= \sqrt{\frac{2m_b^*(V_0-E)}{\hbar^2}}\end{aligned}\right\}\rightarrow QW;\quad \left.\begin{aligned}\alpha_1 &= \sqrt{\frac{m_w^* E}{\hbar^2}}\\ \beta_1 &= \sqrt{\frac{m_b^*(V_0-E)}{\hbar^2}}\end{aligned}\right\}\rightarrow QWW;\quad \left.\begin{aligned}\alpha_2 &= \sqrt{\frac{2m_w^* E}{3\hbar^2}}\\ \beta_2 &= \sqrt{\frac{2m_b^*(V_0-E)}{3\hbar^2}}\end{aligned}\right\}\rightarrow QD \tag{5}$$

N_{1s} is the normalization constant, B is obtained from the continuity condition and the subscript w-stands for well and b-stands for barrier.

The approximate ground states for the confined two electrons have been calculated using the variational approach. The variational ansatz is written as

$$\Psi_{QW} = f(z)e_{1s}^{-\lambda \quad r};\ \Psi_{QWW} = f(x,y)e_{1s}^{-\lambda \quad r};\ \Psi_{QD} f(x,y,z)e_{1s}^{-\lambda \quad r} \tag{6}$$

where, λ is the variational parameter.

The lowest energy level E_0 without donor impurity can be computed by solving the transcendental equation

$$\alpha \tan\alpha\, L/2 = \beta \tag{7}$$

The expectation value of **H** is minimized with respect to λ_{1s} and the electron-electron interaction energy is obtained by computing

$$E_{e-e} = \langle \Psi_{QW,QWW,QD}(r_1,r_2)\left|\frac{2}{|\vec{r}_1 - \vec{r}_2|}\right|\Psi_{QW,QWW,QD}(r_1,r_2)\rangle \tag{8}$$

The binding energy of the two electrons in the presence of magnetic field is found by solving the Schrödinger equation variationally, and is given by

$$E_B = E_0 + \gamma - \langle H\rangle_{min} \tag{9}$$

The CdTe parameters used in our calculations are $\varepsilon_0 = 10.2$; $m_w^* = 0.090$; $R^* = 11.76$ meV; $a_B^* = 60$ Å.

3. Results and discussion

The variation of binding energy for the He-like impurity confined inside a CdTe/$Cd_{1-x}Mn_xTe$ Square Quantum Well with and without the application of magnetic field ($\gamma = 0$, $\gamma = 3$, $\gamma = 6$) as a function of well width is depicted in Fig. 1 for the composition of Mn^{2+} ion x = 0.3.

It is noted from the figure that for the case with $\gamma = 0$, the binding energy increases gradually as the well width is reduced from the bulk regime towards the Quasi two dimensional regime and it attains maximum when the well width reaches approximately the effective Bohr radius of the confining system (60 Å). This is due to the fact that the impurity potential energy becomes more negative with decreasing well width which leads to larger binding of the carriers in that regime even though there is an increase in the kinetic energy of the particles. The variation of Coulomb interaction between the two electrons as a function of well width is plotted in Fig. 2.

The interaction energy is maximum for the narrower well width where the confinement is more and thereafter a gradual decrease is observed as the well width increases since the Coulomb interaction scales inversely proportional to the dimension of the well as $V_{Coulomb}$ ~1/L [29]. But, when the external magnetic field of strength $\gamma = 3$ and $\gamma = 6$ are applied, the Coulomb interaction gets decreased as shown in Fig. 2. This is because, the applied magnetic field tremendously suppresses the confining potential barrier (333.27 meV, 67.65 meV, 8.39 meV for $\gamma = 0$, $\gamma = 3$ and $\gamma = 6$ respectively) and thereby shrinking the spatial extend of the two particle wavefunction which causes tunnelling of electrons through the barrier $Cd_{1-x}Mn_xTe$. In addition to this, when the strength of magnetic field is more the angular momentum gets increased and the electrons in states with higher angular momentum are further apart from each other and thereby decreasing the Coulomb interaction between them. The expectation value of binding energy of the two electrons confined in a QW also follows the same trend (given in Fig. 1) with the magnetic field as that of the interaction energy. The decrease of the binding energy (Fig. 1) with the magnetic field can be attributed to the decrease in the kinetic energy, impurity potential energy as well as the subband energy due to the reduction in the potential barrier height. The variation of subband energy with the magnetic field for the two electrons confined inside the QW for various well widths is reported in Table 1.

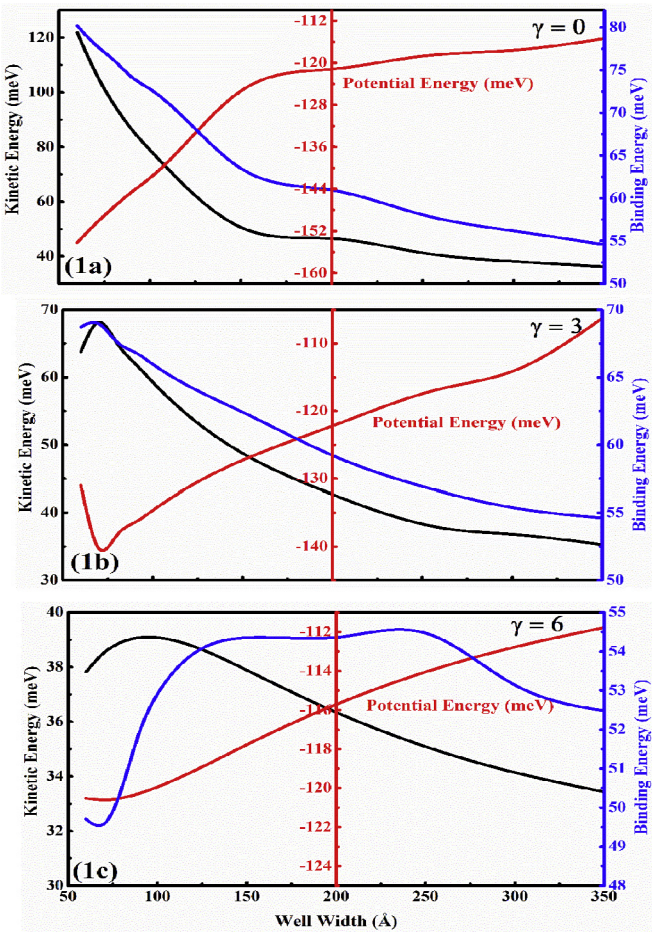

Fig. 1. Variation of Kinetic Energy, Potential energy and the Binding energy of the two electrons confined inside the QW as a function of well width for $\gamma = 0$, $\gamma = 3$ and $\gamma = 6$.

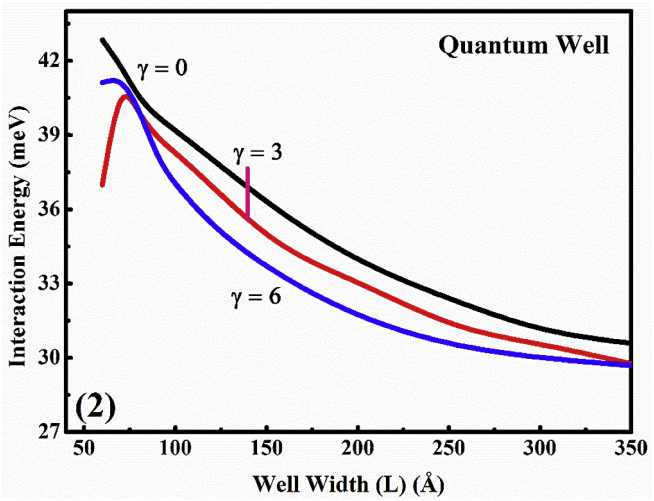

Fig. 2. Variation of interaction energy of the two electrons confined inside the QW as a function of well width for (a) $\gamma = 0$, $\gamma = 3$ and (c) $\gamma = 6$.

Table 1
Subband Energy *vs* well width for different magnetic fields.

Well Width (Å)	Subband Energy (meV)		
	$\gamma = 0$	$\gamma = 3$	$\gamma = 6$
60	63.27	33.42	7.34
100	28.70	18.97	6.08
150	14.39	10.79	4.63
200	8.614	6.90	3.54
300	4.08	3.5026	2.19

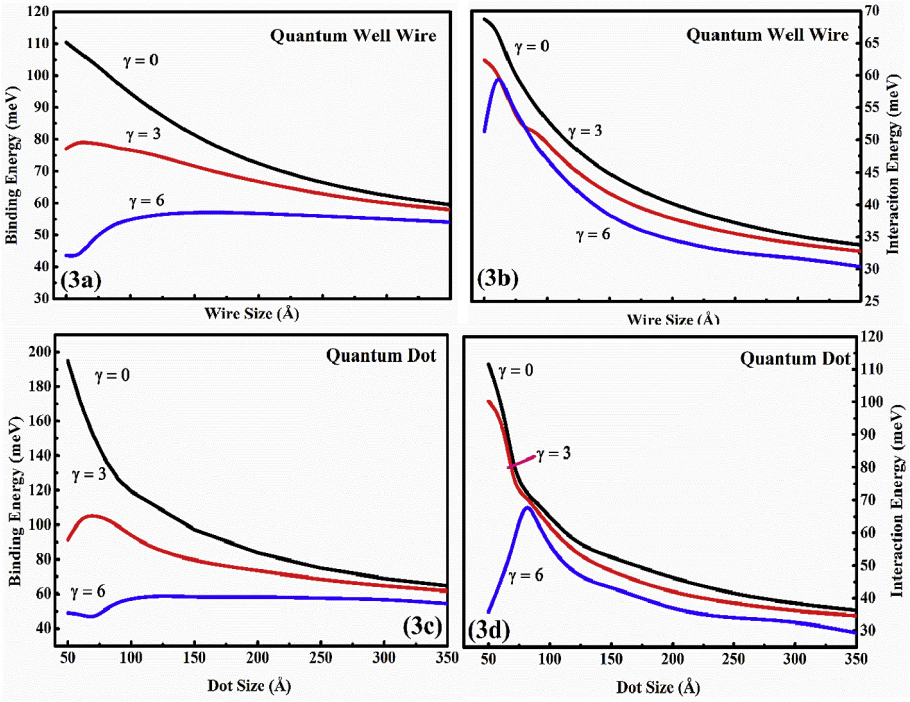

Fig. 3. Variation of binding energy for the two electrons confined inside (a) QWW, (c) QD and the interaction energy in (b) QWW, (d) QD as a function of well width for different magnetic fields.

When the magnetic field of strength $\gamma = 3$ is applied, the turnover in the binding energy is seen in the Quasi 2D region. This is because, the reduction in the potential barrier height due to the application of magnetic field keeps the expectation value of impurity potential to be more negative until the well width reaches around the effective Bohr radius when it is decreased from the bulk value. But, thereafter, it allows the carrier to be far apart from each other and leads to less negative value in the impurity potential with decreasing well width and therefore the carriers get loosely bound to the donor atom which results in lower binding energy.

But when the magnetic field of strength $\gamma = 6$ is applied, the binding energy increases as the well width increases and attains a maximum value around L = 100 Å and thereafter it gets saturated until L reaches 250 Å and beyond that the binding energy starts to fall again. The reason for this behaviour is the competition between the kinetic energy and the potential

Table 2
Subband Energy *vs* Well Width for different magnetic fields in QWW and QD.

Well Width (Å)	Subband Energy (meV)					
	QWW			QD		
	$\gamma = 0$	$\gamma = 3$	$\gamma = 6$	$\gamma = 0$	$\gamma = 3$	$\gamma = 6$
60	100.807	43.93	7.82	127.945	49.44	8.0013
100	49.648	28.422	7.02	66.844	34.60	7.411
150	26.035	17.5738	5.886	36.224	22.655	6.507
200	15.952	11.77	4.854	22.583	15.684	5.59645
300	7.74	6.27316	3.323	11.57684	8.666	4.080

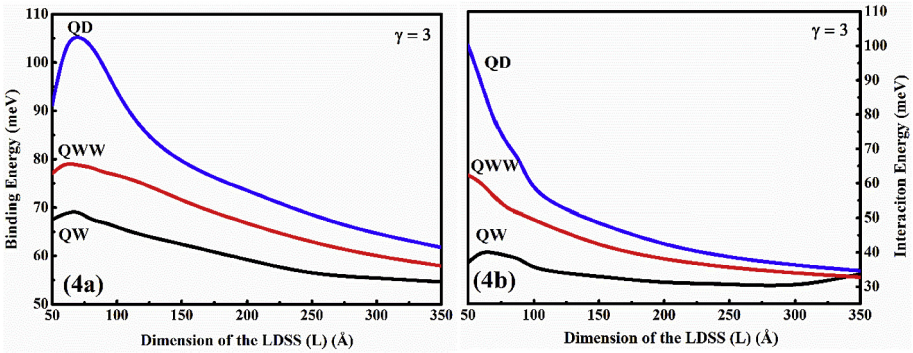

Fig. 4. Variation of (a) binding energy and (b) interaction energy for the two electrons confined inside QW, QWW and QD as a function of dimension of the LDSS for the magnetic field $\gamma = 3$.

energy as shown in Fig. 1c. The contribution of the kinetic energy to the total energy is much greater than the potential energy in the range L < 100 Å and vice versa in the ranges L > 100 Å. But this variation of the binding energy with the well width for $\gamma = 6$ is not as rapid as the variation observed for $\gamma = 0$ and $\gamma = 3$. This can be understood on the basis of the following qualitative argument. The strength of the applied magnetic field $\gamma = 6$ is very nearer to the critical magnetic field ($\gamma = 7.35$) at which the barrier vanishes completely and the QW gets disappeared and the carriers become unconfined as in the bulk system. Moreover, the binding energy for all the values of magnetic field converges when the well width is increased towards the bulk value.

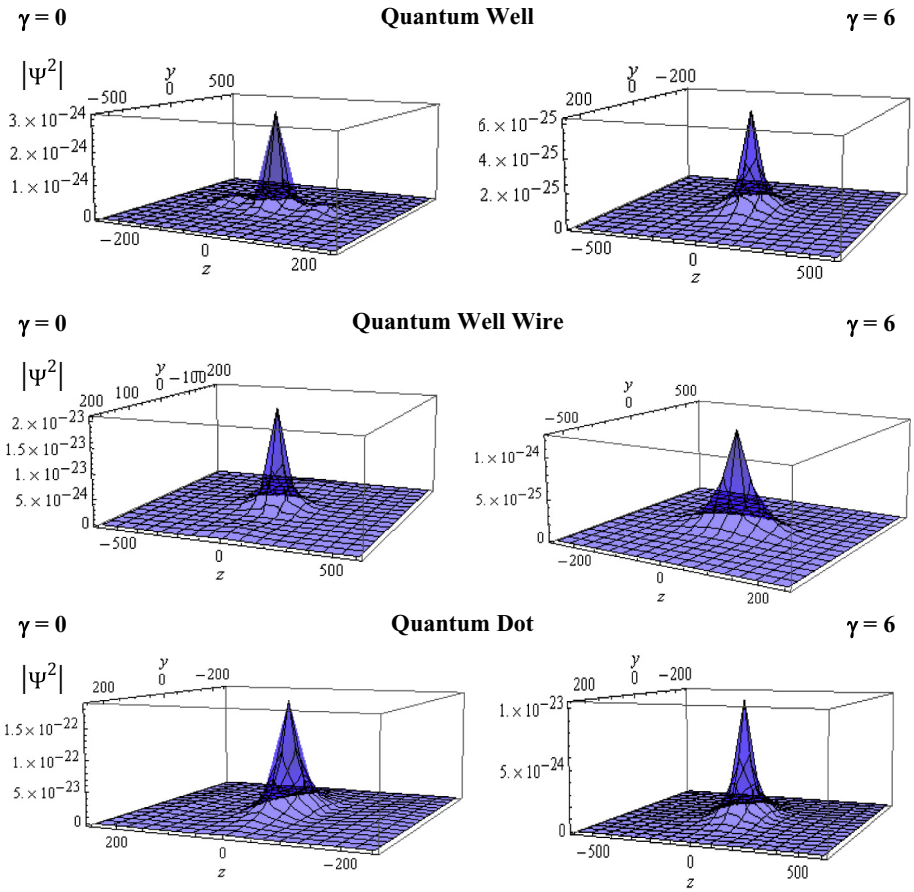

Fig. 5. Probability density $|\psi^2|$ of the He − like impurity confined inside the QW, QWW and QD under $\gamma = 0$ and $\gamma = 6$ for Mn ion concentration of x = 0.3.

The graphs for binding energy and interaction energy for QWW and QD are plotted in Fig. 3 for the cases with and without the application of magnetic field and the variation of subband energy for these QWW and QD have also been presented in Table 2. It is clearly seen from these figures that the trend of the binding energy with the dimension of the system is as same as the trend seen in the QW but with the larger magnitude in binding as well as interaction energy as the confinement of the system is increased from 2D → 1D (QW → QWW) and then 1D → 0D (QWW → QD). The Binding energy and the interaction energy for QW, QWW and QD for a typical value of $\gamma = 3$, has been given in Fig. 4a and b respectively.

This is because, when the confinement is increased, there is a less possibility for the electrons to undergo tunnelling because of its highly localized wavefunction. Since the degree of freedom for the two electrons is restricted as the dimensionality of the system is reduced which increases the effective strength of the Coulomb interaction between them and hence affects the binding energy.

It is worth noticing from all the graphs portrayed above that the binding of the two electrons and their Coulomb interaction is tremendously affected by the applied magnetic field only when the impurity is confined inside the QD rather than in the QW and QWW. This can be justified as one can note that the magnitude of decrease in the binding energy and the interaction energy with respect to the applied magnetic field increases as the confinement of the carrier increases from 2D → 1D → 0D. The above said qualitative arguments can be justified from the three dimensional probability function shown in Fig. 5 for the two electrons confined inside the $CdTe/Cd_{1-x}Mn_xTe$ QW, QWW and QD with $\gamma = 0$ and $\gamma = 6$ by noticing, the $|\Psi^2|$ decreases when the magnetic field is applied and it increases as the dimensionality of the system is reduced.

To conclude, we have calculated the Coulomb interaction between the two electrons confined in the LDSS and their binding to the donor impurity as a function of magnetic field. The most appealing feature of the Coulomb interaction in DMS systems in response to the applied magnetic field as compared to other non-magnetic systems may be instrumental in understanding the strong influence of the spectral properties of the LDSS which can be interpreted as transition to Quantum Chaos and may also shed some light on the fabrication of spintronic devices.

Acknowledgement

The authors thank University Grants Commission, New Delhi, India for the financial support under Major Research Project (F. No.42-816/2013(SR)).

References

[1] T. Kasuya, Anamalous transport phenomena in Eu-chalcogenide alloys, Rev. Mod. Phys. 40 (1968) 684–696, http://dx.doi.org/10.1103/RevModPhys.40.684.
[2] U. Thibblin, Theory of bound magnetic polarons in diluted magnetic semiconductors, Int. J. Mod. Phys. B 3 (1989) 337–366, http://dx.doi.org/10.1142/S0217979289000269.
[3] J.A. Gaj, J. Ginter, Exchange interaction of manganese, Phys. Status Solidi Basic Res. 655 (1978) 655–662, http://dx.doi.org/10.1002/pssb.2220890241.
[4] J.P. Lascaray, D. Coquillat, J. Deportes, A.K. Bhattacharjee, Zeeman splitting of exciton and magnetization in $Cd_{1-x}Mn_xTe$:anomalous behavior at high x, Phys. Rev. B 38 (1988) 7602–7606, http://dx.doi.org/10.1103/PhysRevB.38.7602.
[5] P. Nithiananthi, K. Jayakumar, Laser induced semiconductor- metal transition in a semimagnetic quantum well, Int. J. Nanosci. 10 (2011) 611–615, http://dx.doi.org/10.1142/S0219581X11009180.
[6] P. Kalpana, P. Nithianathi, K. Jayakumar, Donor states in a semimagnetic double quantum well, Superlatt. Microstruct. 102 (2017) 246–258, http://dx.doi.org/10.1016/j.spmi.2016.12.042.
[7] R. Khordad, H.R. Rastegar Sedhi, Application of non − extensive entropy to study of decoherence of RbCl quantum dot qubit : tsallis entropy, Superlatt. Microstruct. 101 (2017) 559, http://dx.doi.org/10.1016/j.spmi.2016.10.041.
[8] R. Khordad, Hydrogenic impurity states in a quantum pseudodot: spin − orbit interaction, relativistic correction and diamagnetic susceptibility, Int. J. Theor. Phys. 52 (2013) 837–848, http://dx.doi.org/10.1007/s10773-012-1393-2.
[9] P. Nithiananthi, K. Jayakumar, Pressure study on the semiconductor − metal transition in a quantum well, Phys. Status. Solidi (b) 246 (2009) 1238–1242, http://dx.doi.org/10.1002/pssb.2000945023.
[10] P. Nithiananthi, K. Jayakumar, Diamagnetic susceptibility of a hydrogenic donor in low lying excited states in a quantum well, Superlatt. Microstruct. 40 (2006) 174–179, http://dx.doi.org/10.1016/j.spmi.2006.07.013.
[11] A. Merwyn Jasper, D. Reuben, K. Jayakumar, Diamagnetic susceptibility of a hydrogenic donor in a quantum dot, Phys. Status. Solidi (b) 243 (2006) 4020–4024, http://dx.doi.org/10.1022/pssb.200642091.
[12] Zhen − Yan Deng, Tatsuki Ohji, Xiaoshuang Chen, Shallow acceptor impurities in V − shaped GaAs − Ga1-xAlxAs quantum wires, J. Phys. Condens. Matter 12 (2000) 3019–3027, http://dx.doi.org/10.1088/0953-8984/12/13/312.
[13] Y. Yakar, B. Cakir, A. Ozman, Computation of ionization and various excited state energies of Helium and Helium − like quantum dots, Int. J. Quantum Chem. 111 (2011) 4139–4149, http://dx.doi.org/10.1002/qua.22973.
[14] Frederico V. Prudente, Luis S. Costa, Jose David M. Vianna, A study of two electron quantum dot spectrum using discrete variable representation method, J. Chem. Phys. 123 (2005) 224701, http://dx.doi.org/10.1063/1.2131068.
[15] R.K. Pandey, Manoj H. Harbola, Vijay A. Singh, Helium like donors in semiconductor quantum dots, J. Phys. Condens. Matter 16 (2004) 1769–1776, http://dx.doi.org/10.1088/0953-8984/16/10/009.
[16] S.E. Okan, H. Akbas, S. Aktas, Binding energies of helium − like impurities in parabolic quantum wells under an applied electric field, Superlatt. Microstruct. 28 (2000) 171–176, http://dx.doi.org/10.1006/spmi.2000.0901.
[17] M. Brasken, M. Lindberg, D. Sundholm, J. Olsen, Carrier − carrier correlation in strain − induced quantum dots, Phys. Stat. Sol. (b) 221 (2000) 37–41, http://dx.doi.org/10.1002/1521-3951 (200009) 221:1.
[18] Ya M. Blanter, N.E. Kaputkina, Yu E. Lozovik, Two-electron quanutm dots in magnetic field, Phys. Scr. 54 (1996) 539–541, http://dx.doi.org/10.1088/0031-8949/54/5/016.
[19] E.C. Niculescu, Binding energy of a double donor in a parabolic quantum well, Phys. Lett. A 197 (1995) 330–334, http://dx.doi.org/10.1016/S0375-9601(05) 80012-X.
[20] P.A. Maksym, T. Chakraborty, Quantum dots in a magnetic field: role of electron −electron interactions, Phys. Rev. Lett. 2 (1990) 108–111, http://dx.doi.org/10.1103/PhysRevLett.65.108.
[21] A. Glodeanu, Helium like impurities in semiconductors, Phys. Stat. Sol.(b) 19 (1967) K43, http://dx.doi.org/10.1002/pssb.19670190158.

[22] H.G. Grimmeiss, E. Janzen, B. Skarstam, Deep sulfar related centers in silicon, J. Appl. Phys. 51 (1980) 4212, http://dx.doi.org/10.1063/1.328279.
[23] H.G. Grimmeiss, E. Janzen, K. Larsson, Multivalley spin splitting of 1s states for sulfur, selenium and tellurium donors in silicon, Phys. Rev. B 25 (1982) 2627, http://dx.doi.org/10.1103/PhysRevB.25.2627.
[24] G.Y. Hu, R.F. O'Connell, Electron – electron interactions in quasi one dimensional electron systems, Phys. Rev. B 42 (1990) 1290, http://dx.doi.org/10.1103/PhysRevB.42.1290.
[25] D. Pfannkuche, R. Gerhardts, A. Maksym, V. Gudmundsson, Theory of quantum dot helium, Phys. B 189 (1993) 6–15, http://dx.doi.org/10.1016/0921-4526 (93) 90141–R.
[26] U. Merkt, J. Huser, M. Wagner, Energy spectra of two electrons in a harmonic quantum dot, Phys. Rev. B 43 (1991) 7320–7323, http://dx.doi.org/10.1103/PhysRevB.43.7320.
[27] R. Correa, W. Gutierrez, I. Mikhailov, M.R. Fulla, J.H. Marin, Dimensionality effect on two electron energy spectrum: a fractional dimension- based formulation, Phys. Lett. A 379 (2015) 1457–1463, http://dx.doi.org/10.1016/j.physleta.2015.02.043.
[28] A. Merwyn Jasper, D. Reuben, K. Jayakumar, Coulomb interaction energy of double donor in a semimagnetic quantum dot, Superlatt. Microstruct. 52 (2012) 732–737, http://dx.doi.org/10.1016/j.spmi.2012.06.020.
[29] Daniela Pancakes, Aspects of Coulomb interaction in semiconductor nanostrucutres, Phys. Habil – Schr. 28 (1999).

Bound Magnetic Polaron in a Semimagnetic Double Quantum Well

P. Kalpana, K. Jayakumar

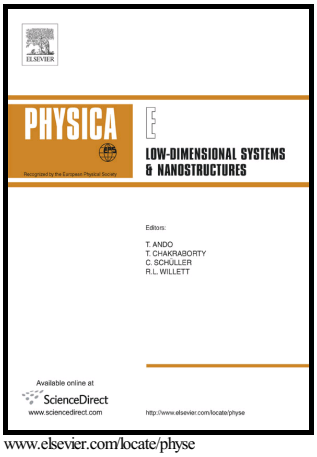

www.elsevier.com/locate/physe

PII: S1386-9477(17)30682-3
DOI: http://dx.doi.org/10.1016/j.physe.2017.06.025
Reference: PHYSE12847

To appear in: *Physica E: Low-dimensional Systems and Nanostructures*

Received date: 10 May 2017
Accepted date: 22 June 2017

Cite this article as: P. Kalpana and K. Jayakumar, Bound Magnetic Polaron in a Semimagnetic Double Quantum Well, *Physica E: Low-dimensional Systems and Nanostructures,* http://dx.doi.org/10.1016/j.physe.2017.06.025

Bound Magnetic Polaron in a Semimagnetic Double Quantum Well

P Kalpana and K Jayakumar*

Nanostructure Lab, Department of Physics, Gandhigram Rural University, Gandhigram-624 302, Tamilnadu, India.

Abstract

The effect of different combinations of the concentration of Mn^{2+} ion in the Quantum well $Cd_{1-x_{in}}Mn_{x_{in}}Te$ and the barrier $Cd_{1-x_{out}}Mn_{x_{out}}Te$ on the Bound Magnetic Polaron (BMP) in a Diluted Magnetic Semiconductors (DMS) Double Quantum Well (DQW) has been investigated. The Schrodinger equation is solved variationally in the effective mass approximation through which the Spin Polaronic Shift (SPS) due to the formation of BMP has been estimated for various locations of the donor impurity in the DQW. The results show that the effect of the increase of Mn^{2+} ion composition with different combinations on SPS is predominant for On Centre Well (OCW) impurity when compared to all other impurity locations when there is no application of magnetic field ($\gamma = 0$), γ being a dimensionless parameter for the magnetic field, and the same is predominant for On Centre Barrier (OCB) impurity with the application of external magnetic field ($\gamma = 0.15$).

Keywords: Double Quantum Well; Dilute Magnetic Semiconductors; Bound Magnetic Polaron; Exchange interaction; Impurity Locations

1. Introduction

The Diluted Magnetic Semiconductors (DMS) have many unusual features like Zeeman Splitting [1], Bound Magnetic Polaron [2], Giant Faraday Rotation [3], magnetic field induced metal – insulator transition due to the exchange interaction between the magnetic Mn^{2+} ions and the confined carrier through sp-d exchange. The formation of spin – glass phase is possible for arbitrarily less concentration of Mn^{2+} ion ($x < 0.2$) at low temperatures which leads to the frustration of antiferromagnetic interaction between the Mn^{2+} ions resulting in a high magnetization of the material.

*Corresponding author. Tel.: +91 9443461177; Fax: +91 451 2454466.

E-mail address: kjkumar_gri@rediffmail.com

These unique properties of DMS presents an entirely new set of challenges for the successful preparation of the Multiple Quantum Wells and the Superlattices. The modification of the barrier height in such QWs made up of DMS materials can be achieved either by adjusting the composition x of the alloy used in the barrier and well material or by the application of the external magnetic field. Many theoretical investigations [4-7] on the energy levels of Bound Magnetic Polaron do already exist. However, no such investigations have been made to study the effect of BMP on the energy levels especially in a DQW with respect to the impurity position as a function of various combinations of the composition of Mn^{2+}ion in the well (x_{in}) and the barrier (x_{out}) of DMS materials in such a way that the difference between the two composition ($x_{out} - x_{in} = x$) is same. The present paper attempts for such an investigation in $Cd_{1-x_{in}}Mn_{x_{in}}Te/Cd_{1-x_{out}}Mn_{x_{out}}Te$ DQW with and without the application of magnetic field for the resultant composition of x = 0.1 as a function of central barrier width and the impurity positions.

2. Theoretical Formalism

The Hamiltonian of a hydrogenic donor impurity inside the DQW made up of $Cd_{1-x_{in}}Mn_{x_{in}}Te/Cd_{1-x_{out}}Mn_{x_{out}}Te$ DMS materials in the effective mass approximation in the presence of applied magnetic field along the direction of growth axis (z-axis) is written as

$$\mathbf{H}_0 = -\nabla^2 - \frac{2}{r} + V_B(z) + \gamma L_z + \frac{\gamma^2 \rho^2}{4} \qquad (1)$$

where $\gamma = \hbar\omega_c / 2R^*$ (ω_c – cyclotron frequency) is the parameter of the strength of the magnetic field and $\gamma = 1$ corresponds to ≈30Tesla; $r = \sqrt{x^2 + y^2 + z^2}$ is the mean distance of the parent donor atom and the carrier attached to it.

The contribution from the exchange interaction between the electron and the Mn^{2+} ion to the Hamiltonian can be written as [8],

$$\mathbf{H}_{exc} = -\sum_i \mathbf{J}_e(\boldsymbol{r}_e - \boldsymbol{R}_i)\mathbf{s}_e.\mathbf{S}_i \qquad (2)$$

where, J_e is the coupling constant for the exchange interaction between the electron of spin $\mathbf{s_e}$ located at $\mathbf{r_e}$ and Mn^{2+} ions of spin $\mathbf{S_i}$ located at $\mathbf{R_i}$. Using the mean field theory with modified Brillouin function [6], the exchange interaction between the carrier and magnetic

impurity which causes the Spin Polaronic Shift (SPS) in the presence of an external magnetic field **B** can be written as[6]

$$E_{exc} = \frac{\beta N_0}{2}\left\{\langle\Psi \left| x_{in} S_0(x_{in}) B_s(y_1)\right|\Psi\rangle + \langle\Psi \left| x_{out} S_0(x) B_s(y_2)\right|\Psi\rangle\right\} \quad (3)$$

$$B_s(y_j) = \frac{2S+1}{2S}\coth\frac{2S+1}{2S}y_j - \frac{1}{2S}\coth\frac{y_j}{2S}\ ; \quad y_j = \frac{S\beta\left|\Psi_j\right|^2}{2\,k_B T_{eff}} + \frac{g\mu_B SB}{k_B T_{eff}}$$

where, S is the spin of Mn^{2+} (=5/2), N_0 = 2.94 × 10^{22} cm^{-3} and β - exchange coupling parameter and its value is obtained from the experimental value of the s – d coupling constant, βN_0 = 220meV [8]. Also $g_{Mn} \approx 2$, k_B is the Boltzmann constant and $B_s(y)$ is the modified Brillouin function. For the DMS of arbitrary x, it is inevitable to choose the phenomenological fitting parameters of saturation value S_0 and the effective temperature $T_{eff} = T + T_0$ with T_0 for the various concentrations of Mn^{2+} ion which numerical values can be taken from [8].

The various combinations (C_i) of x_{in} and x_{out} in such a way that the difference between x_{out} and x_{in} is 0.1 (x_{out} - x_{in} = x = 0.1) and the various impurity positions (z_i) accounted for the study are as follows:

$$\begin{aligned} &C_1: x_{in} = 0.005,\ x_{out} = 0.1 \\ &C_2: x_{in} = 0.01,\ x_{out} = 0.1 \\ &C_3: x_{in} = 0.1,\ x_{out} = 0.2 \\ &C_4: x_{in} = 0.2,\ x_{out} = 0.3 \end{aligned} \quad (4)$$

and

(i) On Centre Barrier impurity (OCB) (z_i = 0)

(ii) On Edge Barrier impurity (OEB) ($z_i = L_b / 2$)

(iii)On Centre Well impurity (OCW) ($z_i = L_b / 2 + L_w / 2$)

(iv)On Edge Well impurity (OEW) ($z_i = L_b / 2 + L_w$ =

The said scheme is shown in fig.1 for which the profile of the confining potential V_B (z) for the carriers in symmetric DQW structures is given as

$$V_{B(z)}=\begin{cases} 0 & \frac{L_b}{2} \le |z| \le (\frac{L_b}{2}+L_w) \\ V_0 & |z| \le \frac{L_b}{2} \text{ and } (\frac{L_b}{2}+L_w) < |z| < \infty \end{cases} \quad (5)$$

L_w is the width of the each well and L_b is the central barrier width and V_0=70% ΔE_g^B, where, ΔE_g^B is the band gap difference with magnetic field and is given by [5]

$$\Delta E_g^B = \Delta E_g^0 \left[\frac{\eta \exp^{\zeta\gamma} - 1}{\eta - 1} \right] \quad (6)$$

ΔE_g^0 is the band gap difference without magnetic field. $\eta = e^{\zeta\gamma_0}$ is chosen with ζ as a parameter (= 0.5) and γ_0 as the critical magnetic field which depends upon the value of the composition 'x' of Mn^{2+} ion. The critical magnetic field B_0 in Tesla for different composition is given as $B_0 = A\ e^{nx}$ with A = 0.734 and n = 19.082 which gives the best fit to the extrapolated experimentally available critical fields and the band gap of $Cd_{1-x}Mn_xTe$ is 1.606+1.587x eV.

The approximate ground state energy for confined donor impurity has been calculated using the variational method. The envelop function f (z) is considered as

$$f(z)=\begin{cases} A\exp[\beta(z+L_e)] & , \ z \le -L_e \\ -B\,\mathrm{Sin}[\alpha(z+\frac{L_b}{2})]+C\,\mathrm{Cos}[\alpha(z+\frac{L_b}{2})] & , \ -Le < z < -\frac{L_b}{2} \\ \mathrm{Cosh}[\beta z] & , \ -\frac{L_b}{2} < z < \frac{L_b}{2} \\ B\,\mathrm{Sin}[\alpha(z-\frac{L_b}{2})]+C\,\mathrm{Cos}[\alpha(z-\frac{L_b}{2})] & , \ \frac{L_b}{2} < z < L_e \\ A\exp[-\beta(z-L_e)] & , \ z \ge L_e \end{cases} \quad (7)$$

Here, $\alpha = (2m^*E)^{1/2}$ and $\beta = (2m^*(V_0-E))^{1/2}$. The unknown constants A, B and C are found out using the proper boundary conditions at the interfaces $z_i = L_b / 2$ and $z_i = L_e$.

The trial wavefunction of the ground state is chosen as,

$$\psi(r) = N\, f(z)\, e^{-\lambda r} \quad (8)$$

where, N is the normalization constant and λ is the variational parameter.

The expectation value of **H** is minimized with respect to λ and the SPS of the donor impurity in the presence of magnetic field is found by solving the Schrödinger equation variationally.

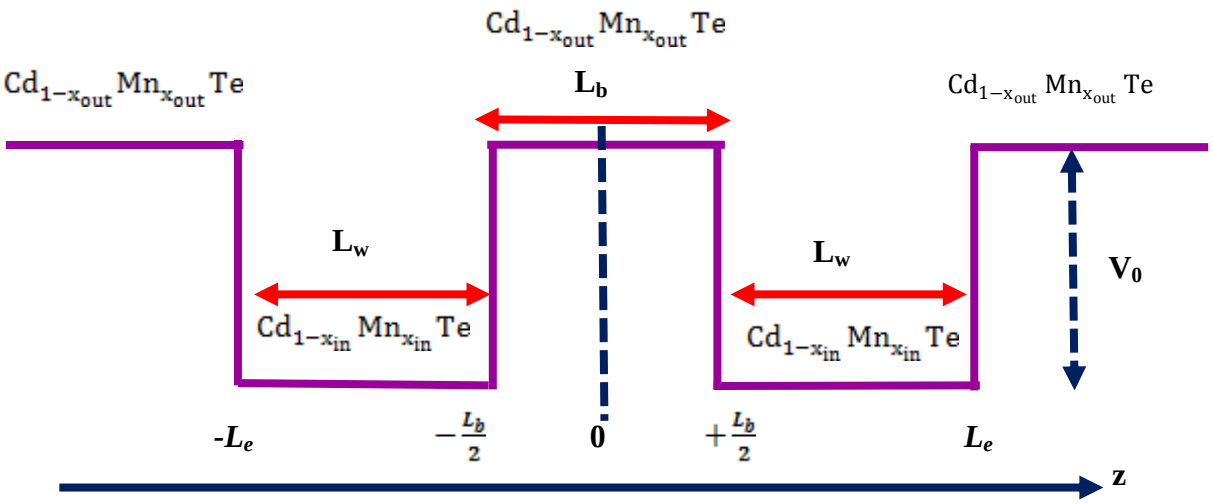

Figure 1: Schematic view of the potential profile for a DQW

3. Results and Discussions

The Fig. 2a, 2b, 2c and 2d corresponding to OCB, OEB, OCW and OEW impurity locations shows the variation of Spin Polaronic Shift (SPS) against the central barrier width in a $Cd_{1-x_{in}}Mn_{x_{in}}Te/Cd_{1-x_{out}}Mn_{x_{out}}Te$ DQW for various combinations of x_{in} and x_{out} in such a way that the difference between x_{out} and x_{in} is 0.1 (x_{out} - x_{in} = x =0.1). It is noted from the figure that the trend of the variation of SPS with the barrier width is as same as the trend of the variation of binding energy of the donor impurity with the barrier width of the DQW under zero magnetic field (γ = 0) as given in [4]. An attempt has been made on how the exchange interaction between the Mn^{2+} ions and the confined carrier in a DQW is affected by the composition of the magnetic impurity ion (x_{in} and x_{out}) which are varied simultaneously as given in (4) both in the well and in the barrier material. For all the impurity locations, the SPS increases with the increase of the composition of Mn^{2+} ion as given in (4) except for the combination (C_4) of x_{in} = 0.2 and x_{out} = 0.3. This is because, when the concentration of Mn^{2+} ion in both well and barrier increases, the exchange interaction between the magnetic moment of the Mn^{2+} ions and the spin of the localized carrier also increases which results in larger shift in the polaronic energy. This may be justified as follows: When the concentration of Mn^{2+} ions is low , x < 0.005, the interaction between the magnetic moments of the Mn^{2+} ions is very low[9]. Hence, all the Mn^{2+} ions can contribute to the total magnetic moment with the average spin per magnetic ions $<S_z>$.

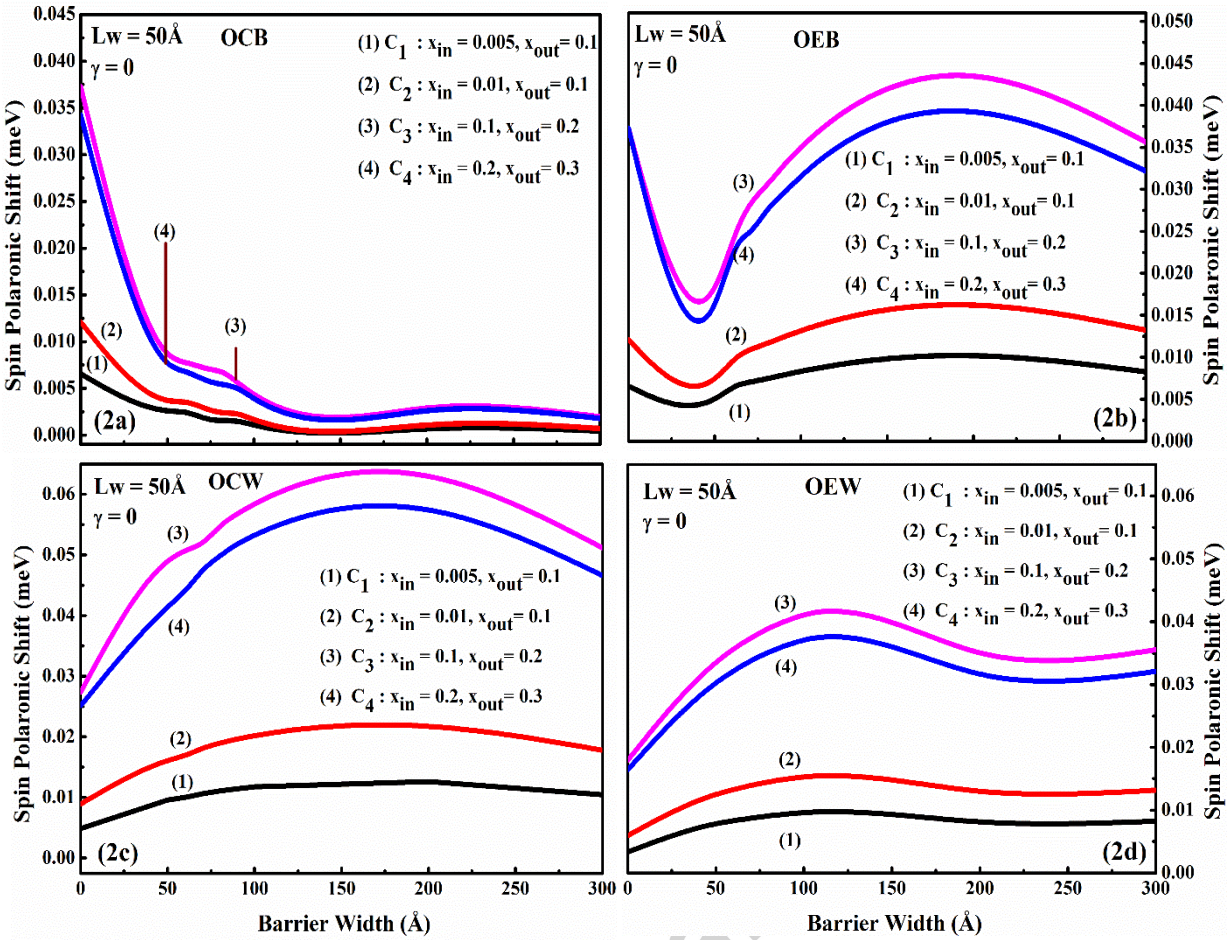

Figure 2: Variation of SPS against the barrier width for different combinations C_i of concentration of Mn^{2+} for composition of x = 0.1 (x_{out} -x_{in}=C_i) in a DQW with a well width of L_w = 50Å for (a) OCB, (b) OEB, (c) OCW and (d) OEW impurities without the application of magnetic field (γ = 0).

But when x increases beyond 0.005, spins of nearest neighbour cancels out due to the antiferromagnetic interaction between the Mn^{2+} ions which reduces the number of ions contributing to the total magnetic moment. Eventually only an effective concentration $\bar{x}$ of Mn^{2+} ions which is always less than x contributes to the total magnetic moment. From the results reported in [9], one can understand that the $\bar{x}$ increases upto x = 0.2 and then starts to decrease when x increases beyond 0.3. It is because of this fact one gets lower SPS for the combination of Mn^{2+} ions which involves x_{out} = 0.3.

When the barrier width is limited to zero ($L_b \rightarrow 0$), the rate of increase of the shift with respect to the increase of the concentration of Mn^{2+} ions as in (4) is high, only when the impurity is at OCB and OEB when compared to the other two impurity locations. This is due

to the fact that the DQW effectively becomes the Single Quantum Well (SQW) as $L_b \rightarrow 0$ and it exhibits the characteristic behaviour ascribed to the SQW. However, when the barrier width starts to increase in between the two wells, the rate of increase of SPS is high, only for the OCW impurity compared to all the other impurity locations as shown in Fig 2c.

The results of SPS against barrier width is presented in Fig.3 for L_w = 300Å.

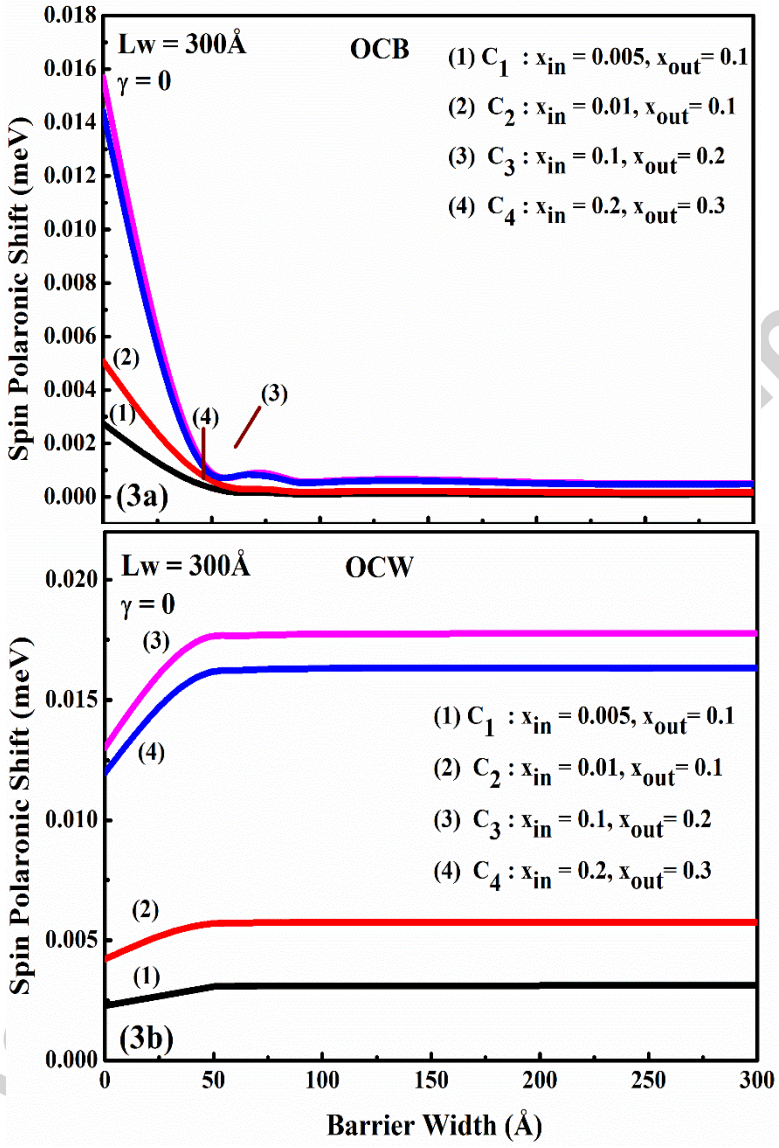

Figure 3: Variation of SPS against the barrier width for different combinations C_i of concentration of Mn^{2+} for composition of x = 0.1 (x_{out} -x_{in}=C_i) in a DQW with a well width of L_w = 300Å for (a) OCB, (b) OCW impurities without the application of magnetic field.

It is seen from the figure that the effect on SPS due to the variation of the concentration of Mn^{2+} ion for any combinations (C_i : $x_{out} - x_{in}$) is predominant only for the lower well width of L_w=50Å rather than for the well width approaching the bulk value like L_w=300Å.

The variation of the SPS against the barrier width for all the combinations of composition of Mn^{2+} ions and for all the impurity locations under the external applied magnetic field is given in Fig.4. It is well known that the applied magnetic field tremendously reduces the confining potential (111. 09meV, 7.865meV for $\gamma = 0$ and $\gamma = 0.15$ respectively) [5] in which the carrier has been confined.

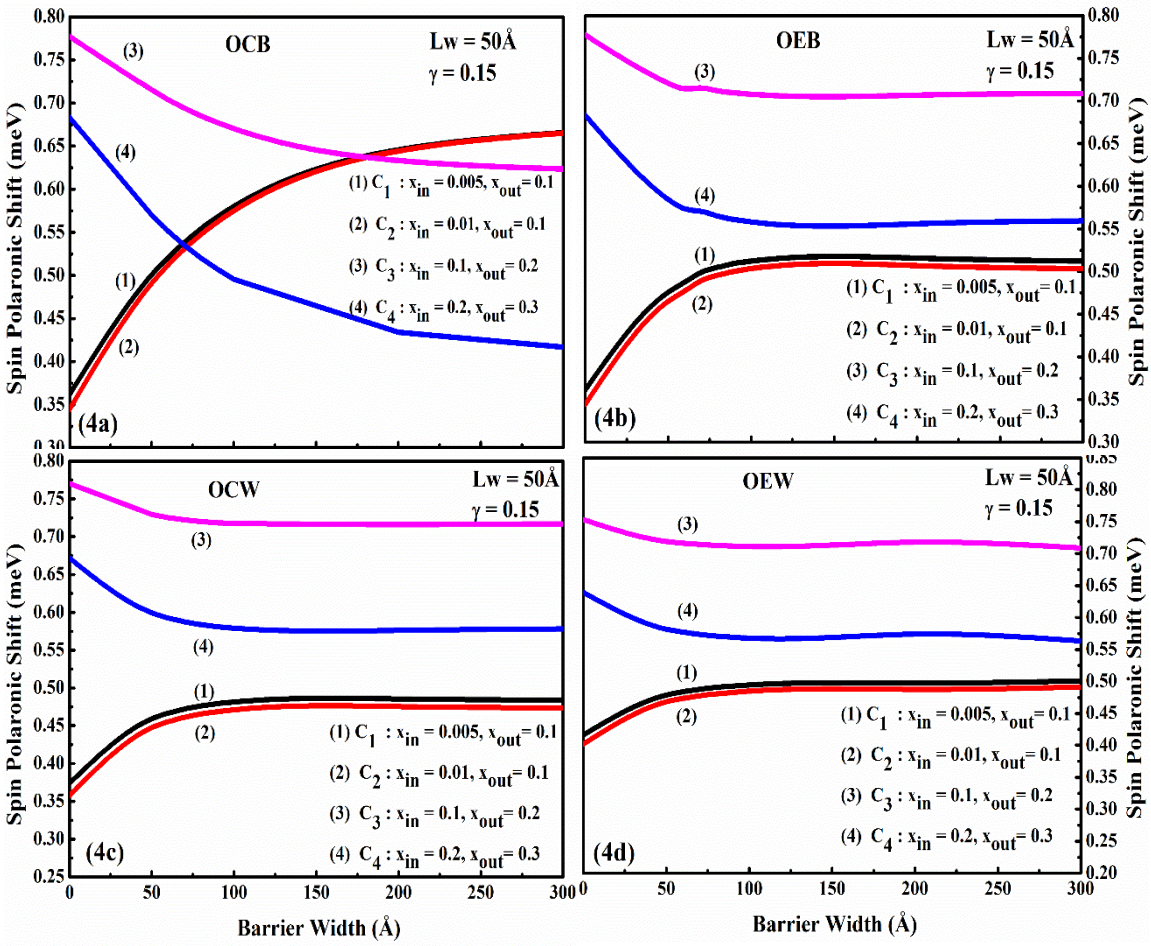

Figure 4: Variation of SPS against the barrier width for different combinations C_i of Mn^{2+} composition of x = 0.1 in a DQW with a well width of L_w = 50Å for (a) OCB, (b) OEB, (c) OCW and (d) OEW impurities with the application of magnetic field ($\gamma = 0.15$).

When the external magnetic field is applied, the exchange interaction between the Mn^{2+} ions and the carrier is enhanced thereby increasing the shift largely as one can see from the numerical values of SPS for both $\gamma = 0$ and $\gamma = 0.15$ from the respective figures. The trend of the variation of SPS with the barrier width under the applied magnetic field is same for all the impurity locations except for OCB impurity with respect to different combinations of Mn^{2+} ions as shown in Fig. 4.

In the case of OCB impurity as given in Fig.4a, when the combinations of C_1 and C_2 are considered, the SPS increases as the barrier width increases and one observes the reverse trend for the combinations of C_3 and C_4. This is because when the barrier width increases, the coupling between the two QWs is reduced which causes the carrier to interact with the Mn^{2+} ions presented in the well material alone. Therefore, only for the combination for which $x_{in} \leq 0.01$ alone only can show its influence to the maximum extent with the carrier, thereby increasing the shift. But when the width of the central barrier becomes thin, the maximum of SPS is observed only for the combinations of C_3 and C_4 which is due to the strong alignment of the spins of Mn^{2+} ions with the applied magnetic field. It is also worth to note from the Fig.4d that the SPS is maximum for OEW impurity as compared to all other impurity locations for the combination of C_1 and C_2. This is because there is a possibility of finding lesser number of antiferromagnetically paired Mn^{2+} ions along the interface of DQW, which can effectively contribute to a larger <Sz>. Therefore, the magnetization of the material becomes larger since these ions can easily be aligned in the external magnetic field.

4. Conclusion

The calculation of the SPS due to the formation of BMP with and without the application of external magnetic field in DQW for various impurity locations and for the different combinations of the concentration of Mn^{2+} ions in the well and the barrier DMS materials giving rise to x = 0.1 has been made. From our investigation it has been observed that even though the Mn^{2+} concentration x = 0.1 ($x_{out} - x_{in} = 0.1$) determines the effective confining potential well of the DQW, the SPS is different and depends on the concentration of Mn^{2+} ion in the well (x_{in}) and in the barrier (x_{out}). The large spin – splitting of energy levels due to the sp-d exchange interaction in such DMS materials corresponds to the far – infrared (FIR) region of the spectrum which causes the possibility of a tunable coherent circularly polarized

FIR emitter and for the resonant tunnelling devices using superlattices involving wide – gap DMS for which our study may throw some light.

5. Acknowledgement

The authors thank University Grants Commission, New Delhi, India for the financial support under Major Research Project (F. No.42-816/2013(SR)).

5. References

[1] J. A. Gaj, J. Ginter, Exchange interaction of Manganese $3d^5$ states with band electrons in $Cd_{1-x}Mn_xTe$, Phys. Stat. sol. (b) 89 (1978) 655-662.

[2] U. Thibblin, Theory of Bound Magnetic Polarons in Diluted Magnetic Semiconductors, Int. J. Mod. Phys. B. 3 (1989) 337–366.

[3] J. A. Gaj, R. R. Galazka and M. Nowrocki, Giant Exciton Faraday Rotation in $Cd_{1-x}Mn_xTe$ mixed crystals, Solid State Commun. 25 (1978) 193-195.

[4] P. Kalpana, P. Nithiananthi and K. Jayakumar, Donor states in a semimagnetic Double Quantum Well, Superlatt.Microstruct., 102 (2017) 246-258.

[5] K. Jayakumar, P. Nithiananthi, Excited states of a magnetic polaron in a Quantum Well, J. Nano. Electron. Phys. 3 (2011) 375-379.

[6] K. Gnanasekar and K. NavaneethaKrishnan, Spin Polaron in a Quantum Dot of the Diluted Magnetic Semiconductors, Mod. Phys. Lett. B. 18 (2004) 419-426.

[7] W. E. Hagston, T. Stirner, P. Harrison, O. F. Holbrook and J. P. Goodwin, "Impurity – bound magnetic polarons in diluted magnetic semicondcutors, Phys. Rev. B. 50 (1994) 5264-5271.

[8] J. A. Gaj, R. Planel and G. Fishman, Relation of Magneto – Optical Properties of free excitons to spin allignment of Mn^{2+} ions in $Cd_{1-x}Mn_xTe$, Solid.State Commun. 29 (1979) 435-438

[9] S. Lee, M. Dobrowolska, J.K. Furdyna, H. Luo, L.R. RamMohan, Magneto-Optical study of interwell coupling in double Quantum Well using Diluted Magnetic Semiconductors, Phys. Rev. B. 54 (1996) 16939–16951.

Highlights:

- Impurity states in a Triangular GaAs/$Al_{1-x}Ga_xAs$ Quantum Well has been studied.
- Effect of Γ-X band crossover on the χ_{dia} of a donor impurity has been investigated.
- χ_{dia} abruptly increases at a particular pressure for 1s and $2p_{\pm}$ states.
- A steady increase of χ_{dia} is noticed for 2s state as a function of applied pressure.
- This work shows the possibility of SMT in such triangular nanostructure systems.

Coulomb interaction of acceptors in Cd 1 x Mn x Te / CdTe quantum dot

P. Kalpana, A. Merwyn Jasper D. Reuben, P. Nithiananthi, and K. Jayakumar

Citation: AIP Conference Proceedings **1591**, 1176 (2014); doi: 10.1063/1.4872894
View online: http://dx.doi.org/10.1063/1.4872894
View Table of Contents: http://scitation.aip.org/content/aip/proceeding/aipcp/1591?ver=pdfcov
Published by the AIP Publishing

Coulomb Interaction of Acceptors in $Cd_{1-x}Mn_xTe$/CdTe Quantum Dot

P.Kalpana[1], A.Merwyn Jasper D Reuben[2], P.Nithiananthi[1] and K.Jayakumar[1,*]

[1]*Department of Physics, Gandhigram Rural University, Gandhigram-624302, TamilNadu, India,*
[2]*Department of Physics, School of Engineering, Saveetha University, Thandalam, Chennai- 600104, TamilNadu, India*
[*]*E-mail:kjkumar_gri@rediffmail.com*

Abstract. The investigation on the effect of confining potential like isotropic harmonic oscillator type potential on the binding and the Coulomb interaction energy of the double acceptors in the presence of magnetic field in a $Cd_{1-x}Mn_xTe$/CdTe Spherical Quantum Dot has been made for the Mn ion composition x=0.3 and compared with the results obtained from the square well type potential using variational procedure in the effective mass approximation.

Keywords: Double acceptors, Square well potential, Parabolic potential, Coulomb Interaction energy
PACS: 73.21.La, 71.15.Nc, 75.75-C, 75.50.Pp, 75.30.Hx.

INTRODUCTION

One of the best known magnetic semiconductors that can be made p-type is $Cd_{1-x}Mn_xTe$[1].The effect of exchange interaction of a hole with magnetic ions on the acceptor states which gives rise to Bound Magnetic Polaron is a special feature in this Semimagnetic Semiconductors. In the absence of magnetic field, the spins of the magnetic ions are not ordered and hence there is no net exchange interaction of these ions with a hole. Recently[2] results are available on the Coulomb interaction of the carriers in square well type potential confinement in Quantum Dots (QD). But still there are uncertainties in the nature and type of potential that exists in QD. Brey et al.[3] and Yip[4] have demonstrated the evidences for the assumption of parabolic potential confinement in QD which is the motivation for the present work. In this work, we investigate the effect of confining potential like harmonic oscillator type on the Coulomb interaction between the acceptors and their binding energy in the presence of magnetic field in $Cd_{1-x}Mn_xTe$/CdTe spherical QD for Mn composition of x=0.3 using variational principle in the effective mass approximation.

THEORETICAL FORMALISM

Defining effective Bohr radius $a_B^* = \hbar^2\varepsilon_0/m^*e^2$ as unit of length, effective Rydberg $R^* = e^2/2\varepsilon_0 a_B^*$ as unit of energy and the strength of the magnetic field parameter $\gamma = \hbar\omega_c/2R^*$ (ω_c – cyclotron frequency), the Hamiltonian of the double acceptor impurities in $Cd_{1-x}Mn_xTe$/CdTe QD in the effective mass approximation in the presence of magnetic field applied along the growth direction is given as

$$H_{hh} = -\nabla_1^2 - \nabla_2^2 - \frac{2}{r_1} - \frac{2}{r_2} + V_B(r_1) + V_B(r_2) + \gamma L_{z_1} + \gamma L_{z_2} + \frac{\gamma^2(r_1^2\sin^2\theta_1)}{4} + \frac{\gamma^2(r_2^2\sin^2\theta_2)}{4} + \frac{2}{\left|\vec{r_1} - \vec{r_2}\right|} \quad (1)$$

The Parabolic confining potential for $Cd_{1-x}Mn_xTe$ Spherical Quantum Dot is given by

$$V_B = \begin{cases} \frac{1}{2}m^*\omega^2 r^2 & r < R \\ V_0 & r > R \end{cases} \quad (2)$$

where R is the radius of the Quantum Dot and $V_0 = 30\%\Delta E_g^B$, where, ΔE_g^B is the band gap difference with magnetic field and is given by[2].

$$\Delta E_g^B = \Delta E_g^0 \left[\frac{\eta e^{\zeta\gamma} - 1}{\eta - 1}\right] \quad (3)$$

Solid State Physics
AIP Conf. Proc. 1591, 1176-1178 (2014); doi: 10.1063/1.4872894

where ΔE_g^0 is the band gap difference without magnetic field given as $\eta=e^{\zeta\gamma_0}$ is chosen with ζ as a parameter(=0.5) and γ_0 as the critical magnetic field.

The trial wavefunction for the ground state of double acceptor impurities in spherical polar co-ordinates with parabolic confinement is given by,

$$\psi_{1s}(r_1, r_2) = N_{hh} \begin{cases} e^{-\frac{1}{2}\alpha_1^2} e^{-\frac{1}{2}\alpha_2^2} e^{-\lambda_{hh}\left|\vec{r_1}-\vec{r_2}\right|} & r < R \\ B \dfrac{e^{-\beta r_1}}{r_1} \dfrac{e^{-\beta r_2}}{r_2} e^{-\lambda_{hh}\left|\vec{r_1}-\vec{r_2}\right|} & r > R \end{cases} \quad (4)$$

where, $\alpha=(2m^*E)^{1/2}$, $\beta=(2m^*(V_0-E))^{1/2}$ and λ_{hh} is the variational parameter.
The subband energy (E) is the lowest energy without the acceptor impurity which is obtained by solving the transcendental equation

$$\alpha + \beta \tan(\alpha R) = 0 \quad (5)$$

RESULTS AND DISCUSSIONS

Fig.1a. gives the variation of Coulomb interaction between acceptors confined in a parabolic and square well potential in QD in the absence of magnetic field (γ=0). Fig.1b. gives the same in the presence of magnetic field (γ=0.075).

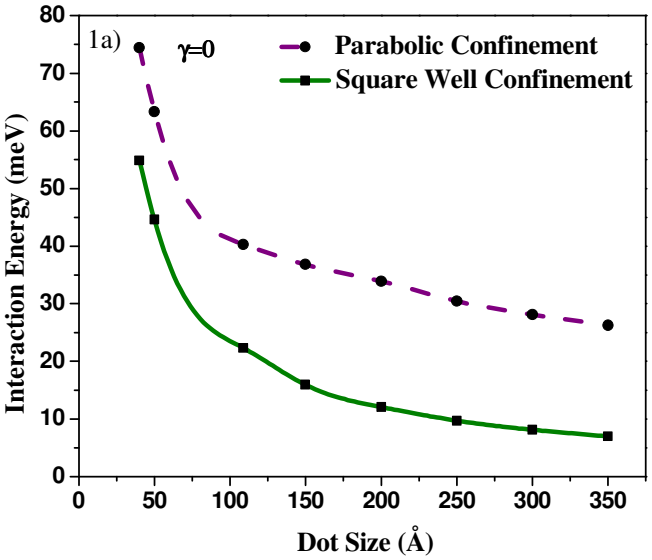

FIGURE 1a. Variation of Coulomb interaction of double acceptors *vs.* dot radius for γ=0.

From these figures one observes that the carriers show more interaction in parabolic confinement than for square well type potential confinement. Moreover, in the presence of the magnetic field a turnover occurs for the smaller radius of QD. A shift in the turnover towards the smaller radius of QD under parabolic confinement in the presence of magnetic field (γ=0.075) has also been noticed. This turnover feature is due to the interplay between three forces, the first being an attractive force due to the confining potential in a dot that tends to confine the holes together, the second being the repulsive force due to the Coulomb interaction between the hole themselves and the third being the magnetic field which reduces the confinement and aids the repulsive forces. At a lower QD radius the repulsive force gains in strength and causes tunneling which in turn reduce the interaction energy when the magnetic field is applied.

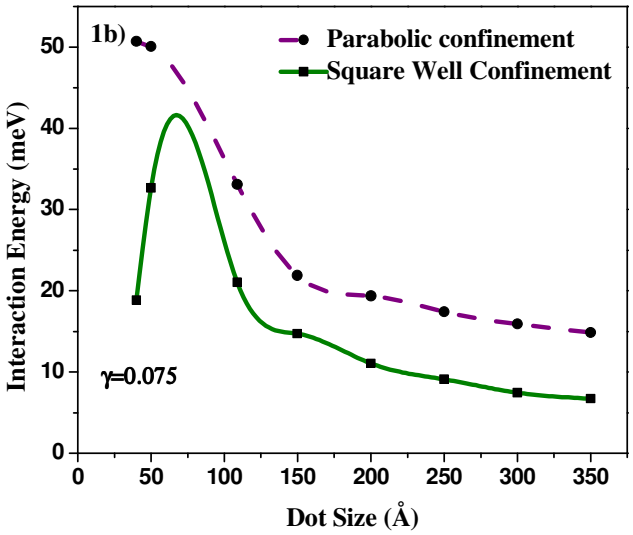

FIGURE 1b. Variation of Coulomb interaction of double acceptors *vs.* dot radius for γ=0.075.

Fig.2a and 2b gives the binding energy of the acceptors as a function of dot size without and with magnetic field respectively. Fig.2a. reveals the binding of acceptor is more in parabolic confinement than in square well type confinement in the absence of magnetic field justifying the trend of the results of fig.1a. In the presence of the magnetic field (γ=0.075), one sees an enhanced binding of acceptors under parabolic confinement than the square well type confinement justifying the results of fig.1b.

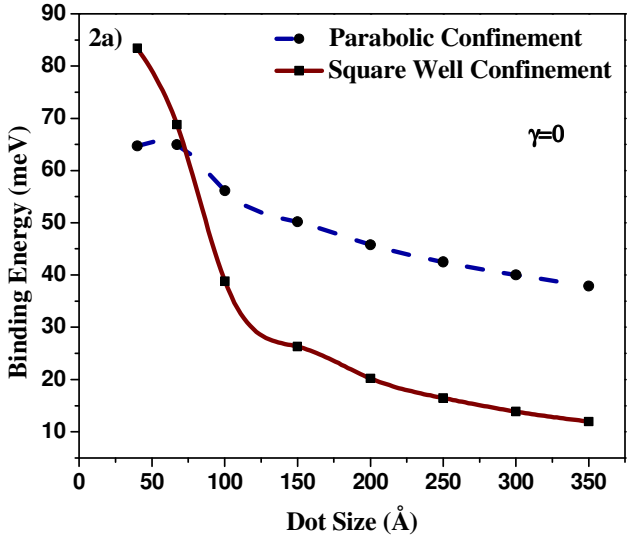

FIGURE 2a. Variation of binding energy of double acceptors *vs*. dot size for a) γ=0.

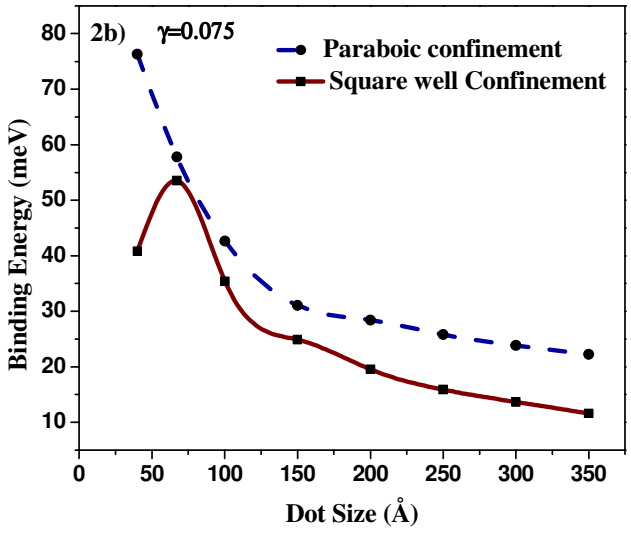

FIGURE 2b. Variation of binding energy of double acceptors *vs*. dot size for γ=0.075.

CONCLUSION

The present investigation can help in understanding the mechanism of two particle spectra and the formation of Wigner crystal in low dimensional systems like Quantum Dot, Quantum Wire and Quantum Well.

ACKNOWLEDGMENTS

The authors thank University Grants Commission, New Delhi, India for the financial support under Major Research Project. (F.No.42-816/2013 (SR)).

REFERENCES

1. R.R. Galazka, *Physiscs of Narrow Gap Semiconductors*, Springer, Berlin 294 (1982).
2. A. Merwyn Jasper D Reuben, K. Jayakumar, *Superlat. and Microstruct* **52** 732–737 (2012) .
3. L. Brey, N. F. Johnson, and B. I. Halperin, *Phys.Rev.B* **40** 10647-10649 (1989).
4. S. K. Yip, *Phys. Rev B* **43**, (1991).

Magnetic field effect on the Coulomb interaction of acceptors in semimagnetic quantum dot

P. Kalpana, A. Merwyn, Jasper D. Reuben, P. Nithiananthi, and K. Jayakumar

Citation: AIP Conference Proceedings **1665**, 090005 (2015); doi: 10.1063/1.4917985
View online: http://dx.doi.org/10.1063/1.4917985
View Table of Contents: http://scitation.aip.org/content/aip/proceeding/aipcp/1665?ver=pdfcov
Published by the AIP Publishing

Magnetic field Effect on the Coulomb Interaction of Acceptors in Semimagnetic Quantum Dot

P. Kalpana[1], A. Merwyn[1], Jasper D. Reuben[2], P. Nithiananthi[1] and K. Jayakumar[1,*]

[1]*Nanostructure Lab, Department of Physics, Gandhigram Rural University, Gandhigram-624302, India*
[2]*Department of Physics, School of Engineering, Saveetha University, Thandalam, Chennai- 600104, India*
[*]*E-mail: kjkumar_gri@rediffmail..com*

Abstract. The Coulomb interaction of holes in a Semimagnetic $Cd_{1-x}Mn_xTe$ / CdTe Spherical and Cubical Quantum Dot (SMQD) in a magnetic field is studied using variational approach in the effective mass approximation. Since these holes in QD show a pronounced collective behavior, while distinct single particle phenomena is suppressed, their interaction in confined potential becomes very significant. It has been observed that acceptor-acceptor interaction is more in cubical QD than in spherical QD which can be controlled by the magnetic field. The results are presented and discussed.

Keywords: Acceptor**,** Semimagnetic system , Quantum Dot, Coulomb interaction, Binding Energy
PACS: 73.60.cs, 75.30.Hx. 73.21.La,75.50Pp

INTRODUCTION

Magnetic and Semi-magnetic nanostructure systems like $Cd_{1-x}Mn_xTe$ / CdTe (where x is the concentration of magnetic impurity Mn) Quantum Dot (QD) is drawing considerable attention due to Spintronic applications, possibility of realizing the optoelectronic devices and exhibiting the switch over of the system from type – I to type – II[1]. It is well known that Coulomb interaction between acceptor states leads to increased significance of many body effects. The Mn concentration in nonmagnetic Semiconductor gives rise to ferromagnetism and metallic transport. Coulomb interaction within the QD gives rise to the phenomenon of Coulomb blockade of transport and its influence strongly depends on the size of the QD[2]. Moreover, the infrared spectra of acceptor-acceptor interaction in Si and Ge show a small splitting which cannot be explained unless one considers the acceptors interaction[3]. In the light of the above, in the present work, the acceptor – acceptor Coulomb interaction in $Cd_{1-x}Mn_xTe$/CdTe QD (both spherical (SQD) and cubical (CQD)) have been investigated in the effective mass theory. The theoretical formulation is given in the next section and in the last section, results and discussions are presented.

THEORETICAL FORMALISM

The double acceptor states are determined by solving the hole effective mass Schrödinger equation and the Coulomb interaction between these two acceptors is screened by the background dielectric constant ε. The effective mass Hamiltonian is written in dimensionless form as

$$H_{hh} = \left\{ \begin{array}{l} -\nabla_1^2 - \nabla_2^2 - \frac{2}{r_1} - \frac{2}{r_2} + V_B(r_1) + V_B(r_2) + \gamma L_{z_1} \\ \qquad + \gamma L_{z_2} + \frac{\gamma^2 (r_1^2 \sin^2\theta_1)}{4} + \frac{\gamma^2 (r_2^2 \sin^2\theta_2)}{4} + \frac{2}{|\vec{r_1} - \vec{r_2}|} \end{array} \right\} \quad (1)$$

where, $\gamma = \hbar\omega_c/2R^*$ (ω_c – cyclotron frequency) is the parameter of the strength of the magnetic field and γ=1 corresponding to 1131.71Tesla.

The effective confinement potential for both the cubical and spherical QD is given as,

$$\left. \begin{array}{ll} V_B = \begin{cases} 0 & r < R \\ V_0 & r > R \end{cases} & \rightarrow SQD \\ V_B = \begin{cases} 0 & |x|,|y|,|z| \le L/2 \\ V_0 & |x|,|y|,|z| > L/2 \end{cases} & \rightarrow CQD \end{array} \right\} \quad (2)$$

Solid State Physics
AIP Conf. Proc. 1665, 090005-1–090005-3; doi: 10.1063/1.4917985

where, R, L are the radius and size of the SQD as well as CQD respectively and V_0=30%ΔE_g^B. The external applied magnetic field strongly changes the difference in the band gap between $Cd_{1-x}Mn_xTe$ and CdTe by[4]

$$\Delta E_g^B = \Delta E_g^0 \left[\frac{\eta e^{\zeta\gamma} - 1}{\eta - 1} \right] \tag{3}$$

so that, the strength of the confinement potential is rapidly reduced and results in the modifications of electrical and optical properties. $\eta = \exp[\alpha\gamma_0]$and α is a parameter(α=0.5) and γ_0 as the critical magnetic field. ΔE_g^B and ΔE_g^0 are the band gap difference with and without magnetic field respectively. The band gap of the material is given by E_g ($Cd_{1-x}Mn_xTe$) = 1606 + 1587x (meV). The critical magnetic field γ_0 depends upon the value of composition. This critical field (in Tesla) for other values of composition can be obtained using the formulae $B_0 = A_2 \exp[nx]$, where, A_2 = -0.57 and n=16.706

The approximate ground states for confined double acceptors have been calculated using the variational approach. The variational wavefunction Ψ is chosen to be a product of the lowest energy subband states of the two holes confined inside the QD.Considering the correlation between the double acceptors, the trial wavefunctions for both the spherical and cubical dot are written as

$$\left.\begin{aligned} \Phi_{wSQD}(r1,r2) &= \frac{Sin[\alpha r1]}{r1}\frac{Sin[\alpha r2]}{r2} \\ \Phi_{bSQD}(r1,r2) &= C_h \frac{e^{-\beta r1}}{r1}\frac{e^{-\beta r2}}{r2} \\ \Psi_{SQD}(r1,r2) &= N_{hh}\begin{cases} \Phi_{wSQD}(r1,r2)\, e^{-\lambda|\overrightarrow{r1}-\overrightarrow{r2}|}, & r<R \\ \Phi_{bSQD}(r1,r2)\, e^{-\lambda|\overrightarrow{r1}-\overrightarrow{r2}|}, & r>R \end{cases} \end{aligned}\right\} \tag{4}$$

$$\left.\begin{aligned} \Phi_{bCQD}(r1,r2) &= Cos[\alpha x1]Cos[\alpha y1]Cos[\alpha z1]Cos[\alpha x2]Cos[\alpha y2]Cos[\alpha z2] \\ \Phi_{bCQD}(r1,r2) &= C_h e^{-\beta(x1+y1+z1)} e^{-\beta(x2+y2+z2)} \\ \Psi_{CQD}(r1,r2) &= N_{hh}\begin{cases} \Phi_{wCQD}(r1,r2)\, e^{-\lambda|\overrightarrow{r1}-\overrightarrow{r2}|}, & |x1|,|y1|,|z1|,|x2|,|y2|,|z2| \le L/2 \\ \Phi_{bCQD}(r1,r2)\, e^{-\lambda|\overrightarrow{r1}-\overrightarrow{r2}|}, & |x1|,|y1|,|z1|,|x2|,|y2|,|z2| > L/2 \end{cases} \end{aligned}\right\} \tag{5}$$

(w-stands for well and b-stands for barrier), where, N_{hh} is the normalization constant, $\alpha=(2m^*E)^{1/2}$, $\beta=(2m^*(V_0-E))^{1/2}$, λ is the variational parameter and C_h is obtained from the continuity condition.

The lowest energy level E_0 without acceptor impurity can be computed by solving the transcendental equation

$$\begin{aligned} \alpha + \beta\tan(\alpha R) = 0 \quad &\rightarrow SQD \\ \alpha\tan(\alpha L/2) = \beta \quad &\rightarrow CQD \end{aligned} \tag{6}$$

The expectation value of H is minimized with respect to λ and the hole-hole interaction energy is obtained by computing

$$E_{hh} = \left\langle \Psi_{SQD,CQD}(r1,r2) \left| \frac{2}{|\overrightarrow{r1}-\overrightarrow{r2}|} \right| \Psi_{SQD,CQD}(r1,r2) \right\rangle \tag{7}$$

and the binding energy of double acceptors in the presence of magnetic field is found by solving the Schrödinger equation variationally, and is given by

$$E_B = E + \gamma - \left\langle H \right\rangle_{\min} \tag{8}$$

The CdTe parameters used in our calculations are ε = 10.2; m_h = 0.67. Energies are scaled by hole effective Rydberg $R_h = m_h e^2/2\hbar^2\varepsilon^2$ and the effective Bohr radius $a_h = \hbar^2\varepsilon/m_h e^2$.

RESULTS AND DISCUSSION

Fig.1 and 2 presents the binding energy and the Coulomb Interaction energy of double acceptors as a function of dot size for three different barrier height(143,67,10.4meV) corresponding to the magnetic field strength of (γ = 0, 0.04, 0.07) respectively for both cubical and spherical dot. It can be seen that there is a rapid reduction in the Coulomb interaction energy as well as the binding energy when the magnetic field (γ) is increased, since the applied magnetic field greatly alters the barrier height of the QD according to eqn.(3).

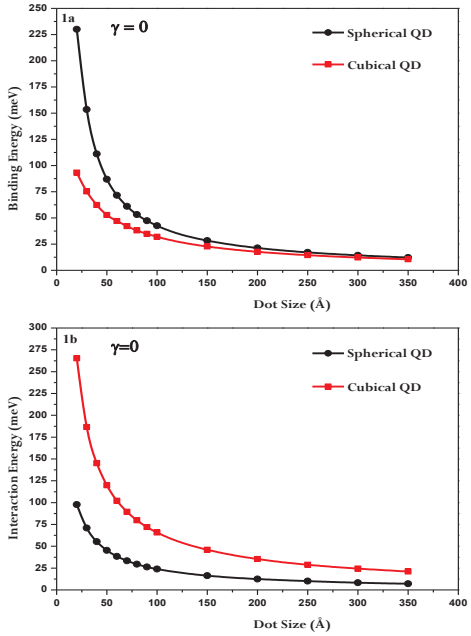

FIGURE 1. Variation of the ground state double acceptor **a)** binding and **b)** interaction energy as a function of dot size for cubical and spherical Quantum dot with x=0.3 for γ=0.

In both cases (CQD & SQD) the binding and the interaction of the two holes increases to a maximum around 30Å without applying magnetic field ($\gamma = 0$) as shown in Fig.1a and 1b.

This is due to the effective confinement frequency scales with the inverse square of the dot size ($\Omega \alpha 1/L^2$) and the typical interaction energy drops inversely with increasing dot size ($V_{Coulomb} \alpha 1/L$), which may be due to the fact that decreasing the dot size, the wavefunction is more squeezed in CdTe dot, leading to the stronger binding. However beyond a certain value of dot size, the wavefunction is spread into the barrier $Cd_{1-x}Mn_xTe$, leading to the reduced confinement of the holes in the well region.

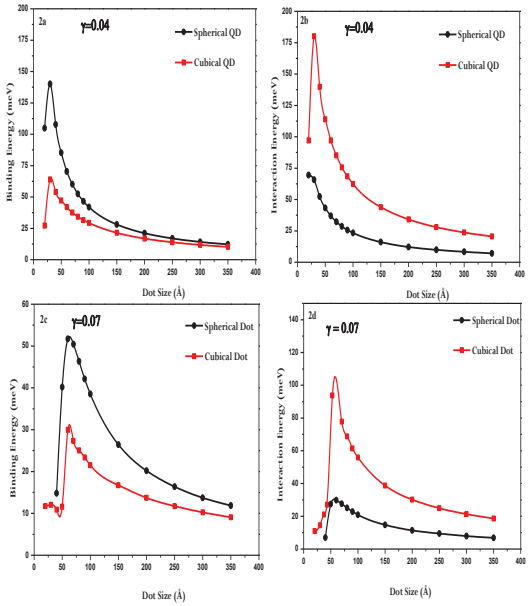

FIGURE 2. Variation of the ground state double acceptor binding energy and interaction energy as a function of dot size for Cubical and spherical Quantum dot with x=0.3 for **a,b)** γ=0.04 and **c,d)** γ=0.07.

When the strength of the magnetic field is increased towards the critical value (vanishing of V_0), the energy maximum shifts towards the dot size < 70Å. This behavior of the energy as a function of dot size (for a given magnetic field) can be attributed by the following facts. (i) For extremely narrow dot size (~30Å) the repulsive force between the two holes gain in strength and causes tunneling. (ii) When the dot size is larger (30Å< (R,L)<70Å), an attractive force due to the confining potential and the magnetic field induced localization win over tunneling and tend to confine the holes together inside CdTe dot. From the above arguments, one expects the onset of quasilowdimensionality effects to occur when the effective Bohr radius of the hole-hole pair is comparable to the size of the QD.

The ionization energy of the double holes is larger in Spherical confinement than in Cubical dot as shown in figures 1 and 2 which is justified by the distribution function of holes inside the dot as shown in fig.3. Hence, the Coulomb interaction between the holes is strongly enhanced only in dot with cubical geometry rather than in spherical geometry. This is due to the fact that the confinement in spherical geometry decreases the kinetic energy of the double holes thus leading to the enhanced binding energy.

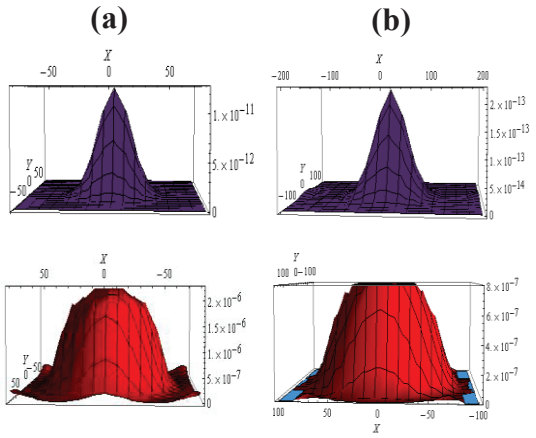

FIGURE 3. Probability distribution of the holes inside the QD of size 50Å for (a)γ=0, (b) γ=0.07 for Cubical (Blue) and Spherical(Red) Quantum Dot

CONCLUSIONS

The Coulomb interaction of acceptors in CQD and SQD is very effective and can be controlled by the external magnetic field. This Coulomb interaction in SMQD is significant in the light of Coulomb blockade of transport. Moreover, this two particle interaction can be very helpful to understand the two particle energy spectra.

ACKNOWLDGEMENTS

The authors (P.Kalpana, K.Jayakumar) thank University Grants Commission, New Delhi, India for the financial support under Major Research Project. (F.No.42-816/2013 (SR)).

REFERENCES

1. G.Bastard, J.A.Brum and R.Rerreire, *Solid St.Phys*, **44**, 229 (1991).
2. U.Merkt, J.Huser and M.Wagner, *Phys.Rev.B* **43**, 7320 (1991)
3. A.Giesekus, *Phys. Rev.B* **42**, 11725 (1991)
4. A. Merwyn Jasper D Reuben, K. Jayakumar, *Superlat. and Microstruct* **52** 732–737 (2012) .

Effect of magnetic field on the donor impurity in CdTe/Cd1-xMnxTe quantum well wire

P. Kalpana, A. Merwyn Jasper D. Reuben, P. Nithiananthi, and K. Jayakumar

Citation: AIP Conference Proceedings **1731**, 090027 (2016); doi: 10.1063/1.4947991
View online: http://dx.doi.org/10.1063/1.4947991
View Table of Contents: http://scitation.aip.org/content/aip/proceeding/aipcp/1731?ver=pdfcov
Published by the AIP Publishing

Effect of Magnetic Field on the Donor Impurity in CdTe/ $Cd_{1-x}Mn_xTe$ Quantum Well Wire

P.Kalpana[1], A.Merwyn Jasper D Reuben[2], P.Nithiananthi[1] and K.Jayakumar[1]*

[1]*Nanostructure Lab, Department of Physics, Gandhigram Rural University, Gandhigram – 624 302, Tamilnadu.*
[2]*Department of Physics, School of Engineering, Saveetha University, Thandalam, Chennai- 600104, TamilNadu, India*
[*]*Email:kjkumar_gri@rediffmail.com*

Abstract. The donor impurity binding energy in CdTe / $Cd_{1-x}Mn_xTe$ QWW with square well confinement along x – direction and parabolic confinement along y – direction under the influence of externally applied magnetic field has been computed using variational principle in the effective mass approximation. The spin polaronic shift has also been computed. The results are presented and discussed.

Keywords: Parabolic Well, Square Well, Quantum Well Wire, Diluted Magnetic Semiconductors, Binding Energy
PACS: 73.63.Nm, 73.21.Hb, 75.50.Pp, 73.63.Hs, 71.38.-k, 75.75.-c

INTRODUCTION

Compound Semiconductors incorporating low concentration of transition metals like Mn which are called "Diluted Magnetic Semiconductors (DMS)". $Cd_{1-x}Mn_xTe$, have opened a new field of spin – functional semiconductor physics. The exchange interaction between the extended (band) and local (usually d) electrons (i.e. the p-d and the s-d exchange interaction), which are responsible for the formation of Bound Magnetic Polaorn (BMP), underlies important spin- amplified properties in these materials [1]. Several theoretical formalisms for evaluating BMP energies have been developed and also an abundance of experimental results exists on both acceptor – BMP and donor - BMP in various semimagnetic materials [2]. The physical nature of impurity states associated with semiconducting heterostructures is a subject of considerable technical and scientific relevance because of their potential device applications. With the technological progresses in the fabrication of semiconductor structures like chemical lithography, Molecular Beam Epitaxy and etching, it has been made possible to fabricate a wide variety of Quantum Well Wires (QWW) with well controlled shape and composition to achieve the high electron mobility [3] due to strong suppression of both impurity and optical – phonon scattering. The spatial confinement of the wavefucntion in these QWW mainly depends on both the shape of the potential and the impurity position along these structures and thereby number of studies concerning QWW with rectangular, T-Shaped, V-groove, triangular and other cross sections [4,5]. Hence lot of attention were shown during the last few decades. In the present work, we investigate theoretically the binding energy of donor impurity in a CdTe/$Cd_{1-x}Mn_xTe$ QWW with square type potential confinement along x-direction and parabolic type confinement along y-direction, V(x, y) under the influence of externally applied uniform magnetic field for Mn composition of x=0.3. Calculations are carried out in the effective mass approximation using variational method.

THEORY

The Hamiltonian of a hydrogenic donor impurity in the presence of magnetic field in CdTe/$Cd_{1-x}Mn_xTe$ Quantum Well Wire in the effective mass approximation is given as

$$H = -\frac{d^2}{dx^2} + V(x) - \frac{d^2}{dy^2} + V(y) - \frac{d^2}{dz^2} - \frac{2}{\varepsilon r} + \gamma L_Z + \frac{\gamma^2 \rho^2}{4} \qquad (1)$$

Defining effective Bohr radius $a_B^* = \hbar^2 \varepsilon_0 / m^* e^2$ as unit of length, effective Rydberg $R^* = e^2 / 2\varepsilon_0 a_B^*$ as unit of energy and the strength of the magnetic field parameter $\gamma = \hbar\omega_c / 2R^*$ (ω_c – cyclotron frequency and $\gamma = 1$ corresponds to 30.5604Tesla), where m* is the

DAE Solid State Physics Symposium 2015
AIP Conf. Proc. 1731, 090027-1–090027-3; doi: 10.1063/1.4947991
Published by AIP Publishing. 978-0-7354-1378-8/$30.00

effective mass of electron in CdTe and $\rho = \sqrt{x^2 + y^2}$, $r = \sqrt{\rho^2 + z^2}$; ε is the static dielectric constant of CdTe. *V(x)* and *V(y)* are the finite confinement potentials in the x- and y-direction, respectively. *V(x)* is a square well potential of height V_0 and *V(y)* is a parabolic well potential of $\frac{1}{2}m\omega^2 y^2$, which are given by,

$$V(x) = \begin{cases} 0 & , |x| \le L/2 \\ V_0 & , |x| > L/2 \end{cases}$$
$$V(y) = \begin{cases} \frac{1}{2}m\omega^2 y^2 & , |y| \le L/2 \\ V_0 & , |y| > L/2 \end{cases} \quad (2)$$

L is the width of the rectangular cross section of the wire and V_0 = 70%ΔE_g^B; ΔE_g^B is the band gap difference with magnetic field [6] and is given by,

$$\Delta E_g^B = \Delta E_g^0 \left[\frac{\eta \exp[\varsigma\gamma] - 1}{\eta - 1} \right] \quad (3)$$

where ΔE_g^0 is the band gap difference without magnetic field given as $\eta = e^{\zeta\gamma_0}$is chosen with ζ as a parameter (=0.5) and γ_0 as the critical magnetic field which depends upon the value of the Mn ion composition 'x'. The critical magnetic field for different composition $B_0 = Ae^{nx}$ is given in Tesla with A=0.734 and n=19.082 which gives the best fit to the extrapolated experimentally available critical fields. The band gap of $Cd_{1-x}Mn_xTe$ is given to be 1.606+1.587x eV.

The trial wavefunction for ground state donor impurity in such QWW with different confinements along two directions is given by

$$\Psi = N_{1s}\, \psi(x)\, \psi(y)\, \mathrm{Exp}[-\lambda r] \quad (4)$$

where,

$$\psi(x) = \begin{cases} \mathrm{Cos}[\alpha 1 x] & , |x| \le L/2 \\ B1\, \mathrm{Exp}[-\beta 1 x] & , |x| > L/2 \end{cases}$$
$$\psi(y) = \begin{cases} \mathrm{Exp}[-\frac{1}{2}\alpha 2 y^2] & , |x| \le L/2 \\ B2\, \mathrm{Exp}[-\beta 2 y] & , |y| > L/2 \end{cases} \quad (5)$$

where N_{1s} is the normalization constant $\alpha 1 = (2m^*E)^{1/2}$ and $\beta 1 = (2m^*(V_0 - E))^{1/2}$, λ is the variational parameter, 'B1' and 'B2' is obtained from the continuity condition.

The binding energy of the donor impurity in the presence of magnetic field is found by solving the Schrodinger equation variationally and is given by

$$E_B^{QWW} = E_x + E_y + \gamma - \langle H_{min} \rangle \quad (6)$$

Spin polaronic effect

The modified Brillouin function [6] to invoke the exchange interaction between the carrier and magnetic impurity in the presence of an external magnetic field **B**, yielding the magnetic polaronic shift which is given by

$$E_{sp} = \tfrac{1}{2}\beta S N_0 \left\{ \langle \Psi_1 | x_1 B_S(y_1) | \Psi_1 \rangle + \langle \Psi_2 | x_2 B_S(y_2) | \Psi_2 \rangle \right\}$$
$$B_S(y_j) = \frac{2S+1}{2S}\coth\frac{2S+1}{2S}y_j - \frac{1}{2S}\coth\frac{y_j}{2S} \quad (7)$$
$$y_j = \frac{S\beta|\Psi_j|^2}{2kT} + \frac{g\mu_B S\beta}{kT}$$

where β - exchange coupling parameter, S is the spin of Mn^{2+} (=5/2), and xN_0 is the Mn ion concentration with N_0 = 2.94 × 10^{22} cm^{-3} and βN_0 = 220 meV for CdTe. Also $g_{Mn} \approx 2$ and B is the strength of the external magnetic field, k is the Boltzmann constant and $B_s(y)$ is the modified Brillouin function.

RESULTS and DISCUSSIONS

Observations have been made on the binding energy and spin polaronic shift of the hydrogenic donor impurity confined in a QWW with square confinement along x-direction and parabolic confinement along y-direction for the various magnetic fields applied along the free direction 'z'.

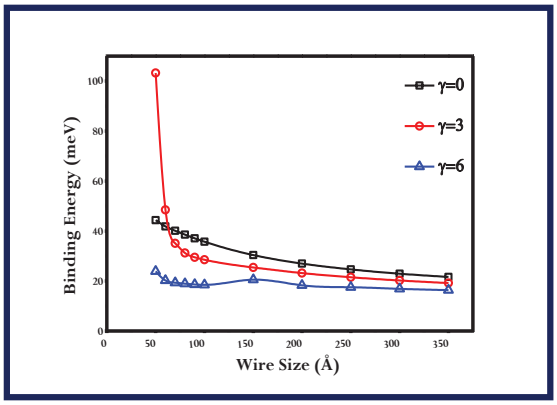

Fig.1: Donor Binding Energy *vs* Wire Size for x=0.3 for various magnetic fields

It can be seen from the Fig (1) that the donor binding energy decreases with increase in magnetic field. This is due to the fact that the application of magnetic field reduces the confining potential barrier height according to eqn (3) thus making the donor less

confined in the wire. This can be justified from the probability distribution function plotted in Fig (2) for γ=0 and γ=6.

γ=0 and L=100Å

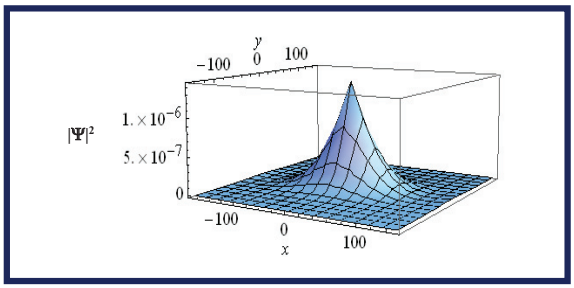

γ=6 and L=100Å

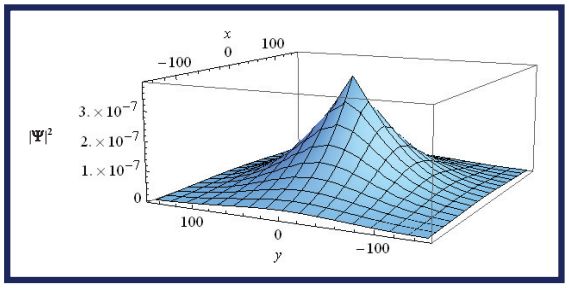

Fig.2: Probability distribution for γ=0 and γ=6 for wire size L=100Å.

It can be seen from the figure that the Probability density of donor inside the wire is higher in magnitude in the absence of magnetic field than in the presence of magnetic field. It is also observed that the binding energy decreases as the wire size increases which is an expected one in any low dimensional systems. The reliability of our results can be verified as:

$$E_B^{QWW} \text{ approches to } \begin{cases} E_B^{\text{Square Well}} & \text{, for } V(x,0) \\ E_B^{\text{Parabolic Well}} & \text{, for } V(0,y) \end{cases}$$

where, $E_B^{\text{Square / Parabolic Well}}$ is the donor binding energy of a Quantum Well with Square / Parabolic potential confinement [7].

The variation of magnetic polaronic shift of the donor impurity for γ=0, γ=3 and γ=6 is given for x=0.3. It is noticed that there is a drastic increase in the spin polaronic shift with increase in magnetic field as there is an increase in the exchange interaction between the magnetic ions and donor impurity.

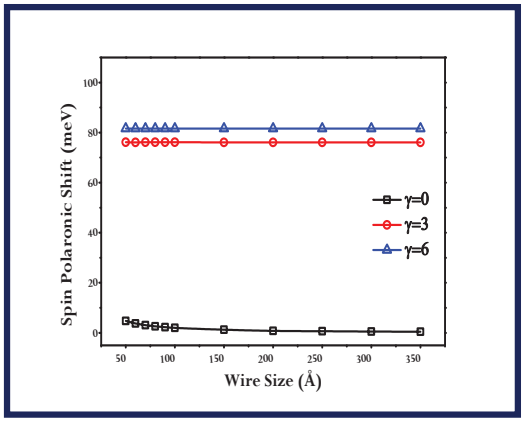

Fig.3: Spin Polaronic shift *vs* Wire Size for x = 0.3 for various magnetic fields

CONCLUSION

The study of the magnetic effect on the donor impurity confined in such a QWW with various confinements along two directions is important since it is possible to investigate the various properties like magnetic excitations and other magneto optical transitions and also to simulate and fabricate QWW of different cross sectional geometry and confining potential according to the requirement for various device applications.

ACKNOWLEDGMENT

The authors (P. Kalpana and K.Jayakumar) thank University Grants Commission, New Delhi, India for the financial support under Major Research Project (F.No.42-816/ 2013(SR)).

REFERENCES

1. Wolff P A, "Theory of Bound Magnetic Polarons in Semimagnetic Semiconductors", in *Semiconductors and Semimetals*, edited by J.K.Furdyna and J.Kossut, New York, Vol.**25** Academic Press Inc., 1987, p413
2. Hagstn W E and Stirner T et.al. *Phys.Rev.* **B 50,** (1994)
3. Sakaki H, *Jpn.J.Apply.Phys.***19**, 94, (1980)
4. Kasapoglu E et.al. *Physica E.* **19**, 332-335, (2003)
5. Khordad R et.al. *Current Appl.Phys.***10**, 199-202 (2010)
6. Nithiananthi P, Jayakumar K, *J. Nano. Electron. Phys.* **3**, 375-379 (2011)
7. Nithiananthi P et.al., *Proc.ICONN-2010*, 291-292, (2010)

Impurity States and diamagnetic susceptibility of a donor in a triangular quantum well

P. Kalpana, A. Merwyn Jasper D. Reuben, P. Nithiananthi, and K. Jayakumar

Citation: AIP Conference Proceedings **1832**, 090032 (2017); doi: 10.1063/1.4980585
View online: http://dx.doi.org/10.1063/1.4980585
View Table of Contents: http://aip.scitation.org/toc/apc/1832/1
Published by the American Institute of Physics

Impurity states and Diamagnetic Susceptibility of a donor in a Triangular Quantum Well

P. Kalpana[1], A. Merwyn Jasper D Reuben[2], P. Nithiananthi[1] and K. Jayakumar[1*]

[1] *Nanostructure Lab, Department of Physics, Gandhigram Rural University, Gandhigram-624302, Tamilnadu, India*

[2] *Department of Physics, School of Engineering, Saveetha University, Thandalam, Chennai-600104, Tamilnadu, India*

[*] *E-mail: kjkumar_gri@rediffmail.com*

Abstract. We have calculated the binding energy and the diamagnetic susceptibility(χ_{dia}) of the ground (1s) and few low lying excited states (2s and $2p_{\pm}$) in a GaAs/$Al_xGa_{1-x}As$ Triangular Quantum Well (TQW) for the Al composition of x = 0.3. Since the estimation of $\langle r^2 \rangle$ gives the carrier localization in nanostructured systems and also the calculation of (χ_{dia}) involves the $\langle r^2 \rangle$, the same has also been estimated as a function of well width. The Schrodinger equation has been solved using variational technique involving Airy functions in the effective mass approximation. The results are presented and discussed.

Keywords: Triangular Quantum Well, Donor Impurity, Binding Energy, Diamagnetic Susceptibility, Excited states
PACS: 73.63.Hs, 73.61.Ey, 78.47.da, 75.75.-c

INTRODUCTION

The potential energy of the conduction band in GaAs is lower than that of $Al_xGa_{1-x}As$ causing electrons to transfer to lower energy region which is opposed by the electric field between the electron and the donor ion which alters the band potential confining carrier within a Triangular Quantum Well (TQW). These TQW appear in Si MOSFETS, GaAs/AlGaAs MODFETS and in biological sensors for pH and dipole moment measurements of polar liquids. The electrons confined in a TQW has attracted much attention in recent times. Jiang et al[1] have calculated the binding energy of the on center donor impurity in a GaAs/$Al_xGa_{1-x}As$ TQW involving Airy functions using variational principle and the same has also been extended for various impurity locations inside the TQW by Zhang et al[2]. Many theoretical works have been devoted to study the impurity states as well as the diamagnetic susceptibility through which one can explain the Semiconductor – Metal Transition [3, 4]. In this present communication, we have investigated the binding energy and the diamagnetic susceptibility for ground state and few excited states of a donor confined in a GaAs/$Al_xGa_{1-x}As$ Triangular Quantum Wells for x = 0.3.

THEORETICAL FORMALISM

The Hamiltonian of the donor impurity confined in a GaAs/ $Al_xGa_{1-x}As$ TQW under the single – band effective mass approximation is given by

$$H = \frac{-\hbar^2}{2m^*}\nabla^2 - \frac{e^2}{\varepsilon_0 r} + V_B(z) \quad (1)$$

where m^* is the effective mass of the charge carrier ε_0 is the static dielectric constant of GaAs and $V_B(z)$ is the electrostatic confining potential and r is the distance between the charge carrier and the donor impurity which is given by $r=\sqrt{\rho^2+z^2}$.

The potential profile of the TQW is given as,

$$V_B(z) = \begin{cases} \dfrac{V_0|z|}{b}, -b < z < b \\ V_0 \quad , |z| > b \end{cases} \quad (2)$$

where, b is the half of the well width i.e. L=2b and V_0 is the potential well height for the electron which is given as 60% of the total energy band gap difference between GaAs and $Al_xGa_{1-x}As$ layers.

DAE Solid State Physics Symposium 2016
AIP Conf. Proc. 1832, 090032-1–090032-3; doi: 10.1063/1.4980585
Published by AIP Publishing. 978-0-7354-1500-3/$30.00

The envelop function without the donor impurity inside the TQW is defined as

$$f(z)=\begin{cases} c_1 e^{\beta(z+b)} & , \ z<-b \\ c_2 \mathrm{Ai}\left[\left(\frac{2m^* V_0}{a\hbar^2}\right)^{1/3}\left(-z-\frac{bE_0}{V_0}\right)\right]+c_3 \mathrm{Bi}\left[\left(\frac{2m^* V_0}{a\hbar^2}\right)^{1/3}\left(-z-\frac{bE_0}{V_0}\right)\right] & , \ -b<z<0 \\ c_4 \mathrm{Ai}\left[\left(\frac{2m^* V_0}{a\hbar^2}\right)^{1/3}\left(z-\frac{bE_0}{V_0}\right)\right]+c_5 \mathrm{Bi}\left[\left(\frac{2m^* V_0}{a\hbar^2}\right)^{1/3}\left(z-\frac{bE_0}{V_0}\right)\right] & , \ 0<z<b \\ c_5 e^{-\beta(z-b)} & , \ z>b \end{cases} \quad (3)$$

where, Ai[z] and Bi[z] are Airy functions, E_0 is the energy of the lowest conduction band subband. The constants c_1, c_2, c_3, c_4 and c_5 and E_0 are obtained by choosing the proper boundary conditions. The trial wavefunction of the donor impurity for 1s state, 2s and $2p_{\pm}$ states are given by,

$$\Psi_{1s} = N_{1s} f(z) e^{(-\lambda_{1s} r)}$$

$$\Psi_{2s} = N_{2s} f(z) (1-\delta r) e^{(-\lambda_{2s} r)} \quad (4)$$

$$\Psi_{2p_{\pm}} = N_{2p_{\pm}} f(z) \rho e^{(\pm im\varphi)} e^{(-\lambda_{2p_{\pm}} r)}$$

where, $\beta = \left(\frac{2m^*(V_0 - E_0)}{\hbar^2}\right)^{1/2}$, N_{1s}, N_{2s}, $N2_{p\pm}$ and λ_{1s}, λ_{2s}, $\lambda_{2p\pm}$ are the Normalization constants and variational parameters for 1s, 2s and $2p_{\pm}$ respectively. δ is the orthogonality parameter which is calculated through $\iiint \Psi^*_{2s} \Psi_{1s} \rho d\rho d\phi dz = 0$.

The variational calculation is implemented by adjusting the variational parameter in order to minimize the expectation value of the Hamiltonian operator and there by the binding energy of the donor state is obtained by

$$E_B = E_0 - < H >_{min} \quad (5)$$

The Diamagnetic susceptibility (χ_{dia}) of the hydrogenic donor confined in a $GaAs/Al_xGa_{1-x}As$ TQW, in atomic units, is given by[3]

$$\chi_{dia} = \frac{-e^2}{6m^* \varepsilon_0 c^2} < r^2 > \quad (6)$$

Results and Discussions

Fig.1. displays the binding energy (E_B) of the donor impurity in the ground state (1s) and in some low lying excited states like 2s and $2p_{\pm}$ state as a function of well width in a potential well with triangular geometry for the Al composition of x = 0.3. The reliability of the results have been verified by setting the two extreme limits as $L \to 0$ and $L \to \infty$ as done in square quantum well[3]. In the bulk limit, $L \to \infty$, the binding energy $E_B \to 1R^*$ (5.3meV) for 1s state and $E_B \to 0.25R^*$ (1.3meV) for 2s and $2p_{\pm}$ states and it should follow the same when the quantum limit approaches to the perfect two dimensional, i.e. $L \to 0$. In addition to this, the supporting evidence can be given to confirm the obtained results are more reliable by calculating the ratio between the binding energy of 1s and 2s states which results in the number approximately as 4 as mentioned in [5].

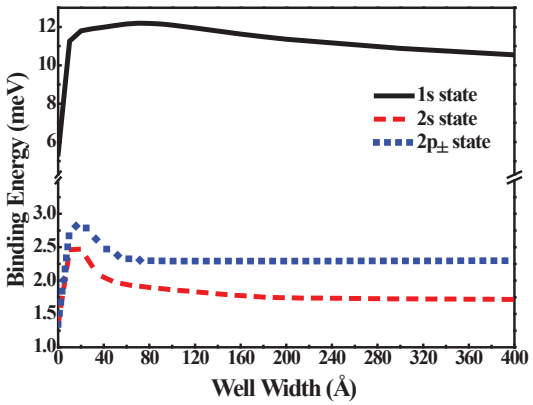

FIGURE 1. Variation of binding energy of donor impurity against well width for ground and low lying excited states.

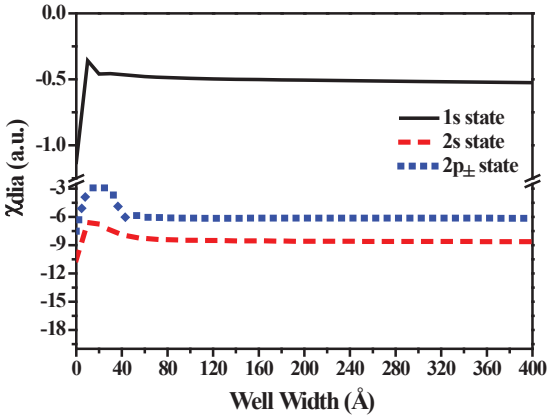

FIGURE 2. Variation of χ_{dia} of the donor impurity against well width for ground state and low lying excited states

As the width of the quantum well is increased widely (bulk limit), the two levels 2s and $2p_{\pm}$ will converge towards 1.3meV, as expected since in this limit both levels are degenerate. The diamagnetic susceptibility (χ_{dia}) has been calculated as a function of well width for various impurity states and is presented in fig.2.

To substantiate our results further, we present the profile of $< r^2 >$ against well width in fig.3, since the calculation of χ_{dia} involves $< r^2 >$ which plays a vital

role in determining the carrier localization in such quantum wells.

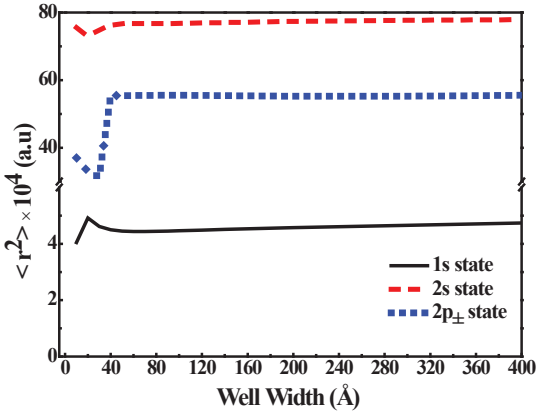

FIGURE 3. Variation of $< r^2 >$ of the donor impurity against well width.

It is obvious from fig.2 that for all the impurity states the χ_{dia} increases to the maximum as the well width goes form perfect 2D quantum region to quasi 2D region and it decreases with a "turn over" when the well width is increased beyond the quasi 2D region and approaches towards the bulk limit which is similar to the one observed in the binding energy against well width as shown in fig.1. The results again have been checked for its veracity by setting the limiting cases. In the bulk limit, $L \rightarrow \infty$, $< r^2 > \rightarrow 42\, a_B^{*2}$, hence $\chi_{dia} \rightarrow$ -15.82 a.u. and in the limit $L \rightarrow 0$, $\chi_{dia} \rightarrow$ -10.53 a.u. for 2s state. Similarly, for $2p_{\pm}$ state, in the bulk limit, $L \rightarrow \infty$, $< r^2 > \rightarrow 30\, a_B^{*2}$, hence $\chi_{dia} \rightarrow$ -11.3 a.u. and in the limit $L \rightarrow 0$, $\chi_{dia} \rightarrow$ -7.52 a.u.[3]. We could not compare our results as there is no explicit experimental results available for Triangular Quantum well.

CONCLUSIONS

We have calculated the Binding energy and the diamagnetic susceptibility for the ground state and few low lying excited states of a hydrogenic donor impurity in a GaAs/$Al_xGa_{1-x}As$ TQW of finite depth. Since this study reveals the effect of confining potential on the χ_{dia} which can be exploited to demonstrate the Semiconductor – Metal Transition at critical carrier concentration in such nanostructured systems.

ACKNOWLEDGMENTS

The authors thank University Grants Commission, New Delhi, India for the financial support under Major Research Project (F. No.42-816/2013(SR)).

REFERENCES

1. G. Z. Jiang and C. Z. Wen, *Phys. Rev. B* **50**, 2689-2692 (1994).
2. Zhang Ji-ye and Liang Xi-xia, *Optoelectron. Lett.* **1**, 0088-0091 (2005).
3. P. Nithiananthi and K. Jayakumar, *Superlattice Microstruct.* **40**, 174-179 (2006).
4. R. Khordad, *Eur. Phys. J. B* **78**, 399-403 (2010).
5. P. Harrison, *Quantum Wells, Wires and Dots,* UK: Wiley, 2005, pp. 180-184.

International Journal of Computational Materials
Science and Engineering
Vol. 4, No. 3 (2015) 1550018 (13 pages)

DOI: 10.1142/S2047684115500189

Imperial College Press
www.icpress.co.uk

Effect of geometry on the pressure induced donor binding energy in semiconductor nanostructures

P. Kalpana, K. Jayakumar and P. Nithiananthi*

Nanostructure Lab, Department of Physics
Gandhigram Rural University
Gandhigram 624302, Tamilnadu, India
**nithyauniq@gmail.com*

Received 8 April 2015
Revised 10 August 2015
Accepted 11 August 2015
Published 10 September 2015

The effect of geometry on an on-center hydrogenic donor impurity in a GaAs/(Ga,Al)As quantum wire (QWW) and quantum dot (QD) under the influence of Γ–X band mixing due to an applied hydrostatic pressure is theoretically studied. Numerical calculations are performed in an effective mass approximation. The ground state impurity energy is obtained by variational procedure. Both the effects of pressure and geometry are to exert an additional confinement on the impurity inside the wire as well as dot. We found that the donor binding energy is modified by the geometrical effects as well as by the confining potential when it is subjected to external pressure. The results are presented and discussed.

Keywords: Quantum well; quantum wire; quantum dot; III–V semiconductors; impurity levels; hydrostatic pressure; Γ–X band mixing.

1. Introduction

As a consequence of the quantum confinement in one, two and three dimensions, quantum well (QW), Quantum Well Wire (QWW) and quantum dots (QD) have interesting nonlinear optical properties with large changes in the optical absorption and index of refraction. All the electronic and optical properties of the semiconductor devices depend on the bandstructure and hence, band engineering has become one of the driving forces in semiconductor physics. Bandgap tailoring in heterostructures is possible by varying the composition of the constituent element or by applying external perturbations like temperature, pressure, laser, etc. The two most important features of GaAs as a micromechanical material are the piezoelectricity and the possibility of integrating optically active elements monolithically

*Corresponding author.

[Hjort and Schweitz, 1994]. The effect of hydrostatic pressure on the shallow donor impurities in $GaAs/Al_xGa_{1-x}As$ low-dimensional systems have been studied extensively by many researchers both experimentally [Burnett *et al.*, 1993] and theoretically [Rezaei *et al.*, 2011; Elabsy, 1994; Nithianathi and Jayakumar, 2005]. Application of hydrostatic pressures ($P > 35$ Kbar) changes the band structures of heterostructure semiconductors and converts them from direct to indirect by lowering the X-conduction band below Γ-conduction band. This results in the unconfined electrons in the well. It was shown that Γ–X crossing influences donor binding tremendously, especially at the crossover points. Investigations on the effect of change in the band structures on the electronic and optical properties have been made extensively [Wolford and Bradley, 1985; Venkateswaran *et al.*, 1986; Perez-Merchancano *et al.*, 2007]. Recently, theoretical investigations have been made to demonstrate pressure induced semiconductor–metal transition in a QW through the abrupt change in the diamagnetic susceptibility [Nithiananthi and Jayakumar, 2007; Nithiananthi and Jayakumar, 2009]. In addition to that, the geometrical effects on the low-dimensional systems raise a great attention since it has strong influence on the properties of these systems. The effect of the shape of microstructures on the binding energy was first addressed by Bryant [1985] and he studied these effects in QWW. Ribeiro and Latge [1994] made a comparative study on the geometrical effects on the impurities in cubical QD. Many research works have been carried out on the influence of shape effects on the electronic and optical properties of QD [Figen *et al.*, 2009; Chun Yong Ngo *et al.*, 2006; Bolcatto and Proetto, 1999]. A study on the confinement effect on the shallow donor impurity in a QWW has been carried out by Kasapogalu *et al.* [2003]. Recently, Rajamohan *et al.* [2008] reported the modification of diamagnetic susceptibility under the influence of the shape in nanostructured semiconductor systems. Most recently, theoretical study of both the pressure and geometrical effects on the metal–insulator transition in a cubical QD has been considered by Rajashabala and Kannan [2011]. Trzeciakowski *et al.* [1992] have experimentally demonstrated that $GaAs/Al_xG_{1-x}As$ QWs can be used as optical pressure sensors upto 40 Kbar in a wide range of temperatures. The effect of hydrostatic pressure which changes the refractive index of the material leading to the change in the geometrical cross-section can be exploited as a transducer [Hjort and Schweitz, 1994]. The influence of cross-sectional geometry is inevitable in the fabrication of devices, since they alter the electron mobility of the system [Mazumdar *et al.*, 2014]. During the fabrication of devices, one can have a control over the mobility exploiting these features. In the light of all these works, in this paper, we report a critical investigation of how the binding energy of an on-center donor impurity in $GaAs/Al_xG_{1-x}As$ QWW and QD is affected by the combined effect of cross-sectional geometry and externally applied hydrostatic pressure.

2. Theoretical Formalism

The pressure dependent Hamiltonian of the donor electron in a GaAs QWW and QD in atomic unit is given by

$$\mathbf{H} = \frac{-\nabla^2}{2m^*_{w,b}(P)} - \frac{1}{\varepsilon_{w,b}(P)\mathbf{r}} + V_B(P), \tag{1}$$

where $r = \sqrt{x^2 + y^2 + z^2}$ and $m^*{}_{w,b}$ is pressure dependent effective mass of electron in GaAs well and $Al_xGa_{1-x}As$ barrier is given by [Elbasy, 1994; Nithianathi and Jayakumar, 2005]

$$m^*_w(P) = \frac{1}{[1 + 7.51\{\frac{2}{\Gamma_w}(P,T) + [\Gamma_w(P,T) + 0.341]^{-1}\}]}, \tag{2}$$

$\Gamma_w(P)$ is the pressure dependent energy gap of GaAs at the Γ point and is given by Nithianathi and Jayakumar [2005]

$$\Gamma_w(P) = \frac{(1.519 + \alpha^{\Gamma}_w P - 5.405 \times 10^{-4} T^2)}{(T + 204)}, \tag{3}$$

where α^{Γ}_w is the pressure coefficient of GaAs at the Γ point and $T = 4\,\mathrm{K}$.

The $Al_xGa_{1-x}As$ barrier effective mass [Adachi, 1985] is given by

$$m^*_b(P) = m^*_w(P) + 0.083x, \tag{4}$$

where x being Al composition.

The pressure dependent dielectric constant for GaAs and $Al_xGa_{1-x}As$ are given by

$$\varepsilon_w(P) = \varepsilon_w(0)e^{\delta P} \quad \text{where } \varepsilon_b(P) = \varepsilon_w(P) - 3.12x. \tag{5}$$

Pressure dependent confinement potential of $Al_xGa_{1-x}As$ barrier

$$\left.\begin{aligned} V_B(x,y,P) &= \begin{cases} 0 & |x|,|y| \le L(P)/2 \\ V_0(P) & |x|,|y| > L(P)/2 \end{cases} \rightarrow \text{QWW} \\ V_B(x,y,z,P) &= \begin{cases} 0 & |x|,|y|,|z| \le L(P)/2 \\ V_0(P) & |x|,|y|,|z| > L(P)/2 \end{cases} \rightarrow \text{QD} \end{aligned}\right\}. \tag{6}$$

The pressure dependent Γ–X band mixing strength coefficient

$$S_{\Gamma X}(P) = S_0 x(P - P_1)/P. \tag{7}$$

P_1 and P_2 are the critical crossover pressures between X_b-band and Γ_b-band and X_b-band and Γ_w-band, respectively.

The variation of X_b-band with pressure is

$$X_b(P) = X_b(0) + \alpha^b_x(P) \tag{8}$$

α^b_x being the pressure coefficient for the barrier.

Choosing the trial wave function of the donor impurity in its ground state as

$$\Psi_{1s} = N_{1s}\begin{cases}\mathrm{Cos}\,\zeta|x|\mathrm{Cos}\,\zeta|y|e^{-\alpha_{1s}r} & |x|,|y| \le L(P)/2 \\ B\exp[-\beta(|x|+|y|)]e^{-\alpha_{1s}r} & |x|,|y| > L(P)/2 \end{cases} \rightarrow \mathrm{QWW}\Bigg\},$$
$$\Psi_{1s} = N_{1s}\begin{cases}\mathrm{Cos}\,\alpha|x|\mathrm{Cos}\,\alpha|y|\mathrm{Cos}_{\alpha}|z|e^{-\alpha_{1s}r} & |x|,|y|,|z| \le L(P)/2 \\ B\exp[-\delta(|x|+|y|+|z|)]e^{-\alpha_{1s}r} & |x|,|y|,|z| > L(P)/2 \end{cases} \rightarrow \mathrm{QD}\Bigg\}, \tag{9}$$

where,

$$\zeta = [2m_w^*(P)E(P)/2]^{1/2} \quad \beta = \{2m_b^*(P)[(V_0(P) - E(P)]/2]\}^{1/2},$$
$$\alpha = [2m_w^*E(P)/3]^{1/2} \quad \delta = \{2m_b^*(P)[(V_0(P) - E(P)]/3]\}^{1/2}.$$

The variation of the width of the well as a function of the pressure is given by [Morales *et al.*, 2002]

$$L(P) = L(0)[1 - (S_{11} + 2S_{12})P]. \tag{10}$$

The pressure dependent subband energy is obtained by solving the transcendental equation

$$\tan\zeta L(P)/2 = \left[\frac{m_w^*(P)}{m_b^*(P)}\left(\frac{V_0(P)}{E(P)} - 1\right)\right]^{1/2}. \tag{11}$$

The normalization constant B is obtained by applying the boundary conditions at $L_x = L_y = \pm L(P)/2$ on the wavefunction in QWW and $L_x = L_y = L_z = \pm L(P)/2$ in QD.

The pressure dependent binding energy is given by

$$E_B(P) = E(P) - \langle H(P)\rangle_{\min}. \tag{12}$$

The parameters used in the calculation are taken from the experimental results [Burnett *et al.*, 1993] and is given in Table 1.

A comparative study of the influence of Γ–X band mixing on the donor binding in GaAs–$Ga_{1-x}Al_xAs$ low-dimensional systems has been made for the following three geometries of the QWW as GW1 ($L_x = L_y = L$), GW2 ($L_x = L, L_y = L/2$), GW3 ($L_x = L/2, L_y = L/4$) and about five geometries of a QD as GD1 ($L_x = L_y, L_z = L$), GD2 ($L_x = L_y = L, L_z = L/2$), GD3 ($L_x = L_y = L, L_z = L/4$), GD4 ($L_x = L, L_y = L/2, L_z = L/4$), GD5 ($L_x = L_y = L/2, L_z = L/4$).

Table 1. The parameters taken from the experimental results.

$\Gamma_b(0)$ (eV)	$X_b(0)$ (eV)	$\alpha^{\Gamma}_{w,b}$ (meV/Kbar)	α^{x}_{b} (meV/Kbar)	Critical pressure		$\varepsilon_0(T_0)$
				P_1 (Kbar)	P_2 (Kbar)	
1.755	1.918	10.7	−1.3	13.5	33.2	12.74

3. Results and Discussion

The observations are made in QW, QWW and QD of different sizes by subjecting them to various pressure from $P = 0$ Kbar to 35 Kbar. The behavior of the system is investigated in three regions say at $P < 13.5$ Kbar, $13.5 < P < 33.2$ Kbar and $33.2 < P < 35$ Kbar, and the results are presented and discussed.

3.1. *Effect of pressure on subband energy*

Γ-conduction band of GaAs (well) and $Al_xGa_{1-x}As$ (barrier) has positive pressure coefficient and X-band of both the materials has negative pressure coefficient. Increase of pressure raises Γ-band and lowers X-band as given in Table 1. With increase of pressure upto P_1, Γ–X crossover does not take place and hence, the potential barrier height remains constant [Burnett *et al.*, 1993]. With increase of pressure above P_1, the X-band of barrier drops below Γ-band of the barrier and the barrier height becomes shallower which is determined by Γ–X crossover. Hence, when $P > P_1$, subband energy decreases with pressure. Since, subband energy increases with decrease of width of the well, it is larger for a smaller width for a certain P which can be seen in Table 2.

3.2. *Binding energy with pressure*

The binding energy of the donor impurity for different pressure for various sizes of the wire and dot has been calculated at $T = 4$ K for $x = 0.3$ and the results are compared with the QW already established result [Elabsy, 1994; Nithiananthi and Jayakumar, 2005] and are displayed in Figs. 1(a)–1(c), respectively.

3.2.1. *Case* 1: *Upto pressure* P_1

The curve for QW of width $L = 50$ Å shows that the binding energy increases linearly with pressure up to P_1 (= 13.5 Kbar), gradually upto $P_2 = 33.2$ Kbar and starts decreasing thereafter.

This is due to the fact that on the application of pressure up to P_1, the potential barrier height remains constant but the well size reduces as given in Eq. (10). This increase of energy is well-understood from the variation of conduction band effective mass and the dielectric constant with pressure. Since, the effective mass

Table 2. Variation of subband energy with pressure.

P (Kbar)	Subband energy (R^*)						
	QWW			QD			
	GW1	GW2	GW3	GD1	GD3	GD4	GD5
0	0.00211	0.00257	0.00553	0.00275	0.00278	0.00338	0.00594
13.5	0.00200	0.00244	0.00536	0.00261	0.00268	0.00325	0.00585
33.2	0.00092	0.00109	0.00147	0.00107	0.00109	0.00124	0.0015

Table 3. Pressure dependent parameters used in the calculation.

P (Kbar)	$m_w^*(P)$	$m_b^*(P)$	$\varepsilon_w(P)$	$\varepsilon_b(P)$
0	0.067	0.0919	12.6545	11.7185
10	0.07115	0.09605	12.445	11.509
13.5	0.07259	0.09749	12.3724	11.4364
20	0.07525	0.10015	12.2389	11.3029
25	0.07729	0.10219	12.1371	11.2011
33.2	0.08062	0.10552	11.972	11.1002

strongly depends on the curvature of band structure, it is modified due to the applied pressure. The increase of pressure enhances the effective mass leading to the decrease of kinetic energy. Dielectric constant (ε) decreases with increase of pressure and leads to low potential energy. Both these effects reflect in the binding energy calculation and end up with the enhancement in the binding energy upto pressure P_1. These parameters are tabulated in Table 3. The increase in binding energy with pressure in QWW and QD follow the same trend as QW but with higher value of binding.

3.2.2. *Case* 2: *For* $P_1 < P < P_2$

At pressure P ($P_1 < P < P_2$), in the QW system, besides the well size, the potential barrier height also reduces due to the Γ–X band crossover in the barrier region as given in Eq. (7). This results in the small increase in binding energy in this region. But, when the dimension of the system is reduced to QWW and QD, the effect of Γ–X band crossover significantly affects the binding energy when the size of the system is 50 Å which is seen from the reduction in binding energy.

3.2.3. *Case* 3: *For* $P > P_2$

For $P > P_2$, the system enters into an indirect bandgap regime as a consequence of the lowering of X minima below the Γ minima both in the well and in the barrier. The effect of barrier height dominates the other effects in this pressure range and reduces the donor binding after pressure P_2. In spite of the effect in effective mass and dielectric constant, the reduction in the barrier height reduces the subband energy and decreases the binding energy thereafter. This is significant in the narrower well width region which is manifested in Fig. 1. The conduction band alignment due to the effect of Γ–X mixing on applying pressure can be well understood from the insets in Fig. 1(c). Similar behavior is observed in QWW and QD also. When the dimension of the system is reduced from two to one and zero dimensions, the coulomb interaction between the charge carrier and the host material is enhanced resulting in the increase of binding energy as expected. It is observed that the effect of Γ–X band crossover strongly alters the barrier height and it is prominent in narrow regions in all the three systems. In all these three systems, one can see that at higher well sizes ($L = 300$ Å), the effect of Γ–X crossover is

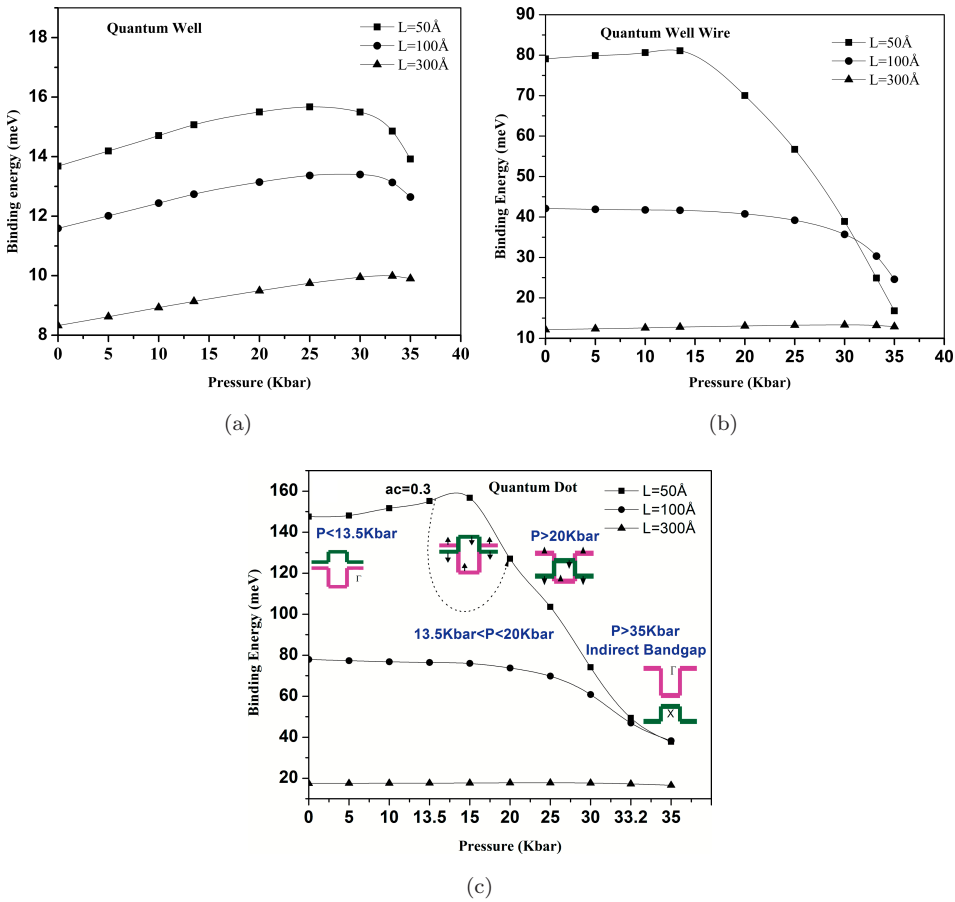

Fig. 1. Variation of donor binding energy as a function of pressure for (a) QW, (b) QWW and (c) QD.

insignificant and there is constant increase in binding energy with pressure reflecting the bulk behavior.

Figures (2a) and (2b) give the variation of binding energy with pressure for various geometries for $L = 100\,\text{Å}$ and $L = 300\,\text{Å}$ respectively. When $L = 100\,\text{Å}$, binding energy increases with pressure upto P_1 and starts decreasing thereafter irrespective of the geometry. But, this variation is drastic in the lower geometry GW3. When $L = 300\,\text{Å}$, there is no significant variation of binding energy with pressure upto P_2. Even beyond P_2, there is only a slight decrease in the binding value, and almost reaches saturation.

Similar behavior is observed in QD also as the geometry GD5 shows a drastic variation in the binding energy with pressure. This effect gradually reduces as the geometry is increased in steps as seen in Figs. (2c) and (2d).

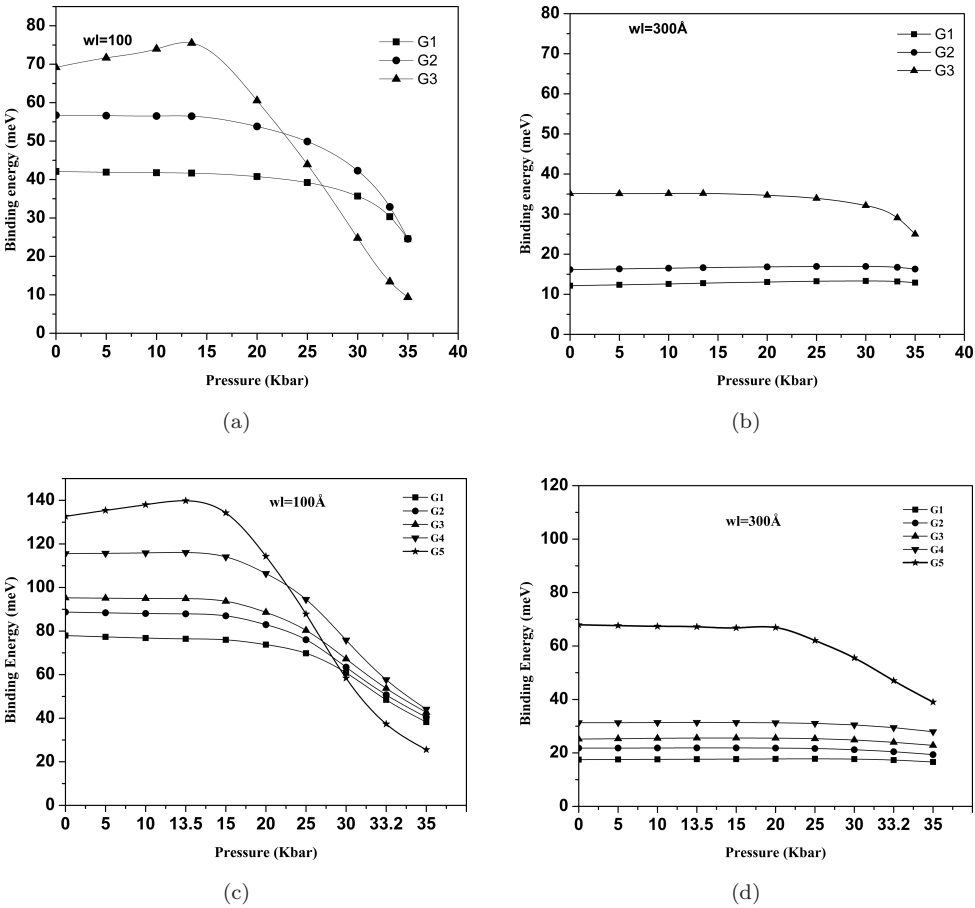

Fig. 2. Variation of donor binding energy as a function of pressure for QWW (a) $L = 100$ Å, (b) 300 Å and for QD (c) $L = 100$ Å and (d) 300 Å of various cross-sectional geometries.

3.3. *Binding energy of wire and dot against size*

Figures 3(a)–3(c) give the variation of binding energy with wire size for the three geometries at zero pressure and at two critical pressures. Similar profile is given in Figs. 4(a)–4(c) in QD for five geometries.

Comparing Figs. 3(a) and 3(c), the behavior of binding energy with wire size is the same. The value of the binding energy is maximum for $L = 120$ Å for G3 at zero pressure. The peak value shifts to the larger wire sizes when the geometry is reduced. This is because when the geometry is reduced, the confinement of the carrier is increased and hence even $L = 100$ Å falls in the quasi-1D region.

The numerical results of the variation of binding energy as a function of cross-sectional geometry for the wire and dot size of 100 Å is given in Fig. 5. for different values of pressure.

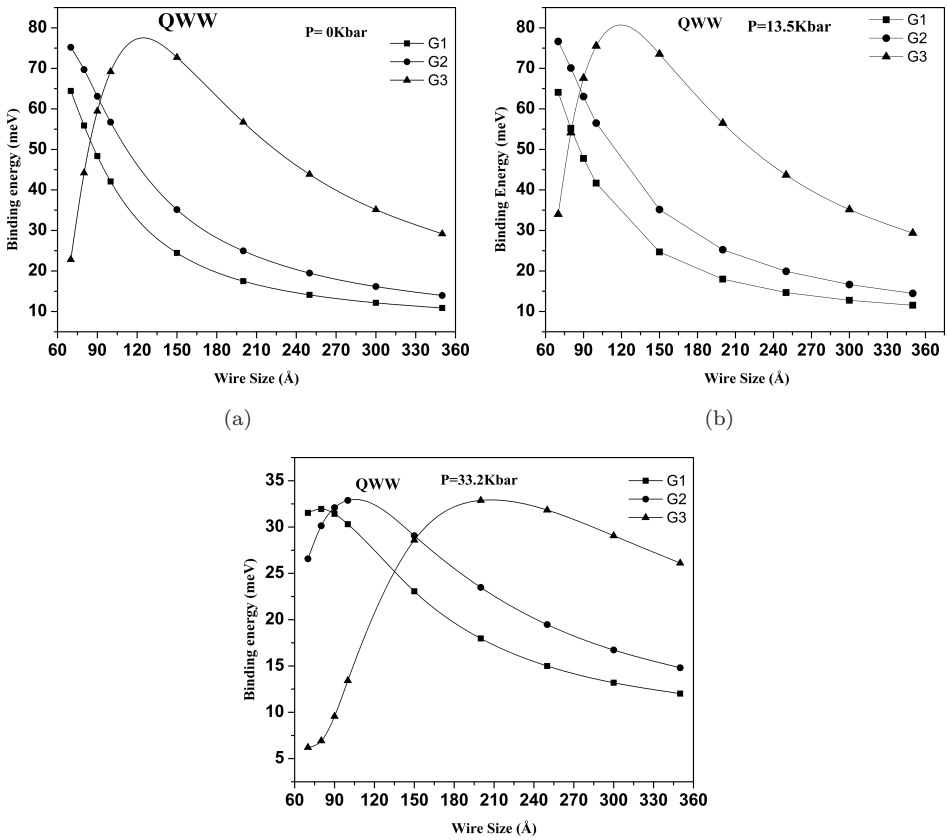

Fig. 3. Variation of donor binding energy as a function of wire size for three different pressure values of (a) $P = 0$, (b) 13.5 and (c) 33.2 Kbar for various cross-sectional geometries.

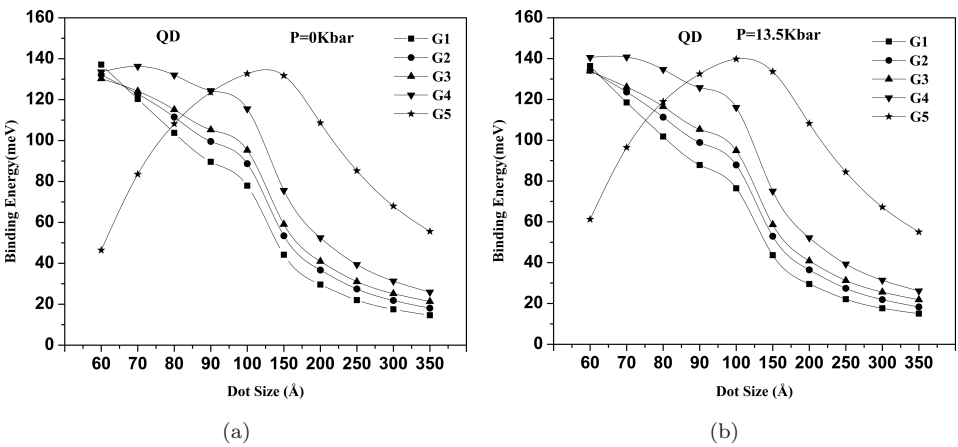

Fig. 4. Variation of donor binding energy as a function of dot size for three different pressure values of (a) $P = 0$, (b) $P = 13.5$ and (c) 33.2 Kbar for various cross-sectional geometries.

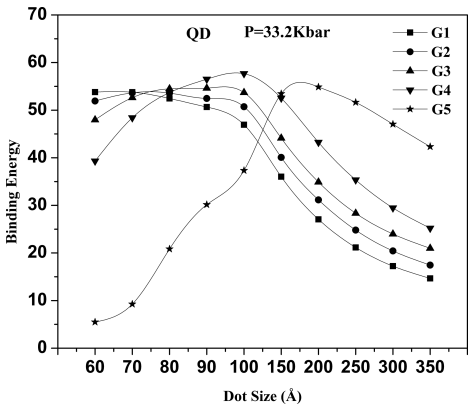

(c)

Fig. 4. (*Continued*)

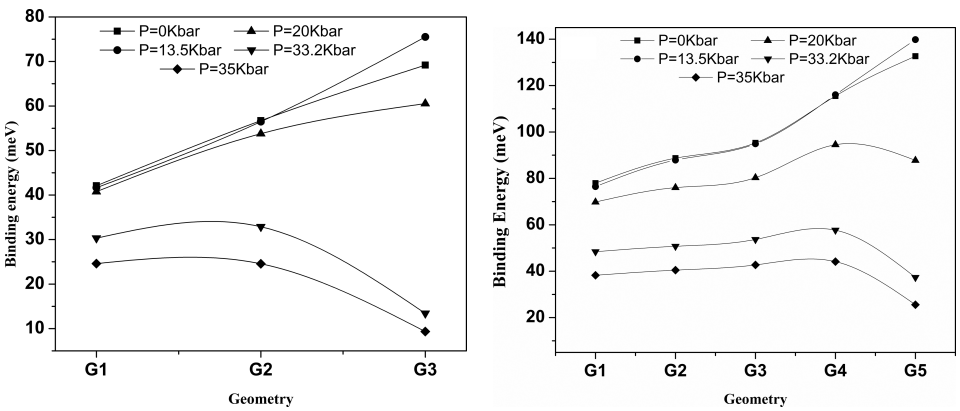

(a) (b)

Fig. 5. Variation of binding energy as a function of cross-sectional geometry for (a) QWW of $L = 100$ Å and (b) QD of $L = 100$ Å.

The rate of increase of binding energy with geometry is considerable at $P \leq 20$ Kbar for QWW and at $P \leq 13.5$ Kbar for QD. The combined effect of pressure and geometry on the binding energy play a vital role especially in the narrower QWW (G3), and smaller QD (G5), as one may note from the reduction in the impurity localization with pressure $P > 20$ Kbar and $P > 13.5$ Kbar respectively, unlike that of other geometries.

We have also demonstrated the degree of localization of donor impurity as position probability density $|\Psi|^2$ for various geometries of wire and dot size $L = 100$ Å in Fig. 6 which clearly justifies the above discussions.

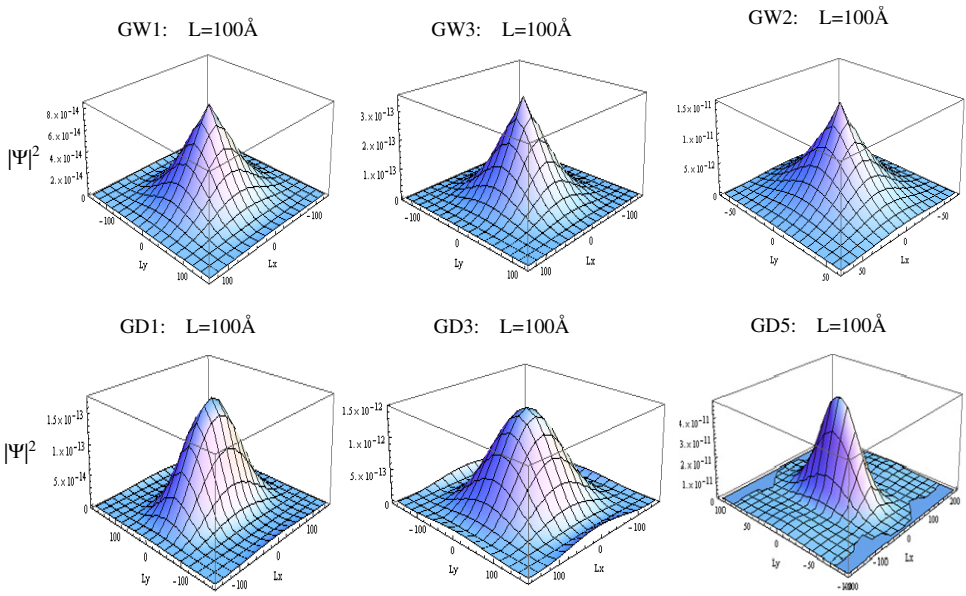

Fig. 6. 3D plot of $|\Psi|^2$ for various cross-sectional geometries of Quantum Well Wire and QD size $L = 100$ Å.

4. Conclusion

Summing up, we have presented a theoretical study on the combined effect of geometry and the Γ–X mixing on the donor impurity binding energy in a GaAs-$Ga_{1-x}Al_xAs$ QWW and QD under the influence of hydrostatic pressure. From our observations we conclude the following. The effect of hydrostatic pressure on the energy levels are strongly dependent on the barrier and well size and mixing of Γ–X states is stronger in narrow sized system [Rezaei *et al.*, 2011]. All the above behavior of donor impurity, can be well expressed in terms of electron localization, which is modified by the confining potential as a result of Γ–X mixing and also by the geometrical effects. We expect that this work will be of great help for describing the behavior of hydrogenic impurities in quantum well wires and QDs with different geometry, which may be useful in technological applications especially in sensors. Micromechanical sensors using such heterostrucutres can be achieved by altering the piezooptic [Issac *et al.*, 1987], piezoelectric [Fricke, 1991], piezoresistive and thermoresisitve properties. Piezoresistive response can be achieved due to pressure induced transfer of electrons from the high mobility bandgap minimum Γ to low mobility minimum X due to a change in their relative energy. To model and simulate nanostructure-based micromechanical, piezoelectric pressure sensor, optical pressure sensor, the critical study of pressure and geometry becomes necessary. This work may be useful in the fabrication of such devices in that direction.

Acknowledgement

The authors thank The University Grants Commission, India for the financial support through Major Research Project.

References

Adachi, S. [1985] "GaAs, AlAs and $Al_xGa_{1-x}As$: Material parameters for use in research and device applications," *J. Appl. Phys.* **58**, R1–R29.

Bolcatto, P. G. and Proetto, C. R. [1999] "Shape and dielectric mismatch effects in semiconductor quantum dots," *Phys. Rev. B* **59**, 12488–12498.

Bryant, G. W. [1985] "Hydrogenic impurity states in quantum-well wires: Shape effects," *Phys. Rev. B* **31**, 7814.

Burnett, H., Cheong, H. M., Paul, W., Koteles, E. S. and Elman, B. [1993] "Γ–X mixing in $GaAs/Al_xGa_{1-x}As$ coupled double quantum wells under hydrostatic pressure," *Phys. Rev. B* **47**, 1991–1997.

Chun, Y. N., Soon, F. Y., Weijun, F. and Soo, J. C. [2006] "Effect of size and shape on electronic states of quantum dots," *Opt. Quant. Electron.* **38**, 981–991.

Elabsy, A. M. [1994] "Effect of Gamma–X crossover on the binding energies of confined donors in single $GaAs/Al_xGa_{1-x}As$ quantum well microstructures," *J. Phys.: Condens. Matter.* **6**, 10025.

Figen, K. B., Sban, A., Abdullah, B. and Sevket, E. O. [2009] "Geometric effects on energy states of a hydrogenic impurity in multilayered spherical quantum dot," *Appl. Surf. Sci.* **255**, 6561–6564.

Fricke, K. [1991] "Piezoelectric properties of GaAs for application in stress transducers," *J. Appl. Phys.* **70**, 914–918.

Hjort, K. and Schweitz, J. [1994] "Gallium arsenide as a mechanical material," *J. Micromech. Microeng.* **4**, 5.

Isaac, J. J., Rue, R. M. D. L. and Wong, K. K. [1987] "An optical pressure sensor in III-V semiconductor material," *Proc. of Institute of Physics Short Meeting Series No.* 7 : *Fiber Optic Sensors*, Bristol, UK, pp. 105-108.

Kasapoglu, E., Sari, H. and Sokmen, I. [2003] "Geometrical effects on shallow donor impurities in quantum wires," *Physica E* **19**, 332–335.

Mazumdar, K., Jha, A., Begum, R. and Ghosal, A. [2014] "Mobility of 1D GaAs quantum wire limited by polar optic scattering," *Int. J. Innov. Res. Sci. Eng. Technol.* **3**, 16638–16641.

Morales, A. L., Montes, A., Lopez, S. Y. and Duque, C. A. [2002] "Simultaneous effects of hydrostatic stress and an electric field on donors in a GaAs–(Ga, Al)As quantum well," *J. Phys.: Condens. Matter.* **14**, 987.

Nithiananthi, P. and Jayakumar, K. [2005] "Effect of Γ–X crossover on the donor binding energy in a quantum well," *Int. J. Mod. Phys. B* **19**, 3861.

Nithiananthi, P. and Jayakumar, K. [2007] "Influence of pressure on the diamagnetic susceptibility of hydrogenic donor in some low-lying excited states in a quantum well," *Int. J. Nanosci.* **6**, 1.

Nithiananthi, P. and Jayakumar, K. [2009] "Pressure study on the semiconductor–metal transition in a quantum well," *Phys. Stat. Sol. B* **246**, 1238.

Perez-Merchancano, S. T., Paredes-Gutierrez, H. and Silva-Valencia, J. [2007] "Hydrostatic-pressure effects on the donor binding energy in GaAs–(Ga, Al)As quantum dots," *J. Phys.: Condens. Matter.* **19**, 026225.

Rajamohan, C., Merwyn Jasper, D., Reuben, A., Nithiananthi, P. and Jayakumar, K. [2008] "Shape effect of diamagnetic susceptibility of a hydrogenic donor in a nanostructured semiconductor systems," *J. Math. Chem.* **44**, 743.

Rajashabala, S. and Kannan, R. [2011] "Simultaneous effets of hydrostatic pressure and geometry on metal–insulator transition in a cubical quantum dot," *J. Nano-Electron. Phys.* **3**, 1041–1047.

Rezaei, G., Doostimotlagh, N. A. and Vaseghi, B. [2011] "Simultaneous effects of hydrostatic pressure and conduction band Non-parabolicity on binding energies and diamagnetic susceptibility of a hydrogenic impurity in spherical quantum dots," *Commun. Theor. Phys.* **56**, 377.

Ribeiro, F. J. and Latge, A. [1994] "Impurities in a quantum dot: A comparative study," *Phys. Rev. B* **50**, 4914–4915.

Trzeciakowski, W., Perlin, P. and Teisseyre, H. [1992] "Optical pressure sensors based on semiconductor quantum wells," *Sens. Actuators A* **32**, 632–638.

Venkateswaran, U., Chandrasekar, M., Chandrasekar, H. R., Vojak, B. A., Chamber, F. A. and Meese, J. M. [1986], *Phys. Rev. B* **33**, 8416.

Wolford, J. and Bradley, J. A. [1985] "Pressure dependence of shallow bound states in gallium arsenide," *Solid State Commun.* **53**, 1069.

6th ICONSAT 2014

International Conference on Nano Science and Technology

the flagship nanoscience meeting of NANO MISSION, DST, Govt. of India

2nd-5th MARCH, 2014

iCONSAT2014

800 Participants & Galaxy of Speakers

Sponsored by

सत्यमेव जयते

NANO MISSION
Dept. of Science and Technology
Govt. of India

NANO MISSION,
DST, GOVT OF INDIA

Institute of Nano Science and Technology

Organized by

INSTITUTE OF NANO SCIENCE & TECHNOLOGY (INST)
Mohali, Punjab

Venue:

UNIVERSITY AUDITORIUM, PANJAB UNIVERSITY

WWW.ICONSAT2014.IN

INST-LANGMUIR LECTURE

Prof CNR Rao, FRS
ICMS & JNCASR, Bangalore, India
will deliver the inaugural
INST LANGMUIR lecture

INST-FEYNMAN LECTURE

Prof James Heath,
California Institute of Technology, USA
will deliver the inaugural
INST FEYNMAN lecture

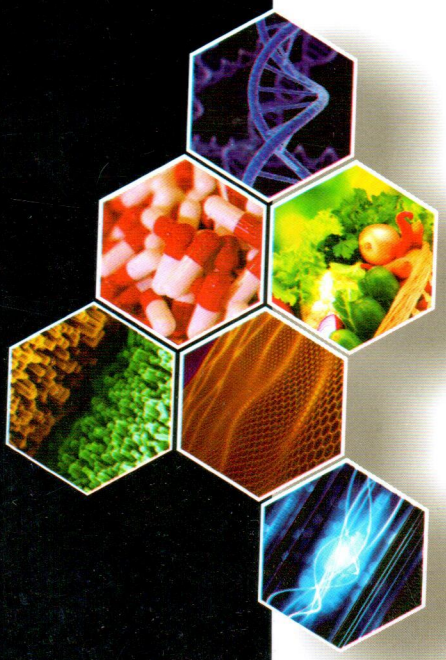

and many more eminent speakers

LECTURE ABSTRACTS

iCONSAT2014

P-05 (T-2)

Enhanced Coulomb Interaction due to Spatial Dielectric Screening in Semimagnetic Quantum Dot

P. Kalpana[a], A. Merwyn Jasper D Reuben[b], P. Nithiananthi[a], K. Jayakumar[a*]

[a]*Department of Physics, Gandhigram Rural Institute, Gandhigram-624302, Tamilnadu, India*
[b]*Department of Physics, School of Engineering, Saveetha University, Thandalam, Chennai-600104, Tamilnadu, India*
kjkumar_gri@rediffmail.com

The electronic structure of the Quantum Dots (QD) with enhanced Coulomb interaction in magnetic field displays a rich scenario of different phases in the ground state. A novel approach can be made to reduce the charged impurity induced scattering[1] and to calculate the vibrational spectra, the carrier interactions in exciton problems and impurity potentials via wave vector dependent and spatial dielectric screening[2,3]. The purpose of the present work is to investigate the significance of spatial dielectric screening (r) in working out the Coulomb interaction between the acceptors[4] in a CdTe/$Cd_{1-x}Mn_xTe$ Semimagnetic Spherical QD assuming the confining potential to be square well type within the effective mass approximation using variational principle. It is seen from the results that the carriers show more interaction (an enhancement of ~13%) when they are screened by spatial dielectric function in the absence of external magnetic field as well as the presence of magnetic field. This work provides the foundation to study the intrinsic transport properties of the carriers in low dimensional systems and to explore the potential applications in spintronic and electronic devices.

Reference: 1. Fang Chen, Jilin Xia, David K Ferry and Nongjian Tao, *Nano Letters*, **2009**, *9*, 2571. 2. Zhen-Yan Deng, Jing-Kan Guo and Ting-Rong Lai, *Phys. Rev. B*, **1994**, 50. 3. J Hermanson, *Phys.Rev.* **1966**, *150*,660. 4. A.Merwyn Jasper D Reuben, K. Jayakumar, *Superlat. and Microstruct.*, **2012**, *52*, 732.

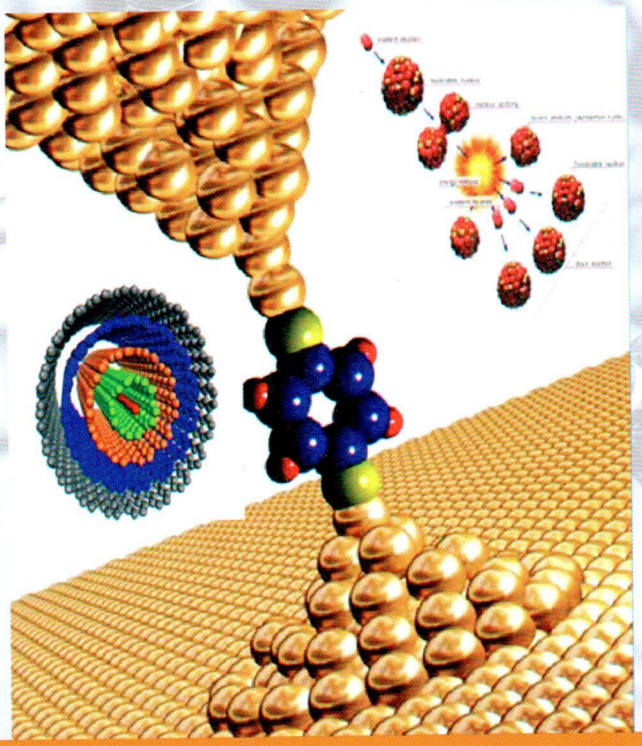

Abstact Proceeding

NCFCM 2015

NATIONAL CONFERENCE ON FRONTIERS OF CHEMISTRY AND MATERIALS

ORGANIZED BY

POST GRADUATE DEPARTMENT OF CHEMISTRY,

(12th -14th Feb. 2015)

Anekant Education Society's

TULJARAM CHATURCHAND COLLEGE,

Baramati, Dist. Pune, (Maharashtra), 413102

Jain Religous Minority College | NAAC Reaccredited College | ISO 9001:2008 Certified | DST FIST "O" LEVEL |

O-5

COULOMB INTERACTION OF He- LIKE IMPURITY IN SEMIMAGNETIC QUANTUM DOT

P.Kalpana, P.Nithiananthi and K.Jayakumar*

Nanostructure Lab, Department of Physics, Gandhigram Rural University, Gandhigram-624302, Tamilnadu, India

*Corresponding Author: kjkumar_gri@rediffmail.com, Contact no. +91 9443461177

Keywords: *Semimagnetic Quantum Dot, He-like donor Impurity, Coulomb Interaction, Magnetic Field*

ABSTRACT

Semimagnetic Nanostructured Systems wherein magnetic material like MnTe is a constituent in Semiconductor material CdTe is drawing considerable interest [1,2]. Interest in these materials arises mainly because of the fact that the band offsets can be tailored by an external magnetic field [3], which opens up the possibility of realising Optoelectronic devices. In the present work, the He-like impurity in a Semimagentic Quantum Dot like CdTe – $Cd_{1-x}Mn_xTe$ is considered and the Coulomb interaction of electrons confined in such Quantum Dot has been computed for the on - centre and on - edge impurities under the influence of external magnetic field in the effective mass approximation using variational principle. It is noticed that the Coulomb interaction for the on - centre impurity is higher than the on - edge impurity for both in the presence and absence of magnetic field for all the sizes of the Dot. It is also observed that the Coulomb interaction is lowered by the external magnetic field as expected because of the tailoring of band offset as mentioned earlier. Results are presented and discussed.

1) Bastard G, Brum J.A. and R.Ferreira: *Solid State Physics* 1991, **44**: 229.
2) Falicov L. M, *Physics Today* 1992, **45**:46
3) Von Ortenberg M, *Phys.Rev. Lett.* 1982, **49**:104

SECOND INTERNATIONAL CONFERENCE ON MATERIALS SCIENCE AND TECHNOLOGY

ICMST 2016

05-08 JUNE 2016

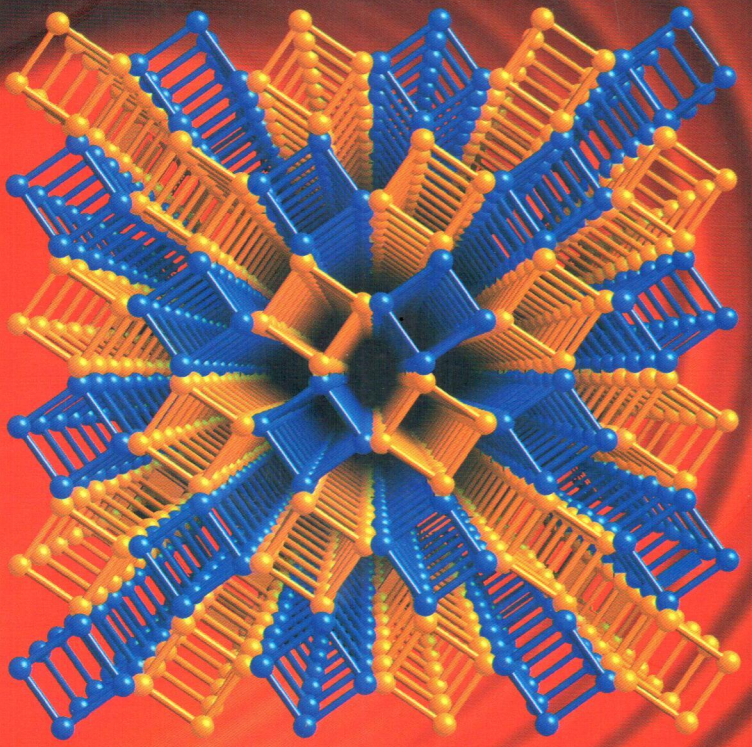

DEPARTMENT OF PHYSICS
ST. THOMAS COLLEGE PALAI
KERALA - 686 574, INDIA

COLLEGE WITH POTENTIAL FOR EXCELLENCE

FO518.

Effect of Er_2O_3 addition of densification characteristics of nanocrystallineZnobased varistors

Samarpita Roy[1], Debdulal Das[1],TapateeKundu Roy[2]
[1]*Department of Metallurgy and Materials Engineering, Indian Institute of Engineering Science and Technology, Shibpur, Howrah - 711 103, West Bengal, India*
[2]*Variable Energy Cyclotron Centre, 1/AF Bidhan Nagar, Kolkata-700064, West Bengal, India*

Varistor is variable resistor that exhibitsnon-ohmic current–voltage characteristic as it consists of semiconducting ZnO grains surrounded by thin insulating intergranular layers. In recent times, continued efforts have been directed to develop high performance varistors specifically by reducing the grain size of ZnO, because the breakdown voltage of a varistor is known to be inversely proportional to the grain size. However, economical production of ultrafine grained varistor remains a technological challenge owing to rapid grain coarsening during sintering. A simple approach to retard grain growth of nanocrystalline varistor powders during sintering is addition of appropriate rare earth oxides. They should act as grain growth inhibitor, in one hand, and must be beneficial for electrical properties, on the other hand. The present study examines the effect of Er_2O_3 addition (0 to 2 mol. %) on densification and grain growth behavior of nanocrystalline $ZnO–V_2O_5–MnO_2–Nb_2O_5$varistor powders prepared by using high energy ball milling. Ball milled powders have been densified by conventional single stage sintering at 900, 1100 and 1300 °C for 1h. Microstructure of ball milled powders and sintered pellets have been characterized by SEM and TEM examinations as well as XRD and image analyses in addition to density measurement of sintered pellets. TEM and XRD results confirm the generation of nanometeric sized ZnO particles by high energy ball milling. Microstructural characterization of sintered pellets assists to infer that while addition of Er_2O_3 reduces densification process, it significantly retards the grain coarsening during sintering particularly at elevated temperatures. These effects are found to enhance with increasing addition of Er_2O_3. It has been established that Er_2O_3 is an effective grain growth inhibitor for the ZnO based varistor systems.

FO523.

Acceptor States in a SemimagneticCdTe/$Cd_{1-x}Mn_xTe$ Double Quantum Well

P.Kalpana, P.Nithiananthi and K. Jayakumar
Nanostructure Lab, Department of Physics, Gandhigram Rural University, Gandhigram, 624302, Tamilnadu, India

The Diluted Magnetic Semiconductors are becoming an interesting test ground for variousthoreticalideassinceitsbandstructurecanbetailoredsothatboth the electronic and magnetic properties can also bealtered. The distinctive behaviour of Double Quantum Wells (DQW)can be observed when compared with a Single Quantum Well (SQW) especially when the density of states gets modified from 2D to 0D due to the formation of Landau levels in these structures under the influence of the magnetic field. In the present work, we have studied the electronic states of the acceptor impurity as well as the influence of Bound Magnetic Polaron by calculating the Spin Polaronic Shift in $Cd_{1-x}Mn_xTe$ / CdTe DQW under the external applied magnetic field in the effective mass approximation using variational technique for various composition of magnetic impurity Mn ion (x = 0.1, 0.3) and also for various impurity locations. It is observed that the acceptor impurity is highly localized only when it is situated at the center of the well region and it is less bound with increase in magnetic field (79.21Tesla), near critical magnetic field due to the reduction in the confining potential barrier height because of the applied magnetic field which can

4TH INTERNATIONAL CONFERENCE ON NANOSCIENCE AND NANOTECHNOLOGY

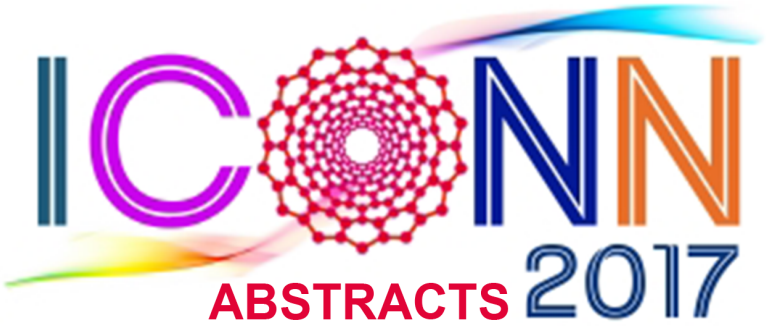

August 9-11,2017
Organised by
Department of Physics and Nanotechnology
SRM University
Kattankulathur, India

IN ASSOCIATION WITH
SHIZUOKA UNIVERSITY, JAPAN
GNS SCIENCE, NEW ZEALAND
NATIONAL CHIAO TUNG UNIVERSITY (NCTU), TAIWAN

CO-SPONSORED BY
SCIENCE AND ENGINEERING RESEARCH BOARD (SERB), DST, GOVT.OF INDIA
COUNCIL FOR SCIENTIFIC AND INDUSTRIAL RESEARCH (CSIR), GOVT OF INDIA

scholarlink.com

First Published by Scholarink 2017

An imprint of
Notion Press Media Private Limited

Old No. 38, New No. 6 McNichols Road,
Chetpet Chennai - 600 031

ISBN 978-1-947697-83-6

confirming highly stable silver nanoparticles while the XPS reveals the zero oxidation state of nano silver. Further, the structural information of formulated silver nanoparticles is characterized through HR SEM, TEM that yields 5-10 nm sized nanoparticles. Again the symmetrical distribution of metal nanoparticles is thoroughly examined through mapping of TEM. The designed silver nanoparticles are highly stable and regularly arranged; and can be employed in various technological applications of sensing, drug delivery along with device formulation.

***Keywords*:**AHMT, Silver nanoparticle, Sensing, Drug delivery.

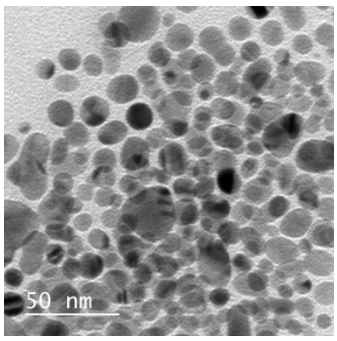

Fig 1 TEM images of regularly arranged silver nanoparticles

DONOR STATES IN SEMIMAGNETIC TRIANGULAR QUANTUM WELL

KALPANA P[1], JAYAKUMAR K[1*]

Nanostrucutre Lab, Department of Physics, Gandhigram Rural Institute – Deemed University, Gandhigram – 624 302, Tamilnadu, Indina

[*]kjkumar_gri@rediffmail.com

[*]+91 9443461177.

Abstract

The effect of Bound Magnetic Polaron (BMP) on the donor binding in a Semimagnetic Triangualr Quantum Well (TQW) as a function of various combinations of the compostion of Mn^{2+} ion in the well (x_{in}) and the barrier (x_{out}) in such a way that $x_{out} - x_{in} = x$ is same has been investigated. The binding energy of the donor is calculated using variational technique in the effective mass approximation and the interaction between the magnetic moment of the Mn^{2+} ion and the spin of the carrier is treated using Mean Field Theory. The magnetic field alters the barrier height of the TQW which drastically changes the binding of the donor as well as the Spin Polaronic Shift (SPS). The results have been computed for the cases with and without the application of magnetic field for the resultant composition of x = 0.1 and x = 0.2 as a function of well width of the TQW. The binding energy decreases as the applied magnetic field (γ, a dimensionless parameter) increases and the shift in the binding occurs towards the higher well width as the γ approaches the critical value. The results show that the SPS increases with the increase in Mn^{2+} ion.

***Keywords*:** Triangular Quantum Well, , Bound Magnetic Polaron, Binding Energy, Donor Impurity, Spin Polaronic Shift

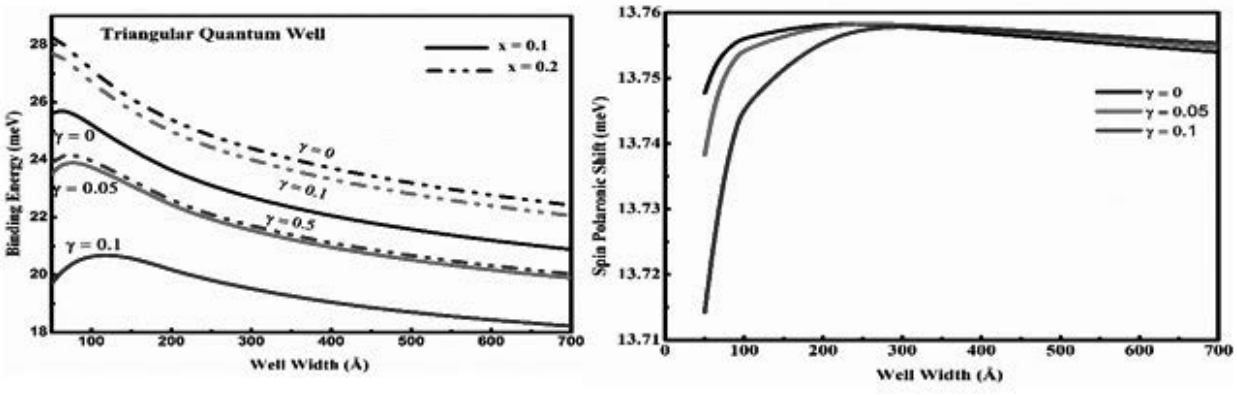

Fig 1. (a) Variation of Bidning Energy for x = 0.1 and 0.2, (b) SPS for x= 0.1 as a function of Well Width for various magnetic fields (γ).

$BATIO_3:EU^{3+}$ PEROVSKITE RED EMITTING PHOSPHOR: STRUCTURAL AND TEMPERATURE DEPENDENT PHOTOLUMINESCENCE STUDIES FOR THE LIGHTING APPLICATIONS

DHANANJAY KUMAR SINGH[A)], J. MANAM[B)]

Department of Applied Physics, Indian Institute of Technology (Indian School of Mines), Dhanbad-826004, India

***Corresponding author:* a) dksism89@gmail.com**

Abstract

One of the most sophisticated approaches to produce white light emitting diode (W-LED) is Phosphor converted (PC) LED which may be treated as the next generation energy efficient lighting source to substitute traditional incandescent and fluorescent lamps because of their long lifetime, higher energy efficiency, and environment-friendly characteristics. $BaTiO_3:Eu^{3+}$, a promising candidate for the same applications have been prepared by the facile solid state reaction method. The synthesized phosphors were characterized through various technique such as XRD, FESEM, Photoluminescence, temperature dependent spectroscopy, decay time analysis and UV-Visible spectroscopy for the studies of crystal structure, morphology and optical properties. XRD analysis confirmed that $BaTiO_3$ phosphor have the tetragonal structure with space group P4mm (99). FESEM images of $BaTiO_3$ exhibited the particle sizes in irregular spherical shape with high resolution and agglomerated in nature. The Eu^{3+} activated perovskite $BaTiO_3$ phosphors have been effectively excited under the wavelength 397nm ($^7F_0 \rightarrow {}^5L_6$) which exhibits very intense and sharp red emission peak at 615nm due to the hypersensitive electric dipole transition $^5D_0 \rightarrow {}^7F_2$. The critical distance between Eu^{3+} ions were estimated as 10.20 Å, refers to multipole-multipole (dipole -dipole) interaction which was most probable reason for the concentration quenching. Temperature dependent PL studies for the optimum composition $Ba_{(0.95)}TiO_3:0.05Eu^{3+}$, reveals the enough thermal stability even at 427 K. Furthermore, using diffuse reflectance spectra the E_g value was estimated to be about 3.250, 3.257eV for $BaTiO_3$, $BaTiO_3:0.05Eu^{3+}$ respectively. Therefore, based on the experimental results, $BaTiO_3:Eu^{3+}$ perovskite phosphors could be a suitable red candidate in phosphor converted white light emitting diode applications.